Development of High-Throughput Methods for Testing Neurotoxicity of Environmental Samples

Dissertation

der Mathematisch-Naturwissenschaftlichen Fakultät der Eberhard Karls Universität Tübingen

zur Erlangung des Grades eines Doktors der Naturwissenschaften

(Dr. rer. nat.)

vorgelegt von

M. Sc. Jungeun Lee

aus Seoul, Südkorea

Tübingen

2022

Gedruckt mit Genehmigung der Mathematisch-Naturwissenschaftlichen Fakultät der Eberhard Karls Universität Tübingen.

Tag der mündlichen Qualifikation: 22.07.2022

Dekan: Prof. Dr. Thilo Stehle

1. Berichterstatterin: Prof. Dr. Beate I. Escher

2. Berichterstatter: Prof. Dr. Marcel Leist

Contents

Summary

Micropollutants in the aquatic environment pose a risk to human and environmental health. Effect-based tools have been applied in environmental monitoring for diverse toxicity endpoints but testing method for neurotoxicity is still limited. The goal of this PhD thesis was to develop and implement high-throughput methods for testing neurotoxicity of typical environmental organic pollutants and mixtures of chemicals extracted from water samples. Neurite outgrowth inhibition and acetylcholinesterase (AChE) inhibition were considered as key neurotoxicity endpoints and human neuroblastoma SH-SY5Y cells were used for both assays. The assays were set up in 384-well plates for high-throughput and repeatable concentration-response assessment. The AChE inhibition assay using purified enzyme has been applied widely, but there has been an issue that natural organic matters such as dissolved organic carbon (DOC) contained in environmental samples can suppress AChE inhibition in the assay. In the cellular assay, AChE inhibition by paraoxon-ethyl was not impacted by DOC up to 68 mg_C/L and binary mixtures of paraoxon-ethyl and water extracts showed concentration-additive effects, which indicates no disturbance by DOC and applicability of the cell-based AChE inhibition assay for testing of environmental samples. Chemicals with potential developmental neurotoxicity (DNT) are often hydrophobic. Hydrophobic chemicals can easily intercalate into the cell membrane and provoke effects via nonspecific manner, i.e., baseline toxicity. To investigate whether DNT of chemicals is driven via specific modes of action or merely via baseline toxicity, test chemicals were selected based on their potential DNT from literature or a combination of occurrence data and effects detected in water samples. The effects on neurite outgrowth and cytotoxicity were directly measured in SH-SY5Y cells and the observed effects were compared with predicted baseline cytotoxicity. Since existing prediction models for baseline toxicity had limited application, a prediction model was newly established using a mass balance model based on constant critical membrane concentrations, which can be applied for chemicals of a wide range of hydrophobicity and speciation. When comparing the measured effects in SH-SY5Y with the predicted baseline toxicity, more hydrophobic chemicals tended to trigger toxicity on neurite outgrowth and cell viability via baseline toxicity. The hydrophobic chemicals were still often highly potent while some more hydrophilic chemicals exhibited high specificity but often lower potency. Environmental pollutants with specific modes of action targeting neurite outgrowth were identified by comparing the effects on neurite outgrowth and cytotoxicity. Highly specific effects

were observed for two carbamate insecticides, the pharmaceutical mebendazole, the biocide 1,2-benzisothiazolin-3-one, and many other chemicals that were detected in surface water and wastewater treatment plant (WWTP) effluent samples. The two types of water samples were tested in neurite outgrowth assay and the effects on neurite outgrowth were even observed when the samples were diluted by a factor of 5. While overall cytotoxicity was similar between two types of samples, higher toxicity on neurite outgrowth was observed for surface water than WWTP effluent. This led to more specific inhibition of neurite outgrowth by surface water, indicating that higher concentrations of chemicals and/or more potent chemicals acting on neurite outgrowth were contained in the surface water samples. Subsequently, the measured mixture effects were further explained by measured effects of single chemicals and overall, chemicals with high effect potency and/or high occurrence were identified as major mixture effect drivers. While main contributors were different between individual samples for surface water, mebendazole was a dominant contributor for the effects observed in WWTP effluent. The detected chemicals still explained only a small fraction of the measured mixture effects of surface water (up to 4.4%) and WWTP effluent (up to 6.8%). When the two neurotoxicity endpoints were assessed in identical samples, the effects appeared not to be related to each other and both neurotoxicity endpoints were sensitive enough to capture toxicity even when the samples were diluted. The experiments with single chemicals and the applications in case studies demonstrated that both neurotoxicity assays are suitable for environmental monitoring of neurotoxicants. Further testing of various chemicals and environmental mixtures can be useful to identify more effect drivers in the environment. Consideration of more diverse neurotoxicity endpoints would enable more comprehensive assessment of water quality. In the future, these assays have also the potential to be used for human biomonitoring and can be applied to other complex environmental matrices such sediments or biota.

Zusammenfassung

Mikroverunreinigungen in der aquatischen Umwelt stellen ein Risiko für die Gesundheit von Mensch und Umwelt dar. Bei der Umweltüberwachung wurden wirkungsbasierte Instrumente für verschiedene Toxizitätsendpunkte eingesetzt, doch die Testmethoden für die Neurotoxizität sind noch begrenzt. Das Ziel dieser Doktorarbeit war die Entwicklung und Implementierung von Hochdurchsatzmethoden zur Prüfung der Neurotoxizität von typischen organischen Umweltschadstoffen und Chemikaliengemischen, die aus Wasserproben extrahiert wurden. Die Hemmung des Neuritenwachstums und die Hemmung der Acetylcholinesterase (AChE) wurden als zentrale Endpunkte der Neurotoxizität betrachtet, und für beide Tests wurden menschliche SH-SY5Y-Neuroblastomzellen verwendet. Die Biotestverfahren wurden in 384-Well-Platten durchgeführt, um einen hohen Durchsatz und eine wiederholbare Konzentrations-Wirkungs-Bewertung zu ermöglichen. Der AChE-Hemmtest unter Verwendung von gereinigtem Enzym ist weit verbreitet, aber es besteht das Problem, dass natürliche organische Stoffe wie gelöster organischer Kohlenstoff (DOC), die in Umweltproben enthalten sind, die eine falsch-positive AChE-Hemmung im Test erzeugen können. Im zellulären Biotestverfahren wurde die AChE-Hemmung durch Paraoxon-Ethyl durch DOC bis zu 68 mg_C/L nicht beeinträchtigt, und auch binäre Mischungen von Paraoxon-Ethyl und Wasserextrakten zeigten konzentrationsadditive Effekte, was darauf hindeutet, dass DOC nicht störend wirkt und der zellbasierte AChE-Hemmtest für die Untersuchung von Umweltproben geeignet ist. Chemikalien mit potenzieller Entwicklungsneurotoxizität (DNT) sind häufig hydrophob. Hydrophobe Chemikalien können sich leicht in die Zellmembran einlagern und auf unspezifische Weise Wirkungen hervorrufen, d.h. eine Grundlinientoxizität. Um zu untersuchen, ob die DNT von Chemikalien über spezifische Wirkungsweisen oder lediglich über die Grundlinientoxizität gesteuert wird, wurden Testchemikalien auf der Grundlage ihrer potenziellen DNT aus der Literatur oder einer Kombination von Daten über ihr Vorkommen und in Wasserproben festgestellten Wirkungen ausgewählt. Die Auswirkungen auf das Neuritenwachstum und die Zytotoxizität wurden direkt in SH-SY5Y-Zellen gemessen, und die beobachteten Effekte wurden mit der vorhergesagten Basis-Zytotoxizität verglichen. Bestehende Prognosemodelle für die Basistoxizität waren jedoch nur begrenzt anwendbar. Daher wurde ein neues Prognosemodell unter Verwendung eines Massenbilanzmodells entwickelt, das für Chemikalien mit einem breiten Spektrum an Hydrophobie und Speziierung angewendet werden kann. Beim Vergleich der gemessenen

Wirkungen in SH-SY5Y mit der vorhergesagten Basistoxizität zeigte sich, dass hydrophobere Chemikalien eher eine Toxizität auf das Neuritenwachstum und die Lebensfähigkeit der Zellen über die Basistoxizität auslösen. Die hydrophoben Chemikalien waren oft noch hochwirksam, während einige hydrophilere Chemikalien eine hohe Spezifität, aber oft eine geringere Wirksamkeit aufwiesen. Umweltschadstoffe mit spezifischer Wirkungsweise auf das Neuritenwachstum wurden durch den Vergleich der Auswirkungen auf das Neuritenwachstum und die Zytotoxizität ermittelt. Hochspezifische Wirkungen wurden bei zwei Carbamat-Insektiziden, dem Arzneimittel Mebendazol, dem Biozid 1,2-Benzisothiazolin-3-on und vielen anderen Chemikalien beobachtet, die in Oberflächenwasser und Abwasserproben von Kläranlagen nachgewiesen wurden. Die beiden Arten von Wasserproben wurden im Neuritenwachstumstest getestet, und die Auswirkungen auf das Neuritenwachstum wurden sogar dann beobachtet, wenn die Proben um den Faktor 5 verdünnt wurden. Während die allgemeine Zytotoxizität zwischen den beiden Probenarten ähnlich war, wurde bei Oberflächenwasser eine höhere Toxizität für das Neuritenwachstum festgestellt als bei Kläranlagenabwasser. Dies führte zu einer spezifischeren Hemmung des Neuritenauswuchses durch Oberflächenwasser, was darauf hindeutet, dass in den Oberflächenwasserproben höhere Konzentrationen von Chemikalien und/oder stärkere Chemikalien mit Wirkung auf den Neuritenauswuchs enthalten waren. Anschließend wurden die gemessenen Mischungseffekte durch die gemessenen Effekte einzelner Chemikalien weiter erklärt, und insgesamt wurden Chemikalien mit hoher Effektstärke und/oder hohem Vorkommen als Hauptfaktoren für Mischungeffekte identifiziert. Während sich die Hauptverursacher in den einzelnen Proben des Oberflächenwassers unterschieden, war Mebendazol der Hauptverursacher der im Kläranlagenablauf beobachteten Effekte. Die nachgewiesenen Chemikalien erklärten jedoch nur einen kleinen Teil der gemessenen Mischungseffekte von Oberflächenwasser (bis zu 4,4 %) und Kläranlagenabwasser (bis zu 6,8 %). Bei der Bewertung der beiden Neurotoxizitätsendpunkte in den identischen Proben schienen die Wirkungen nicht miteinander verbunden zu sein, und beide Neurotoxizitätsendpunkte waren empfindlich genug, um die Toxizität zu erfassen, selbst wenn die Proben verdünnt wurden. Die Experimente mit einzelnen Chemikalien und die Anwendungen in Fallstudien haben gezeigt, dass beide Neurotoxizitätstests für die Umweltüberwachung von neurotoxischen Stoffen geeignet sind. Weitere Tests mit verschiedenen Chemikalien und Umweltgemischen können nützlich sein, um weitere Wirkfaktoren in der Umwelt zu

identifizieren. Die Berücksichtigung vielfältigerer Neurotoxizitätsendpunkte würde eine umfassendere Bewertung der Wasserqualität ermöglichen. In Zukunft könnten diese Tests auch für das Biomonitoring beim Menschen eingesetzt und auf andere komplexe Umweltmatrices wie Sedimente oder Umweltorganismen angewendet werden.

Acknowledgements

I am grateful that I had the opportunity to grow not only academically but also personally over the past few years, having good people around me. I would like to thank the following people, without whom I would not have been able to complete this thesis. I deeply thank my three supervisors for providing guidance and feedback with great support through my research. Thank you all for stimulating my curiosity, giving me advice, and helping me grow as a better researcher. We were the best team I could ever imagine! I would like to express my sincere thanks to Beate Escher, who always encouraged me to explore new things and gave a lot of help and support for me to do so. Thank you for going through this adventure with me from the beginning to the end with consistent support and dedication. I wouldn't have developed myself this much without you. I would like to thank Rita Schlichting for helping me a lot to adapt to new life and research environment in Germany when I was wandering around in the beginning. I was able to come this far without getting lost because you helped me to make wise decisions whenever I encountered challenges. I would also like to thank Stefan Scholz for always taking interest in my research and being willing to give academic advice. While doing research with you, I learned a lot about how to ask and approach research questions and your warm words have made me to stay motivated. I would like to say special thanks to the CELLTOX members for helping me in every way, especially to Sandy Schöne, Julia Huchthausen, Niklas Wojtysiak, Sophia Mälzer, Jenny Braasch, and Luise Henneberger. They were always willing to help me with experiments and research direction, and all the chats I had with them in the lab, office, or hallway were great happiness in my daily life. From the bottom of my heart I would like to say big thank you to Maria König, who is my colleague and also my best friend, for always being there to rejoice and grieve with me and helping me not to lose myself through difficult times. I also thank all my friends in Leipzig (especially to Jieying Zhou, Chaeyoon Lee, Juhwi Lee, Sungju Han, and Maria Paula da Silva), who made me precious and colorful memories during my life of studying abroad and made me realize that I was not alone during difficult times. I also want to say thank you to all my friends in Korea for always encouraging, supporting and worrying about me, especially to my old friends Dami and Jihyun. My deepest thanks go to my beloved mother, father, and brother, who would have always missed their daughter or sister from afar. You have been a great source of support and thank you for always staying by my side.

1. Introduction

1.1 Micropollutants in the environment

Contamination of the aquatic environment poses a risk to human and environmental health. Anthropogenic chemicals such as pharmaceuticals, industrial chemicals, and pesticides mainly contribute to the contamination through various routes (Yang et al., 2022). Chemicals can be released into the aquatic environment via effluent from wastewater treatment plants (WWTP) (Loos et al., 2013; Alygizakis et al., 2019; Gago-Ferrero et al., 2020), or agricultural and road runoff during rain events (Leu et al., 2004; Halbach et al., 2021; Crawford et al., 2022). The released chemicals into the environment would constitute complex mixtures of individual chemicals at very low concentrations, often below the limit of detection. These micropollutants can cause toxicity via diverse modes of action (MOA), ranging from baseline toxicity to specific toxicity (Verhaar et al., 1992; Escher and Hermens, 2002). Many bioassays have been already applied for water quality assessment targeting diverse endpoints relevant for human and environmental health (Escher et al., 2021). However, some toxicity endpoints such as neurotoxicity are only covered to a limited extent despite a raising concern for associated adverse effects (Legradi et al., 2018).

The bioassay results can be linked with chemical analysis via iceberg modelling (Escher, 2020). While individual chemicals contained in the environmental samples can be identified and quantified based on chemical analysis, bioassays can be used to assess mixture effects by covering detected chemicals as well as the chemicals that are below the detection limit or transformation products. Hence, the iceberg modelling approach has been used to explain the mixture effects from environmental samples using bioassays and chemical analysis in a complementary way (Neale et al., 2020; Escher et al., 2021). The iceberg modelling can evaluate how much of measured effects of environmental mixture can be explained by detected chemicals with effect measurement as shown in Figure 1. Bioanalytical equivalent concentrations BEQ_{bio} are derived by measuring mixture effects with bioanalysis and can capture entire mixture effects. This can be partially explained by BEQ_{chem}, which predicts the mixture effects considering effect concentrations and detected concentrations of individual chemicals. By comparing these two BEQs, we can identify potential toxicity drivers and evaluate how much of the observed effects are driven by unknown chemicals.

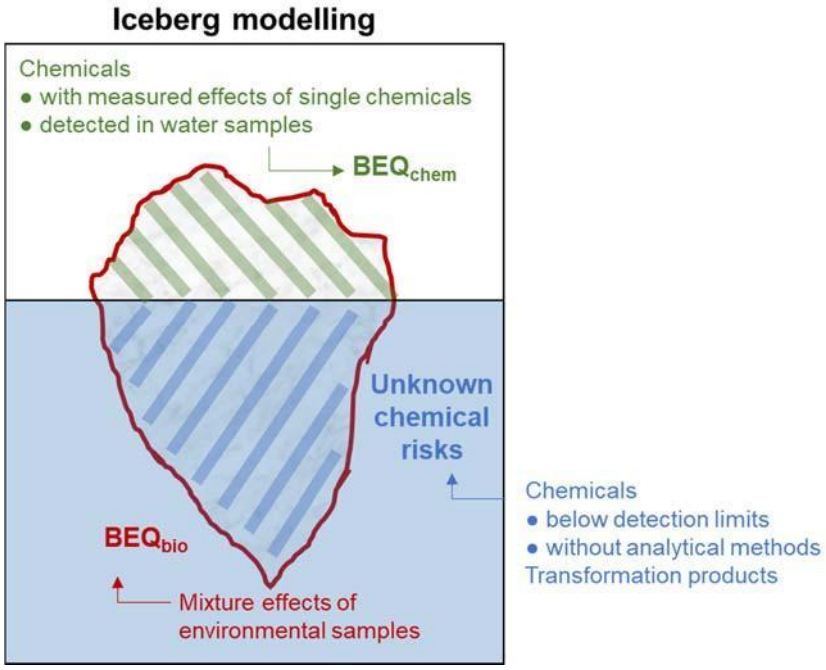

Figure 1: Iceberg modelling approach based on bioassays and chemical analysis (figure adapted from Escher et al. (2021)). Bioanalytical equivalent concentrations BEQ_{chem} estimate risk driven by detected chemicals with known effects, which is just the tip of iceberg. BEQ_{bio} can be derived by testing environmental samples in bioassays and capture not only the known risk BEQ_{chem} but also unknown chemical risks.

1.2 Baseline toxicity

Baseline toxicity (also called narcosis) is a nonspecific MOA of chemicals and caused by membrane intercalation of chemicals. Baseline toxicity represents the minimal level of toxicity, hence chemicals with specific MOAs would elicit toxic effects at lower exposure concentrations compared to concentrations that cause baseline toxicity. Baseline toxicity can be measured based on cytotoxicity caused by baseline toxicity. Since hydrophobic chemicals can intercalate the membrane more easily, baseline cytotoxicity can occur at lower nominal concentration for more hydrophobic chemicals. However, concentration of chemicals in the membrane leading to 10% baseline cytotoxicity, i.e., critical membrane burden (CMB), was found to be constant irrespectively of the test system used. For instance, a constant level of 69 $mmol \cdot L_{lip}^{-1}$ was found in eight reporter gene cell lines (Escher et al., 2019).

Quantitative structure-activity relationships (QSAR) have been established to predict nominal concentrations causing baseline cytotoxicity in human and mammalian cell lines but also in aquatic organisms. The nominal concentrations for baseline toxicity can be described by hydrophobicity of chemicals, e.g., liposome-water partition constants ($K_{lip/w}$). QSAR equations for baseline toxicity have been developed for eight reporter gene cell lines with $K_{lip/w}$ as a hydrophobicity descriptor (Escher et al., 2019). Since the existing QSARs for *in vitro* assays were established based on neutral and hydrophilic chemicals ($0.5 < \log K_{lip/w} < 4.5$), they could not be applied to charged and more hydrophobic organic chemicals. This necessitates the development of an improved prediction model for baseline toxicity which is applicable for wide variety of chemicals.

By comparing predicted baseline toxicity level with observed toxicity level, we can identify whether chemicals just act via baseline toxicity or more specific MOAs. Such approach has been already applied based on toxic ratio (TR), the ratio between baseline toxicity and experimental cytotoxicity. TR is a measure for involvement of specific MOAs in cytotoxicity of chemicals (Verhaar et al., 1992; Maeder et al., 2004).

1.3 Neurotoxicity

Neurotoxicity represents adverse effects on nervous system of organisms. But in a narrow sense, neurotoxicity only refers to so-called adult neurotoxicity, which is the adverse effects on already differentiated nervous system. More sensitive neurotoxicity can occur from early life exposure. Exposure to toxicants at early life stage can lead to irreversible and life-long damage in the developing nervous system, which is called developmental neurotoxicity (DNT). Current testing guidelines for neurotoxicity with regulatory purposes require assessment in *in vivo* system, which is time- and resource-intensive. For example, OECD technical guideline 424 and 426 evaluates neurobehavioural and neuropathological effects of chemicals in adult rats or after in utero exposure.

1.3.1 Neurite outgrowth: an endpoint for developmental neurotoxicity

Development of the nervous system is a complex process, and several fundamental neurodevelopmental processes are essential for the development: proliferation, migration, differentiation, apoptosis, network formation and function (Aschner et al., 2017; Bal-Price et al., 2018). Many epidemiological studies reported the potential adverse effects of developmental neurotoxicants, which may impair learning, memory, and cognitive functions and cause neurodevelopmental disorders (Grandjean and Landrigan, 2014). Diverse environmental chemicals such as pesticides and industrial chemicals have been reported to cause DNT (Grandjean and Landrigan, 2006; Bjorling-Poulsen et al., 2008) and various MOAs involved in DNT have been suggested. Due to the limited mechanistic information and diversity in molecular initiating events (MIE) for DNT, the key neurodevelopmental processes that may capture various MIEs have been considered as endpoints for testing DNT of chemicals (Lein et al., 2005; Smirnova et al., 2014; Bal-Price et al., 2015). Especially, neurite outgrowth is crucial for connectivity of neural network and its function and has been used as an endpoint in screening research for potential DNT chemicals (Ryan et al., 2016; Delp et al., 2018).

1.3.2 Challenges in testing effects on neurite outgrowth

Since neurite outgrowth is an apical phenotype, its inhibition can be caused by secondary effects of cytotoxicity. Therefore, specificity assessment is necessary to discriminate DNT-specific

effects from general cytotoxicity (Aschner et al., 2017; Bal-Price et al., 2018). In previous studies using neurite outgrowth assays, specificity of the DNT effects has been quantified based on the ratio between effect concentrations or benchmark concentrations for neurite outgrowth inhibition and cytotoxicity (Ryan et al., 2016; Delp et al., 2018). Despite the raising concern, DNT was assessed only for the limited number of chemicals, hence identification of specific DNT among environmental pollutants is even more of a knowledge gap.

Another specificity measure exists, which quantifies specificity of DNT by comparing the observed DNT effects with cytotoxicity in non-neuronal cells (Delp et al., 2021). This neuronal-specificity can evaluate the degree of toxicity that occurs specifically in neuronal cells. However, it is questionable, which cell model could be considered as non-neuronal cells since availability of targets would differ between cell types, which may impact the degree of responses. In this regard, baseline toxicity can be used to refine this approach since it is nonspecific toxicity independent of cell type. Another possible advantage of this approach would be that it enables to identify whether the observed effects are driven by specific MOAs of chemicals or merely baseline toxicity arising from their hydrophobicity. For instance, certain pesticides have been discussed to cause DNT but many of them are also highly hydrophobic. Hence the observed low effect concentration may be mainly driven by baseline toxicity. Therefore, this additional specificity measure can help to investigate further details of observed DNT effects.

While DNT *in vitro* testing battery was already well established for testing of single chemicals (Masjosthusmann et al., 2020), high-throughput screening tools for environmental monitoring are still lacking (Legradi et al., 2018). Since the neurite outgrowth assay showed relatively sensitive responses among the key DNT endpoints and the assay duration is shorter compared to other DNT endpoints (Masjosthusmann et al., 2020), it is suitable as a candidate high-throughput tool for testing environmental samples.

1.3.3 Acetylcholinesterase inhibition: an endpoint for adult neurotoxicity

Neuronal cells play an important role in communication between cells and information-storage. The communication involves two processes: nerve impulse and neurotransmission. Nerve impulse is mediated by electrochemical potential generated along the membrane of a neuron. When the nerve impulse reaches at the synapse, messenger chemicals, i.e., neurotransmitters, are released into synaptic cleft and deliver the signal to postsynaptic neurons. These communication

processes can be hindered by diverse chemicals that target specific sites in nervous system (Casida, 2009; Lushchak et al., 2018). Previously, 16 different neurotoxicity mechanisms were identified from hundreds of chemicals detected in three European river catchments (Legradi et al., 2018). Especially, the highest hazard quotient was observed for acetylcholinesterase (AChE) inhibition considering both detected concentrations and effect concentrations for relevant chemicals. AChE is an enzyme that breaks down the neurotransmitter acetylcholine (ACh) and modulates the neurotransmission. Chemicals with affinity to the active site of AChE can reduce its activity, which could disrupt the neurotransmission and lead to acute toxicity in organisms (Pohanka, 2011; Čolović et al., 2013).

1.3.4 Challenges in AChE inhibition assays

Diverse AChE inhibition assays have been already well established and applied for screening the inhibitory potency of chemicals and even environmental samples. Inhibition in AChE activity was screened for chemicals in Tox21 program using purified enzyme, neural stem cells, and human neuroblastoma SH-SY5Y cells (Li et al., 2021). This study revealed that approximately 2.25% of 8,312 chemicals can have inhibitory potency on AChE. For environmental monitoring, the purified enzyme-based assay has been widely applied to assess inhibition of AChE activity by micropollutants in water samples considering its simplicity (Hamers et al., 2000; Molica et al., 2005; Escher et al., 2009; Macova et al., 2011).

A limitation of the purified enzyme-based AChE inhibition assay is the reduced sensitivity due to natural organic matter contained in environmental sample extracts. During extraction of environmental samples, a small fraction of natural organic matter such as dissolved organic carbon (DOC) can be co-extracted with the micropollutants, and this might lead to interferences with the AChE inhibition assay. Such matrix effects were observed for diverse water samples in the purified enzyme-based AChE inhibition assay, which was supported by the observation of suppressed AChE inhibition after co-exposure to DOC and an AChE inhibitor (Neale and Escher, 2013). This disturbance by DOC was not observed in several cell-based bioassays, which could be explained by intracellular localization of target sites (Neale 2014). Since AChE are anchored to outer side of cell membrane or localized in the cytoplasm in neuronal cells (Thullbery et al., 2005; Hicks et al., 2013), the direct interaction between DOC and AChE could potentially be avoided in a cell-based AChE inhibition assay.

1.4 Aim and approach of this thesis

The goal of this thesis was to implement high-throughput screening tools for testing neurotoxicity of environmental samples. Two neurotoxicity endpoints, inhibition of neurite outgrowth and AChE, were mainly discussed as potential endpoints for environmental monitoring of neurotoxicity. Baseline toxicity would be additionally investigated to measure specificity of the observed toxic effects. Therefore, multiple endpoints will be covered in this thesis: cytotoxicity (including baseline cytotoxicity), neurite outgrowth inhibition, and AChE inhibition (Figure 2).

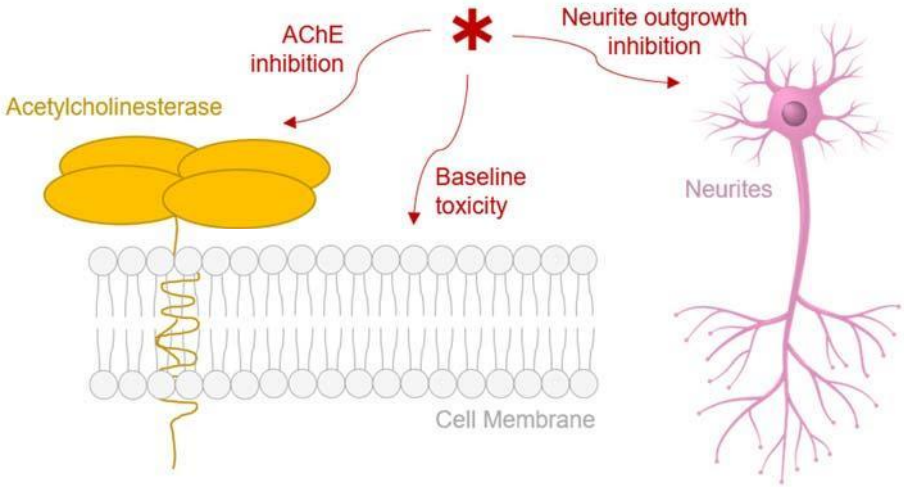

Figure 2: Baseline toxicity, acetylcholinesterase (AChE) inhibition, and neurite outgrowth inhibition.

The outline of the thesis and associated publications is shown in Figure 3. In order to support assessment of specificity of DNT compared to baseline toxicity, baseline toxicity needs to be predicted for individual chemicals. Existing prediction models for baseline toxicity are only applicable for neutral chemicals with limited hydrophobicity (Escher et al., 2019), hence *Publication I* aimed to develop an improved predictive model for baseline toxicity with wider applicability.

The existing test method for neurite outgrowth was mainly designed for testing single chemicals with low- or medium-throughput method, hence it is not proper to apply as a high-throughput screening tool for testing environmental samples. *Publication II* and *III* aimed to

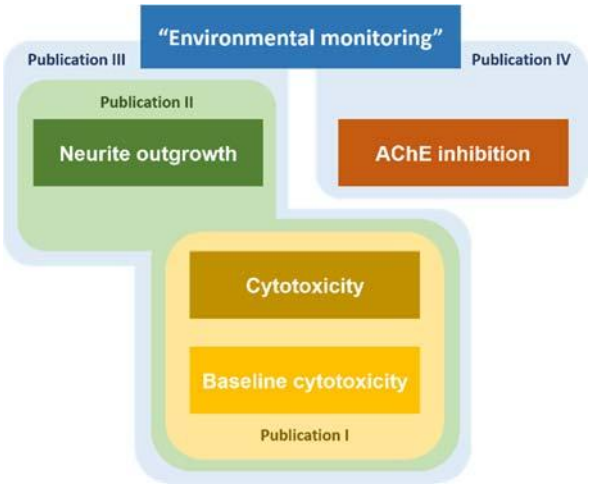

Figure 3: Outline of this thesis.

develop or optimize the assays for testing neurotoxicity of not only single chemicals but also environmental samples. In *Publication II*, diverse environmental chemicals with potential DNT (e.g., pesticides) and high environmental relevance were to be assessed for their effects on neurite outgrowth and cytotoxicity. Since hydrophobic chemicals can cause neurotoxicity in a nonspecific manner via baseline toxicity, it was investigated whether the neurite outgrowth inhibition and cytotoxicity in neuronal cells are driven by baseline toxicity or other specific MOAs using the proposed prediction tool for baseline toxicity from *Publication I*. Furthermore, enhanced toxicity on neurite outgrowth and cytotoxicity compared to baseline toxicity was explored using different specificity measures. The neurite outgrowth assays have not been applied to environmental mixtures and thus its applicability should be investigated. Therefore, *Publication III* aimed to compare the responses from different types of water samples in neurite outgrowth assay. The observed mixture effects were investigated based on measured effects from single chemicals to identify which chemicals contribute to the mixture effects in the environment using the iceberg modelling approach.

Since the purified enzyme-based AChE inhibition assay is not suitable for testing environmental samples due to disturbance by DOC (Neale and Escher, 2013), it should be investigated whether AChE inhibition in the cell-based assay could avoid this impact by DOC. AChE inhibition assay using SH-SY5Y cells has been already used for testing single chemicals (Li et al., 2021), but the used assay condition was not proper to evaluate AChE inhibition precisely (e.g., short exposure duration) and needs to be optimized to improve assay quality and

performance. Therefore, *Publication IV* aimed to optimize the AChE inhibition assay to be applicable for testing single chemicals as well as environmental samples. Additionally, volatility of well-known AChE inhibitors was predicted to be high, hence the chemical loss of the AChE inhibitors was further investigated in the AChE inhibition assay.

2. Baseline toxicity

2.1 Mass balance model to predict nominal baseline toxicity

Baseline toxicity is mediated by intercalation of chemicals with membranes and can be predicted based on hydrophobicity of chemicals. Previous baseline toxicity QSARs were established for neutral chemicals with limited hydrophobicity (Escher et al., 2019). To expand the applicability of baseline QSAR in terms of speciation and hydrophobicity of chemicals, the concept of critical membrane burden (CMB) was considered since the CMB is known to be constant independently of speciation and hydrophobicity of chemicals (van Wezel and Opperhuizen, 1995; Escher et al., 2002; Escher et al., 2017; Klüver et al., 2019). The CMB is also similar across various cell types (Escher et al., 2002; Escher et al., 2019) and various aquatic species (van Wezel and Opperhuizen, 1995; Escher et al., 2011). The uniform CMB can be converted into chemical concentration in the medium, i.e., nominal concentration causing 10% baseline cytotoxicity ($IC_{10,baseline}$) in a given cellular assay using a mass balance model (MBM) as outlined in Figure 4. A MBM describes distribution of test chemicals between protein, lipid, and water compartment of medium and cells in bioassays using partition constants (Fischer et al., 2017). Liposome and bovine serum albumin (BSA) serve as surrogates for lipids and proteins in bioassays, respectively. The baseline toxicity QSAR was proposed for differentiated human neuroblastoma SH-SY5Y cells for subsequent application to neurotoxicity in the following chapters and additionally for three reporter gene cell lines (ARE, AhR, and PPARγ), which can be found in *Publication I*.

Multiple input parameters from chemicals as well as cells and medium were required to establish a MBM for baseline toxicity. In case of chemicals, two partition constants that describe chemical distribution between liposome and water ($K_{lip/w}$) and between protein and water ($K_{BSA/w}$) were needed, which can be either experimentally determined or predicted. To unify the input parameters from chemicals, a linear relationship was derived to connect the two partition constants $K_{lip/w}$ and $K_{BSA/w}$ based on published QSARs (Endo et al., 2011; Endo and Goss, 2011). This linear relationship was verified for neutral chemicals and further for ionizable chemicals with experimental distribution ratios $D_{BSA/w}$(pH 7.4) and $D_{lip/w}$(pH 7.4), which are the partition constants that considered speciation of chemicals. The experimental values $D_{BSA/w}$(pH 7.4) and $D_{lip/w}$(pH 7.4) aligned well with the linear relationship derived from the published QSARs for

neutral chemicals, bases, and multiprotic chemicals but those of anionic chemicals highly deviated (Figure 2 in *Publication I*). For the chemicals, for which the linear relationship between $K_{lip/w}$ and $K_{BSA/w}$ holds, the MBM for baseline toxicity could only requires $D_{lip/w}$(pH 7.4) as an input parameter from chemicals. In case of the input parameters from cells and media, the protein, lipid, and water contents in cells and media were retrieved from literature or newly determined for each bioassay (Table 1 in *Publication I*; Escher et al. (2019)) to derive bioassay-specific models for the four mammalian cell lines (SH-SY5Y, ARE, AhR, and PPARγ). This resulted in the simulation in Figure 4 and $IC_{10,baseline}$ could be predicted merely from the log $D_{lip/w}$(pH 7.4) of individual chemicals.

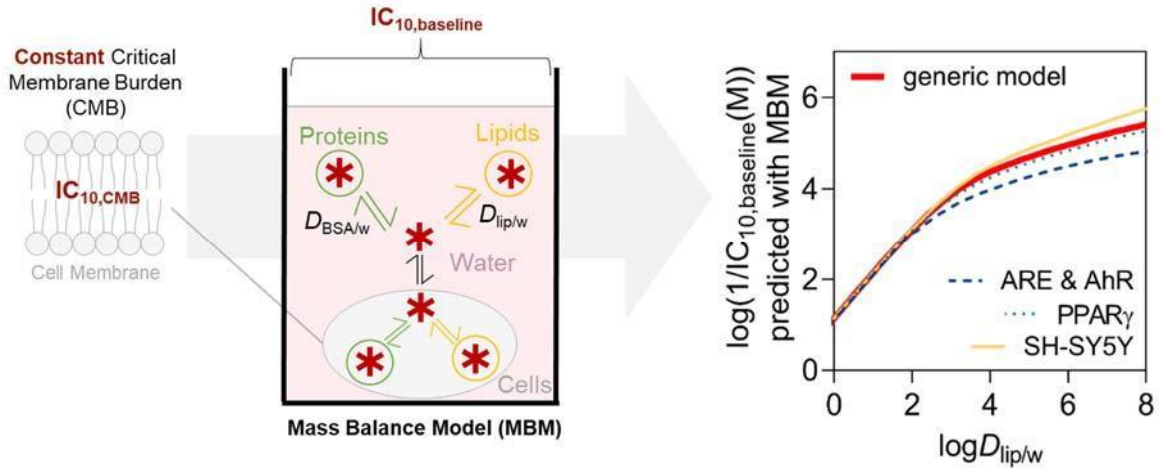

Figure 4: Critical membrane burden (CMB) was used to derive the nominal concentration that would lead to 10% baseline cytotoxicity ($IC_{10,baseline}$) using a mass balance model (MBM) as described in *Publication I*. The MBM describes distribution of a chemical (✱) between the protein, lipid, and water compartment of medium and cells. The MBM for $IC_{10,baseline}$ was simulated based on log $D_{lip/w}$(pH 7.4) for four bioassays and generic condition. Chemical partitioning to plastic of well plates was considered as is negligible (Fischer et al., 2018). This MBM is not suitable for chemicals that can highly partition into the air (Escher et al., 2019).

2.2 Bioassay-specific baseline toxicity QSAR

The reverse of logarithmic effect concentrations represents the degree of toxicity and the log ($1/IC_{10,baseline}$) increased with increasing log $D_{lip/w}$(pH 7.4), i.e., hydrophobicity of chemicals. This means hydrophobic chemicals can provoke baseline toxicity at lower exposure concentration due to their high membrane affinity. The relationship started to level off at log $D_{lip/w}$(pH 7.4) around 2 and the curve flattened the most for the assays whose medium had the highest protein and lipid content (AREc32 and AhR-CALUX supplemented with 10% FBS). $IC_{10,baseline}$ was lower for PPARγ-BLA, whose medium is only supplemented with 2% FBS, which was followed by SH-SY5Y cells with low protein and negligible lipid content of their medium. In the bioassays with medium containing less protein and lipid contents, bioavailable portion of chemicals would be higher due to less sorption to the biomolecules in the medium, hence the CMB can be reached with smaller amount of chemicals, which results in lower $IC_{10,baseline}$.

Despite the single input parameter, the original equation for baseline toxicity MBM was rather complex (eq. 18 in *Publication I*). Therefore, an exponential fit equation was derived for each bioassay for practical applications, which was visually identical with the original equation. The baseline toxicity QSAR for SH-SY5Y cells is given in eq. 1, and bioassay-specific models for the other three cell lines can be found in *Publication I* (Table 2 and eq. 19 in *Publication I*). Based on the similarity of the bioassay-specific models, a generic model for baseline toxicity can be proposed by averaging medium and cell composition of the four cell lines, which can be used to predict baseline toxicity of chemicals in any adherent cell lines even when protein and lipid contents of the cells and the medium have not been quantified.

$$\log(1/IC_{10,baseline}(M)) = 1.26+5.63\times\left(1-e^{-0.202 \log D_{lip/w}}\right) \quad (1)$$

When the bioassay-specific models were compared with experimental cytotoxicity from 392 chemicals with diverse hydrophobicity and speciation, experimental cytotoxicity IC_{10} aligned well with the baseline toxicity QSAR (Figure 5A-C in *Publication I*). Also, known baseline toxicants were classified as baseline toxicants in all four bioassays, having the ratio between $IC_{10,baseline}$ and IC_{10} , i.e., toxic ratio (TR) less than 10 (Verhaar et al., 1992; Maeder et

al., 2004). The alignment of experimental cytotoxicity along the baseline toxicity QSARs and verification using known baseline toxicants demonstrated the validity of the proposed baseline toxicity QSAR. Even organic acids aligned well with the QSAR (Figure 5C in *Publication I*) although the linear relationship between $K_{lip/w}$ and $K_{BSA/w}$ was not satisfied for organic acids. Therefore, the proposed baseline toxicity QSAR is applicable for chemicals with broad range of hydrophobicity and speciation, but more reliable prediction model might be required for organic acids. The derived models for baseline toxicity can be applied to investigate whether chemicals act on target endpoints via specific MOAs or merely via baseline toxicity arising from hydrophobicity. The baseline toxicity QSAR for SH-SY5Y cells (eq. 1) will be used for this specificity analysis of observed effects in neurotoxicity assays in the following chapters.

3. Neurotoxicity

3.1 Neurite outgrowth inhibition and cytotoxicity

3.1.1 Method development

In vitro models and assay condition were optimized to develop an assay for evaluating effects on neurite outgrowth and cytotoxicity of single chemicals and environmental samples. For routine environmental monitoring, high-throughput method is required for testing many samples (Escher et al., 2021), hence the cellular assay was established in 384-well plate format. Human neuroblastoma SH-SY5Y cells and Lund human mesencephalic (LUHMES) cells were considered as candidate *in vitro* models for the assay. While LUHMES cells are mainly used in neurite outgrowth assay in the current DNT *in vitro* battery (Masjosthusmann et al., 2020), poly-L-ornithine/fibronectin-coated plates were required for LUHMES cells and the plates had to be coated manually, which could result in inconsistent quality of test plates. SH-SY5Y cells enabled high-throughput screening due to their easier maintenance and availability of commercial 384-well plates with appropriate coating for adherence of cells. Therefore, SH-SY5Y cells were selected for screening effects on neurite outgrowth in this thesis. SH-SY5Y cells were differentiated with retinoic acid for the assay since more mature neuron-like characteristics and longer neurites can be achieved after differentiation (Biedler et al., 1973; Påhlman et al., 1984; de Medeiros et al., 2019). Experimental procedure is outlined in Figure 5 and the detailed protocol of the neurite outgrowth assay can be found in *Publication II*. The effect concentrations leading to 10% reduction in cell viability (IC_{10}) and neurite length (EC_{10}) were experimentally determined in differentiated SH-SY5Y cells using image analysis.

3.1.2 Chemical selection criteria

Diverse chemicals were selected to assess their effects on neurite outgrowth and cytotoxicity. Potential DNT chemicals based on literature were selected in *Publication II* and chemicals that occurred in water samples with possible DNT were tested in *Publication III*. Endpoint-specific controls are highly specific positive controls for neurite outgrowth (Krug et al., 2013; Aschner et al., 2017). Four organic endpoint-specific controls were tested: including narciclasine, colchicine, cycloheximide, and rotenone. Six established baseline toxicants (Vaes et al., 1998) were applied as negative controls. Since pesticides have been reported to cause DNT (Grandjean

and Landrigan, 2006), pesticides from diverse MOA classes were also investigated for their effects on cell viability and neurite outgrowth: acetylcholinesterase (AChE) inhibitors, nicotinic acetylcholine receptor (nAChR) agonists, γ-aminobutyric acid (GABA)-gated chloride channel blockers, voltage-gated sodium channel agonists, mitochondrial toxicants, and redox cyclers. Furthermore, the U.S. National Toxicology Program (NTP) provided a proof-of-concept chemical library (Behl et al., 2019) for testing neurotoxicity and DNT, and some chemicals from this NTP library were additionally tested for comparison: polycyclic aromatic hydrocarbons (PAH), polybrominated diphenyl ethers (PBDE), polychlorinated biphenyls (PCB), and endocrine disrupting chemicals (EDC). Most importantly, environmental chemicals that were detected in water samples and presumed to cause high neurotoxic effects were also included as test chemicals (detailed selection strategy in method section and Figure S1 in *Publication III*).

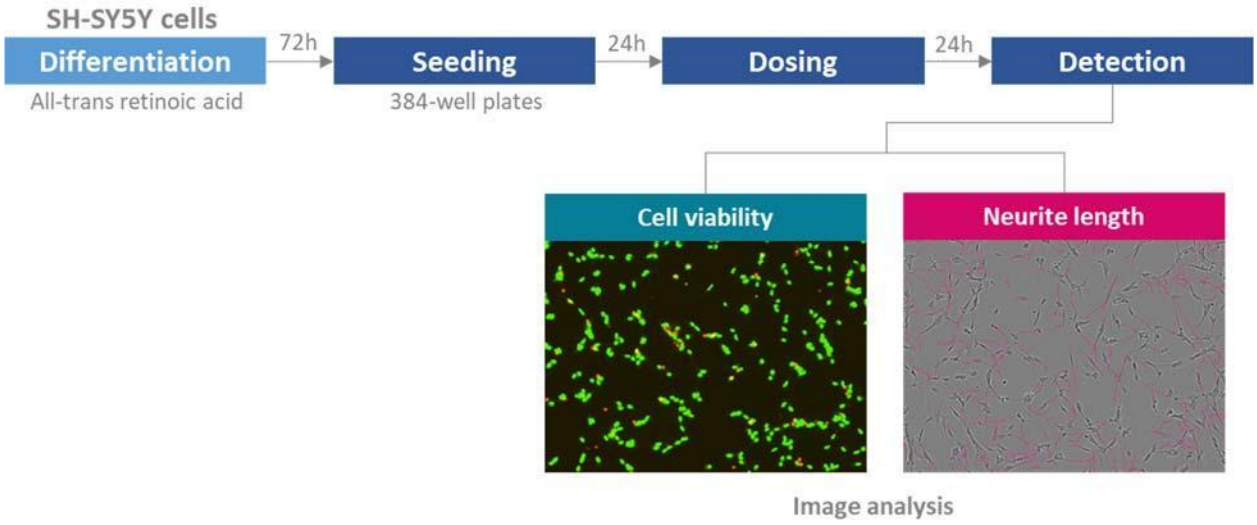

Figure 5: Experimental procedure of neurite outgrowth assay using differentiated SH-SY5Y cells. Effects of single chemicals or environmental samples were tested in 384-well plates for 24 h and cytotoxicity (IC_{10}), and neurite outgrowth inhibition (EC_{10}) were measured using image analysis.

3.1.3 Specificity of effects compared to baseline toxicity

Chemicals with potential DNT are often hydrophobic, such as some pesticides and PCBs (Grandjean and Landrigan, 2006). Hydrophobic chemicals can elicit toxicity at low nominal concentration, but the toxicity may occur from baseline toxicity due to their hydrophobicity rather than from specific MOAs of the chemicals. Hence it was investigated whether toxicity of

potential DNT chemicals was driven by specific MOAs or just by baseline toxicity. To compare baseline toxicity level with observed effect level, cytotoxicity IC_{10} and neurite outgrowth inhibition EC_{10} were measured for the test chemicals in neurite outgrowth assay using SH-SY5Y cells. Baseline cytotoxicity ($IC_{10,baseline}$) was predicted from $D_{lip/w}$(pH 7.4) using the baseline QSAR developed for differentiated SH-SY5Y cells as outlined in the previous chapter. By comparing the effect concentrations, toxic ratio TR and specificity ratios SR were derived as specificity measures of chemicals (Maeder et al., 2004; Escher et al., 2020) as visualized in Figure 6.

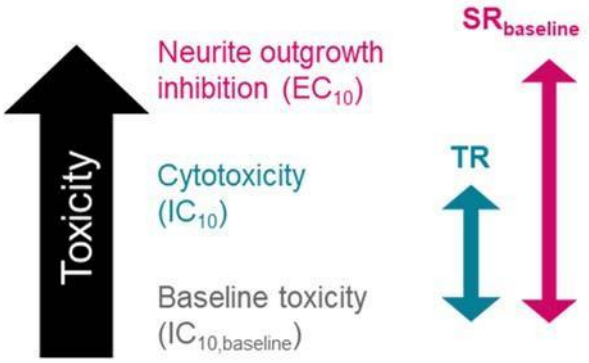

Figure 6: Baseline cytotoxicity ($IC_{10,baseline}$), cytotoxicity (IC_{10}), and neurite outgrowth inhibition (EC_{10}) were predicted or measured in SH-SY5Y cells. The effect concentrations were used to calculate toxic ratio (TR) and specificity ratio (SR), which quantify specificity of the observed effects.

Since baseline toxicity is the minimal toxicity, any enhanced cytotoxicity observed above the baseline toxicity would mean that the chemicals can act through specific MOAs (including also reactive and uncoupling). To quantify the enhanced level, toxic ratios (TR; eq. 2) can be calculated based on the ratio between experimental cytotoxicity IC_{10} and predicted baseline cytotoxicity $IC_{10,baseline}$ (Verhaar et al., 1992; Maeder et al., 2004). Typically, chemicals with $0.1 < TR < 10$ are considered as baseline cytotoxicants while those with $TR > 10$ indicate that the chemicals can cause cytotoxicity via specific MOAs.

$$TR = \frac{IC_{10,baseline}}{IC_{10}} \quad (2)$$

Analogously, $SR_{baseline}$ (eq. 3) was calculated to quantify how specifically chemicals can act on neurite outgrowth compared to predicted baseline toxicity. It enables to identify whether specific MOAs other than baseline toxicity contribute to the observed effects on neurite outgrowth. Since baseline toxicity is independent of cell type, $SR_{baseline}$ can quantify any enhanced toxicity in neuronal cells compared to the nonspecific toxicity (Delp et al., 2021). In line with the definitions by Escher et al. (2020), the effects were considered as "neuronal-specific" toxicity when $SR_{baseline} > 10$.

$$SR_{baseline} = \frac{IC_{10,baseline}}{EC_{10}} \quad (3)$$

Most of the hydrophobic chemicals (log $D_{lip/w} > 4$) were classified as baseline toxicants, which means that the hydrophobic chemicals caused both cytotoxicity and neurite outgrowth inhibition via baseline toxicity (Figure 7). Considering higher TR and $SR_{baseline}$ that were observed for more hydrophilic chemicals (log $D_{lip/w} < 4$), hydrophilic chemicals were more likely to act through specific MOAs and show enhanced toxicity on both cell viability and neurite outgrowth compared to baseline toxicity. The enhanced toxicity on cell viability and neurite outgrowth was distinct for endpoint-specific controls. Excess toxicity was also observed for some pesticides and pharmaceuticals, indicating and/or confirming the specificity of their MOAs. In contrast, highly hydrophobic chemicals with log $D_{lip/w} > 4$ (e.g., 4 PAHs, 3 PBDEs, 5 PCBs, and some pesticides) did not show excess toxicity or even inactive up to $IC_{10, baseline}$. Although many hydrophobic chemicals triggered toxicity in a nonspecific manner, they were highly potent considering their IC_{10} and EC_{10}, which were as low as those for some chemicals with highly enhanced toxicity. Our results agree well with the previous observation that highly hydrophobic chemicals elicit strong toxic effects but act through baseline toxicity (Escher and Hermens, 2002). However, neurite outgrowth is only one of many DNT endpoints and may not capture all potential DNT driven by a chemical. Thus, it is possible that DNT of pesticides is not mediated by neurite outgrowth inhibition and hence, their effects on other DNT endpoints should be further investigated.

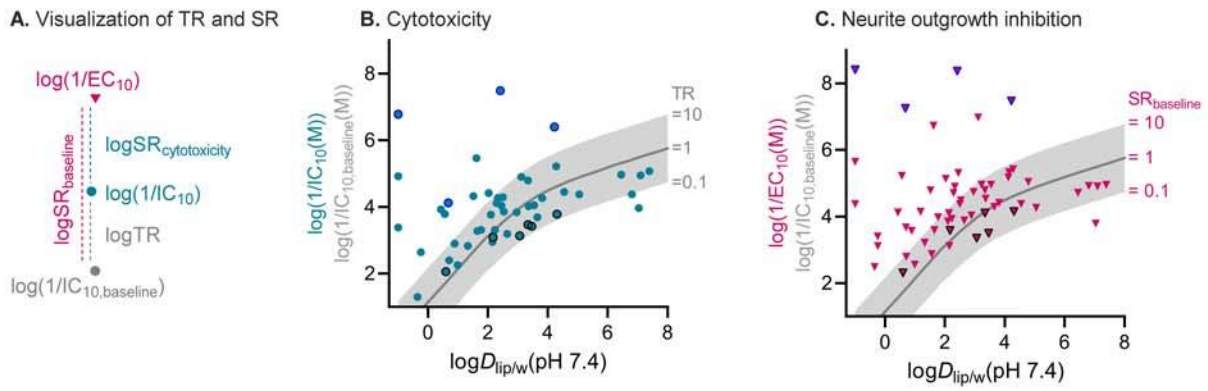

Figure 7: Effect concentrations for cytotoxicity and neurite outgrowth inhibition in differentiated SH-SY5Y cells against hydrophobicity of test chemicals as described in *Publication II*. (A) Visualization of the toxic ratio TR as well as the specificity ratios $SR_{cytotoxicity}$ and $SR_{baseline}$. (B) Cytotoxicity as a function of the hydrophobicity expressed as liposome-water partition constants ($D_{lip/w}$). The turquoise circles indicate the experimental inhibitory concentration for cytotoxicity (IC_{10}). (C) Neurite outgrowth inhibition as a function of $D_{lip/w}$. Magenta triangles indicate concentration leading to 10% reduction in neurite length (EC_{10}). In both plots (B) and (C), endpoint-specific controls were encircled in blue and known baseline toxicants were encircled in black. Thick grey lines correspond to predicted baseline toxicity causing 10% cytotoxicity ($IC_{10,baseline}$) as a function of $D_{lip/w}$. The grey areas indicate when TR or $SR_{baseline}$ is between 0.1 and 10.

3.1.4 Neurite-specific environmental pollutants and their modes of action

While neuronal-specific chemicals can cause enhanced toxicity compared to baseline toxicity, it is still questionable whether chemicals have specific MOAs that only target neurite outgrowth or rather inhibit neurite outgrowth secondarily via cytotoxicity. Therefore, another specificity measure $SR_{cytotoxicity}$ (eq. 4) can be used to quantify specific effects on neurite outgrowth compared to measured cytotoxicity, which has been already applied for DNT assessment (Krug et al., 2013; Delp et al., 2018). Chemicals with $SR_{cytotoxicity} > 4$ were considered as "neurite-specific" according to Krug et al. (2013) and the validity of threshold was confirmed based on independent calculation in our test system using SH-SY5Y cells.

$$SR_{cytotoxicity} = \frac{IC_{10}}{EC_{10}} \quad (4)$$

To verify the threshold based on experimental values, endpoint-specific controls and baseline toxicants were considered. All four endpoint-specific controls (narciclasine, colchicine, cycloheximide, and rotenone) showed neurite-specific effects, and narciclasine was selected as an assay positive control considering its highest potency. In addition, all six confirmed baseline toxicants did not show neurite-specific effects but an exception was provided by 4-chloro-3-methylphenol whose $SR_{cytotoxicity}$ was 4.3, just above the threshold. This chemical can be considered as nonspecific considering its standard error, hence the chemicals close to the threshold must be regarded with caution.

Among all the tested chemicals, 20 neurite-specific chemicals were identified as neurite-specific chemicals. The neurite-specific chemicals were highly diverse, ranging from pesticides to industrial chemicals. More than half of the neurite-specific chemicals were pesticides such as AChE inhibitors, redox cyclers, and mitochondrial toxicants. It was noteworthy that 9 neurite-specific chemicals had known or potential AChE inhibitory potency and 3-hydroxycarbofuran showed the highest $SR_{cytotoxicity}$ among the AChE inhibitors. Reversible AChE inhibitors were more likely to show more neurite-specific effects than irreversible AChE inhibitors, whose $SR_{cytotoxicity}$ were just above the threshold.

All tested chemicals were plotted together based on their $SR_{cytotoxicity}$ and $SR_{baseline}$ to visualize neurite- and neuronal-specific toxicity (Figure 8). Highly neurite-specific effects were more likely to be accompanied by the neuronal-specific effects and specificity of effects was rather low for only neurite-specific chemicals. Only neuronal-specific effects were observed for 4 chemicals (clarithromycin, 2-naphthalene sulfonic acid, citalopram, and roxithromycin), which indicates that there exist specific MOAs for these chemicals that are not specific for neurite outgrowth and rather generally affect the cells. Since the mechanistic understanding is limited for DNT, potential MOAs of the test chemicals leading to the neurite-specific effects were assigned. The neurite-specific chemicals were marked in different colors according to their MOAs potentially relevant to the effects on neurite outgrowth in SH-SY5Y cells (Figure 8B). The details of uses, MOAs, and $SR_{cytotoxicity}$ for neurite-specific chemicals are given in Table 1.

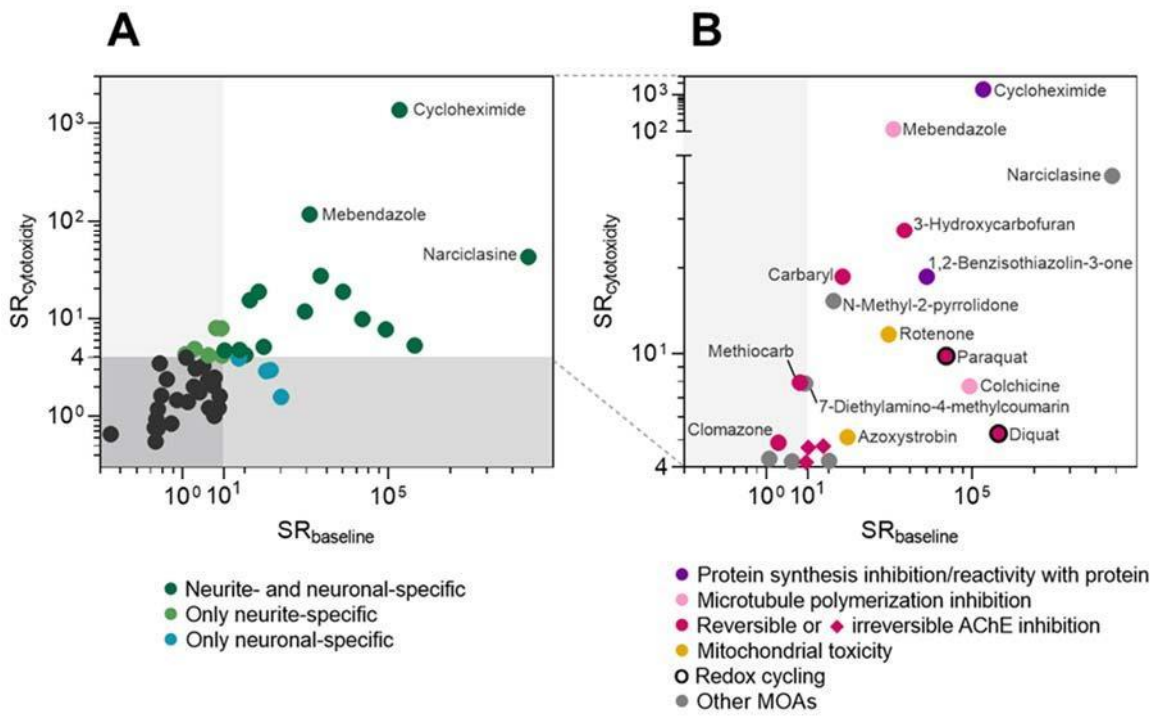

Figure 8: Specificity ratios $SR_{cytotoxicity}$ and $SR_{baseline}$ for the tested chemicals as described in *Publication II*. (A) Chemicals grouped based on neurite-specific effects ($SR_{cytotoxicity} > 4$) and neuronal-specific effects ($SR_{baseline} > 10$). (B) Neurite-specific chemicals and their specific modes of action (MOA) that can be linked to effects on neurite outgrowth.

Potential MOAs relevant to neurite-specific effects are relatively well known for the two endpoint-specific controls, narciclasine and colchicine. Narciclasine is known to activate Rho signaling pathway, which can lead to contraction of actomyosin. Colchicine could possibly act on neurite outgrowth via binding to tubulin and inhibiting microtubule polymerization. Another neurite-specific chemical mebendazole, which was detected in water samples, is known to bind to the colchicine-binding site of tubulin and thus could provide additional evidence that inhibition of microtubule polymerization can be related to neurite-specific effects.

Two neurite-specific chemicals had specific MOAs relevant to protein: cycloheximide and 1,2-benzisothiazolin-3-one (BIT). Cycloheximide showed the highest $SR_{cytotoxicity}$ among all tested chemicals and is known to interfere with translocation leading to protein synthesis inhibition. BIT is an electrophile and could react with enzymes or other proteins (Lindner, 2004; Silva et al., 2020), which can be linked to one of the molecular initiating event (MIE) established

for DNT, chemical reactivity to seleno proteins (Spinu et al., 2019). However, the MOAs relevant to proteins appear to trigger rather general toxicity and hence, the direct relationship between the MOAs and the observed DNT effects should be further investigated.

Two mitochondrial toxicants, rotenone and azoxystrobin, showed neurite-specific effects. The degree of specificity differed considerably between rotenone and azoxystrobin, which can be explained by difference in MIE (Delp et al., 2019). In LUHMES cells, it was observed that inhibitors of mitochondrial complex I such as rotenone were more likely to show neurite-specific effects compared to complex III inhibitors such as azoxystrobin, which agrees well with our observation.

Two redox cyclers, which were also expected to affect cells rather in a general way, showed neurite-specific effects with extremely neuronal-specific effects. This indicates that their specific MOAs contributed to neurite-specific effects as well as strongly to cytotoxic effects. Reactive oxygen species (ROS) generated by redox cycling can not only generally affect cell health but also were reported to regulate cytoskeleton dynamics in neuronal cells, which might cause the specific effects on neurite outgrowth (Wilson and Gonzalez-Billault, 2015). Furthermore, there are other specific MOAs reported for diquat and paraquat, such as reversible AChE inhibition (Seto and Shinohara, 1987; Ahmed et al., 2007), and hence it is possible that their effects might be contributed by multiple MOAs.

Six of 21 neurite-specific chemicals are known to inhibit AChE reversibly and their $SR_{cytotoxicity}$ was higher than those from irreversible AChE inhibitors. The role of AChE in neurite outgrowth can be explained by both enzymatic and non-enzymatic way (Grisaru et al., 1999; Paraoanu and Layer, 2008). In enzymatic way, released ACh could bind to AChE of adjacent cells for directing neurite outgrowth. In case of non-enzymatic way, AChE can support the neurite outgrowth via structural interaction with extracellular matrix proteins. However, the difference in specificity between reversible and irreversible AChE inhibitors should be further elucidated and involvement of other specific MOAs should also be taken into account.

For the remaining of neurite-specific chemicals, their underlying MOAs were not clear or the degree of specificity was not very high with low $SR_{cytotoxicity}$. Considering that several chemicals had $SR_{cytotoxicity}$ just above the threshold of 4 including the known baseline toxicant 4-chloro-3-methylphenol, an extended set of chemicals would need to be investigated to improve reliability of the thresholds for $SR_{cytotoxicity}$.

Table 1: Uses, modes of action (MOA), and specificity ratio ($SR_{cytotoxicity}$) for neurite-specific chemicals identified in this thesis.

Chemical name	Uses	MOAs in SH-SY5Y cells[1]	$SR_{cytotoxicity}$[2]
Narciclasine	Natural plant toxins	Activation of Rho signaling pathway	42
Mebendazole	Pharmaceuticals	Microtubule polymerization inhibition	118
Colchicine	Natural plant toxins; pharmaceuticals	Microtubule polymerization inhibition	7.7
Rotenone	Natural plant toxins; pesticides/insecticides (banned)	Mitochondrial complex I inhibition	12
Azoxystrobin	Fungicides	Mitochondrial complex III inhibition	5.1
3-Hydroxycarbofuran	Insecticides (metabolites)	Reversible AChE inhibition	27
Carbaryl	Insecticides	Reversible AChE inhibition	19
Methiocarb	Insecticides	Reversible AChE inhibition	7.9
Paraquat	Herbicides	Reversible AChE inhibition; redox cycling	9.8
Diquat	Herbicides	Reversible AChE inhibition; redox cycling	5.3
Clomazone	Herbicides	(Reversible) AChE inhibition	4.9
Diazoxon	Insecticides (metabolites)	Irreversible AChE inhibition	4.8
Paraoxon-ethyl	Insecticides (metabolites)	Irreversible AChE inhibition	4.7
Chlorpyrifos-oxon	Insecticides (metabolites)	Irreversible AChE inhibition	4.2
1,2-Benzisothiazolin-3-one	Preservatives; antimicrobials	Reactivity with functional groups in proteins	19
Verapamil	Pharmaceuticals	Blocking calcium channels	4.2
Cycloheximide	Natural plant toxins; fungicides	Protein synthesis inhibition	1370
N-Methyl-2-pyrrolidone	Industrial use as solvent	Unknown	15
7-Diethylamino-4-methylcoumarin	Fluorescent dyes	Unknown	7.9
2(4-Morpholinyl)benzothiazole	A vulcanization accelerator in car tires	Unknown	4.2

[1]MOAs relevant to effects on neurite outgrowth in SH-SY5Y cells.

[2]$SR_{cytotoxicity}$ derived from measured cytotoxicity and neurite outgrowth inhibition in SH-SY5Y cells.

3.1.5 Application to environmental samples

The neurite outgrowth assay has not been applied for testing environmental samples. To confirm the applicability of the assay for environmental monitoring and identify major effect drivers in the environment, two types of water samples were investigated. Surface water from small German streams was collected, which has diverse contamination source such as agricultural runoff, street runoff, and combined sewer overflows. Wastewater treatment plant (WWTP) effluents collected across Europe were also considered together. The collected water samples were extracted and enriched to be tested in the bioassays and their effect concentrations were expressed in the unit of relative enrichment factor (REF; $L_{water}/L_{bioassay}$). Mixture effects were measured in SH-SY5Y cells for 85 surface water and 55 WWTP effluent samples. In parallel, the environmental samples were used for chemical analysis to quantify concentrations of single chemicals in individual samples. The detailed sampling, analytical method, and detected concentrations for individual chemicals can be found in *Publication III*.

IC_{10} for cytotoxicity was from REF 2.8 to 147, which means that the samples were enriched 3 to 147 times to cause 10% cytotoxicity (Figure 9A). The EC_{10} for neurite outgrowth inhibition ranged from REF 0.2 to 80 and the effects on neurite outgrowth were observed even when the samples were diluted by a factor of 5. For the samples with similar cytotoxicity, the toxicity on neurite outgrowth tended to be stronger in surface water than in WWTP effluent. The ratio between the two effect concentrations, i.e., $SR_{cytotoxicity}$, was calculated as done for single chemicals but the specific effects observed in the environmental mixtures would be contributed by many chemicals at low concentrations. Overall, surface water showed higher $SR_{cytotoxicity}$ (from 1.8 to 49; median 5.8) than WWTP effluents (from 0.9 to 8.2; median 3.7) as shown in Figure 9B.

While bioassays can capture entire mixture effects, chemical analysis can identify and quantify individual chemicals. Hence, these two methods can complement each other in the iceberg modelling approach to explain the mixture effects (Escher, 2020; Neale et al., 2020). BEQ_{bio} and BEQ_{chem} were derived to explain neurite outgrowth inhibition and expressed in the unit of a reference chemical, i.e., narciclasine, which resulted in narciclasine-EQ_{bio} and narciclasine-EQ_{chem}. The measured mixture effects on neurite outgrowth were converted into narciclasine-EQ_{bio} and compared with narciclasine-EQ_{chem}. Narciclasine-EQ_{chem} was calculated

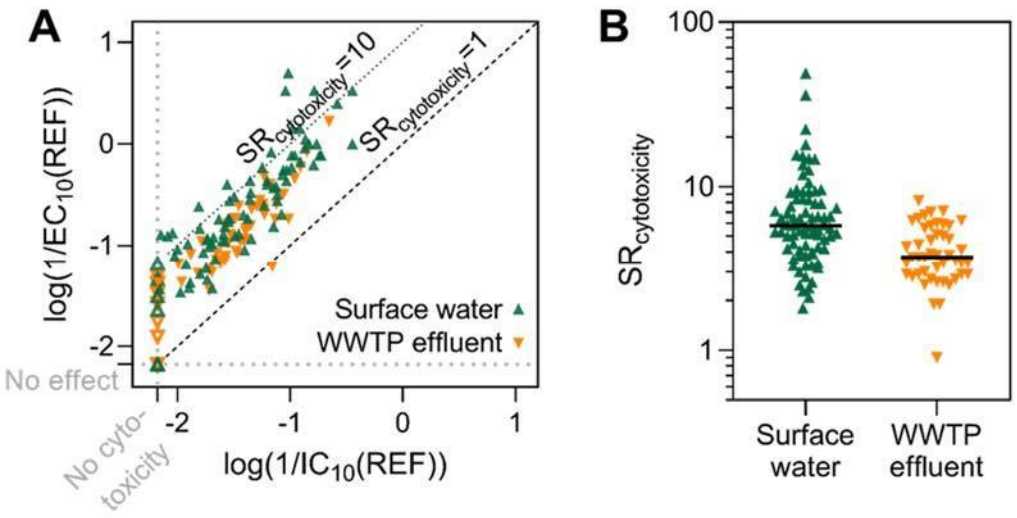

Figure 9: Specificity of effects on neurite outgrowth compared to cytotoxicity for surface water and WWTP effluent samples in SH-SY5Y cells as described in *Publication III*. (A) Comparison of IC_{10} and EC_{10} and (B) their ratio $SR_{cytotoxicity}$ as an indicator of specificity of effect. Empty symbols in (A) stands for no effects on cell viability or neurite outgrowth. The bold line in (B) indicates median values. The figure was taken from *Publication III*.

based on measured effect concentrations of single chemicals from previous chapter and detected concentrations from chemical analysis. The details of calculation method can be found in *Publication III*.

Overall, measured mixture effects for neurite outgrowth inhibition were explained by detected chemicals to higher extent in WWTP than in surface water (Figure 4 in *Publication III*). Up to 4.4% and 6.8% of the measured mixture effects on neurite outgrowth (narciclasine-EQ_{bio}) were explained by the estimated effects from detected chemicals (narciclasine-EQ_{chem}) for surface water and WWTP effluent, respectively. In the highly explained samples more than 1%, there were dominant contributors such as BIT or 7-diethylamino-4-methylcoumarin, which were highly detected at the micromolar level. Except for a few samples, less than 1% of measured mixture effects were explained by single chemical effects for majority of samples. This can be because the number of chemicals included for iceberg modelling was too small and/or substantial amount of the mixture effects were driven by chemicals below detection limits or transformation products.

The contribution of individual chemicals to narciclasine-EQ_{chem} was pronounced when the chemicals were detected at high concentration and/or had high effect potency. The major effect drivers are visualized in Figure 10 for surface water and WWTP effluent samples. In case of surface water, the average contribution to narciclasine-EQ_{chem} was the highest for azoxystrobin, followed by N-methyl-2-pyrrolidone, benzothiazole, and propiconazole. The main drivers were highly different between samples for surface water and this could be related to diversity of source contributions for individual surface water samples, i.e., the different level of contribution by agricultural runoff, street runoff, and combined sewer overflows. In case of WWTP effluent, mebendazole dominantly contributed to the narciclasine-EQ_{chem} in half of the WWTP effluent extracts, indicating mebendazole was one of the major effect drivers in WWTP effluent. There were overlapping mixture effect contributors for both sample types such as propiconazole and 7-diethylamino-4-methylcoumarine. While management in a broad scale should be discussed to reduce level of these overlapping chemicals, site-specific identification of effect drivers would be useful to investigate the contamination source and potential reduction of emissions from these sources. More assessment information of single chemicals can facilitate further identification of effect drivers in the environment.

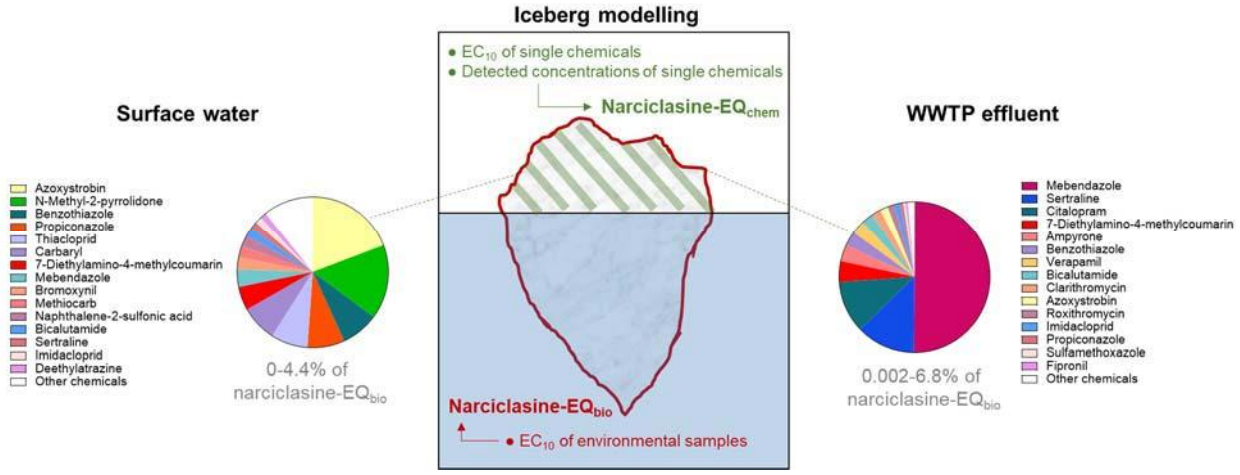

Figure 10: Iceberg modelling to explain mixture effects on neurite outgrowth of surface water and WWTP effluent. Measured mixture effects in bioanalysis (narciclasine-EQ_{bio}) were explained by detected chemicals with effect measurement (narciclasine-EQ_{chem}). Top 15 contributors (pie graph) were identified based on average contribution of individual chemicals to narciclasine-EQ_{chem}.

Toxic unit (TU) is an analogous concept that can be applied for cytotoxicity and can be calculated without reference chemicals (Kuzmanovic et al., 2015; Beckers et al., 2018). The detailed discussion on TU can be found in *Publication III*. In addition, the iceberg modelling was performed for identical samples in three reporter gene assays (AhR-CALUX, PPARγ-BLA, and AREc32). Their sensitivity of responses and the major effect drivers were compared with those observed in SH-SY5Y cells, which also can be found in *Publication III*.

3.2 Acetylcholinesterase inhibition

3.2.1 Assay optimization

SH-SY5Y cells were used to analyze AChE inhibition since they are known to express AChE, mainly localized on neurites and partially distributed throughout the cytoplasm (Thullbery et al., 2005). AChE inhibition assay using SH-SY5Y cells has been already used for testing single chemicals, which identified many potential AChE inhibitors from the Tox21 chemicals (Li et al., 2021). However, in the original assay protocol, exposure duration was too short to capture inhibitory effects and medium containing FBS, which can be another source of AChE, was used for the assay, hence the assay condition needed to be optimized to improve assay quality and performance. The condition of AChE inhibition assay was optimized based on well-known AChE inhibitors. Three irreversible inhibitors organothiophosphates (OTP) and their metabolites organophosphates (OP) as well as three reversible inhibitors carbamates were investigated for the optimization process. SH-SY5Y cells were differentiated to increase AChE activity and assay performance (de Medeiros et al., 2019). The assessment of AChE in SH-SY5Y cells will allow comparison to other neurotoxicity endpoints such as neurite outgrowth that can be measured in the same cell line. Since commonly used assay medium for AChE inhibition assays contains FBS and showed AChE activity themselves, the optimized assay medium was not supplemented with FBS to avoid any bias in AChE inhibition assessment. The assay was performed as outlined in Figure 11 and the detailed experimental procedure can be found in *Publication IV*.

Nine AChE inhibitors were tested from 1 to 6 h to assess the changes in EC_{50} over time and determine a suitable exposure duration (Figure 1 in *Publication IV*). EC_{50}s, the effect concentrations causing 50% of maximum AChE inhibition, decreased over time for all six irreversible AChE inhibitors. EC_{50} for AChE inhibition rapidly decreased at 1 to 2 h exposure and leveled off after longer exposure for the irreversible inhibitors. In contrast, EC_{50}s for AChE inhibition reached the minimum level already after 1 h of exposure for two reversible inhibitors, carbofuran and 3-hydroxycarbofuran. This faster reaction observed from carbamates can be explained by their structural similarity to ACh, leading to good structural fitness and also due to the high reactivity of carbamyl moiety at the AChE active sites (Fukuto, 1990). Unlike carbofuran and 3-hydroxycarbofuran, the EC_{50}s of another reversible inhibitor carbaryl increased over time. This decrease in toxicity may be explained by degradation of carbaryl by hydrolysis (Sogorb et al., 2004; Sogorb et al., 2007). Continuous degradation of carbaryl would occur when

they are released from AChE by reverse reaction, leading to decrease in exposure concentration over time. Given that the maximal AChE inhibition was achieved after a few hours for OPs and decreasing AChE inhibition over time observed for carbaryl, 3 h was determined as the optimal exposure duration.

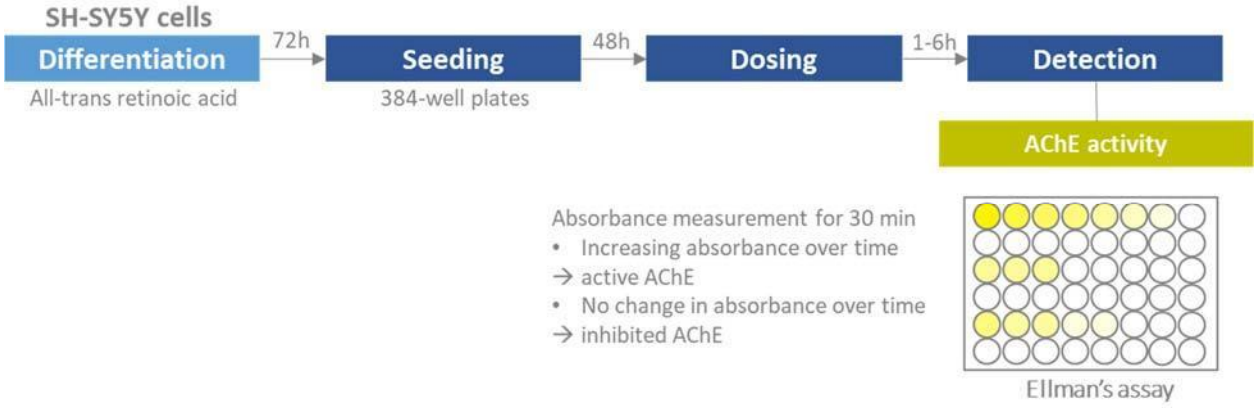

Figure 11: Experimental procedure of AChE inhibition assay using differentiated SH-SY5Y cells. Effects of single chemicals or environmental samples were tested in 384-well plates and inhibitory effects on AChE activity (EC_{50}) were measured based on absorbance using Ellman's assay (Ellman et al., 1961). Active AChE can react with detection mixture and the product with color can be formed while inhibited AChE cannot react with the detection mixture and no change in absorbance can be observed.

3.2.2 Loss of volatile AChE inhibitors from the test system

Chemical loss can occur during exposure due to partitioning of chemicals to the air space in bioassays. According to Escher et al. (2019), volatility cutoff based on medium-air partition constants ($K_{medium/air}$) was defined, which can be used to predict chemical loss due to volatilization of chemicals in cellular bioassays. Chemicals with log $K_{medium/air} < 4$ were considered as volatile chemicals in the assays with 24 h exposure duration. When $K_{medium/air}$ was predicted for the 9 AChE inhibitors (Table 1 in *Publication IV*), three OPs (chlorpyrifos, diazinon, and parathion) had log $K_{medium/air}$ from 3.6 to 5.1, which are below or just above the previously defined cutoff (Figure 12). Therefore, the chemical loss of the three OPs was investigated using solid-phase microextraction and chemical analysis. Assay medium was spiked with the chemicals at the highest test concentration used in the previous chapter (maximum

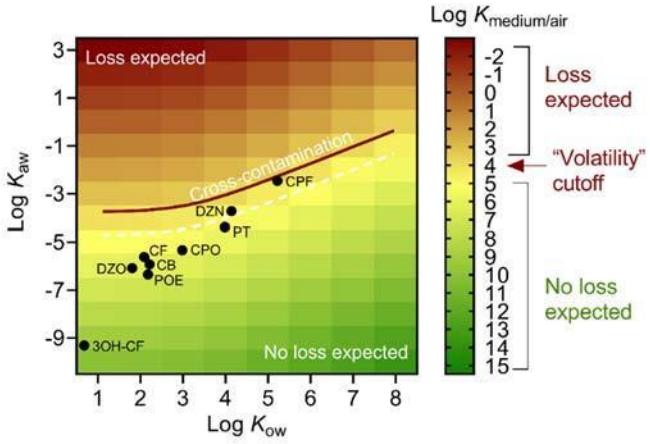

Figure 12: Medium-air partition constants ($K_{medium/air}$, colored squares) of 9 AChE inhibitors were estimated from air-water partition constants (K_{aw}) and octanol-water partition constants (K_{ow}) as described in *Publication IV*. The previously established volatility cutoff (24 h exposure) of $K_{medium/air}$ of 10^4 is shown as solid red line, which is also applicable for the 3 h-AChE inhibition assay. The white broken line ($K_{medium/air}$ of 10^5) indicates there can be partial losses after exposure duration of 24 h. CPF: chlorpyrifos; DZN: diazinon, PT: parathion; CPO: chlorpyrifos-oxon; DZO: diazoxon; POE: paraoxon-ethyl; CF: carbofuran; 3OH-CF: 3-hydroxycarbofuran; CB: carbaryl. The figure was taken from *Publication IV*.

solubility level) and incubated in closed vials or 384-well plates for 3 h and 24 h. The incubation was performed without cells to exclude possible loss from metabolism by cells.

The chemical amount after incubation was compared with the initial amount of chemicals at 0 h (Figure 2 in *Publication IV*). When chemicals were incubated in closed vials, the amount of chemicals stayed relatively stable over 24 h of incubation (> 85% of initial level). After incubation of chemicals for the assay duration of 3 h in the 384-well plates, no cross-contamination was observed, and the majority of chemicals stayed in the medium from spiked wells for all three OPs (> 66 % of initial level). After 24 h of incubation, a higher loss was observed in the spiked wells for the chemicals with lower $K_{medium/air}$. While parathion (log $K_{medium/air}$ = 5.1) still had 71.5% of the initial level, chlorpyrifos (log $K_{medium/air}$ = 3.6.) only had 28.7% left in the spiked wells. In case of diazinon (log $K_{medium/air}$ = 4.4), 46.3% of the initial level was found in the spiked wells and in addition, slight cross-contamination was observed in neighboring wells (< 5%). This trend agrees well with the previous observation that chemicals with $K_{medium/air}$ closer to the volatility cutoff were more likely to contaminate the neighboring

wells while chemicals with $K_{medium/air}$ well below the cutoff, i.e., highly volatile chemicals, were just volatilized without cross-contamination (Escher et al., 2019).

Considering that more than 64% of chemicals were retained in the medium and no cross-contamination was observed for our assay duration of 3 h, the previously defined volatility cutoff appears also valid for the AChE inhibition assay. However, it should be noted that substantial loss can occur for the three typically tested OPs in bioassays with longer exposure duration. Therefore, it could be necessary to verify the exposure concentrations using chemical analysis for testing of single chemicals with log $K_{medium/air}$ close to the cutoff of 4.

3.2.3 Evaluation of the influence of DOC on the cell-based AChE inhibition assay

In purified enzyme-based AChE inhibition assay, DOC suppressed AChE inhibition by a chemical and this can hinder precise toxicity assessment of environmental samples (Neale and Escher, 2013). This disturbance by DOC was not observed in several other cell-based bioassays, which could be explained by intracellular localization of target sites (Neale 2014). In SH-SY5Y cells, AChE are anchored to outer side of cell membrane or localized in the cytoplasm (Thullbery et al., 2005; Hicks et al., 2013), hence it was investigated whether disturbance by DOC can be avoided in a cell-based AChE inhibition assay. A commercially available DOC, Aldrich humic acid, was used to represent DOC according to Neale and Escher (2013) and paraoxon-ethyl was applied as a reference chemical.

Constant level of paraoxon-ethyl was exposed together with different concentrations of Aldrich humic acid, and the inhibition of AChE by paraoxon-ethyl was not influenced by Aldrich humic acid up to 68 mg_C/L (Figure 13A). This means no suppressive effects by humic acid were observed, which is in contrast to what was observed previously in free enzyme-based AChE inhibition assay where humic acid suppressed AChE inhibition already at 2 mg_C/L (Neale and Escher, 2013). In purified enzyme-based AChE assays, DOC is freely accessible to AChE, hence freely interact to each other. However, in the cell-based assay, AChE location in the cellular assay, i.e., on outer cell membrane or in cytoplasm, could sterically protect it from DOC and potential nonspecific binding.

Binary mixtures of paraoxon-ethyl and two surface water extracts with different AChE inhibitory potency were tested to confirm the applicability of cell-based assay to environmental

samples. The mixtures were prepared in different combination ratio, leading to different levels of DOC in each mixture. If DOC has an impact on AChE inhibition in the assay, unexpected mixture effects, i.e., deviation from the predicted mixture effect, would be observed. Based on an isobologram approach (Altenburger et al., 1990), paraoxon-ethyl and the water extracts were mixed in different effect concentration fractions and tested in serial dilution as described in *Publication IV*. Briefly, experimental toxic units (TU) were derived from the EC_{50} of the individual binary mixtures with diverse combination ratio. The sum of TUs would be ideally 1 (dotted line in Figure 13B) when the chemicals or samples behave in a concentration-additive manner without any synergistic or antagonistic effects. As a result, the experimentally derived TU aligned well with the concentration addition prediction for binary mixtures of water extracts and paraoxon-ethyl (Figure 13B), which indicates there was no interference with AChE inhibition by DOC. On the contrary, in a previous isobologram study using purified AChE, the experimental TUs highly deviated from the predictions for binary mixtures of oxidized parathion with water samples, indicating disturbance by DOC (Neale and Escher, 2013). Therefore, SH-SY5Y cell-based AChE inhibition assay can avoid the artefacts from DOC, and hence can be applied for screening of DOC-rich environmental samples.

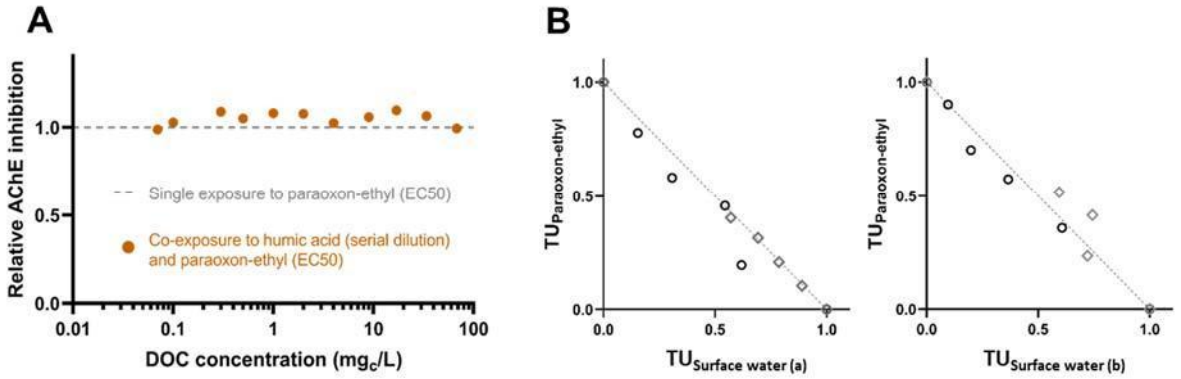

Figure 13: (A) Relative inhibition of AChE after 3 h-exposure to constant level of paraoxon-ethyl and variable concentrations of Aldrich humic acid (dissolved organic carbon, DOC) in SH-SY5Y cells. (B) Isobolograms for binary mixtures of paraoxon-ethyl with two surface water extracts in AChE inhibition assay using SH-SY5Y cells. The line indicates the concentration addition prediction. Each data point represents the TU derived from EC_{50} of individual binary mixtures as described in *Publication IV*.

3.3 Neurotoxicity in environmental samples

Thirteen surface water samples were selected based on detected concentrations of known AChE inhibitors and analyzed for AChE inhibition potency. The samples were partially impacted by agricultural runoff, hence several insecticides including AChE inhibitors (e.g. carbaryl, diazinon, pirimicarb) were detected in the samples. The identical surface water samples were already tested for the neurite outgrowth assay, hence the responses were compared together.

EC_{50} for AChE inhibition by surface water samples ranged from REF 0.5 to 10 (Figure 14). This means that 50% of AChE inhibition was achieved by diluting samples by two to enriching them up to ten times. The samples with higher detected concentrations of AChE inhibitors did not necessarily show higher inhibitory potency on AChE. This may indicate the presence of unknown AChE inhibitors and/or mixture effects from many chemicals below the detection limit.

Since IC_{10} for cytotoxicity and EC_{10} for neurite outgrowth inhibition were available for these samples, the responses were compared for the three endpoints: neurite outgrowth, AChE inhibition, and neuronal cytotoxicity (Figure 14A). Among the 13 samples, the strongest effects were observed for AChE inhibition in 6 samples despite the shorter exposure duration than the other two endpoints. The responses of neurite outgrowth inhibition were the most sensitive in the remaining 7 samples, and the lowest effect concentration among all endpoints and extracts was observed for neurite outgrowth inhibition when the extract was diluted by a factor of 5.

When the two specific endpoints were compared with cytotoxicity (Figure 14B), EC_{50} for AChE inhibition was independent of cytotoxicity while samples with lower EC_{10} for neurite outgrowth inhibition were more likely to also exhibit lower IC_{10}. This could be because neurite outgrowth represents a more apical endpoint than the AChE inhibition. Although AChE inhibition was proposed as a specific MOA that can drive neurite-specific effects for single chemicals in chapter 3.1.4, the effects on neurite outgrowth would be contributed by other diverse mechanisms from many micropollutants in the mixtures. Hence, there was no clear relationship observed between effect concentrations for AChE inhibition and neurite outgrowth inhibition.

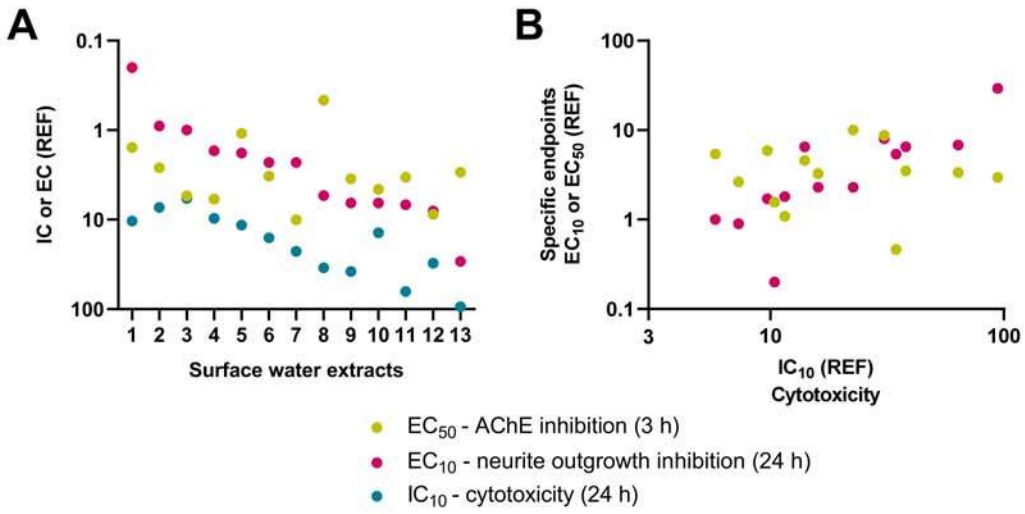

Figure 14: Comparison of effect concentrations for three endpoints after exposure to surface water extracts in SH-SY5Y cells. REF: relative enrichment factor (REF; $L_{water}/L_{bioassay}$). Samples were sorted according to their effect concentrations for neurite outgrowth inhibition in (A).

4. Implications

4.1 Key findings

In this thesis, applicability of baseline toxicity was expanded for chemicals with various hydrophobicity and speciation (*Publication I*). This QSAR formed the basis to quantify specificity of the effects on neurite outgrowth. A major observation was that the toxicity of hydrophobic chemicals is likely to be triggered by baseline toxicity (*Publication II*). Neurite-specific toxicants were identified, and their specific MOAs were compiled and linked to neurite-specific effects (*Publication II* and *III*). The neurite outgrowth assay was applied for environmental monitoring and identified major chemicals driving the effects on neurite outgrowth in environmental mixtures (*Publication III*). Finally, it was demonstrated that AChE inhibition of DOC-rich samples could be analyzed without any bias due to DOC when the cell-based assay was used (*Publication IV*). Therefore, the two assays for testing effects on neurite outgrowth and AChE could provide high-throughput tool for environmental monitoring of neurotoxicants with the advantage of being measurable in the same cell line.

4.2 Testing strategy in bioassays for single chemicals

Typically, identical maximum dosing concentration is applied for testing of chemicals in bioassays without considering different effect potency of various chemicals. In this approach, often no toxic effects are observed until at the highest tested concentration, which can result in false negative responses. Based on the proposed baseline toxicity QSAR, the minimal toxicity level can be predicted for individual chemicals and it can be used for planning dosing concentration. Dosing strategy for testing chemicals in cellular bioassays has been proposed considering multiple factors (e.g., stability of chemicals, FBS content, and solubility of chemicals), which could be considered together for the planning (Fischer et al., 2019). Furthermore, the proposed generic baseline QSAR can be broadly applied to other bioassays even when protein and lipid content of cells and medium are unavailable. Unlike the previous QSAR which was only applicable for chemicals with certain ranges of hydrophobicity ($0.5 < \log K_{lip/w} < 4.5$), the proposed baseline QSAR is suitable for any type of chemicals including hydrophobic and ionizable chemicals. However, its application to organic acids needs to be further investigated to develop more reliable prediction model. Given that the prediction of

baseline toxicity entirely depends on $D_{lip/w}$(pH 7.4), more accurate, ideally experimental $D_{lip/w}$(pH 7.4) would improve the confidence of the prediction.

Another limitation when testing chemicals in bioassays is that chemicals could be lost during exposure, e.g., by volatilization, which can hinder precise quantification of their toxicity. Volatile loss of chemicals can also lead to false negatives of the volatile chemicals or incorrect effect concentration determination in the neighboring wells due to cross-contamination. Therefore, a volatility cutoff should be also considered for experimental planning of testing chemicals. The volatility cutoff at log $K_{medium/air}$ of 4 was previously defined based on cytotoxic effects in multiple bioassays (Escher et al., 2019) and its validity was confirmed in the AChE inhibition assay with 3 h of assay duration using chemical analysis. The volatility cutoff would be valid for bioassays with exposure duration up to 24 h but chemicals with $K_{medium/air}$ close to the cutoff need caution, especially when the bioassays have sensitive endpoints or the test chemical can elicit the effects at low concentration. For volatile chemicals, alternative dosing strategy could be used such as system with defined headspace (Birch et al., 2017).

4.3 Use of baseline toxicity to estimate the specificity of responses

The degree of toxicity of chemicals is usually estimated based on nominal concentrations that cause certain level of effects, i.e., effect concentrations. Lower effect concentrations indicate higher degree of toxicity, however, the degree of specificity is often not discussed properly. For example, hydrophobic chemicals can often trigger effects at low effect concentrations for any toxicity endpoints, but it is questionable whether the observed effects are induced by specific MOAs of the chemicals or just by baseline toxicity arising from their high hydrophobicity. Baseline toxicity can be the trigger of neurotoxicity particularly for hydrophobic chemicals since they have high tendency to accumulate in the membrane (Escher and Hermens, 2002). Based on the newly established baseline toxicity QSAR, it was observed that hydrophobic chemicals were more likely to act on neurite outgrowth in a nonspecific manner via baseline toxicity. Similar observation was already made for reactive but also hydrophobic chemicals (Freidig et al., 1999).

Although baseline toxicity is the minimal toxicity of chemicals, cytotoxicity can be induced at as low as a few micromolar level via baseline toxicity for hydrophobic chemicals. This can secondarily cause toxicity on other endpoints such as neurite outgrowth and the effect concentration would be determined at lower level. This would indicate strong toxicity although it

is not specific on neurite outgrowth. Likewise, neuronal-specific chemicals might not cause neurite-specific effects but nevertheless can elicit high degree of toxicity on neurite outgrowth due to enhanced cytotoxicity caused by specific MOAs occurred in neuronal cells.

The current DNT *in vitro* testing strategy use $SR_{cytotoxicity}$ as the specificity measure and I proposed assessment of neuronal-specific effects based on $SR_{baseline}$ to complement the current approach. While $SR_{cytotoxicity}$ can be used identify chemicals that specifically affect neurite outgrowth, $SR_{baseline}$ enables to identify chemicals affecting the entire neuronal cell and induce neurite degeneration via enhanced level of toxicity compared to baseline toxicity. Since multiple *in vitro* models are used to cover diverse endpoints in the current DNT testing battery, $SR_{baseline}$ enables comparison of effect potency for a given chemical between cell models and can quantify cell-specific toxicity since baseline toxicity is independent of cell types. Furthermore, when no cytotoxicity was observed, $SR_{baseline}$ could provide a surrogate to estimate specificity and replace the use of the highest tested concentration as reference level in specificity analysis (Delp et al., 2018).

4.4 Modes of action for neurite-specific effects

Current DNT testing strategy recommends use of key event-based approach using *in vitro* cell models (Masjosthusmann et al., 2020). Evaluation of toxicity for chemicals based on key event level provide an efficient way to cover multiple MOAs that can provoke DNT and facilitate assessment of toxicity for single chemicals. A wide variety of neurite-specific chemicals with also high environmental relevance were identified in this thesis. Highly neurite-specific effects were commonly observed for inhibitors of microtubule polymerization (e.g., mebendazole, colchicine) and reversible AChE inhibitors (e.g. carbaryl, 3-hydroxycarbofuran). This could provide an evidence to reveal MOAs relevant to neurite-specific effects. However, the known or primary MOAs of the chemicals are not necessarily the only specific MOA involved in their specific inhibition of neurite outgrowth. For example, insecticides are known to be less potent in mammals due to species specificity and metabolic detoxification and they can induce toxic effects in non-target organisms possibly via secondary targets (Lushchak et al., 2018). Therefore, direct relationship between the potential MIEs and neurite outgrowth should be further elucidated. Such efforts have already been made for mitochondrial toxicants (Delp et al., 2019; Delp et al., 2021), which can provide evidence for establishment of AOPs for DNT. It is also

possible that multiple MOAs arise from a single chemical and contribute to the observed cytotoxic or neurite-specific effects. Hence, key event-based approaches and mechanistic research should be performed complementarily.

One limitation can occur when connecting the MOAs to the observed effects in SH-SY5Y. SH-SY5Y cells have been commonly applied as an *in vitro* model to test effects on neurite outgrowth and SH-SY5Y cells were selected in this study considering practical aspects to develop high-throughput method. However, there can be an abnormal physiology due to their tumor origin (Do et al., 2007), which could result in misinterpretation of the observed effects. Therefore, the current DNT testing strategy recommends use of non-oncogenic cells such as LUHMES cells. The effects observed in SH-SY5Y should be compared with those from non-oncogenic cell models to improve reliability of the model.

4.5 Neurotoxicity observed in the environmental samples

The neurite outgrowth inhibition assay using SH-SY5Y cells was successfully applied for the first time to water samples including WWTP effluent and diverse surface water, which demonstrated its wide applicability. It was revealed that the mixture effects were contributed not only by the effect potency of chemicals but also by their occurrence in the environment. Since the assessment for single chemicals and MOA information relevant to DNT are highly limited, testing of mixture in the bioassays would provide efficient monitoring tool to evaluate DNT effects in the environment. Different chemicals dominated or contributed to the mixture effects in each sample and therefore site-specific identification of effect drivers would be useful to identify the contamination source.

The AChE inhibition assays were also successfully established for environmental sample assessment. AChE inhibition has been widely applied as an endpoint for environmental monitoring already but the previously measured toxicity using purified enzyme-based assays might have been underestimated due to the suppressive effects of DOC on AChE inhibition. SH-SY5Y cell-based AChE inhibition assay was provided, which can evaluate inhibition of AChE more precisely without disturbance by DOC. I also confirmed its applicability in environmental samples and the inhibitory effects on AChE were observed even when the water extracts were diluted by a factor of two. This bioassay-based monitoring would complement chemical analysis-based approach very well considering that mixture effects of environmental samples are

driven by many chemicals at low concentrations. Especially, there are highly specific AChE inhibitors such as OPs and carbamates and they would contribute to mixture effects even at very low concentrations.

Based on the complementary approach using bioassays and chemical analysis, neurite-specific chemicals or known AChE inhibitors were detected in the environmental samples. Considering low concentration of chemicals in the environment, chemicals with common MOA need to reach certain level to cause effects. Hence, detection by chemical analysis does not necessarily mean that the mixtures could elicit observable effects in the mixture. In this regard, bioassays can complement chemical analysis since bioassay-based approach can even cover the effects driven by chemicals below the detection limit or chemicals with unknown MOAs.

5. Recommendations for Future Work

5.1 Diverse sources of chemical loss

Chemical loss in bioassays can occur not only from volatilization of chemicals but also from other degradation processes. Physicochemical properties differ a lot for individual chemicals and thus the loss can arise from diverse processes, e.g., hydrolysis, protein reactivity, and photodegradation (Proenca et al., 2021; Huchthausen et al., 2022). Therefore, the degradation processes in bioassays for highly degradable chemicals should be investigated to evaluate their toxicity more precisely. In addition, in cell-based assays, uptake and metabolism by cells can affect the effect of chemicals. In case of AChE inhibition assay, cellular metabolism of chemicals can play an important role by increasing or decreasing their inhibitory potency on AChE. For example, OTPs can be oxidized by cells into OPs with extremely high inhibitory potency, hence the metabolic activity of cells and their contribution to toxicity of chemicals should be clarified.

5.2 Diverse neurotoxicity endpoints

Neurite outgrowth inhibition and AChE inhibition were suggested as potent neurotoxicity endpoints for environmental monitoring, but other neurotoxicity endpoints may be considered for DNT assessment of individual chemicals and future monitoring studies. The effects on neurite outgrowth indicate potential DNT but it may only partially explain DNT that can be induced by a chemical and fail to detect DNT related to other key events. Therefore, consideration of diverse DNT endpoints such as migration and synaptogenesis may allow to capture wider range of chemicals causing DNT and make the water quality monitoring more comprehensive (Harrill et al., 2018; Behl et al., 2019; Masjosthusmann et al., 2020). Given that the current *in vitro* DNT battery is established in the context of human toxicology, the test system can be rather complex and less high-throughput to be considered as environmental monitoring tool. Therefore, the relevance to DNT as well as practical aspects such as high-throughput applicability should be considered in the context of environmental monitoring. In case of adult neurotoxicity, high environmental risk would be posed not only by AChE inhibition but also by several receptor-mediated toxicity endpoints such as nicotinic acetylcholine receptor (nAChR) agonism and voltage-gated sodium channel antagonism (Legradi et al., 2018). Therefore, these

environmentally relevant endpoints can be also considered to monitor neurotoxicity in the environment more comprehensively.

5.3 Strategies for environmental monitoring

At present, chemicals with measured effects on neurite outgrowth are limited, which makes it difficult to identify major effect drivers effectively. Therefore, more chemicals need to be assessed for their neurotoxicity to evaluate their contributions to mixture effects. It is not realistic to test all detected chemicals in the environment and thus priority can be given to chemicals that occur more frequently in the environment. Hence, chemical analysis can be applied to prioritize chemicals for further testing. Assessment information of many chemicals can also be utilized for derivation of so-called effect-based trigger values that may allow one to differentiate between acceptable and poor water quality (Escher et al., 2018). If effect-based trigger values were implemented, it can be evaluated whether the toxicity observed in surface water and WWTP effluent would be acceptable or strict regulation is necessary to manage the water quality. Considering that specific effects on neurite outgrowth were more pronounced for surface water than WWTP effluent, future monitoring can be performed with more focus on surface water. In case of the AChE inhibition assay, insecticides can be potent effect drivers for AChE inhibition, hence the monitoring can be focused on agricultural sites. Additionally, the neurotoxicity assays could be applied for comparative assessment of treatment option or buffer strip to manage release of chemicals into the environment.

6. References

Ahmed, M., Rocha, J.B., Mazzanti, C.M., Morsch, A.L., Cargnelutti, D., Correa, M., Loro, V., Morsch, V.M., Schetinger, M.R., 2007. Malathion, carbofuran and paraquat inhibit Bungarus sindanus (krait) venom acetylcholinesterase and human serum butyrylcholinesterase in vitro. Ecotoxicology 16, 363-369.

Altenburger, R., Bodeker, W., Faust, M., Grimme, L.H., 1990. Evaluation of the isobologram method for the assessment of mixtures of chemicals. Combination effect studies with pesticides in algal biotests. Ecotoxicol Environ Saf 20, 98-114.

Alygizakis, N.A., Besselink, H., Paulus, G.K., Oswald, P., Hornstra, L.M., Oswaldova, M., Medema, G., Thomaidis, N.S., Behnisch, P.A., Slobodnik, J., 2019. Characterization of wastewater effluents in the Danube River Basin with chemical screening, in vitro bioassays and antibiotic resistant genes analysis. Environ Int 127, 420-429.

Aschner, M., Ceccatelli, S., Daneshian, M., Fritsche, E., Hasiwa, N., Hartung, T., Hogberg, H.T., Leist, M., Li, A., Mundy, W.R., Padilla, S., Piersma, A.H., Bal-Price, A., Seiler, A., Westerink, R.H., Zimmer, B., Lein, P.J., 2017. Reference Compounds for Alternative Test Methods to Indicate Developmental Neurotoxicity (DNT) Potential of Chemicals: Example Lists and Criteria for their Selection and Use. ALTEX 34, 49-74.

Bal-Price, A., Crofton, K.M., Leist, M., Allen, S., Arand, M., Buetler, T., Delrue, N., FitzGerald, R.E., Hartung, T., Heinonen, T., Hogberg, H., Bennekou, S.H., Lichtensteiger, W., Oggier, D., Paparella, M., Axelstad, M., Piersma, A., Rached, E., Schilter, B., Schmuck, G., Stoppini, L., Tongiorgi, E., Tiramani, M., Monnet-Tschudi, F., Wilks, M.F., Ylikomi, T., Fritsche, E., 2015. International STakeholder NETwork (ISTNET): creating a developmental neurotoxicity (DNT) testing road map for regulatory purposes. Arch. Toxicol. 89, 269-287.

Bal-Price, A., Hogberg, H.T., Crofton, K.M., Daneshian, M., FitzGerald, R.E., Fritsche, E., Heinonen, T., Bennekou, S.H., Klima, S., Piersma, A.H., Sachana, M., Shafer, T.J., Terron, A., Monnet-Tschudi, F., Viviani, B., Waldmann, T., Westerink, R.H.S., Wilks, M.F., Witters, H., Zurich, M.G., Leist, M., 2018. Recommendation on Test Readiness Criteria for New Approach Methods in Toxicology: Exemplified for Developmental Neurotoxicity. ALTEX 35, 306-352.

Beckers, L.M., Busch, W., Krauss, M., Schulze, T., Brack, W., 2018. Characterization and risk assessment of seasonal and weather dynamics in organic pollutant mixtures from discharge of a separate sewer system. Water Res. 135, 122-133.

Behl, M., Ryan, K., Hsieh, J.H., Parham, F., Shapiro, A.J., Collins, B.J., Sipes, N.S., Birnbaum, L.S., Bucher, J.R., Foster, P.M.D., Walker, N.J., Paules, R.S., Tice, R.R., 2019. Screening for Developmental Neurotoxicity at the National Toxicology Program: The Future Is Here. Toxicol Sci 167, 6-14.

Biedler, J.L., Helson, L., Spengler, B.A., 1973. Morphology and growth, tumorigenicity, and cytogenetics of human neuroblastoma cells in continuous culture. Cancer Res. 33, 2643-2652.

Birch, H., Andersen, H.R., Comber, M., Mayer, P., 2017. Biodegradation testing of chemicals with high Henry's constants - Separating mass and effective concentration reveals higher rate constants. Chemosphere 174, 716-721.

Bjorling-Poulsen, M., Andersen, H.R., Grandjean, P., 2008. Potential developmental neurotoxicity of pesticides used in Europe. Environ. Health 7.

Casida, J.E., 2009. Pest toxicology: the primary mechanisms of pesticide action. Chem. Res. Toxicol. 22, 609-619.

Čolović, M.B., Krstić, D.Z., Lazarevic-Pasti, T.D., Bondzic, A.M., Vasic, V.M., 2013. Acetylcholinesterase Inhibitors: Pharmacology and Toxicology. Curr Neuropharmacol 11, 315-335.

Crawford, S.E., Brinkmann, M., Ouellet, J.D., Lehmkuhl, F., Reicherter, K., Schwarzbauer, J., Bellanova, P., Letmathe, P., Blank, L.M., Weber, R., Brack, W., van Dongen, J.T., Menzel, L., Hecker, M., Schuttrumpf, H., Hollert, H., 2022. Remobilization of pollutants during extreme flood events poses severe risks to human and environmental health. J Hazard Mater 421, 126691.

de Medeiros, L.M., De Bastiani, M.A., Rico, E.P., Schonhofen, P., Pfaffenseller, B., Wollenhaupt-Aguiar, B., Grun, L., Barbe-Tuana, F., Zimmer, E.R., Castro, M.A.A., Parsons, R.B., Klamt, F., 2019. Cholinergic Differentiation of Human Neuroblastoma SH-SY5Y Cell Line and Its Potential Use as an In vitro Model for Alzheimer's Disease Studies. Mol Neurobiol 56, 7355-7367.

Delp, J., Cediel-Ulloa, A., Suciu, I., Kranaster, P., van Vugt-Lussenburg, B.M., Munic Kos, V., van der Stel, W., Carta, G., Bennekou, S.H., Jennings, P., van de Water, B., Forsby, A., Leist, M., 2021. Neurotoxicity and underlying cellular changes of 21 mitochondrial respiratory chain inhibitors. Arch Toxicol 95, 591-615.

Delp, J., Funke, M., Rudolf, F., Cediel, A., Bennekou, S.H., van der Stel, W., Carta, G., Jennings, P., Toma, C., Gardner, I., van de Water, B., Forsby, A., Leist, M., 2019. Development of a neurotoxicity assay that is tuned to detect mitochondrial toxicants. Arch. Toxicol. 93, 1585-1608.

Delp, J., Gutbier, S., Klima, S., Hoelting, L., Pinto-Gil, K., Hsieh, J.H., Aichem, M., Klein, K., Schreiber, F., Tice, R.R., Pastor, M., Behl, M., Leist, M., 2018. A high-throughput approach to identify specific neurotoxicants/ developmental toxicants in human neuronal cell function assays. ALTEX 35, 235-253.

Do, J.H., Kim, I.S., Park, T.K., Choi, D.K., 2007. Genome-wide examination of chromosomal aberrations in neuroblastoma SH-SY5Y cells by array-based comparative genomic hybridization. Mol Cells 24, 105-112.

Ellman, G.L., Courtney, K.D., Andres, V., Jr., Feather-Stone, R.M., 1961. A new and rapid colorimetric determination of acetylcholinesterase activity. Biochem Pharmacol 7, 88-95.

Endo, S., Escher, B.I., Goss, K.U., 2011. Capacities of Membrane Lipids to Accumulate Neutral Organic Chemicals. Environ. Sci. Technol. 45, 5912-5921.

Endo, S., Goss, K.U., 2011. Serum albumin binding of structurally diverse neutral organic compounds: data and models. Chem. Res. Toxicol. 24, 2293-2301.

Escher, B.I., 2020. Tracking complex mixtures of chemicals in our changing environment. Science.

Escher, B.I., Ashauer, R., Dyer, S., Hermens, J.L., Lee, J.H., Leslie, H.A., Mayer, P., Meador, J.P., Warne, M.S., 2011. Crucial role of mechanisms and modes of toxic action for understanding tissue residue toxicity and internal effect concentrations of organic chemicals. Integr Environ Assess Manag 7, 28-49.

Escher, B.I., Asmall yi, U.-A.y.U.S., Behnisch, P.A., Brack, W., Brion, F., Brouwer, A., Buchinger, S., Crawford, S.E., Du Pasquier, D., Hamers, T., Hettwer, K., Hilscherova, K., Hollert, H., Kase, R., Kienle, C., Tindall, A.J., Tuerk, J., van der Oost, R., Vermeirssen, E., Neale, P.A., 2018. Effect-based trigger values for in vitro and in vivo bioassays performed on surface water extracts supporting the environmental quality standards (EQS) of the European Water Framework Directive. Sci Total Environ 628-629, 748-765.

Escher, B.I., Baumer, A., Bittermann, K., Henneberger, L., König, M., Kühnert, C., Klüver, N., 2017. General baseline toxicity QSAR for nonpolar, polar and ionisable chemicals and their mixtures in the bioluminescence inhibition assay with *Aliivibrio fischeri*. Environ. Sci. Process. Impacts 19, 414-428.

Escher, B.I., Bramaz, N., Ort, C., 2009. JEM spotlight: Monitoring the treatment efficiency of a full scale ozonation on a sewage treatment plant with a mode-of-action based test battery. J Environ Monit 11, 1836-1846.

Escher, B.I., Eggen, R.I.L., Schreiber, U., Schreiber, Z., Vye, E., Wisner, B., Schwarzenbach, R.P., 2002. Baseline toxicity (narcosis) of organic chemicals determined by *in vitro* membrane potential measurements in energy-transducing membranes. Environ. Sci. Technol. 36, 1971-1979.

Escher, B.I., Glauch, L., König, M., Mayer, P., Schlichting, R., 2019. Baseline Toxicity and Volatility Cutoff in Reporter Gene Assays Used for High-Throughput Screening. Chem. Res. Toxicol. 32, 1646-1655.

Escher, B.I., Henneberger, L., König, M., Schlichting, R., Fischer, F.C., 2020. Cytotoxicity Burst? Differentiating Specific from Nonspecific Effects in Tox21 in Vitro Reporter Gene Assays. Environ. Health Perspect. 128.

Escher, B.I., Hermens, J.L.M., 2002. Modes of action in ecotoxicology: Their role in body burdens, species sensitivity, QSARs, and mixture effects. Environ. Sci. Technol. 36, 4201-4217.

Escher, B.I., Neale, P.A., Leusch, F., 2021. Bioanalytical Tools in Water Quality Assessment (2nd edition). IWA Publishing: London, UK.

Fischer, F., Henneberger, L., König, M., Bittermann, K., Linden, L., Goss, K.-U., Escher, B., 2017. Modeling exposure in the Tox21 *in vitro* bioassays. Chem. Res. Toxicol. 30, 1197−1208.

Fischer, F.C., Cirpka, O.A., Goss, K.U., Henneberger, L., Escher, B.I., 2018. Application of Experimental Polystyrene Partition Constants and Diffusion Coefficients to Predict the Sorption of Neutral Organic Chemicals to Multiwell Plates in *in Vivo* and *in Vitro* Bioassays. Environ. Sci. Technol. 52, 13511-13522.

Fischer, F.C., Henneberger, L., Schlichting, R., Escher, B.I., 2019. How To Improve the Dosing of Chemicals in High-Throughput in Vitro Mammalian Cell Assays. Chem. Res. Toxicol. 32, 1462-1468.

Freidig, A.P., Verhaar, H.J.M., Hermens, J.L.M., 1999. Comparing the potency of chemicals with multiple modes of action in aquatic toxicology: Acute toxicity due to narcosis versus reactive toxicity of acrylic compounds. Environ. Sci. Technol. 33, 3038-3043.

Fukuto, T.R., 1990. Mechanism of Action of Organophosphorus and Carbamate Insecticides. 87, 245-254.

Gago-Ferrero, P., Bletsou, A.A., Damalas, D.E., Aalizadeh, R., Alygizakis, N.A., Singer, H.P., Hollender, J., Thomaidis, N.S., 2020. Wide-scope target screening of >2000 emerging contaminants in wastewater samples with UPLC-Q-ToF-HRMS/MS and smart evaluation of its performance through the validation of 195 selected representative analytes. J Hazard Mater 387, 121712.

Grandjean, P., Landrigan, P.J., 2006. Developmental neurotoxicity of industrial chemicals. Lancet 368, 2167-2178.

Grandjean, P., Landrigan, P.J., 2014. Neurobehavioural effects of developmental toxicity. Lancet Neurol 13, 330-338.

Grisaru, D., Sternfeld, M., Eldor, A., Glick, D., Soreq, H., 1999. Structural roles of acetylcholinesterase variants in biology and pathology. European Journal of Biochemistry 264, 672-686.

Halbach, K., Moder, M., Schrader, S., Liebmann, L., Schafer, R.B., Schneeweiss, A., Schreiner, V.C., Vormeier, P., Weisner, O., Liess, M., Reemtsma, T., 2021. Small streams-large concentrations? Pesticide monitoring in small agricultural streams in Germany during dry weather and rainfall. Water Res. 203, 117535.

Hamers, T., Molin, K.R., Koeman, J.H., Murk, A.J., 2000. A small-volume bioassay for quantification of the esterase inhibiting potency of mixtures of organophosphate and carbamate insecticides in rainwater: development and optimization. Toxicol Sci 58, 60-67.

Harrill, J.A., Freudenrich, T., Wallace, K., Ball, K., Shafer, T.J., Mundy, W.R., 2018. Testing for developmental neurotoxicity using a battery of in vitro assays for key cellular events in neurodevelopment. Toxicol. Appl. Pharmacol. 354, 24-39.

Hicks, D.A., Makova, N.Z., Nalivaeva, N.N., Turner, A.J., 2013. Characterisation of acetylcholinesterase release from neuronal cells. Chem Biol Interact 203, 302-308.

Huchthausen, J., Henneberger, L., Malzer, S., Nicol, B., Sparham, C., Escher, B.I., 2022. High-Throughput Assessment of the Abiotic Stability of Test Chemicals in In Vitro Bioassays. Chem. Res. Toxicol.

Klüver, N., Bittermann, K., Escher, B.I., 2019. QSAR for baseline toxicity and classification of specific modes of action of ionizable chemicals in the zebrafish embryo toxicity test. Aquat. Toxicol. 207, 110-119.

Krug, A.K., Balmer, N.V., Matt, F., Schonenberger, F., Merhof, D., Leist, M., 2013. Evaluation of a human neurite growth assay as specific screen for developmental neurotoxicants. Arch. Toxicol. 87, 2215-2231.

Kuzmanovic, M., Ginebreda, A., Petrovic, M., Barcelo, D., 2015. Risk assessment based prioritization of 200 organic micropollutants in 4 Iberian rivers. Sci Total Environ 503-504, 289-299.

Legradi, J.B., Di Paolo, C., Kraak, M.H.S., van der Geest, H.G., Schymanski, E.L., Williams, A.J., Dingemans, M.M.L., Massei, R., Brack, W., Cousin, X., Begout, M.L., van der Oost, R., Carion, A., Suarez-Ulloa, V., Silvestre, F., Escher, B.I., Engwall, M., Nilen, G., Keiter, S.H., Pollet, D., Waldmann, P., Kienle, C., Werner, I., Haigis, A.C., Knapen, D., Vergauwen, L., Spehr, M., Schulz, W., Busch, W., Leuthold, D., Scholz, S., vom Berg, C.M., Basu, N., Murphy, C.A., Lampert, A., Kuckelkorn, J., Grummt, T., Hollert, H., 2018. An ecotoxicological view on neurotoxicity assessment. Environ Sci Eur 30.

Lein, P., Silbergeld, E., Locke, P., Goldberg, A.M., 2005. In vitro and other alternative approaches to developmental neurotoxicity testing (DNT). Environ Toxicol Phar 19, 735-744.

Leu, C., Singer, H., Stamm, C., Muller, S.R., Schwarzenbach, R.P., 2004. Simultaneous assessment of sources, processes, and factors influencing herbicide losses to surface waters in a small agricultural catchment. Environ. Sci. Technol. 38, 3827-3834.

Li, S., Zhao, J., Huang, R., Travers, J., Klumpp-Thomas, C., Yu, W., MacKerell, A.D., Jr., Sakamuru, S., Ooka, M., Xue, F., Sipes, N.S., Hsieh, J.H., Ryan, K., Simeonov, A., Santillo, M.F., Xia, M., 2021. Profiling the Tox21 Chemical Collection for Acetylcholinesterase Inhibition. Environ. Health Perspect. 129, 47008.

Lindner, W., 2004. Fields of application: surface coatings. In: Paulus, W. (Ed.), Directory of microbicides for the protection of materials. Kluwer Academic, 347-376.

Loos, R., Carvalho, R., Antonio, D.C., Comero, S., Locoro, G., Tavazzi, S., Paracchini, B., Ghiani, M., Lettieri, T., Blaha, L., Jarosova, B., Voorspoels, S., Servaes, K., Haglund, P., Fick, J., Lindberg, R.H., Schwesig, D., Gawlik, B.M., 2013. EU-wide monitoring survey on emerging polar organic contaminants in wastewater treatment plant effluents. Water Res. 47, 6475-6487.

Lushchak, V.I., Matviishyn, T.M., Husak, V.V., Storey, J.M., Storey, K.B., 2018. Pesticide Toxicity: A Mechanistic Approach. Excli Journal 17, 1101-1136.

Macova, M., Toze, S., Hodgers, L., Mueller, J.F., Bartkow, M., Escher, B.I., 2011. Bioanalytical tools for the evaluation of organic micropollutants during sewage treatment, water recycling and drinking water generation. Water Res 45, 4238-4247.

Maeder, V., Escher, B.I., Scheringer, M., Hungerbuhler, K., 2004. Toxic ratio as an indicator of the intrinsic toxicity in the assessment of persistent, bioaccumulative, and toxic chemicals. Environ. Sci. Technol. 38, 3659-3666.

Masjosthusmann, S., Blum, J., Bartmann, K., Dolde, X., Holzer, A.K., Stürzl, L.C., Keßel, E.H., Förster, N., Dönmez, A., Klose, J., Pahl, M., Waldmann, T., Bendt, F., Kisitu, J., Suciu, I., Hübenthal, U., Mosig, A., Leist, M., Fritsche, E., 2020. Establishment of an a priori protocol for the implementation and interpretation of an in-vitro testing battery for the assessment of developmental neurotoxicity. EFSA Supporting Publications 17.

Molica, R.J.R., Oliveira, E.J.A., Carvalho, P.V.V.C., Costa, A.N.S.F., Cunha, M.C.C., Melo, G.L., Azevedo, S.M.F.O., 2005. Occurrence of saxitoxins and an anatoxin-a(s)-like anticholinesterase in a Brazilian drinking water supply. Harmful Algae 4, 743-753.

Neale, P.A., Braun, G., Brack, W., Carmona, E., Gunold, R., König, M., Krauss, M., Liebmann, L., Liess, M., Link, M., Schafer, R.B., Schlichting, R., Schreiner, V.C., Schulze, T., Vormeier, P., Weisner, O., Escher, B.I., 2020. Assessing the Mixture Effects in In Vitro Bioassays of Chemicals Occurring in Small Agricultural Streams during Rain Events. Environ. Sci. Technol. 54, 8280-8290.

Neale, P.A., Escher, B.I., 2013. Coextracted dissolved organic carbon has a suppressive effect on the acetylcholinesterase inhibition assay. Environ Toxicol Chem 32, 1526-1534.

Påhlman, S., Ruusala, A.I., Abrahamsson, L., Mattsson, M.E., Esscher, T., 1984. Retinoic acid-induced differentiation of cultured human neuroblastoma cells: a comparison with phorbolester-induced differentiation. Cell Differ. 14, 135-144.

Paraoanu, L.E., Layer, P.G., 2008. Acetylcholinesterase in cell adhesion, neurite growth and network formation. FEBS J 275, 618-624.

Pohanka, M., 2011. Cholinesterases, a target of pharmacology and toxicology. Biomedical Papers of the Medical Faculty of Palacky University in Olomouc 155.

Proenca, S., Escher, B.I., Fischer, F.C., Fisher, C., Gregoire, S., Hewitt, N.J., Nicol, B., Paini, A., Kramer, N.I., 2021. Effective exposure of chemicals in *in vitro* cell systems: A review of chemical distribution models. Toxicol. In Vitro 73, 105133.

Ryan, K.R., Sirenko, O., Parham, F., Hsieh, J.H., Cromwell, E.F., Tice, R.R., Behl, M., 2016. Neurite outgrowth in human induced pluripotent stem cell-derived neurons as a high-throughput screen for developmental neurotoxicity or neurotoxicity. Neurotoxicology 53, 271-281.

Seto, Y., Shinohara, T., 1987. Inhibitory Effects of Paraquat and Its Related-Compounds on the Acetylcholinesterase Activities of Human-Erythrocytes and Electric-Eel (Electrophorus, Electricus). Agricultural and Biological Chemistry 51, 2131-2138.

Silva, V., Silva, C., Soares, P., Garrido, E.M., Borges, F., Garrido, J., 2020. Isothiazolinone Biocides: Chemistry, Biological, and Toxicity Profiles. Molecules 25.

Smirnova, L., Hogberg, H.T., Leist, M., Hartung, T., 2014. Developmental neurotoxicity - challenges in the 21st century and in vitro opportunities. ALTEX 31, 129-156.

Sogorb, M.A., Alvarez-Escalante, C., Carrera, V., Vilanova, E., 2007. An in vitro approach for demonstrating the critical role of serum albumin in the detoxication of the carbamate carbaryl at in vivo toxicologically relevant concentrations. Arch Toxicol 81, 113-119.

Sogorb, M.A., Carrera, V., Vilanova, E., 2004. Hydrolysis of carbaryl by human serum albumin. Arch Toxicol 78, 629-634.

Spinu, N., Bal-Price, A., Cronin, M.T.D., Enoch, S.J., Madden, J.C., Worth, A.P., 2019. Development and analysis of an adverse outcome pathway network for human neurotoxicity. Arch. Toxicol. 93, 2759-2772.

Thullbery, M.D., Cox, H.D., Schule, T., Thompson, C.M., George, K.M., 2005. Differential localization of acetylcholinesterase in neuronal and non-neuronal cells. J Cell Biochem 96, 599-610.

Vaes, W.H.J., Ramos, E.U., Verhaar, H.J.M., Hermens, J.L.M., 1998. Acute toxicity of nonpolar versus polar narcosis: Is there a difference? Environ. Toxicol. Chem. 17, 1380-1384.

van Wezel, A., Opperhuizen, A., 1995. Narcosis Due to Environmental-Pollutants in Aquatic Organisms - Residue-Based Toxicity, Mechanisms, and Membrane Burdens. Crit. Rev. Toxicol. 25, 255-279.

Verhaar, H.J.M., van Leeuwen, C.J., Hermens, J.L.M., 1992. Classifying environmental pollutants. Chemosphere 25, 471-491.

Wilson, C., Gonzalez-Billault, C., 2015. Regulation of cytoskeletal dynamics by redox signaling and oxidative stress: implications for neuronal development and trafficking. Front Cell Neurosci 9, 381.

Yang, Y., Zhang, X.R., Jiang, J.Y., Han, J.R., Li, W.X., Li, X.Y., Leung, K.M.Y., Snyder, S.A., Alvarez, P.J.J., 2022. Which Micropollutants in Water Environments Deserve More Attention Globally? Environ. Sci. Technol. 56, 13-29.

7. Thesis Publications

Publication I

Lee, J., Braun, G., Henneberger, L., König, M., Schlichting, R., Scholz, S., and Escher, B. I. (2021) Critical Membrane Concentration and Mass-Balance Model to Identify Baseline Cytotoxicity of Hydrophobic and Ionizable Organic Chemicals in Mammalian Cell Lines. *Chemical Research in Toxicology* 34, 2100-2109.

Publication II

Lee, J., Escher, B. I., Scholz, S., and Schlichting, R. (2022) Inhibition of neurite outgrowth and enhanced effects compared to baseline toxicity in SH-SY5Y cells. *Archives of Toxicology* 96, 1039-1053.

Publication III

Lee, J., Schlichting, R., König, M., Scholz, S., Krauss, M., and Escher, B. I. (2022) Monitoring mixture effects of neurotoxicants in surface water and wastewater treatment plant effluents with neurite outgrowth inhibition in SH-SY5Y cells. *ACS Environmental Au* 2, 523-535.

Publication IV

Lee, J., Huchthausen, J., Schlichting, R., Scholz, S., Henneberger, L., and Escher, B. I. (2022) Validation of a SH-SY5Y cell-based acetylcholinesterase inhibition assay for water quality assessment. *Environmental Toxicology and Chemistry* 41, 3046-3057.

Publication I

Critical membrane concentration and mass-balance model to identify baseline cytotoxicity of hydrophobic and ionizable organic chemicals in mammalian cell lines

Jungeun Lee,[1] Georg Braun,[1] Luise Henneberger,[1] Maria König,[1] Rita Schlichting[1], Stefan Scholz,[2] and Beate I. Escher,[1,3]*

[1]Department of Cell Toxicology, Helmholtz Centre for Environmental Research – UFZ, Permoserstr. 15, DE-04318 Leipzig, Germany,

[2]Department of Bioanalytical Toxicology, Helmholtz Centre for Environmental Research – UFZ, Permoserstr. 15, DE-04318 Leipzig, Germany,

[3]Environmental Toxicology, Center for Applied Geoscience, Eberhard Karls University Tübingen, Scharrenbergstr. 94-96, DE-72076 Tübingen, Germany

***Address correspondence to:** beate.escher@ufz.de

Published in Chemical Research in Toxicology, DOI: 10.1021/acs.chemrestox.1c00182.

Chemical Research in Toxicology

pubs.acs.org/crt

Article

Critical Membrane Concentration and Mass-Balance Model to Identify Baseline Cytotoxicity of Hydrophobic and Ionizable Organic Chemicals in Mammalian Cell Lines

Jungeun Lee, Georg Braun, Luise Henneberger, Maria König, Rita Schlichting, Stefan Scholz, and Beate I. Escher*

Cite This: *Chem. Res. Toxicol.* 2021, 34, 2100−2109

Read Online

ACCESS | Metrics & More | Article Recommendations | Supporting Information

ABSTRACT: All chemicals can interfere with cellular membranes and this leads to baseline toxicity, which is the minimal toxicity any chemical elicits. The critical membrane burden is constant for all chemicals; that is, the dosing concentrations to trigger baseline toxicity decrease with increasing hydrophobicity of the chemicals. Quantitative structure−activity relationships, based on hydrophobicity of chemicals, have been established to predict nominal concentrations causing baseline toxicity in human and mammalian cell lines. However, their applicability is limited to hydrophilic neutral compounds. To develop a prediction model that includes more hydrophobic and charged organic chemicals, a mass balance model was applied for mammalian cells (AREc32, AhR-CALUX, PPARγ-BLA, and SH-SY5Y) considering different bioassay conditions. The critical membrane burden for baseline toxicity was converted into nominal concentration causing 10% cytotoxicity by baseline toxicity ($IC_{10,baseline}$) using a mass balance model whose main chemical input parameter was the liposome-water partition constants ($K_{lip/w}$) for neutral chemicals or the speciation-corrected $D_{lip/w}$(pH 7.4) for ionizable chemicals plus the bioassay-specific protein, lipid, and water contents of cells and media. In these bioassay-specific models, $\log(1/IC_{10,baseline})$ increased with increasing hydrophobicity, and the relationship started to level off at log $D_{lip/w}$ around 2. The bioassay-specific models were applied to 392 chemicals covering a broad range of hydrophobicity and speciation. Comparing the predicted $IC_{10,baseline}$ and experimental cytotoxicity IC_{10}, known baseline toxicants and many additional chemicals were identified as baseline toxicants, while the others were classified based on specificity of their modes of action in the four cell lines, confirming excess toxicity of some fungicides, antibiotics, and uncouplers. Given the similarity of the bioassay-specific models, we propose a generalized baseline-model for adherent human cell lines: $\log[1/IC_{10,baseline}\ (M)] = 1.23 + 4.97 \times (1 - e^{-0.236 \log D_{lip/w}})$. The derived models for baseline toxicity may serve for specificity analysis in reporter gene and neurotoxicity assays as well as for planning the dosing for cell-based assays.

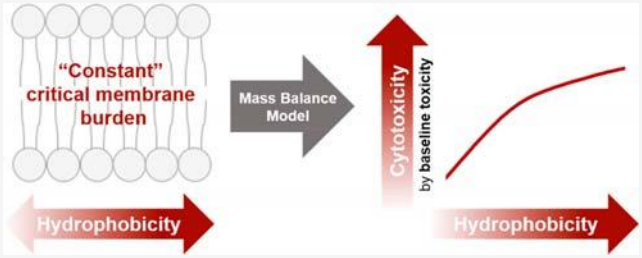

INTRODUCTION

Modes of action (MOA) describe how toxic chemicals act on their target and can be classified into baseline, reactive, and specific toxicity.[1,2] Principally, all chemicals cause baseline toxicity because it is their minimal toxicity caused by the interference of the chemicals with the membrane. Chemicals with more specific MOAs exhibit toxic effects before the baseline toxicity occurs. Therefore, we can identify whether chemicals act through baseline toxicity or more specific MOA by comparing expected baseline toxicity level and the observed toxicity, and the ratio between these two toxicity levels is defined as toxic ratio (TR), which is an indicator for specificity of MOA.[1,3]

Quantitative structure−activity relationships (QSARs) for baseline toxicity describe the relationship between nominal effect concentrations for baseline toxicity and liposome-water partition constants ($K_{lip/w}$), a proxy for biomembrane-water partition constants. Nominal effect concentrations for baseline toxicity depend on hydrophobicity of chemicals. Hydrophobic chemicals can exhibit baseline toxicity at lower nominal concentrations than hydrophilic chemicals as they will accumulate better in cell membranes than hydrophilic chemicals. The QSARs have been established experimentally from effect concentrations of confirmed baseline toxicants in aquatic animals[4−6] and even extended to ionizable organic compounds (IOCs).[7,8] QSAR equations for baseline toxicity have also been developed for eight reporter gene cell lines derived from human and animal cells.[9] The existing QSARs for

Received: May 13, 2021
Published: August 6, 2021

https://doi.org/10.1021/acs.chemrestox.1c00182
Chem. Res. Toxicol. 2021, 34, 2100−2109

in vitro assays were based on hydrophilic and neutral compounds ($0.5 < \log K_{lip/w} < 4.5$), which limits their application to more hydrophobic and charged organic chemicals.

Mass balance models (MBM) can convert nominal concentration (C_{nom}) into membrane concentration (C_{mem}) or freely dissolved concentration (C_{free}) at equilibrium, or *vice versa*, by considering chemical partitioning between different compartments of the bioassay system. C_{nom} is widely used as a dose metric in *in vitro* assays, but the bioavailable portion even from the same C_{nom} may vary for a given chemical depending on the bioassay system. This variability is believed to result mainly from sorption of the chemicals to the biomolecules in the medium such as proteins and lipids, which reduces bioavailability and uptake into cells. Alternatively, C_{mem} and C_{free} have been suggested as more accurate dose metrics than C_{nom} because they better reflect bioavailable concentration and interaction at the target sites, respectively.[10,11] C_{mem} leading to baseline toxicity in cell lines, that is, critical membrane burden (CMB) for 10% reduced cell viability, was found to be constant at 69 mmol L_{lip}^{-1} (95% CI: 49−89) in 8 reporter gene cell lines.[9] The CMB is independent of the type and hydrophobicity of the chemicals,[12] including neutral and charged chemicals,[7,8,13] and is very similar across different cell types[9,13] and various aquatic species.[12,14]

The mass balance models published by Armitage et al.[15] and Fischer et al.[10] described *in vitro* exposure based on chemical partitioning in medium and cells. Each compartment was composed of proteins, lipids, and water, and bovine serum albumin (BSA) and phospholipids represented proteins and lipids in the system, respectively. This model is applicable for both neutral and ionizable compounds; however, the complex behavior of anionic compounds such as specific binding to BSA cannot be modeled simply based on this partitioning process.[16,17] This particularly matters for organic acids that are predominantly negatively charged at the pH 7.4 of the medium.

The aim of this study was to develop a model to predict baseline toxicity, which has a broad applicability in terms of hydrophobicity and speciation (Figure 1). Instead of trying to expand the existing baseline QSAR developed based on hydrophilic known baseline toxicants, we propose a bioassay-specific MBM to predict the nominal inhibitory concentration for cytotoxicity (IC_{10}) from the constant CMB (Figure 1). The predicted nominal baseline toxicity $IC_{10,baseline}$ can then be compared with experimental IC_{10} to identify chemicals that act as baseline cytotoxicants in mammalian cell lines. Our workflow includes evaluation, simplification, and application of the model as outlined in Figure S1. Neutral (253) and ionizable (139) compounds were included, which cover broad ranges of hydrophobicity, speciation, and MOA. Four mammalian cell lines were applied to simulate diverse scenarios with different composition of cells and medium. First, the predicted relationship between partition constants, which is the premise of our model, was verified by experimental partition constants. The MBM was then used to predict $IC_{10,baseline}$ solely based on $K_{lip/w}$ and was applied initially to compounds with experimental partition constants. Lastly, the developed model was simplified for ease of application, and TR was derived from $IC_{10,baseline}$ and experimental IC_{10} to identify baseline toxicants in the test set of chemicals with experimental data.

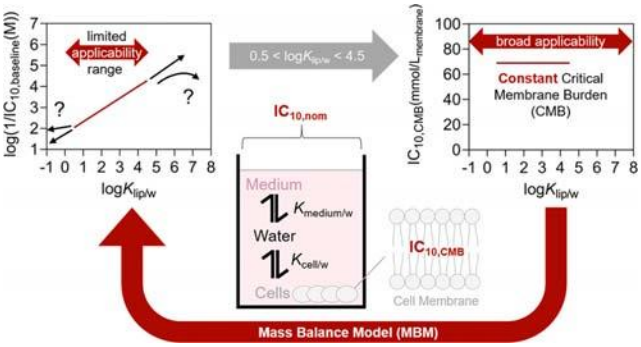

Figure 1. Outline of the study. Chemical distribution between medium, water, and cells was described by $K_{medium/w}$ and $K_{cell/w}$ in a mass balance model (MBM). Nominal concentration causing 10% cytotoxicity by baseline toxicity ($IC_{10,baseline}$) was predicted from critical membrane burden (CMB) for 10% reduced cell viability ($IC_{10,CMB}$) through MBM, and the predicted $IC_{10,baseline}$ was compared with nominal concentration for 10% cytotoxicity from the experiment ($IC_{10,nom}$).

THEORY

Mass Balance Model for Baseline Toxicity. The mass balance model outlined in Figure 1 is a nested model with just two boxes, one for medium and one for cells.[10] Each box is made up of water, proteins, and lipids, albeit with a different composition. Water from the medium connects cells and the other components of the medium and mediates the partitioning processes between the two boxes. The partitioning between the medium and cells ($K_{medium/cell}$) can be broken up into two partitioning processes, the partitioning between medium and water described by the medium-water partition constant ($K_{medium/w}$) and the partitioning between cells and water described by the cell-water partition constant ($K_{cell/w}$).

Within medium and cells, the chemicals can partition between three compartments, i.e., proteins, lipids, and water, and therefore, the $K_{medium/w}$ can be described by the partition constants between proteins and water ($K_{protein/w}$) and the volume fraction of proteins ($Vf_{protein,medium} = V_{protein,medium}/V_{medium}$), the partition constants between lipids and water ($K_{lip/w}$), and the volume fraction of lipids ($Vf_{lip,medium} = V_{lip,medium}/V_{medium}$), as well as the volume fraction of water ($Vf_{w,medium} = V_{w,medium}/V_{medium}$) (eq 1).[10] The analogous equation is defined for $K_{cell/w}$ (eq 2).[10]

$$K_{medium/w} = Vf_{protein,medium} \times K_{protein/w} + Vf_{lip,medium} \times K_{lip/w} + Vf_{w,medium} \quad (1)$$

$$K_{cell/w} = Vf_{protein,cell} \times K_{protein/w} + Vf_{lip,cell} \times K_{lip/w} + Vf_{w,cell} \quad (2)$$

Applying a mass balance, we can then calculate the fraction of chemicals in the medium (f_{medium}, eq 3) and cells (f_{cell}, eq 4).[10]

$$f_{medium} = \frac{1}{1 + \frac{K_{cell/w}}{K_{medium/w}} \frac{V_{cell}}{V_{medium}}} \quad (3)$$

$$f_{cell} = \frac{1}{1 + \frac{K_{medium/w}}{K_{cell/w}} \frac{V_{medium}}{V_{cell}}} \quad (4)$$

The mass balance model inside the cell[9] connects the membrane concentration in the cell ($C_{membrane}$ in general or

https://doi.org/10.1021/acs.chemrestox.1c00182
Chem. Res. Toxicol. 2021, 34, 2100−2109

Table 1. Reporter Gene Cell Lines Evaluated and Descriptors for the Mass Balance Models Taken from Our Previous Study[9] and Determined Newly for SH-SY5Y[a]

cell lines	derived from	number of plated cells/well[b]	mean cell number in assay[c]	total volume of cells V_{cell} (nL)	$Vf_{water,cell}$ (mL/L)	$Vf_{protein,cell}$ (mL/L)	$Vf_{lip,cell}$ (mL/L)
AREc32	MCF7	2500	4300 ± 290	43.0	944[d]	51[d]	5[d]
AhR-CALUX	H4IIe	3000−3250	5360 ± 750	18.9	939[d]	55[d]	6[d]
PPARγ-BLA	HEK293H	4500−5500	5940 ± 760	17.1	887[e]	80[e]	34[e]
SH-SY5Y	SH-SY5Y	3000	3280 ± 20	6.43	942[f]	47[f]	10[f]

[a]Adapted with permission from ref 9 Baseline Toxicity and Volatility Cutoff in Reporter Gene Assays Used for High-Throughput Screening. Copyright 2019 American Chemical Society. [b]The total volume of the medium was 40 μL medium per well in 384-well plates. [c]Cell number is an average between plated cells and final cell number after 24 h of exposure. [d]Henneberger et al.[16] [e]Fischer et al.[10] [f]This study.

specifically for the concentration causing 10% cytotoxicity ($IC_{10,membrane}$) to the total cellular concentration (C_{cell} or $IC_{10,cell}$) by eq 5 with $f_{lip,cell}$ (eq 6) being the fraction of chemical in the lipids of the cell. The $IC_{10,cell}$ can then be converted to nominal concentrations that lead to 10% cytotoxicity, IC_{10}, by eq 7.

$$IC_{10,cell} = IC_{10,membrane} \cdot \frac{Vf_{lip,cell}}{f_{lip,cell}} \quad (5)$$

$$f_{lip,cell} = \frac{1}{1 + \frac{1}{K_{lip/w}}\frac{V_{w,cell}}{V_{lip,cell}} + \frac{K_{protein/w}}{K_{lip/w}}\frac{V_{protein,cell}}{V_{lip,cell}}} \quad (6)$$

$$IC_{10} = \frac{IC_{10,cell}}{f_{cell}} \times \frac{V_{cell}}{V_{medium} + V_{cell}} \quad (7)$$

The critical membrane concentration for baseline toxicity (CMB) corresponds to an $IC_{10,membrane}$ of 69 mM.[9] The associated nominal $IC_{10,baseline}$ for baseline toxicity can be calculated by combining eqs 4, 5, and 7.

$$IC_{10,baseline}(M) = 0.69 \times \frac{Vf_{lip,cell}}{f_{lip,cell}} \times \frac{V_{cell}}{V_{medium} + V_{cell}} \times \left(1 + \frac{K_{medium/w}}{K_{cell/w}} \times \frac{V_{medium}}{V_{cell}}\right) \quad (8)$$

Since $V_{medium} \gg V_{cell}$, we can simplify eq 8 to yield eq 9.

$$IC_{10,baseline}(M) = 0.69 \times \frac{Vf_{lip,cell}}{f_{lip,cell}} \times \left(\frac{V_{cell}}{V_{medium} + V_{cell}} + \frac{K_{medium/w}}{K_{cell/w}}\right) \quad (9)$$

$K_{lip/w}$ as a Sole Descriptor of the Mass Balance Model. In cells, the $K_{protein/w}$ of neutral chemicals can be approximated with BSA as protein surrogate ($K_{BSA/w}$). The liposome-water partition constant ($K_{lip/w}$) uses liposomes as surrogate for the cell lipids, which are mainly membrane lipids.

$K_{BSA/w}$ and $K_{lip/w}$ of neutral organic chemicals can be predicted by simple QSARs from the octanol−water partition constant (log K_{ow}).[18,19]

$$\log K_{BSA/w} = 0.71 \times \log K_{ow} + 0.42 \quad (n = 76,\ R^2 = 0.76,\ SD = 0.43) \quad (10)$$

$$\log K_{lip/w} = 1.01 \times \log K_{ow} + 0.12 \quad (n = 156,\ R^2 = 0.948,\ SD = 0.426) \quad (11)$$

The QSAR for $K_{BSA/w}$ was linear for $1 < \log K_{ow} < 7$,[19] which agreed with the earlier observation that there was approximately a factor of 20 between $K_{BSA/w}$ and $K_{lip/w}$ for neutral chemicals down to log K_{ow} of 2, below which the $K_{BSA/w}$ was leveling off to 1.31 ± 0.62.[20]

The QSAR for $K_{lip/w}$ was linear for $-1 < \log K_{ow} < 8$[18] and stayed virtually constant at a log $K_{lip/w}$ of −1 for log $K_{ow} < -1$.[21]

If eqs 10 and 11 were combined, a direct linear relationship between $K_{lip/w}$ and $K_{BSA/w}$ was obtained (K_{ow} QSAR, eq 12).

$$\log K_{BSA/w} = 0.72 \times \log K_{lip/w} + 0.34 \quad (12)$$

This means that the $IC_{10,baseline}$ can be predicted for chemicals, for which eq 12 holds, merely from the log $K_{lip/w}$ and lipid and protein content of cells and medium. Therefore, this model is theoretically valid only for neutral chemicals. After implementing the model with experimental data for neutral chemicals, we attempted to extend it also to charged chemicals. There are more sophisticated models based on linear solvation energy relationships (LSER), which have been used to retrieve physicochemical properties for the model evaluation, but the baseline toxicity prediction model was meant to be as simple as possible and based on as few input parameters as possible. The log $K_{lip/w}$ can even be substituted by the readily available log K_{ow} (eq 11).

MATERIALS AND METHODS

Chemicals and Partition Constants. We included 392 chemicals in the present analysis (Table S1). All chemicals are listed together with their name, DTXSID, CAS number, and physicochemical properties in Table S2. Experimental octanol−water partition constant log K_{ow} stemmed mainly from PhysPropNCCT or were predicted with using the OPERA model and both were retrieved from the US EPA Comptox Chemistry Dashboard.[22] The acidity constant pK_a and the fraction of neutral and charged species were predicted with ACD/Percepta.[23]

For liposome-water partitioning of the neutral species $K_{lip/w}$, experimental values[7,18,24−31] were preferred over predictions by linear solvation energy relationships (LSER).[32] If no experimental LSER descriptors were available, the $K_{lip/w}$ was predicted from K_{ow} with eq 11 (Table S2). If log $K_{ow} < -1$, $K_{lip/w}$ was fixed at −1.[21] For IOCs with one charged species, the distribution ratio $D_{lip/w}$(pH 7.4) considered their speciation, and experimental values were used, if available,[7,8,16−18,24,26,27,33−35] or calculated from experimental data of the pure species (a few predicted by COSMOmic[8,33]) and the fraction of neutral species ($\alpha_{neutral}$) with eq 13. For the chemicals with multiple charged species, $D_{lip/w}$(pH 7.4) was measured directly at pH 7.4.[16,17,34] If only the $K_{lip/w}$ of the neutral species was available, the $K_{lip/w}$ of the charged species was assumed to be 10 times lower (Δmw = 1) and $D_{lip/w}$(pH 7.4) was calculated with eq 14.[36]

https://doi.org/10.1021/acs.chemrestox.1c00182
Chem. Res. Toxicol. 2021, 34, 2100−2109

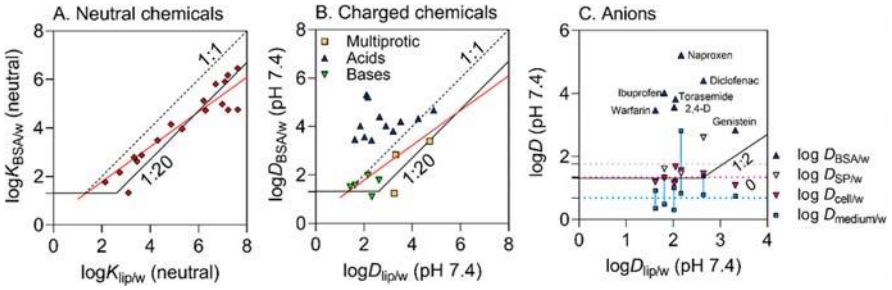

Figure 2. Relationship between liposome-water partitioning ($K_{lip/w}$) and protein (BSA)-water partitioning ($K_{BSA/w}$) of (A) 18 neutral chemicals and (B) ionizable organic chemicals (IOCs; 12 acids, 5 bases, and 3 multiprotic compounds). The data are from Table S2. The red line in both plots is the $K_{BSA/w} - K_{lip/w}$ QSAR (eq 12) and does not constitute a regression of the experimental data. The black line is the 1:20 line reported to be the approximate relationship by DeBruyn and Gobas,[20] which levels off to a constant value of average log $K_{BSA/w}$ of 1.31 at low log K_{ow}. (C) Comparison of $D_{lip/w}$(pH 7.4) (L_w/L_{lip}) with various distribution ratios D, including binding to BSA [$D_{BSA/w}$(pH 7.4) (L_w/L_{BSA})],[38] structural proteins [$D_{SP/w}$(pH 7.4) (L_w/kg$_{SP}$)],[40,47] and distribution between cells and water [$D_{cell/w}$(pH 7.4) (L_w/L_{cell})] and medium and water [$D_{medium/w}$(pH 7.4) (L_w/L_{medium})]. The ranges (blue lines) are given for $D_{medium/w}$ because of nonlinear binding isotherms.[35] The dotted lines represent the mean of the depicted log $D_{SP/w}$, log $D_{cell/w}$, and log $D_{medium/w}$, and the lower value at saturated binding for the medium. Data from Table S3.

$$D_{lip/w}(\text{pH } 7.4) = \alpha_{neutral} \times K_{lip/w}(\text{neutral species}) + (1 - \alpha_{neutral}) \times K_{lip/w}(\text{charged species}) \quad (13)$$

$$D_{lip/w}(\text{pH } 7.4) = K_{lip/w}(\text{neutral species}) \times [\alpha_{neutral} + 10^{-\Delta mw}(1 - \alpha_{neutral})] \quad (14)$$

The binding to proteins was approximated by $K_{BSA/w}$, and only experimental values directly measured at pH 7.4[16−18,37−39] were used for evaluation of the model. For organic acids, BSA is not a suitable model for cellular proteins and therefore experimental distribution ratios to structural proteins ($D_{SP/w}$) as well as experimental distribution ratios between medium and water ($D_{medium/w}$) and cells and water ($D_{cell/w}$) were also retrieved from the literature[16,40] and are listed in Table S3.

Experimental partition constants for, both, lipids and proteins, were available for less than 10% of the chemicals (Table S1) and, therefore, the mass balance model was initially applied only for these chemicals that had both types of experimental data to judge its applicability. After it was established that the model produced reasonable predictions, it was applied to all chemicals that had experimental (23% of the neutral chemicals and 29% of the IOCs) or predicted partition constant for lipids (Table S1).

Cell Lines. Three reporter gene cell lines (AREc32, AhR-CALUX, and PPARγ-BLA) and a human neuroblastoma cell line SH-SY5Y were applied in this study (Table 1). The cell lines were obtained from different sources: AREc32 by courtesy of C. Roland Wolf (Cancer research UK), AhR-CALUX (H4L7.5c2) by courtesy of Michael Denison (UC Davis, USA), PPARγ-BLA from Thermo Fisher Scientific (Schwerte, Germany), and SH-SY5Y from Sigma-Aldrich. SH-SY5Y were differentiated with 10 μM of all-trans retinoic acid (Sigma-Aldrich, R2625) for 72 h before plating. The focus of the study was cytotoxicity and only cytotoxicity was discussed for these four cell lines. For the newly measured hydrophobic compounds (Table S4), the reporter gene activation was additionally reported for the sake of completion. The total volume of the cells (V_{cell}) and their Vf of water, proteins, and lipids were previously quantified or newly calculated for the reporter gene cell lines[9] and measured for differentiated SH-SY5Y cells using the reported methods[10] (Table 1).

Assay Medium. The medium for AREc32 and AhR-CALUX is DMEM GlutaMAX supplemented with 10% FBS and has a protein content $Vf_{protein,medium}$ of 8.93 mL/L and a lipid content $Vf_{lip,medium}$ of 0.14 mL/L.[16] PPARγ-BLA is grown in OptiMEM supplemented with 2% cs-FBS with $Vf_{protein,medium}$ of 4.84 mL/L and a lipid content $Vf_{lip,medium}$ of 0.02 mL/L.[16] The Neurobasal medium (w/o phenol-red) for SH-SY5Y was composed of 2% B-27 Supplement, 2% GlutaMAX Supplement, and was newly characterized with the methods published previously[10] resulting in a $Vf_{protein,medium}$ of 2.58 mL/L and a negligible $Vf_{lip,medium}$. All medium contained 100 U/mL Penicillin and 100 μg/mL Streptomycin, and all medium constituents were purchased from Thermo Fisher Scientific.

Plating. The cells were plated using a MultiFlo Dispenser (Biotek, Vermont, USA) in 384-well plates and incubated for 24 h at 37 °C and 5% CO_2. The number of cells plated is shown in Table 1. The plates were TC-treated for AREc32, poly-D-lysine-coated for AhR-CALUX and PPARγ-BLA, and collagen I-coated plates for SH-SY5Y, and all plates were purchased from Corning (Maine, USA).

Dosing and Cytotoxicity Measurements. For the reporter gene cell lines, chemical stocks dissolved in DMSO were dosed using a Tecan D300e Digital Dispenser (Tecan, Crailsheim, Germany) as described previously, and cell confluency was quantified before dosing and after 24 h of exposure using an IncuCyte S3 live cell imaging system (Essen BioScience, Ann Arbor, Michigan, USA). For SH-SY5Y, chemical stocks were prepared in MeOH due to their high sensitivity to DMSO. The stocks were added into the assay medium, and the dosing medium was diluted and dosed using a pipetting robot (Hamilton Star, Bonaduz, Switzerland). After 24 h exposure, Nuclear Green LCS1 (Abcam, ab138904) and propidium iodide (Sigma-Aldrich, 81845) were added to stain total and dead cells at final concentrations in the well plates of 10 μM and 1 μM, respectively. The cells were stained for 1 h in an incubator, and cell viability was derived by image analysis with the IncuCyte S3.

Cytotoxicity was expressed as % inhibition of cell viability (% cytotoxicity) relative to unexposed cells from measurements of confluency for reporter gene cell lines as described in detail previously.[9] For SH-SY5Y cells, cell viability was calculated based on the ratio of live cell count to total cell count and its relative inhibition to unexposed cells was determined as % cytotoxicity. The concentration causing 10% cytotoxicity (IC_{10}, eq 16) was derived from the slope of the linear portion of the concentration response curve (eq 15), which was typically linear up to a 30 to 40% effect.[41]

$$\%\ \text{cytotoxicity} = \text{slope} \times \text{concentration} \quad (15)$$

$$IC_{10} = \frac{10\%}{\text{slope}} \quad (16)$$

The majority of IC_{10} values listed in Table S2 was already published earlier,[9,42−46] but to expand the MBM also to more hydrophobic chemicals, we measured 75 additional hydrophobic neutral chemicals in AREc32, AhR-CALUX, and PPARγ-BLA; the resulting IC_{10} values are given in Table S4. For SH-SY5Y, cytotoxicity was determined within this study and the resulting IC_{10} values are listed in Table S2. Of the total of 392 chemicals included, 271 of 381 tested chemicals had experimental IC_{10} values in AREc32, 271 of 379 tested chemicals

https://doi.org/10.1021/acs.chemrestox.1c00182
Chem. Res. Toxicol. 2021, 34, 2100−2109

in AhR-CALUX, 216 of 370 tested in PPARγ-BLA, and 22 of 48 in SH-SY5Y. The ones tested but without reported IC_{10} values were either tested at concentrations that were too low (Tox21 data were dosed only up to 100 μM and were reevaluated in our previous study with stricter quality control[44]) or precipitated in the assay and thus could not be used. If precipitation occurred in the newly measured chemicals, which was the case for 17 experiments for reporter gene cell lines, this observation was noted in Table S4. In the case of SH-SY5Y, hydrophobic chemicals had limited solubility from low content of proteins and lipids in the medium and, therefore, precipitates were allowed up to the level where turbidity started to appear. This observation was reported also in Table S4, and these chemicals with a precipitate issue can have uncertainty in the determined IC_{10} values.

Toxic Ratio. The ratio between the predicted IC_{10} for baseline toxicity ($IC_{10,baseline}$) and the experimental IC_{10} is called the toxic ratio (TR, eq 17).[1] Chemicals with TR < 10 are baseline toxicants, and TR ≥ 10 points to an enhanced toxicity due to a specific mode of action or reactive toxicity.[3]

$$TR = \frac{IC_{10,baseline}}{IC_{10}} \quad (17)$$

RESULTS AND DISCUSSION

Distribution Ratios. The mass balance model for baseline toxicity relies on a predictable relationship between liposome-water partitioning and protein−water partitioning. This relationship was derived from published QSARs and resulted in a linear QSAR equation between $K_{lip/w}$ and $K_{BSA/w}$ (eq 12, red line in Figure 2A). For 18 neutral chemicals with cytotoxicity data, both experimental $K_{BSA/w}$ and $K_{lip/w}$ were available and corresponded remarkably well with the QSAR [Figure 2A; mean absolute percentage error (MAPE): 12.7%]. For very hydrophobic neutral chemicals, the $K_{lip/w}$ was approximately 20 times higher than the $K_{BSA/w}$, as already reported by DeBruyn and Gobas,[20] but at lower hydrophobicity the values came closer to each other. At low hydrophobicity (log K_{ow} < 2), the $K_{BSA/w}$ was reported to be 1.31 on average and independent of the hydrophobicity.[20]

For IOCs, their speciation at pH 7.4 should be considered to derive distribution ratios between BSA and water ($D_{BSA/w}$) and between liposomes and water ($D_{lip/w}$). Both experimental distribution ratios $D_{BSA/w}$(pH 7.4) and $D_{lip/w}$(pH 7.4) were available for 12 acids, 5 bases, and 3 multiprotic compounds. Bases and multiprotic chemicals fell well into the prediction range of the QSAR (Figure 2B; MAPE for bases: 25.1%; MAPE for multiprotic chemicals: 26.1%), which is consistent with earlier observations that simple mass balance models can be applied for these types of IOCs.

However, organic acids showed much stronger binding to BSA than predicted from partitioning to lipids (Figure 2B; MAPE: 43.6%). To explore the relationship between $D_{BSA/w}$(pH 7.4) and $D_{lip/w}$(pH 7.4) for organic acids more clearly, we evaluated more organic acids, for which no cytotoxicity data were available, but no clearer pattern emerged (Figure S2), the perfluoroalkyl substances having a ratio of $D_{BSA/w}$(pH 7.4)/$D_{lip/w}$(pH 7.4) of 10 to 1, the carboxylic acids even higher, and the two substituted phenols divergent (10 and 1000). These divergent ratios confirm that binding of anions to BSA cannot be described as a partitioning process. In addition, one needs to consider specific binding to high-affinity sites on BSA that depends on the three-dimensional structure of the molecule and the location of the charge.[38] This specific binding is saturable, which makes binding of anions to BSA concentration-dependent.[16] Therefore, there does not exist a simple relationship between $D_{BSA/w}$(pH 7.4) and $D_{lip/w}$(pH 7.4) for organic anions. The distribution ratios between structural proteins (SP) and water $D_{SP/w}$(pH 7.4) described the binding to cell proteins much better than BSA for organic acids,[16] and their experimental $D_{SP/w}$(pH 7.4) were much smaller than $D_{BSA/w}$(pH 7.4) (Figure 2C, Table S3).

Instead of considering specific types of proteins and lipids as surrogates for proteins and lipids in the medium and cells, the experimental distribution ratios between cells and water ($D_{cell/w}$) and medium and water ($D_{medium/w}$) were explored as alternative descriptors for organic acids (Figure 2C, Table S3). Text S1 discusses some options for how to develop models for anions (Figure S3), but more experimental data would be required for developing a reliable prediction model for organic anions.

Mass Balance Model to Predict Nominal Baseline Toxicity. As we concluded in the theoretical section, $IC_{10,baseline}$ can be predicted merely from the log $K_{lip/w}$ and lipid and protein content of cells and medium for chemicals, for which eq 12 holds. For each cell line, the lipid and protein content of cells (Table 1) and medium (M&M) is known. Therefore, we simulated $IC_{10,baseline}$ (eq 9) with the MBM by assuming that eq 12 is satisfied. In this case, the predicted $IC_{10,baseline}$ (eq 9) only depends on log$K_{lip/w}$ (Figure 3A).

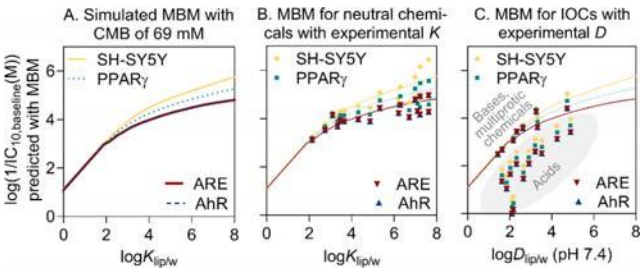

Figure 3. (A) Simulation of $IC_{10,baseline}$ (eq 9) as a function of log $K_{lip/w}$ using the mass balance model (MBM) with a CMB of 69 mM and $K_{BSA/w}$ − $K_{lip/w}$ QSAR (eq 12) to obtain log $K_{BSA/w}$. (B) Evaluation of the simulated MBM (A) with predicted $IC_{10,baseline}$ (symbols) using experimental $K_{lip/w}$ and $K_{BSA/w}$ with the MBM for neutral chemicals. (C) Evaluation of the simulated MBM (A) with predicted $IC_{10,baseline}$ (symbols) using experimental $D_{lip/w}$(pH 7.4) and $D_{BSA/w}$(pH 7.4) with the MBM for IOCs.

Log($1/IC_{10,baseline}$) initially increased linearly with an increase of hydrophobicity with a slope of 1, and there was no difference in the $IC_{10,baseline}$ for the different cell lines (Figure 3A). The relationship started to level off at log $K_{lip/w}$ = 2, and the flattening of the curve was most pronounced for the assays with highest protein content in the medium (AREc32 and AhR-CALUX supplemented with 10% FBS). PPARγ-BLA, whose medium is only supplemented with 1% FBS, shows lower $IC_{10,baseline}$, and the SH-SY5Y have the highest sensitivity due to the low protein content and negligible lipid content of their medium (Figure 3A). The difference in predicted $IC_{10,baseline}$ was largest between AREc32 and SH-SY5Y leading to 9-fold difference at log $K_{lip/w}$ of 8.

The previously published baseline toxicity QSARs[9] were linear but can be interpolated only for 0.5 < log $K_{lip/w}$ < 4.5. The previous QSAR with their slopes of 0.56−0.73 overlays the MBM in this range rather well (Figure S4), confirming the validity of the earlier QSAR. The comparison in Figure S4 demonstrates that the QSAR cannot be linearly extended in

https://doi.org/10.1021/acs.chemrestox.1c00182
Chem. Res. Toxicol. 2021, 34, 2100−2109

either direction because the slope of the linear range of the MBM at log $K_{lip/w}$ < 2 is higher than that of the QSAR equation, and there is further flattening at log $K_{lip/w}$ > 4.5.

The simulated MBM built on the linear relationship of $K_{BSA/w}$ and $K_{lip/w}$ (eq 12) was then compared with $IC_{10,baseline}$ predicted from experimental $K_{BSA/w}$ and $K_{lip/w}$. For neutral compounds, the predictions from experimental values were consistent with the simulated MBM (Figure 3B; MAPE ranges in 4 cell lines between 5.8 and 7.1%), apart from the three very hydrophobic polycyclic aromatic hydrocarbons (PAHs; benzo[a]pyrene, benzo[k]fluoranthene, and benzo[ghi]perylene) that had log $K_{lip/w}$ between 7.0 and 7.6 but log $K_{BSA/w}$ only around 4.7. The equally hydrophobic flame retardants BDE-99, BDE-100, and BDE-153 fell much better on the MBM prediction due to the higher log $K_{BSA/w}$ (5.9−6.5; Table S2). The deviation was larger for the protein-dominated SH-SY5Y medium, which confirms that most likely the cellular protein binding of the PAHs was underestimated by log $K_{BSA/w}$.

IOCs, that is, partially or fully charged organic acids and bases, showed an inconsistent picture (Figure 3C). After applying the speciation-corrected $D_{lip/w}$(pH 7.4) and $D_{BSA/w}$(pH 7.4) (Table S2), agreement between the MBM with predicted and experimental distribution ratios was excellent (ratio 0.3−1.2) for the bases (diphenhydramine, propranolol, metoprolol, verapamil, and venlafaxine; all positively charged at pH 7.4; the range of MAPE in 4 cell lines: 3.1−4.2%) and the multiprotic substances (the range of MAPE in 4 cell lines: 5.3−7.0%) including labetalol (53% cationic, 42% zwitterionic). However, in the case of organic acids, the predicted $IC_{10,baseline}$ values were 7 to 1100 times higher for the experimental D values (Figure 3C; the range of MAPE in 4 cell lines: 109−105678%). The reason for this discrepancy is the high and specific binding affinity of organic acids to BSA that is much higher than predicted by eq 12 as discussed above. We tentatively developed a simplified MBM model for organic acids based on experimental $D_{cell/w}$, $D_{medium/w}$, and $D_{SP/w}$ values, which is preliminarily due to the lack of a sufficient number of data and described in Text S1 and Figure S3.

Simplifying the Baseline MBM to an Empirical QSAR. On the basis of the four bioassays, a generic model for baseline toxicity was established for the following assay condition: mammalian cells, FBS content of medium up to 10%, and 24 h exposure in 384-well plate format (Figure 4). The generic assay condition was determined by averaging the volume fraction of proteins and lipids of the four cell lines ($Vf_{protein,cell}$ of 6% and $Vf_{lip,cell}$ of 1%) and assigning typical medium composition ($Vf_{protein,medium}$ of 0.3% and $Vf_{lip,medium}$ of 0.001%) and total volume of cells V_{cell} of 30 nL in 40 μL medium (V_{medium}). The determined volume fraction for the typical assay conditions was substituted into eq 9 and expanded to IOCs by exchanging $K_{lip/w}$ with $D_{lip/w}$, yielding an equation with only one input parameter, $D_{lip/w}$(pH 7.4) (eq 18, "(pH 7.4)" omitted for simplicity).Figure 4 compares the bioassay-specific simulations from Figure 3A with the simulations for a generic cell and a generic media (eq 18). The lipid and protein content of the medium had a larger influence on the curve shape for more hydrophobic chemicals (Figure 4). The cell composition seems not to have a large influence on the model (simulation not shown).

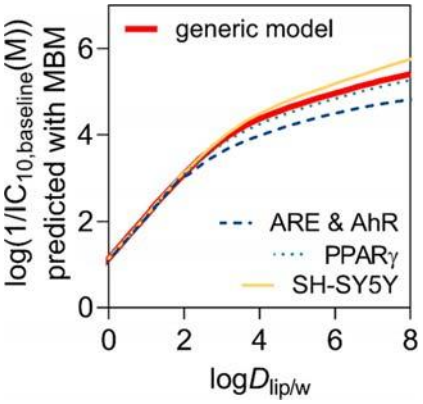

Figure 4. Simulation of hydrophobicity dependence of the MBM with CMB of 69 mM. Comparison of the bioassay-specific models (eq 9 with eq 12 as input) by specific cells and medium and a generic model (thick red line, eqs 18 or 19; mammalian cells, FBS content of medium up to 10%, 24 h exposure in 384-well plate format).

$$IC_{10,baseline}(M) = 6.9 \times 10^{-4} \times \left(1 + \frac{93}{D_{lip/w}} + \frac{6 \times 10^{(0.72 \log D_{lip/w} + 0.34)}}{D_{lip/w}}\right) \times \left(7.5 \times 10^{-4} + \frac{0.003 \times 10^{(0.72 \log D_{lip/w} + 0.34)} + 10^{-5} D_{lip/w} + 0.99}{0.06 \times 10^{(0.72 \log D_{lip/w} + 0.34)} + 10^{-2} D_{lip/w} + 0.93}\right) \quad (18)$$

Despite having only one input parameter, eq 18 remains rather complex and can be simplified into an exponential fit equation (eq 19) for practical applications.

$$\log[1/IC_{10,baseline}(M)] = a + b \times (1 - e^{-c \log D_{lip/w}(pH\ 7.4)}) \quad (19)$$

This model (eq 19) with the fit parameters in Table 2 is visually indistinguishable from eq 18 and can be used for predictions for cell lines, where no protein and lipid contents are available, and the medium has not been characterized under the condition given above. In the same way, the bioassay-specific MBM was also simplified into exponential fit equations using best-fit values (Table 2).

Despite partitioning processes being rather complex and different between neutral chemicals and IOCs, there appears to be a common relationship between log $D_{lip/w}$(pH 7.4) and log($1/IC_{10,baseline}$) independent of the type of chemical and specific for each bioassay combination of cells and medium. Therefore, our simplified model could be applied pragmatically as an "empirical QSAR" for anchoring the measured effects in baseline toxicity. Although the relationship between $D_{lip/w}$(pH 7.4) and $D_{BSA/w}$(pH 7.4) was not satisfied for organic acids (Figure 2B), even organic acids aligned with the predictions of the empirical QSAR (eq 19).

Deriving TR for Classification. $IC_{10,baseline}$ was predicted using the bioassay-specific empirical QSAR for neutral and ionizable compounds and was compared with experimentally determined IC_{10} to calculate TR (Figure 5). As our empirical QSAR entirely depends on $D_{lip/w}$(pH 7.4), more reliable $D_{lip/w}$(pH 7.4) would improve the confidence of our

https://doi.org/10.1021/acs.chemrestox.1c00182
Chem. Res. Toxicol. 2021, 34, 2100−2109

Table 2. Empirical QSAR for Baseline Toxicity: Best-Fit Values from Exponential Fit Equation of Mass Balance Model (MBM) for Baseline Toxicity with Eq 19

			best-fit values (eq 19)		
bioassay	cells	medium	*a*	*b*	*c*
generic[a]	generic cell	generic medium	1.23	4.97	0.236
AREc32	MCF7	DMEM glutamax + 10% FBS	1.25	4.01	0.281
AhR-CALUX	H4lle	DMEM glutamax + 10% FBS	1.25	4.02	0.280
PPARγ-BLA	HEK293H	optiMEM + 2% FBS	1.27	4.71	0.241
SH-SY5Y	SH-SY5Y (differentiated)	neurobasal medium	1.26	5.63	0.202

[a]Mammalian cells, FBS content of medium up to 10%, 24 h exposure in 384-well plate format.

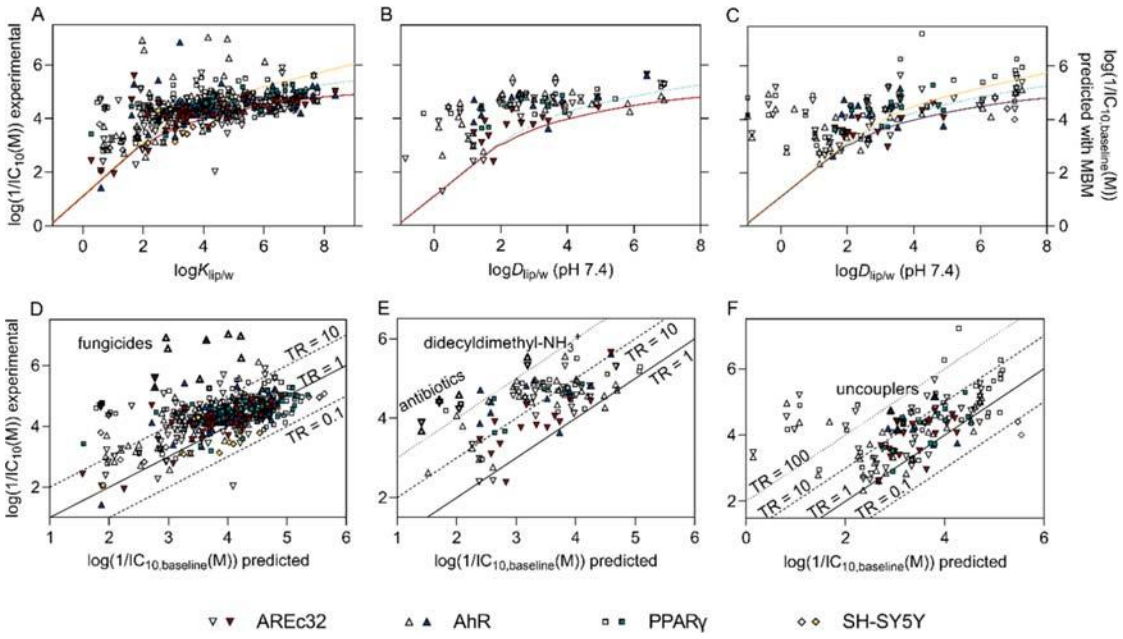

Figure 5. IC_{10} of (A) neutral, (B) cationic and multispecies, and (C) anionic chemicals as a function of experimental (filled symbols) and predicted (empty symbols) $D_{lip/w}$(pH 7.4) overlying the plot of the MBM prediction. Comparison of experimental IC_{10} with $IC_{10,baseline}$ for (D) neutral, (E) cationic and multispecies, and (F) anionic chemicals.

prediction. Due to the limited availability of experimental $D_{lip/w}$(pH 7.4), we took a weight-of-evidence approach to derive $D_{lip/w}$(pH 7.4), which means that experimental values were preferably used over predicted values (LSERD or K_{ow} QSAR) (Table S2). A challenge in our approach is that we cannot decide *a priori* if these chemicals act only as baseline toxicants. Therefore, we also had to take an iterative weight-of-evidence approach and calculate the toxic ratio for all chemicals and evaluate how many classify as baseline toxicants and if that would align with absence of a known specific mode of action. Likewise for those with a TR > 10 it was checked if they have a known specific mode of action.

A general observation can be made from Figure 5 that the more hydrophobic a chemical is, the more likely it is classified as baseline toxicant. Such an observation has been made even for reactive chemicals that are also hydrophobic,[48] suggesting that they might mainly act in the membrane, where they accumulate, rather than on their specific target site.

Classification of Neutral Compounds. Among 59 neutral chemicals with experimental $D_{lip/w}$(pH 7.4), experimental IC_{10} of 51 chemicals fell within a factor of 10 of the $IC_{10,baseline}$ prediction of the MBM and followed the bent baseline toxicity-hydrophobicity curve very well (Figure 5A). These 51 chemicals could be classified as baseline toxicants (TR < 10), while the remaining 8 chemicals indicated specific MOA with TR > 10 in one or more cell lines (Table S5). For further 194 chemicals with predicted $K_{lip/w}$, the majority also aligned well with the prediction of the MBM (Figure 5A). Eighty-eight percent (110/125) were baseline toxicants in AREc32, 79% (99/125) in AhR-CALUX, 80% (80/99) in PPARγ-BLA, and 83% (10/12) in SH-SY5Y (Figure 5D, Table S5). All 7 confirmed baseline toxicants by Vaes et al.[5] fell in the range of 0.1 < TR < 10 either with predicted or experimental $D_{lip/w}$(pH 7.4) and, therefore, were successfully classified as baseline toxicants in all cell lines (experimental IC_{10} was only available for 6 baseline toxicants in PPARγ and SH-SY5Y) (Figure 5A).

Nineteen neutral chemicals (4 chemicals with experimental and 15 with predicted $K_{lip/w}$) had a TR > 10 in AREc32, 32 (6 chemicals with experimental and 26 with predicted $K_{lip/w}$) in AhR-CALUX, 22 (3 chemicals with experimental and 19 with predicted $K_{lip/w}$) in PPARγ-BLA, and 2 (all with predicted $K_{lip/w}$) in SH-SY5Y (Figure 5D, Table S5). Many of those were just around 10, so the TR are quite uncertain given that the partition constant had been predicted. Therefore, we only had a closer look at 21 chemicals whose TR exceeded 50 at least in one cell line. Interestingly, fungicides including diverse strobilurins, dithianon, and isopyrazam were mainly affecting

https://doi.org/10.1021/acs.chemrestox.1c00182
Chem. Res. Toxicol. 2021, 34, 2100−2109

the AhR-CALUX, which could be potentially explained by differences in metabolic capacity of the three cell lines. Especially, strobilurin fungicides showed high TR in AhR-CALUX ranging from 562 to 9176, and they are inhibitors of the electron transport chain in mitochondria and are therefore potent general toxicants.[49,50] In all three reporter gene cell lines, a cancer medicine etoposide showed high TRs between 230 and 271. The antimicrobial agent 1,2-benzisothiazolin-3-one had TRs between 25 and 95 and the fungicide octhilinone had TRs between 19 and 142 in all reporter gene cell lines. Some insecticides had rather high TRs in the reporter gene cell lines, but $D_{lip/w}$(pH 7.4) was predicted, leading to uncertainty of the TR prediction. 3-Hydroxycarbofuran, a metabolite of the acetylcholinesterase inhibitor carbofuran, had a TR of 84 in SH-SY5Y, and the fungicide azoxystrobin also had a TR around 20 for SH-SY5Y. The observed specific toxicity of these chemicals could be aligned with their known mode of action.

Classification of IOCs. The IC_{10} of cationic and multispecies IOCs with experimental $D_{lip/w}$(pH 7.4) generally followed the trend of the empirical QSAR (Figure 5B, Table S6), but the TRs exceeded 10 for many bases and even 50 for a few bases, namely pindolol, irbesartan, and metoprolol (Figure 5E, Table S6). A very large TR was predicted for some medicines, including antibiotics and didecyldimethylammonium, but the $D_{lip/w}$(pH 7.4) for those were predicted and hence uncertain.

A similar picture was seen for the organic anions (Figure 5C, Table S6) with the majority following the empirical QSAR with the exception of highly hydrophilic anionic chemicals, whose $D_{lip/w}$(pH 7.4) were predicted. Among the 25 organic acids with experimental $D_{lip/w}$(pH 7.4), 19 chemicals were baseline toxicants with TR < 10 and only 6 chemicals showed TR > 10 in one or more cell lines. Especially the substituted phenols (2,4-dinitrophenol, bromoxynil, and dinoterb) had TR > 10 (Figure 5F), which is consistent with their specific mode of action of uncoupling. Many of the highly hydrophilic charged chemicals had TRs exceeding 100, but these results are uncertain because in all cases the $D_{lip/w}$(pH 7.4) values were merely predicted and the empirical QSAR uncertain at low $D_{lip/w}$(pH 7.4) values.

Two anionic compounds, hexachlorophene and 3,3′,5,5′-tetrabromobisphenol A, were tested in SH-SY5Y, and both showed TR even lower than 0.1 (Figure 5C, Table S6). This could be due to sorption of compounds to the plates, which was not considered in our prediction model. Larger sorption capacity to the well plastic can be observed especially in the medium with low content of lipids and proteins,[51] which is the case for SH-SY5Y. Furthermore, a positively charged surface of collagen-coated plates could serve as a sink for anionic compounds in SH-SY5Y. The interaction with coating materials especially matters for SH-SY5Y as a large area was uncovered with cells due to a low number of cells used in the assay (Table 1), and collagen has positively charged amino acids at a pH value lower than 9.0.[52] Also, chemicals can be metabolized to less bioactive products, and IC_{10} of these chemicals will also be higher than $IC_{10,baseline}$ and hence may result in TR < 0.1.

CONCLUSION

The developed empirical QSAR would help to predict baseline toxicity of chemicals simply based on their hydrophobicity and is applicable even for chemicals without experimentally determined partition constants simply based on the K_{ow}, but precision and accuracy increase when experimental partition ratios to cell lipids and proteins were used. This empirical QSAR is suitable for any type of chemicals including hydrophobic and ionizable chemicals but needs to be applied for organic acids with caution. The generic model derived from average of our assay condition provides a prediction tool that can be applied broadly to other bioassays with conditions comparable to our assays.

Specificity of MOA can be quantified by comparing the actual toxicity of chemicals with predicted baseline toxicity from the empirical QSAR. The prediction of baseline toxicity also can provide the evidence to determine reasonable dosing concentration considering an expected minimal toxicity level, not merely testing the same concentration over diverse compounds with different toxicity levels.

ASSOCIATED CONTENT

Supporting Information

The Supporting Information is available free of charge at https://pubs.acs.org/doi/10.1021/acs.chemrestox.1c00182.

Detailed information on the workflow, number of available partition constants, experimental physicochemical parameters for organic acids, relationship between liposome-water partitioning and protein-water partitioning of organic acids, comparison of the prediction using the mass balance model for baseline toxicity, empirical QSAR for baseline toxicity for neutral and charged chemicals, predicted $IC_{10,baseline}$, and experimental IC_{10}, as well as toxic ratios (PDF)

Compilation of physicochemical properties, cytotoxicity data, and model results (XLSX)

AUTHOR INFORMATION

Corresponding Author

Beate I. Escher − *Department of Cell Toxicology, Helmholtz Centre for Environmental Research−UFZ, DE-04318 Leipzig, Germany; Environmental Toxicology, Center for Applied Geoscience, Eberhard Karls University Tübingen, DE-72076 Tübingen, Germany;* orcid.org/0000-0002-5304-706X; Phone: +49 341 235-1244; Email: beate.escher@ufz.de; Fax: +49 341 235-1787

Authors

Jungeun Lee − *Department of Cell Toxicology, Helmholtz Centre for Environmental Research−UFZ, DE-04318 Leipzig, Germany*

Georg Braun − *Department of Cell Toxicology, Helmholtz Centre for Environmental Research−UFZ, DE-04318 Leipzig, Germany*

Luise Henneberger − *Department of Cell Toxicology, Helmholtz Centre for Environmental Research−UFZ, DE-04318 Leipzig, Germany;* orcid.org/0000-0002-3181-0044

Maria König − *Department of Cell Toxicology, Helmholtz Centre for Environmental Research−UFZ, DE-04318 Leipzig, Germany*

Rita Schlichting − *Department of Cell Toxicology, Helmholtz Centre for Environmental Research−UFZ, DE-04318 Leipzig, Germany*

Stefan Scholz − *Department of Bioanalytical Toxicology, Helmholtz Centre for Environmental Research−UFZ, DE-04318 Leipzig, Germany*

https://doi.org/10.1021/acs.chemrestox.1c00182
Chem. Res. Toxicol. 2021, 34, 2100−2109

Complete contact information is available at:
https://pubs.acs.org/10.1021/acs.chemrestox.1c00182

Funding

The robotic HTS systems and the D300 dispenser are a part of the major infrastructure initiative CITEPro (Chemicals in the Environment Profiler) funded by the Helmholtz Association with cofunding by the States of Saxony and Saxony-Anhalt.

Notes

The authors declare no competing financial interest.

■ ACKNOWLEDGMENTS

We thank Jenny Braasch, Andreas Baumer, and Niklas Wojtysiak for experimental assistance.

■ REFERENCES

(1) Verhaar, H. J. M., van Leeuwen, C. J., and Hermens, J. L. M. (1992) Classifying environmental pollutants. *Chemosphere 25*, 471−491.

(2) Escher, B. I., and Hermens, J. L. M. (2002) Modes of action in ecotoxicology: Their role in body burdens, species sensitivity, QSARs and mixture effects. *Environ. Sci. Technol. 36*, 4201−4217.

(3) Maeder, V., Escher, B. I., Scheringer, M., and Hungerbuhler, K. (2004) Toxic ratio as an indicator of the intrinsic toxicity in the assessment of persistent, bioaccumulative and toxic chemicals. *Environ. Sci. Technol. 38*, 3659−3666.

(4) Urrestarazu Ramos, E., Vaes, W. H. J., Verhaar, H. J. M., and Hermens, J. L. M. (1998) Quantitative structure-activity relationships for the aquatic toxicity of polar and nonpolar narcotic pollutants. *J. Chem. Inf. Comput. Sci. 38*, 845−852.

(5) Vaes, W. H. J., Ramos, E. U., Verhaar, H. J. M., and Hermens, J. L. M. (1998) Acute toxicity of nonpolar versus polar narcosis: Is there a difference? *Environ. Toxicol. Chem. 17*, 1380−1384.

(6) Klüver, N., Vogs, C., Altenburger, R., Escher, B. I., and Scholz, S. (2016) Development of a general baseline toxicity QSAR model for the fish embryo acute toxicity test. *Chemosphere 164*, 164−173.

(7) Escher, B. I., Baumer, A., Bittermann, K., Henneberger, L., König, M., Kühnert, C., and Klüver, N. (2017) General baseline toxicity QSAR for nonpolar, polar and ionisable chemicals and their mixtures in the bioluminescence inhibition assay with *Aliivibrio fischeri*. *Environ. Sci. Process. Impacts 19*, 414−428.

(8) Klüver, N., Bittermann, K., and Escher, B. I. (2019) QSAR for baseline toxicity and classification of specific modes of action of ionizable chemicals in the zebrafish embryo toxicity test. *Aquat. Toxicol. 207*, 110−119.

(9) Escher, B. I., Glauch, L., Konig, M., Mayer, P., and Schlichting, R. (2019) Baseline Toxicity and Volatility Cutoff in Reporter Gene Assays Used for High-Throughput Screening. *Chem. Res. Toxicol. 32*, 1646−1655.

(10) Fischer, F., Henneberger, L., König, M., Bittermann, K., Linden, L., Goss, K.-U., and Escher, B. (2017) Modeling exposure in the Tox21 *in vitro* bioassays. *Chem. Res. Toxicol. 30*, 1197−1208.

(11) Proenca, S., Escher, B. I., Fischer, F. C., Fisher, C., Gregoire, S., Hewitt, N. J., Nicol, B., Paini, A., and Kramer, N. I. (2021) Effective exposure of chemicals in *in vitro* cell systems: A review of chemical distribution models. *Toxicol. In Vitro 73*, 105133.

(12) van Wezel, A. P., and Opperhuizen, A. (1995) Narcosis Due to Environmental-Pollutants in Aquatic Organisms-Residue-Based Toxicity, Mechanisms and Membrane Burdens. *Crit. Rev. Toxicol. 25*, 255−279.

(13) Escher, B. I., Eggen, R. I. L., Schreiber, U., Schreiber, Z., Vye, E., Wisner, B., and Schwarzenbach, R. P. (2002) Baseline toxicity (narcosis) of organic chemicals determined by *in vitro* membrane potential measurements in energy-transducing membranes. *Environ. Sci. Technol. 36*, 1971−1979.

(14) Escher, B. I., Ashauer, R., Dyer, S., Hermens, J. L., Lee, J. H., Leslie, H. A., Mayer, P., Meador, J. P., and Warne, M. S. (2011) Crucial role of mechanisms and modes of toxic action for understanding tissue residue toxicity and internal effect concentrations of organic chemicals. *Integr. Environ. Assess. Manage. 7*, 28−49.

(15) Armitage, J. M., Wania, F., and Arnot, J. A. (2014) Application of Mass Balance Models and the Chemical Activity Concept To Facilitate the Use of in Vitro Toxicity Data for Risk Assessment. *Environ. Sci. Technol. 48*, 9770−9779.

(16) Henneberger, L., Mühlenbrink, M., Fischer, F. C., and Escher, B. I. (2019) C18-Coated Solid-Phase Microextraction Fibers for the Quantification of Partitioning of Organic Acids to Proteins, Lipids and Cells. *Chem. Res. Toxicol. 32*, 168−178.

(17) Huchthausen, J., Mühlenbrink, M., Konig, M., Escher, B. I., and Henneberger, L. (2020) Experimental Exposure Assessment of Ionizable Organic Chemicals in *In Vitro* Cell-Based Bioassays. *Chem. Res. Toxicol. 33*, 1845−1854.

(18) Endo, S., Escher, B. I., and Goss, K. U. (2011) Capacities of Membrane Lipids to Accumulate Neutral Organic Chemicals. *Environ. Sci. Technol. 45*, 5912−5921.

(19) Endo, S., and Goss, K. U. (2011) Serum albumin binding of structurally diverse neutral organic compounds: data and models. *Chem. Res. Toxicol. 24*, 2293−2301.

(20) deBruyn, A. M. H., and Gobas, F. A. P. C. (2007) The sorptive capacity of animal protein. *Environ. Toxicol. Chem. 26*, 1803−1808.

(21) Gobas, F. A.P.C., Lahittete, J. M., Garofalo, G., Shiu, W. Y., and Mackay, D. (1988) A novel method for measuring membrane-water partition coefficients of hydrophobic organic chemicals: comparison with 1-octanol-water partitioning. *J. Pharm. Sci. 77*, 265−272.

(22) US EPA. (2020) Chemistry Dashboard. https://comptox.epa.gov/dashboard/ (accessed 20 Dec, 2020).

(23) *Build 2726*; Advanced Chemistry Development, Inc./Percepta: Toronto, On, Canada, 2015, http://www.acdlabs.com.

(24) Betageri, G. V., and Rogers, J. A. (1987) Thermodynamics of partitioning of beta-blockers in the normal-octanol-buffer and liposome systems. *Int. J. Pharm. 36*, 165−173.

(25) Vaes, W. H. J., Urrestarazu Ramos, E., Hamwijk, C., van Holsteijn, I., Blaauboer, B. J., Seinen, W., Verhaar, H. J. M., and Hermens, J. L. M. (1997) Solid phase microextraction as a tool to determine membrane/water partition coefficients and bioavailable concentrations in in vitro systems. *Chem. Res. Toxicol. 10*, 1067−1072.

(26) Avdeef, A., Box, K. J., Comer, J. E. A., Hibbert, C., and Tam, K. Y. (1998) pH-metric logP 10. Determination of liposomal membrane-water partition coefficients of ionizable drugs. *Pharm. Res. 15*, 209−215.

(27) Escher, B. I., Schwarzenbach, R. P., and Westall, J. C. (2000) Evaluation of liposome-water partitioning of organic acids and bases. 1. Development of a sorption model. *Environ. Sci. Technol. 34*, 3954−3961.

(28) Jabusch, T. W., and Swackhamer, D. L. (2005) Partitioning of polychlorinated biphenyls in octanol/water, triolein/water and membrane/water systems. *Chemosphere 60*, 1270−1278.

(29) Kwon, J. H., Liljestrand, H. M., and Katz, L. E. (2006) Partitioning of moderately hydrophobic endocrine disruptors between water and synthetic membrane vesicles. *Environ. Toxicol. Chem. 25*, 1984−1992.

(30) Endo, S., Mewburn, B., and Escher, B. I. (2013) Liposome and protein-water partitioning of polybrominated diphenyl ethers (PBDEs). *Chemosphere 90*, 505−511.

(31) Quinn, C. L., van der Heijden, S. A., Wania, F., and Jonker, M. T. O. (2014) Partitioning of Polychlorinated Biphenyls into Human Cells and Adipose Tissues: Evaluation of Octanol, Triolein and Liposomes as Surrogates. *Environ. Sci. Technol. 48*, 5920−5928.

(32) Ulrich, N., Endo, S., Brown, T. N., Watanabe, N., Bronner, G., Abraham, M. H., and Goss, K.-U. (2017) *UFZ-LSER database* v 3.2.1, Helmholtz Centre for Environmental Research-UFZ, Leipzig, Germany,[accessed on 05.02.2021]; http://www.ufz.de/lserd.

(33) Bittermann, K., Spycher, S., Endo, S., Pohler, L., Huniar, U., Goss, K.-U., and Klamt, A. (2014) Prediction of Phospholipid-Water

Partition Coefficients of Ionic Organic Chemicals Using the Mechanistic Model COSMOmic. *J. Phys. Chem. B 118*, 14833−14842.
(34) Ebert, A., Allendorf, F., Berger, U., Goss, K. U., and Ulrich, N. (2020) Membrane/Water Partitioning and Permeabilities of Perfluoroalkyl Acids and Four of their Alternatives and the Effects on Toxicokinetic Behavior. *Environ. Sci. Technol. 54*, 5051−5061.
(35) Henneberger, L., Mühlenbrink, M., Heinrich, D., Teixeira, A., Nicol, B., and Escher, B. I. (2020) Experimental Validation of Mass Balance Models for *in vitro* Cell-based Bioassays. *Environ. Sci. Technol. 54*, 1120−1127.
(36) Escher, B. I., Abagyan, R., Embry, M., Kluver, N., Redman, A. D., Zarfl, C., and Parkerton, T. F. (2020) Recommendations for improving methods and models for aquatic hazard assessment of ionizable organic chemicals. *Environ. Toxicol. Chem. 39*, 269−286.
(37) Vaes, W. H. J., Urrestarazu Ramos, E., Verhaar, H. J. M., Seinen, W., and Hermens, J. L. M. (1996) Measurement of free concentrations using solid phase microextraction: binding to protein. *Anal. Chem. 68*, 4463−4467.
(38) Henneberger, L., Goss, K. U., and Endo, S. (2016) Equilibrium Sorption of Structurally Diverse Organic Ions to Bovine Serum Albumin. *Environ. Sci. Technol. 50*, 5119−5126.
(39) Allendorf, F., Berger, U., Goss, K. U., and Ulrich, N. (2019) Partition coefficients of four perfluoroalkyl acid alternatives between bovine serum albumin (BSA) and water in comparison to ten classical perfluoroalkyl acids. *Environ. Sci. Process. Impacts 21*, 1852−1863.
(40) Henneberger, L., Goss, K. U., and Endo, S. (2016) Partitioning of Organic Ions to Muscle Protein: Experimental Data, Modeling and Implications for *in Vivo* Distribution of Organic Ions. *Environ. Sci. Technol. 50*, 7029−7036.
(41) Escher, B., Neale, P. A., and Villeneuve, D. (2018) The advantages of linear concentration-response curves for *in vitro* bioassays with environmental samples. *Environ. Toxicol. Chem. 37*, 2273−2280.
(42) Escher, B. I., van Daele, C., Dutt, M., Tang, J. Y. M., and Altenburger, R. (2013) Most oxidative stress response in water samples comes from unknown chemicals: the need for effect-based water quality trigger values. *Environ. Sci. Technol. 47*, 7002−7011.
(43) Neale, P. A., Altenburger, R., Ait-Aissa, S., Brion, F., Busch, W., de Aragao Umbuzeiro, G., Denison, M. S., Du Pasquier, D., Hilscherova, K., Hollert, H., Morales, D. A., Novak, J., Schlichting, R., Seiler, T.-B., Serra, H., Shao, Y., Tindall, A. J., Tollefsen, K. E., Williams, T. D., and Escher, B. I. (2017) Development of a bioanalytical test battery for water quality monitoring: Fingerprinting identified micropollutants and their contribution to effects in surface water. *Water Res. 123*, 734−750.
(44) Escher, B. I., Henneberger, L., Konig, M., Schlichting, R., and Fischer, F. C. (2020) Cytotoxicity burst or baseline toxicity? Differentiating specific from nonspecific effects in reporter gene assays. *Environ. Health Perspect. 128*, 077007.
(45) Neale, P. A., Braun, G., Brack, W., Carmona, E., Gunold, R., Konig, M., Krauss, M., Liebmann, L., Liess, M., Link, M., Schafer, R. B., Schlichting, R., Schreiner, V. C., Schulze, T., Vormeier, P., Weisner, O., and Escher, B. I. (2020) Assessing the Mixture Effects in *In Vitro* Bioassays of Chemicals Occurring in Small Agricultural Streams during Rain Events. *Environ. Sci. Technol. 54*, 8280−8290.
(46) Escher, B. I., and Neale, P. A. (2021) Effect-based trigger values for mixtures of chemicals in surface water detected with *in vitro* bioassays. *Environ. Toxicol. Chem. 40*, 487−499.
(47) Endo, S., Brown, T. N., and Goss, K.-U. (2013) General model for estimating partition coefficients to organisms and their tissues using the biological compositions and polyparameter Linear Free Energy Relationships. *Environ. Sci. Technol. 47*, 6630−6639.
(48) Freidig, A. P., Verhaar, H. J. M., and Hermens, J. L. M. (1999) Comparing the potency of chemicals with multiple modes of action in aquatic toxicology: Acute toxicity due to narcosis versus reactive toxicity of acrylic compounds. *Environ. Sci. Technol. 33*, 3038−3043.
(49) Mansfield, R. W., and Wiggins, T. E. (1990) Photoaffinity labelling of the β-methoxyacrylate binding site in bovine heart mitochondrial cytochrome bc1 complex. *Biochim. Biophys. Acta, Bioenerg. 1015*, 109−115.
(50) Müller, M. E., Vikstrom, S., König, M., Schlichting, R., Zarfl, C., Zwiener, C., and Escher, B. I. (2019) Mitochondrial toxicity of micropollutants in water samples measured by the oxygen consumption rate in cells. *Environ. Toxicol. Chem. 38*, 1000−1011.
(51) Fischer, F. C., Cirpka, O. A., Goss, K. U., Henneberger, L., and Escher, B. I. (2018) Application of Experimental Polystyrene Partition Constants and Diffusion Coefficients to Predict the Sorption of Neutral Organic Chemicals to Multiwell Plates in *in Vivo* and *in Vitro* Bioassays. *Environ. Sci. Technol. 52*, 13511−13522.
(52) Uquillas, J. A., and Akkus, O. (2012) Modeling the Electromobility of Type-I Collagen Molecules in the Electrochemical Fabrication of Dense and Aligned Tissue Constructs. *Ann. Biomed. Eng. 40*, 1641−1653.

https://doi.org/10.1021/acs.chemrestox.1c00182
Chem. Res. Toxicol. 2021, 34, 2100−2109

Publication II

Inhibition of neurite outgrowth and enhanced effects compared to baseline toxicity in SH-SY5Y cells

Jungeun Lee,[1] Beate I. Escher,[1,2] Stefan Scholz,[3] and Rita Schlichting[1]

[1]Department of Cell Toxicology, Helmholtz Centre for Environmental Research – UFZ, Leipzig, Germany

[2]Environmental Toxicology, Center for Applied Geoscience, Eberhard Karls University Tübingen, Tübingen, Germany

[3]Department of Bioanalytical Toxicology, Helmholtz Centre for Environmental Research – UFZ, Leipzig, Germany

***Address correspondence to:** beate.escher@ufz.de

Published in Archives of Toxicology, DOI: 10.1007/s00204-022-03237-x.

Archives of Toxicology (2022) 96:1039–1053
https://doi.org/10.1007/s00204-022-03237-x

ORGAN TOXICITY AND MECHANISMS

Inhibition of neurite outgrowth and enhanced effects compared to baseline toxicity in SH-SY5Y cells

Jungeun Lee[1] · Beate I. Escher[1,2] · Stefan Scholz[3] · Rita Schlichting[1]

Received: 6 October 2021 / Accepted: 27 January 2022 / Published online: 19 February 2022

Abstract

Early life exposure to environmental chemicals can cause developmental neurotoxicity (DNT). The impairment of key neurodevelopmental processes such as neurite outgrowth inhibition can be used as endpoints for screening of DNT effects. We quantified neurite-specific effects using the ratio of effect concentrations for cytotoxicity and neurite outgrowth inhibition ($SR_{cytotoxicity}$). Baseline cytotoxicity, the minimal toxicity of any chemical, was used to quantify enhanced cytotoxicity (toxic ratio, TR) and neuronal-specific toxicity ($SR_{baseline}$) by comparing baseline cytotoxicity with the effects on cell viability and neurite outgrowth, respectively. The effects on cell viability and neurite length were measured based on image analysis in human neuroblastoma SH-SY5Y cells. Baseline cytotoxicity was predicted from hydrophobicity descriptors using a previously published model for SH-SY5Y cells. Enhanced cytotoxicity and neuronal-specific toxicity were more often observed for hydrophilic chemicals, which indicates that they are more likely to act through specific modes of action (MOA) on cell viability and neurite outgrowth. Hydrophobic chemicals showed a tendency to act through baseline toxicity without showing specific or enhanced toxicity, but were highly potent considering their low effect concentrations for both cytotoxicity and neurite outgrowth inhibition. The endpoint-specific controls (narciclasine, colchicine, cycloheximide, and rotenone), two carbamates (3-hydroxycarbofuran and carbaryl), and two redox cyclers (diquat and paraquat) showed distinct neurite-specific effects ($SR_{cytotoxicity} > 4$). By comparing neurite-specific effects with enhanced cytotoxicity, one can explain whether the observed effects involve specific inhibition of neurite outgrowth, other specific MOAs, or merely baseline toxicity arising from hydrophobicity.

Keywords Developmental neurotoxicity · Neurite outgrowth · Specificity · Enhanced toxicity · Pesticides

Introduction

The developing nervous system is vulnerable to exposure to environmental chemicals (Giordano and Costa 2012). Despite the high relevance for human health, developmental neurotoxicity (DNT) is only conditionally considered in chemical safety assessment by current OECD test guideline (OECD TG 426). These test guidelines represent in vivo test with developing rats and are very demanding in terms of animal numbers and labor. Therefore, in vitro bioassays may serve as animal-protective and time- and resource-efficient alternatives to animal testing and enable high-throughput screening of environmental chemicals for routine assessment of DNT. Due to the diversity in molecular initiating events (MIE) leading to DNT and limited mechanistic information of the cellular toxicity pathways leading to DNT, the key neurodevelopmental processes are considered as endpoints for testing DNT in vitro rather than the assessment of MIEs (Bal-Price et al. 2015; Lein et al. 2005; Smirnova et al. 2014). Neurite outgrowth, in particular, is an important step in the differentiation of the nervous system as the basis for connectivity and function of neural network in the nervous system, and diverse in vitro models are available to assess effects on neurite outgrowth (Masjosthusmann et al. 2020; Radio and Mundy 2008).

DNT has been reported for many environmental chemicals, in particular, pesticides (Bjorling-Poulsen et al. 2008;

✉ Beate I. Escher
beate.escher@ufz.de

[1] Department of Cell Toxicology, Helmholtz Centre for Environmental Research-UFZ, Leipzig, Germany

[2] Environmental Toxicology, Center for Applied Geoscience, Eberhard Karls University Tübingen, Tübingen, Germany

[3] Department of Bioanalytical Toxicology, Helmholtz Centre for Environmental Research-UFZ, Leipzig, Germany

Grandjean and Landrigan 2006). Pesticides control pests through diverse mechanisms and many insecticides target specific sites in nervous system such as acetylcholinesterase (AChE), acetylcholine receptor (AChR), voltage-gated sodium channel, and γ-aminobutyric acid (GABA) receptor (Casida 2009; Lushchak et al. 2018). DNT of pesticides in non-target organisms is supported by experimental and epidemiological evidence (Bjorling-Poulsen et al. 2008), and commonly used pesticides were confirmed to inhibit neurite outgrowth in PC-12 cells (Christen et al. 2017). Especially, many pesticides of concern for DNT in humans or animals provoked effects in multiple DNT-related endpoints in DNT in vitro testing battery (Masjosthusmann et al. 2020).

In vitro tools have been applied to screen toxicants causing DNT and capture the specific effects on neurite outgrowth. The U.S. National Toxicology Program (NTP) provided a proof-of-concept chemical library (Behl et al. 2019) for testing neurotoxicity and DNT, and high-throughput screening for neurite outgrowth inhibition has been performed on these NTP library compounds (Delp et al. 2018; Ryan et al. 2016). These screening studies quantified specificity of the DNT effects by comparing the ratio between effect concentrations or benchmark concentrations derived for neurite outgrowth inhibition and cytotoxicity, and demonstrated that specific effects on neurite outgrowth inhibition can be distinguished from general cytotoxic effects. Masjosthusmann et al. (2020) applied multiple DNT assays to chemicals presumed to be developmental neurotoxicants and negative controls, and the endpoints related to neurite morphology were the most sensitive in 11% of 119 chemicals if the neuronal network formation assay was excluded and 7% of 60 chemicals if it was included (Masjosthusmann et al. 2020). While specificity of DNT was evaluated by comparing the effect concentrations to levels of cytotoxicity in these studies, the distance to levels of baseline toxicity, which is the minimal toxicity of any chemical, can provide further understanding of the observed DNT effects.

Baseline toxicity represents a nonspecific mode of action (MOA) and results from membrane interference of chemicals. Baseline toxicity is driven by hydrophobicity of chemicals, and can be assessed and predicted easily in experimental systems with a partition-based exposure, but is applicable to any organism and cell type. The interference of chemicals with membranes leads to a critical membrane burden causing 10% cytotoxicity that was reported to stay constant (69 $mmol \cdot L_{lip}^{-1}$) over diverse mammalian cells (Escher et al. 2019). Accordingly, a quantitative structure–activity relationship (QSAR) was developed to predict nominal concentration of baseline cytotoxicity for multiple in vitro assays including also human neuroblastoma SH-SY5Y cells (Lee et al. 2021). Hydrophobicity—described by partition constants between liposomes (membrane bilayer vesicles) and water ($K_{lip/w}$)—serves as a single descriptor of the baseline cytotoxicity QSAR (Lee et al. 2021).

The predicted baseline cytotoxicity has been applied to estimate how potent the observed toxicity is for the target endpoint compared to the minimal toxicity, and the enhanced toxicity over baseline cytotoxicity indicates the involvement of specific MOA (Escher et al. 2020). The current approach using cytotoxicity as a reference for DNT is useful to quantify how important neurite outgrowth is compared to general cytotoxic effects on neuronal cells that integrate all modes of action leading to cytotoxicity. In contrast, baseline toxicity is independent of cell type (or organism), and, therefore, can provide additional metrics to quantify any elevated toxicity that occurs in neuronal cells compared to nonspecific effects from baseline toxicity. Many pesticides are highly hydrophobic, and hence, they already provoke strong toxic effects via baseline toxicity. However, it has not been explored yet if pesticides exert specific MOA leading to enhanced cytotoxicity or toxicity to the target endpoint compared to baseline cytotoxicity in the neuronal cells. Therefore, these additional measures considering baseline toxicity can provide further details to the current approach considering the ratio of effects on neurite outgrowth to cytotoxicity.

We aim to identify the degree of specificity and elevated cytotoxicity of effects for pesticides and environmental chemicals on neurite outgrowth. Differentiated SH-SY5Y cells were used to test the effects of chemicals on cell viability and neurite outgrowth. Effect concentrations were then compared to predicted baseline cytotoxicity using QSAR developed for differentiated SH-SY5Y cells (Lee et al. 2021). SH-SY5Y cells can be differentiated into more mature neuron-like cells, and retinoic acid is commonly applied for differentiation (Agholme et al. 2010; Biedler et al. 1973; Kovalevich and Langford 2013; Påhlman et al. 1984). The cell viability and neurite length were measured by image analysis. The focus was set on pesticides that target nervous system or energy metabolism. For comparison, we included the assessment of endpoint-specific controls, i.e., highly specific positive controls for neurite outgrowth (Aschner et al. 2017; Krug et al. 2013), including narciclasine, colchicine, cycloheximide, and rotenone, all of which are natural plant-derived chemicals. Confirmed baseline toxicants (Vaes et al. 1998) were applied as negative controls. Additional chemicals from the NTP (US National Toxicology Program) library such as endocrine disrupting chemicals were also tested for comparison. The test chemicals were then classified based on their specific effects on neurite outgrowth.

Materials and methods

Chemicals

Endpoint-specific positive controls for neurite outgrowth (Aschner et al. 2017), known baseline toxicants (Vaes et al.

1998), and pesticides with diverse MOAs (Casida 2009) and some endocrine disrupting chemicals (EDCs) were tested in this study (Table S1). Additionally, polycyclic aromatic hydrocarbons (PAHs), polybrominated diphenyl ethers (PBDEs), and polychlorinated biphenyls (PCBs) from the NTP library were tested for comparison (Table S2). The chemical stocks were prepared in methanol. For chemicals with higher water solubility, methanol was evaporated under a stream of nitrogen gas prior to adding the appropriate amount of assay medium. For chemicals with low solubility, the stock solution was directly added to dosing medium and the final concentration of methanol in assay plates was limited to a maximum of 1% which was found to not cause any effects on cell viability and neurite outgrowth inhibition.

Selection of cell model and cell culture

SH-SY5Y cells and Lund human mesencephalic (LUHMES) cells were considered as candidates for developing high-throughput screening assay detecting effects on neurite outgrowth. LUHMES cells are currently used to test effects of chemicals on neurite outgrowth in DNT in vitro battery mainly and they have the advantage of a non-oncogenic origin (Masjosthusmann et al. 2020). In the present study, we selected SH-SY5Y cells for screening effects on neurite outgrowth because of their easier maintenance and availability of commercial 384-well plates with appropriate coating for adherence of cell monolayers.

SH-SY5Y cells (Sigma-Aldrich, 94,030,304) were cultured at 37 °C in 5% CO2 in incubator. Growth medium consisted of 90% of DMEM/F12 (Gibco, 11,320,074) and 10% of heat-inactivated fetal bovine serum (Gibco, 10,500,064) with 100 U/mL penicillin and 100 µg/mL streptomycin (Gibco, 15,140,122). Cells were used from passage 5 only up to passage 15 to avoid senescence.

Plating cells and dosing

Before the assay, SH-SY5Y cells were differentiated in flasks for 72 h using 10 µM all-trans retinoic acid (Sigma-Aldrich, R2625). The differentiation medium was composed of Neurobasal™ medium with phenol-red (Gibco, 21,103,049) supplemented with 2% B-27™ Supplement (Gibco, 17,504,044), 2 mM GlutaMAX™ (Gibco, 35,050,061), and 100 U/mL penicillin and 100 µg/mL streptomycin. For seeding and dosing, phenol-red free Neurobasal™ medium (Gibco, 12,348,017) was used as differentiation medium.

The differentiated cells were plated at density of 3,000 cells/well in Collagen I-coated 384-well plates (Corning, 354,667). 30 µL medium containing differentiated cells and 10 µM all-trans retinoic acid were added into each well using a MultiFlo™ Dispenser (Biotek, Vermont, USA). The last two columns of each plate were used as control with or without cells. The seeded cells were incubated for further 24 h in the incubator.

Dosing medium was prepared either by directly adding chemical stocks or blowing down stock solution with nitrogen gas. The dosing medium was then diluted in serial or linear dilution, and 10 µL of diluted dosing medium was transferred to the plates using a pipetting robot (Hamilton Star, Bonaduz, Switzerland). Eleven concentrations were tested with two technical replicates for each chemical, and exposure concentrations were selected based on predicted baseline toxicity and adjusted in case limited solubility was observed. We allowed turbidity only up to the level it started to be observed by eyes and these chemicals with turbidity issue are flagged. In each assay plate, narciclasine and MeOH were included as positive control (Aschner et al. 2017; Delp et al. 2019) and solvent control, respectively. The tests were repeated at least in three independent experimental runs for the chemicals which showed effects on the first test set. The inactive chemicals were not tested further, but the predicted baseline cytotoxicity values are noted in Table S2. After dosing, the cells were kept in the incubator for 24 h.

Neurite outgrowth measurement

Neurite length was measured and analyzed in phase-contrast image by an IncuCyte® S3 live cell imaging system (Essen BioScience, Ann Arbor, Michigan, USA). After 24 h exposure, phase-contrast images were recorded in each well with a 10X objective lens, which imaged 36% of the well area. The total neurite length per image was quantified by IncuCyte® NeuroTrack software module (Fig. S1), and the neurite length relative to control was used to express the effects on neurite outgrowth. The cells got clustered or partially detached in the wells where most cells were dead; therefore, the neurite length was not normalized by the cell numbers to avoid possible artifacts. In case significant stimulating effects were observed in neurite outgrowth, total neurite length divided by total cell counts was also evaluated for comparison to exclude artifacts from different cell numbers and verify the stimulating effects observed in original data analysis.

For quality assurance, phase-contrast images were taken from each well at 30 min after seeding to quantify artifacts caused by scratches on the plate bottom or fine dust fluff. When this background signal was higher than three times the standard deviation of the mean background signal, the image was flagged and checked if any artifacts were observed.

Viability test

After capturing phase-contrast images, Nuclear Green™ LCS1 (Abcam, ab138904) and propidium iodide

(Sigma-Aldrich, 81,845) were used to stain total and dead cells, respectively. The stains were diluted in phosphate-buffered saline (PBS) to make the final concentration of 10 µM Nuclear Green™ LCS1 and 1 µM propidium iodide. 10 µL of the mixture was added into each well with a multi-channel pipette and the plates were incubated for 1 h in the incubator. Fluorescence images were derived with a 10× objective lens in green (excitation wavelength: 460 nm; emission wavelength: 524 nm; acquisition time: 300 ms) and red (585 nm; 635 nm; 400 ms) fluorescence channel. The stained cell objects were counted with Basic analyzer mode in IncuCyte® S3 software (Fig. S1), and cell viability was calculated by dividing the number of live cells (total-dead cells) by those of total cells. The decrease in cell viability compared to unexposed cells was defined as cytotoxicity.

Data evaluation

The analysis model for the concentration–response curves (CRC) was selected among three models: a linear regression model, a log-logistic model, and the Brain–Cousens model (Brain and Cousens 1989; Ritz et al. 2015).

CRC typically shows linearity up to 30% effect level and the effect concentration can be derived from the slope of interpolation line as described previously by Escher et al. (2018) using Eq. (1).

$$\%\ \text{cell viability or neurite length} = 100\% - \text{slope} \times \text{concentration (M)}, \quad (1)$$

Data up to 30% effect level were included in linear CRC analysis when no plateau was observed. The concentration leading to 10% cytotoxicity (IC_{10}) and 10% neurite outgrowth inhibition (EC_{10}) was determined using Eqs. 1 and 2

$$IC_{10} = \frac{10\%}{\text{slope}}, \quad (2)$$

$$EC_{10} = \frac{10\%}{\text{slope}}. \quad (3)$$

For the log-logistic model (Eq. 4), data of all effect levels were included for analysis and the IC_{10} or EC_{10} were derived with the following equations:

$$\%\ \text{cell viability or neurite length} = 100\% - \frac{100}{1 + 10^{\left(\log\left(\frac{EC_{50}}{\text{concentration(M)}}\right) \times \text{slope}\right)}}, \quad (4)$$

$$\log EC_{50} = \log EC_{10} - \left(\frac{1}{\text{slope}}\right) \times \log\left(\frac{90}{10}\right). \quad (5)$$

Equations 1 and 4 were fitted with GraphPad prism (version 9, San Diego, California, USA). Standard errors were calculated with error propagation according to Escher et al. (2018).

The Brain–Cousens model is for hormetic *U*-shaped curves and was also applied to whole data using the drc package in *R* studio version 4.0.4 (Brain and Cousens 1989; Ritz et al. 2015). The equation that used for Brain–Cousens model is

$$\%\ \text{neurite length} = c + \frac{d - c + f \times \text{concentration}(\mu\text{M})}{1 + \exp(b(\log(\text{concentration}(\mu\text{M})/e))}, \quad (6)$$

where the concentration is given in micromolar units (µM), and b, c, d, f, and e are adjustable parameters. The parameter f quantifies the degree of hormesis, that is, stimulating effects and a higher f implies stronger hormetic effect. The derived best-fit values of model parameters were used as input parameters to calculate EC_{10} for stimulating effects (i.e., 110% of controls) and inhibiting effects (90% of controls). EC_{10} for inhibiting effects were calculated using the ED command in R

The CRC models used to estimate effect concentrations for cell viability and neurite length were selected based on a decision tree as indicated in Fig. S2. Among the three models mentioned above, the linear regression model (Eq. 1) was applied preferentially to fit CRCs of both endpoints. When the IC_{10} and EC_{10} could not be derived with 95% confidence interval from the interpolation line of linear regression or when the data did not follow linearity (e.g., reached a plateau), a log-logistic model (Eq. 4) was applied instead. In case of neurite length, the Brain–Cousens model was applied for chemicals that stimulated neurite outgrowth. When neurite length over 110% was observed in more than two independent experimental sets, the significance of the hormesis parameter f was checked in Brain–Cousens model and the model was applied only when the parameter was significant (p value < 0.05).

Prediction of $IC_{10,baseline}$ from a baseline cytotoxicity QSAR for SH-SY5Y cells

Nominal concentrations for baseline cytotoxicity leading to 10% cytotoxicity ($IC_{10,baseline}$) were predicted with a baseline toxicity prediction model based on a quantitative structure–activity relationship (QSAR) derived specifically for differentiated SH-SY5Y cells (Lee et al. 2021). IC_{10} values reported here were already published and used for application of this baseline cytotoxicity QSAR by Lee et al. (2021). The baseline toxicity prediction model can predict $IC_{10,baseline}$ solely from the liposome–water partition

constants ($K_{lip/w}$) and more details of the baseline toxicity prediction model are given in Text S1. The pH-corrected liposome–water distribution ratios ($D_{lip/w}$) were used for charged chemicals according to Lee et al. (2021).

Calculation of toxic ratio and specificity ratios

The toxic ratio (TR) is a measure to estimate if the cytotoxic effects of tested chemicals are caused by a specific MOA (Maeder et al. 2004). TRs are obtained by comparing the observed cytotoxic effects (experimental IC_{10}) and predicted cytotoxicity caused by baseline toxicity ($IC_{10,baseline}$), as shown in Table 1, using the equation

$$TR = \frac{IC_{10,baseline}}{IC_{10}}. \quad (7)$$

Chemicals with $0.1 < TR < 10$ are typically classified as baseline toxicants, and a specific MOA is suggested for cytotoxic effects when $TR > 10$ (Maeder et al. 2004)

A similar approach has been taken to calculate specific effects on target endpoints compared to either baseline toxicity or cytotoxicity for many different in vitro reporter gene assays (Escher et al. 2020). The specificity ratio, $SR_{cytotoxicity}$, is the ratio between EC_{10} for a specific endpoint in a reporter gene assay and the experimental IC_{10} for cytotoxicity with Eq. 8

$$SR_{cytotoxicity} = \frac{IC_{10}}{EC_{10}}. \quad (8)$$

In case of neurotoxicity addressed in the present study, we applied this equation using the EC_{10} of inhibition of neurite outgrowth and the IC_{10} for cytotoxicity toward differentiated neuronal cell lines. An analogous equation (Table 1) has been applied previously for the neurite outgrowth inhibition assay to identify "DNT-specific" effects (Delp et al. 2018; Masjosthusmann et al. 2020) or for identification of "neurite-specific" effects (Delp et al. 2021). Krug et al. (2013) defined a threshold of 4 to discriminate chemicals specifically acting on neurite outgrowth. We applied the same threshold of 4 for identification of "neurite-specific" effects using $SR_{cytotoxicity}$

The specificity ratio, $SR_{baseline}$, is the ratio of the effect concentration (EC_{10}) and the associated predicted $IC_{10,baseline}$ by Eq. 9

$$SR_{baseline} = \frac{IC_{10,baseline}}{EC_{10}}. \quad (9)$$

$SR_{baseline}$ can quantify how specifically chemicals can act on certain endpoints compared to minimal toxicity caused by baseline toxicity and this helps identify if specific MOAs contribute to the effects on the certain endpoints. According to Escher et al. (2020), $SR_{baseline} \leq 1$ was considered as nonspecific, $1 \leq SR_{baseline} < 10$ as moderately specific (with high uncertainty), $10 \leq SR_{baseline} < 100$ as specific, and $100 \leq SR_{baseline}$ as highly specific. For the purpose of the present study, we only used the threshold of $SR_{baseline}$ of 10 to differentiate between nonspecific and specific effects. $SR_{baseline}$ has not previously been applied for DNT. Delp et al. (2021) had used cytotoxicity in the U2OS osteosarcoma cell line as an indicator of nonspecific toxicity to identify "neuronal-specific" effects. We suggest that the predicted baseline toxicity in the same cell line measured under identical conditions (Lee et al. 2021) is an even better descriptor of nonspecific effects. The specific effects compared to baseline toxicity derived from $SR_{baseline}$ will be referred as "neuronal-specific" toxicity henceforth to distinguish it from "neurite-specific" effects compared to cytotoxicity ($SR_{cytotoxicity}$)

The terms "neurite-specific" $SR_{cytotoxicity}$ and "neuronal-specific" $SR_{baseline}$ allow one to differentiate between an enhanced effect caused by direct interference with neurite

Table 1 Terminology for evaluation of effects in in vitro assays in general and for developmental neurotoxicity (DNT)

Description	General definition	Reference	Definition for DNT	Reference
Toxic ratio TR: specific mode of action if $TR > 10$	$TR = IC_{10,baseline}/IC_{10}$	Maeder et al. (2004)	Enhanced cytotoxicity of neuronal cells relative to baseline toxicity	This study
Specific effects relative to cytotoxicity	$SR_{cytotoxicity} = IC_{10}/EC_{10}$	Escher et al. (2020)	Neurite-specific: effects of neurite outgrowth inhibition relative to cytotoxicity	This study; Delp et al. (2021)
			DNT-specificity = EC_{50}(viability)/EC_{50}(neurite area)	Krug et al. (2013); Delp et al. (2018)
Specific effects relative to baseline toxicity	$SR_{baseline} = IC_{10,baseline}/EC_{10}$	Escher et al. (2020)	Neuronal-specific: effects of neurite outgrowth inhibition relative to baseline toxicity	This study; Delp et al. (2021)

growth and those enhanced effects that are specific (such as mitochondrial toxicity) but not specific to neurites but affects the entire neuronal cell. Even chemicals that do not show neurite-specific effects can still show enhanced neurite degeneration compared to baseline toxicity due to neuronal-specific effects if $SR_{cytotoxicity} < 4$ and $SR_{baseline} > 10$. The highest tested concentration was used to calculate the upper limit of TR, TR_{max}, and lower limits of $SR_{cytotoxicity,min}$ for chemicals that only showed effects on neurite outgrowth and no cytotoxicity. The connection between effect concentrations and ratios is visualized in Fig. 1A, demonstrating that $\log SR_{baseline} = \log SR_{cytotoxicity} + \log TR$.

Results and discussion

Assay performance

Endpoint-specific controls, that is, positive control chemicals for neurite outgrowth, showed high activity in the micromolar-to-nanomolar concentration range and were neurite-specific inhibitors of neurite outgrowth (Table 2). Narciclasine, the assay's positive control, inhibited neurite outgrowth at the lowest EC_{10} showing the strongest effect potency among all tested chemicals. The selection of the endpoint-specific controls was originally based on specific effects on neurite outgrowth observed in LUHMES cells considering the ratio between EC_{50} and IC_{50} (Krug et al. 2013). The effect for all endpoint-specific controls (narciclasine, cycloheximide, colchicine, and rotenone) detected with the present experimental setup in SH-SY5Y cells corresponded well with cytotoxicity and neurite outgrowth inhibition observed in LUHMES cells by Krug et al. (2013), which confirmed the performance of our assay. Although EC_{50} values were derived for LUHMES cells and, therefore, slightly higher effect concentrations were reported than the corresponding IC_{10} or EC_{10} in SH-SY5Y cells, the effect concentrations for neurite outgrowth endpoint align within a factor of 10 (Fig. S3).

It is remarkable that neurite-specific inhibitors were also highly neuronal-specific, that is, their TR and $SR_{baseline}$ were also very high. Only for cycloheximide neurite-specific effects dominated over neuronal-specific effects. Narciclasine, in contrast, had a TR of 6 million, which means that it is highly toxic to neuronal cells, but the specific effect on neurite outgrowth is moderate compared to this with a $SR_{cytotoxicity}$ of 42.

Effects in relation to hydrophobicity of the chemicals

IC_{10} for cytotoxicity and EC_{10} for neurite outgrowth inhibition or stimulation were determined with best-fit model parameters (Table S3) from the CRCs (Fig. S4). The effect concentrations are given with the applied CRC model, calculated ratios, classification, and experimental issues due to turbidity/precipitation for all individual chemicals in Table 2. The IC_{10} (Fig. 1B) and EC_{10} (Fig. 1C) were plotted against the hydrophobicity expressed as $\log K_{lip/w}$ and compared with predictions for $IC_{10,baseline}$ calculated with the baseline cytotoxicity QSAR (Eq. S1; Table 2).

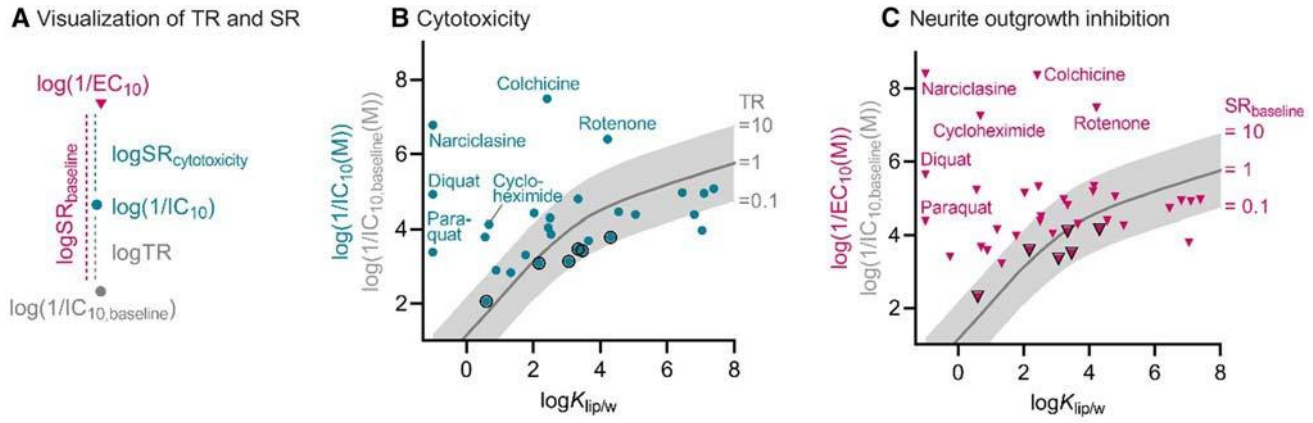

Fig. 1 Inhibitory and effect concentrations against hydrophobicity of test chemicals. **A** Visualization of the toxic ratio TR (Eq. 7), the specificity ratios $SR_{cytotoxicity}$ for neurite-specific effects (Eq. 8), and $SR_{baseline}$ for neuronal-specific effects (Eq. 9). **B** Cytotoxicity as a function of the hydrophobicity expressed as liposome–water partition constants ($K_{lip/w}$). The turquoise circles are the experimental inhibitory concentration for cytotoxicity (IC_{10}; Table 2) with known baseline toxicants encircled in black. **(C)** Neurite outgrowth inhibition as a function of $K_{lip/w}$. Magenta triangles indicate concentration leading to 10% reduction in neurite length (EC_{10}; Table 2) which were experimentally determined in differentiated SH-SY5Y cells with known baseline toxicants encircled in black. Thick gray lines in both plots **B** and **C** correspond to predicted baseline toxicity causing 10% cytotoxicity ($IC_{10,baseline}$; Eq. S1) as a function of $K_{lip/w}$. The gray areas indicate when TR or $SR_{baseline}$ is between 0.1 and 10

Table 2 Toxicity values for quantification of enhanced cytotoxicity (TR), neuronal-specific effects ($SR_{baseline}$), and neurite-specific effects ($SR_{cytotoxicity}$)

Group	Chemical name	Baseline toxicity			Cytotoxicity			Neurite outgrowth inhibition			TR	$SR_{baseline}$	$SR_{cytotoxicity}$	Group classification[e]	Remarks[f]
		log-K_{ow}[a]	log-$K_{lip/w}$[a]	$IC_{10,baseline}$ (M)	IC_{10} (M)[b]	SE or CI[c]	Model[d]	EC_{10} (M)	SE or CI[c]	Model[d]					
Endpoint-specific controls	Narciclasine	− 1.2	− 1	1	$1.7 \cdot 10^{-7}$	$1.6 \cdot 10^{-8}$	L	$3.9 \cdot 10^{-9}$	$3.6 \cdot 10^{-10}$	L	$6.0 \cdot 10^{6}$	$2.5 \cdot 10^{8}$	42	1	
	Cycloheximide	0.6	0.7	$1.0 \cdot 10^{-2}$	$7.7 \cdot 10^{-5}$	[$6.2 \cdot 10^{-5}$, $9.5 \cdot 10^{-5}$]	LL	$5.6 \cdot 10^{-8}$	$7.7 \cdot 10^{-9}$	L	136	$1.9 \cdot 10^{5}$	1370	1	Pl
	Colchicine	1.3	2.4	$3.7 \cdot 10^{-4}$	$3.3 \cdot 10^{-8}$	[$2.2 \cdot 10^{-8}$, $4.7 \cdot 10^{-8}$]	LL	$4.2 \cdot 10^{-9}$	$5.0 \cdot 10^{-10}$	L	$1.1 \cdot 10^{4}$	$8.7 \cdot 10^{4}$	7.7	1	Pl
	Rotenone	4.1	4.2	$3.2 \cdot 10^{-5}$	$4.0 \cdot 10^{-7}$	$4.1 \cdot 10^{-8}$	L	$3.4 \cdot 10^{-8}$	$4.3 \cdot 10^{-9}$	L	81	948	11.7	1	
Baseline toxicants	2-Butoxyethanol	0.8	0.6	$1.3 \cdot 10^{-2}$	$8.7 \cdot 10^{-3}$	$5.9 \cdot 10^{-4}$	L	$4.9 \cdot 10^{-3}$	$1.1 \cdot 10^{-3}$	L	1.5	2.6	1.8	3	
	3-Nitroaniline	1.4	2.2	$5.5 \cdot 10^{-4}$	$8.1 \cdot 10^{-4}$	$4.5 \cdot 10^{-5}$	L	$2.6 \cdot 10^{-4}$	$3.5 \cdot 10^{-5}$	L	0.7	2.1	3.1	3	
	2-Allylphenol	2.6	3.1	$1.4 \cdot 10^{-4}$	$7.3 \cdot 10^{-4}$	$3.6 \cdot 10^{-5}$	L	$4.5 \cdot 10^{-4}$	$4.5 \cdot 10^{-5}$	L	0.2	0.3	1.6	3	
	4-Chloro-3-methylphenol	3.1	3.3	$9.4 \cdot 10^{-5}$	$3.4 \cdot 10^{-4}$	$1.0 \cdot 10^{-5}$	L	$8.0 \cdot 10^{-5}$	$1.0 \cdot 10^{-5}$	L	0.3	1.2	4.3	2	
	2-Phenylphenol	3.1	3.5	$8.0 \cdot 10^{-5}$	$3.8 \cdot 10^{-4}$	[$3.4 \cdot 10^{-4}$, $4.1 \cdot 10^{-4}$]	LL	$3.2 \cdot 10^{-4}$	[$2.8 \cdot 10^{-4}$, $3.5 \cdot 10^{-4}$]	LL	0.2	0.3	1.2	3	
	4-Pentylphenol	4.2	4.3	$2.9 \cdot 10^{-5}$	$1.7 \cdot 10^{-4}$	[$1.6 \cdot 10^{-6}$, $1.8 \cdot 10^{-4}$]	LL	$7.0 \cdot 10^{-5}$	$6.9 \cdot 10^{-6}$	L	0.2	0.4	2.4	3	
AChE inhibitors	3-Hydroxycarbofuran	0.8	0.6	$1.4 \cdot 10^{-2}$	$1.6 \cdot 10^{-4}$	$1.2 \cdot 10^{-5}$	L	$6.0 \cdot 10^{-6}$	$8.8 \cdot 10^{-7}$	L	84	2283	27	1	
	Carbaryl	2.4	2.5	$3.5 \cdot 10^{-4}$	$9.1 \cdot 10^{-5}$	$6.5 \cdot 10^{-6}$	L	$4.9 \cdot 10^{-6}$	$6.6 \cdot 10^{-7}$	L	3.8	71	19	1	
	Diazoxon	2.1	0.9	$6.5 \cdot 10^{-3}$	$1.3 \cdot 10^{-3}$	$1.5 \cdot 10^{-4}$	L	$2.7 \cdot 10^{-4}$	$2.6 \cdot 10^{-5}$	L	5.1	24	4.7	1	
	Paraoxon-ethyl	2	1.8	$1.1 \cdot 10^{-3}$	$4.9 \cdot 10^{-4}$	$3.9 \cdot 10^{-5}$	L	$1.1 \cdot 10^{-4}$	$1.1 \cdot 10^{-5}$	L	2.2	11	4.7	1	
	Chlorpyrifos-oxon	3.3	2.5	$3.0 \cdot 10^{-4}$	$1.4 \cdot 10^{-4}$	[$1.3 \cdot 10^{-4}$, $1.4 \cdot 10^{-4}$]	LL	$3.3 \cdot 10^{-5}$	$3.8 \cdot 10^{-6}$	L	2.2	9.1	4.2	2	
nAChR agonists	Thiamethoxam	− 0.1	− 0.3	$1.1 \cdot 10^{-1}$	I ($3.1 \cdot 10^{-3}$)		–	$3.9 \cdot 10^{-4}$	$3.8 \cdot 10^{-5}$	L	< 35	271	> 7.7	–	
	Imidacloprid	0.6	0.7	$1.0 \cdot 10^{-2}$	I ($4.8 \cdot 10^{-4}$)		–	$2.1 \cdot 10^{-4}$	$2.7 \cdot 10^{-5}$	L	< 21	47	> 2.3	–	
	Thiacloprid	1.3	1.2	$3.4 \cdot 10^{-3}$	I ($1.2 \cdot 10^{-4}$)		–	$7.0 \cdot 10^{-5}$	$1.2 \cdot 10^{-5}$	L	< 28	49	> 1.7	–	
	Acetamiprid	1.2	1.3	$2.6 \cdot 10^{-3}$	$1.5 \cdot 10^{-3}$	$8.1 \cdot 10^{-5}$	L	$6.2 \cdot 10^{-4}$	$6.2 \cdot 10^{-5}$	L	1.8	4.2	2.4	3	
	Clothianidin	0.7	2.9	$1.8 \cdot 10^{-4}$	I ($2.8 \cdot 10^{-4}$)		–	$9.3 \cdot 10^{-5}$	$1.1 \cdot 10^{-5}$	L	< 0.6	1.9	> 3.1	–	
GABA blockers	Fipronil	4.0	2.5	$3.2 \cdot 10^{-4}$	$5.2 \cdot 10^{-5}$	[$5.1 \cdot 10^{-5}$, $5.3 \cdot 10^{-5}$]	LL	$4.3 \cdot 10^{-5}$	–	B	6.2	7.5	1.2	3	Pr
	Fipronil sulfone	3.2	3.3	$9.4 \cdot 10^{-5}$	$1.6 \cdot 10^{-5}$	[$1.5 \cdot 10^{-5}$, $1.7 \cdot 10^{-5}$]	LL	$1.6 \cdot 10^{-5}$	-	B	5.9	5.9	1.0	3	Pr
	α-Endosulfan	3.8	4.6	$2.2 \cdot 10^{-5}$	$3.5 \cdot 10^{-5}$	[$3.2 \cdot 10^{-5}$, $3.8 \cdot 10^{-5}$]	LL	$4.2 \cdot 10^{-5}$	-	B	0.6	0.5	0.8	3	Pr
	Dieldrin	5.4	5.1	$1.4 \cdot 10^{-5}$	$4.1 \cdot 10^{-5}$	$3.0 \cdot 10^{-6}$	L	$5.5 \cdot 10^{-5}$	-	B	0.3	0.2	0.7	3	Pr
Sodium channel agonists	Bifenthrin	6.8	6.5	$4.3 \cdot 10^{-6}$	$1.1 \cdot 10^{-5}$	$6.5 \cdot 10^{-7}$	L	$2.0 \cdot 10^{-5}$	–	B	0.4	0.2	0.6	3	
	4,4'-DDT	6.9	7.1	$2.8 \cdot 10^{-6}$	$1.1 \cdot 10^{-5}$	$9.1 \cdot 10^{-7}$	L	$1.2 \cdot 10^{-5}$	–	B	0.2	0.2	0.9	3	Pr

Table 2 (continued)

Group	Chemical name	Baseline toxicity			Cytotoxicity			Neurite outgrowth inhibition			TR	$SR_{baseline}$	$SR_{cytotoxicity}$	Group classification[e]	Remarks[f]
		log-K_{ow}[a]	log-$K_{lip/w}$[a]	$IC_{10,baseline}$ (M)	IC_{10} (M)[b]	SE or CI[c]	Model[d]	EC_{10} (M)	SE or CI[c]	Model[d]					
Mitochondrial toxicants	Azoxystrobin	2.5	2.0	$7.0 \cdot 10^{-4}$	$3.8 \cdot 10^{-5}$	$2.1 \cdot 10^{-6}$	L	$7.4 \cdot 10^{-6}$	$1.9 \cdot 10^{-6}$	L	18	94	5.1	1	
	Picoxystrobin	3.6	3.2	$1.1 \cdot 10^{-4}$	I ($7.3 \cdot 10^{-5}$)		–	$1.1 \cdot 10^{-5}$	$2.1 \cdot 10^{-6}$	L	< 1.5	10	> 6.7	–	
	Fluoxastrobin	4.0	4.1	$3.6 \cdot 10^{-5}$	I ($3.6 \cdot 10^{-5}$)		–	$6.6 \cdot 10^{-6}$	$9.4 \cdot 10^{-7}$	L	< 1.0	5.4	> 5.4	–	
	Pyraclostrobin	4.0	4.1	$3.5 \cdot 10^{-5}$	I ($3.5 \cdot 10^{-5}$)		–	$4.7 \cdot 10^{-6}$	$8.8 \cdot 10^{-7}$	L	< 1.0	7.4	> 7.4	–	
	Trifloxystrobin	4.5	4.8	$1.8 \cdot 10^{-5}$	I ($3.2 \cdot 10^{-5}$)		–	$9.2 \cdot 10^{-6}$	$2.5 \cdot 10^{-6}$	L	< 0.6	1.9	> 3.4	–	
	Hexachlorophene	7.5	6.8	$3.4 \cdot 10^{-6}$	$4.2 \cdot 10^{-5}$	$3.5 \cdot 10^{-6}$	L	$1.2 \cdot 10^{-5}$	–	B	0.1	0.3	3.5	3	
Redox cyclers	Paraquat	–1.8	– 1	1	$4.2 \cdot 10^{-4}$	[$2.8 \cdot 10^{-4}$, $6.0 \cdot 10^{-4}$]	LL	$4.2 \cdot 10^{-5}$	$6.1 \cdot 10^{-6}$	L	2400	$2.4 \cdot 10^{4}$	9.8	1	Pl
	Diquat	– 2.0	– 1	1	$1.2 \cdot 10^{-5}$	[$9.0 \cdot 10^{-6}$, $1.6 \cdot 10^{-5}$]	LL	$2.3 \cdot 10^{-6}$	$2.6 \cdot 10^{-7}$	L	$8.3 \cdot 10^{4}$	$4.4 \cdot 10^{5}$	5.3	1	Pl
Endocrine disruptors	Bisphenol A	3.3	3.7	$6.3 \cdot 10^{-5}$	$2.0 \cdot 10^{-4}$	$2.7 \cdot 10^{-5}$	L	$5.1 \cdot 10^{-5}$	$6.7 \cdot 10^{-6}$	L	0.3	1.2	4.0	3	
	3,3′,5,5′-Tetra- bromobisphenol A	6.7	7.0	$2.9 \cdot 10^{-6}$	$1.1 \cdot 10^{-4}$	$7.0 \cdot 10^{-6}$	L	$1.6 \cdot 10^{-4}$	–	B	0.03	0.02	0.7	3	
	Di(2-ethylhexyl) phthalate	7.5	7.4	$2.3 \cdot 10^{-6}$	$8.5 \cdot 10^{-6}$	[$6.7 \cdot 10^{-6}$, $1.0 \cdot 10^{-5}$]	LL	$1.1 \cdot 10^{-5}$	[$8.8 \cdot 10^{-6}$, $1.4 \cdot 10^{-5}$]	LL	0.3	0.2	0.8	3	Pr

[a] $\log K_{ow}$ and $\log K_{lip/w}$ were derived as described in Lee et al. (2021)

[b] I: Inactive; highest tested concentration (M) was given in brackets

[c] Standard error (SE) for IC_{10} or EC_{10} in linear regression; 95% confidence interval (CI) for IC_{10} or EC_{10} in log-logistic model

[d] L: linear regression; LL: log-logistic model; B: Brain–Cousens model

[e] Group 1: $SR_{cytotoxicity} > 4$, $SR_{baseline} > 10$; group 2: $SR_{cytotoxicity} > 4$, $SR_{baseline} < 10$; group 3: $SR_{cytotoxicity} < 4$, $SR_{baseline} < 10$

[f] Pr: precipitation/turbidity observed; Pl: Plateau observed in concentration–response curves for cell viability

Many chemicals had TRs, a measure for enhanced cytotoxicity, between 0.1 and 10 and were classified as baseline toxicants in SH-SY5Y cells (Fig. 1B). Among 37 chemicals, 70% were baseline toxicants (26 chemicals including the 6 known baseline toxicants). The remaining 11 chemicals included the 4 endpoint-specific controls and their TR exceeding 10 indicated that specific MOAs rather than baseline toxicity could be involved in cytotoxicity. The analysis for diquat and paraquat is highly uncertain, because they have double cationic charges, are very hydrophilic, and are therefore outside the applicability domain of the baseline cytotoxicity QSAR (Lee et al. 2021). Their $\log K_{lip/w}$ was assumed to be -1 as for other very hydrophilic chemicals (Gobas et al. 1988). This estimate still gave highly elevated cytotoxicity with $TR > 10^3$, which is reasonable given that they act as redox cyclers forming radicals and reactive oxygen species (Bonneh-Barkay et al. 2005; Conning et al. 1969). When we had a closer look at pesticides (24 pesticides except endpoint-specific controls), 71% of them had TRs of baseline toxicants. The chemicals with $TR > 10$ were mostly observed for chemicals with $\log K_{lip/w} < 4$, and therefore, TR was more likely to be higher for hydrophilic chemicals.

Similar trends with respect to hydrophobicity were observed for neuronal-specific effects, i.e., the ratio of $IC_{10,baseline}$ to the EC_{10} for neurite outgrowth inhibition (Fig. 1C). Neuronal-specific effects were again mostly observed for hydrophilic chemicals with $\log K_{lip/w} < 4$. $SR_{baseline}$ ranged from 0.02 to 2.5 $\times 10^8$, and 41% of the tested chemicals exceeded $SR_{baseline}$ of 10, which is only 11% more than those that exceeded TR of 10. When it comes to neurite-specific effects, $SR_{cytotoxicity}$ ranged from 0.6 to 1370, and high specificity was observed especially for endpoint-specific controls, carbamates, and redox cyclers (Table 2).

Hydrophobic chemicals were mostly classified as baseline cytotoxicants and, hence, appear more likely to trigger both cytotoxicity and neurite outgrowth inhibition through baseline toxicity (Fig. 1). However, they are still very potent due to their high hydrophobicity and were with the lowest EC_{10} and IC_{10} among the pesticides. Apart from the known baseline toxicants, 63% of chemicals that did not act neuronal-specific ($SR_{baseline} < 10$) exceeded a $\log K_{lip/w}$ of 4, and IC_{10} and EC_{10} for these chemicals were close to $IC_{10,baseline}$.

Enhanced effects over baseline cytotoxicity (TR and $SR_{baseline}$)

The tested chemicals were categorized into nine MOA classes, and their $IC_{10,baseline}$, IC_{10}, and EC_{10} were grouped in Fig. 2 by their MOA classes with an increasing $K_{lip/w}$ within each class.

The four endpoint-specific controls were extremely neuronal-specific and showed highly enhanced cytotoxicity (Fig. 2). Their effect potency considering nominal concentration was the highest among the MOA groups. TR ranged from 81 to 6.0×10^6 and $SR_{baseline}$ ranged from 948 to 2.5×10^8 for this group of chemicals. Narciclasine, a toxic alkaloid found in *Amaryllidaceae* plants, showed the most neuronal-specific effects ($SR_{baseline} = 2.5 \times 10^8$) and its cytotoxicity also enhanced the most over baseline toxicity ($TR = 6.0 \times 10^6$) among all tested chemicals. Cycloheximide was also extremely neuronal-specific, which are more contributed by specific effects on neurite outgrowth than by cytotoxicity considering $SR_{cytotoxicity} > TR$. In contrast, the neuronal-specific effects were more contributed by enhanced cytotoxicity than specific effects on neurite outgrowth for plant-derived alkaloid colchicine and isoflavone rotenone. The endpoint-specific controls are all naturally occurring toxic substances but also have been synthesized, and cycloheximide and rotenone were used as pesticides (Richardson et al. 2019).

All well-known baseline toxicants (2-butoxyethanol, 3-nitroaniline, 2-allylphenol, 4-chloro-3-methylphenol, 2-phenylphenol, and 4-pentylphenol), which are industrial chemicals, were confirmed as baseline toxicants with respect to cytotoxicity as well as neurite outgrowth inhibition (Fig. 2). They all showed no enhanced cytotoxicity compared to baseline toxicity with TR from 0.2 to 1.5 and no neuronal-specific effects $SR_{baseline}$ from 0.3 to 2.6, which proved our assay quality as negative controls. Despite all of them lacking specific MOAs, they differed in the effect potency by a factor of 50 for cytotoxicity (IC_{10}) and 70 for neurite outgrowth inhibition (EC_{10}) due to the variation in hydrophobicity.

Neuronal-specific toxicity was mostly accompanied by enhanced cytotoxicity, which led to highly elevated effect potency for inhibition of neurite outgrowth compared to baseline toxicity (Fig. 2). Among the pesticides, carbamates (3-hydroxycarbofuran and carbaryl) and redox cyclers (paraquat and diquat) showed high neuronal specificity, and high TRs were also observed for these two groups except carbaryl. This means that these pesticides are neurotoxic, but that inhibition of neurite outgrowth is not the cause but a consequence of their neurotoxic effect triggered by another initiating event, such as potentially mitochondrial toxicity.

The hydrophobicity-dependent trends were maintained within the same MOA group for the pesticides as TR and $SR_{baseline}$ tended to increase with decreasing hydrophobicity within the group. However, except carbamates and redox cyclers, the pesticides with determined IC_{10} were mostly classified as baseline toxicants for the SH-SY5Y cells. The two hydrophobic chemical groups (all with $\log K_{lip/w} > 4$), GABA receptor blockers (fipronil, fipronil sulfone, α-endosulfan, and dieldrin), and sodium channel agonists (bifenthrin, 4,4′-DDT) did not exceed TR nor SR thresholds, and thus classified as baseline toxicants for the tested endpoints. Highly hydrophobic chemicals such as

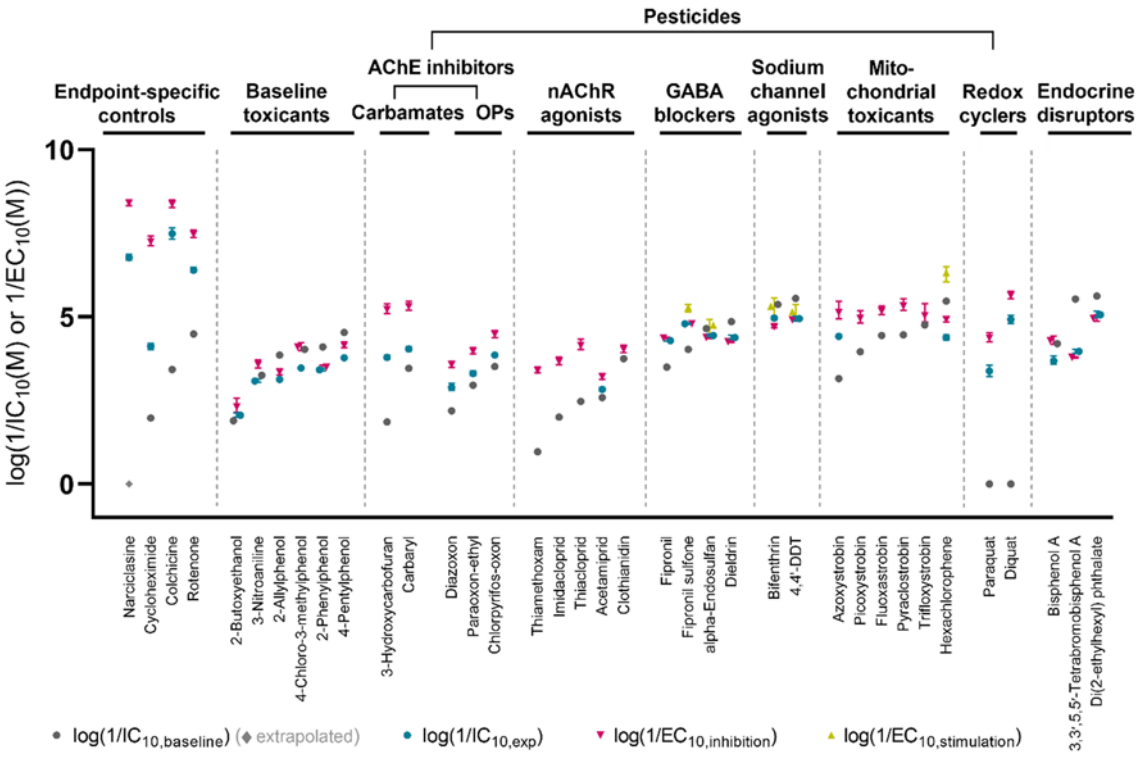

Fig. 2 Effect concentrations for baseline toxicity, cytotoxicity, and neurite outgrowth inhibition or stimulation sorted by MOA class. $IC_{10,baseline}$ for baseline toxicity (extrapolated for very hydrophilic chemicals), $IC_{10,exp}$ for cytotoxicity, and EC_{10} for inhibiting or stimulating effects on neurite outgrowth in different groups of chemicals were shown in the order of increasing $K_{lip/w}$ within each MOA class. The test chemicals include endpoint-specific controls for neurite outgrowth inhibition (Aschner et al. 2017), known baseline toxicants (Vaes et al. 1998), pesticides with diverse mode of action grouped into the MOA classes of acetylcholinesterase (AChE) inhibitors, nicotinic acetylcholine receptor (nAChR) agonists, γ-aminobutyric acid (GABA)-gated chloride channel blockers, voltage-gated sodium channel agonists, mitochondrial toxicants, redox cyclers, and endocrine disruptors. The error bars represent the 95% confidence intervals; in case of very small confidence intervals, error bars are hidden by the symbol

pyrethroids other than bifenthrin, PAHs, PCBs, and PBDEs were inactive up to $IC_{10,\ baseline}$ (Table S2). It has often been observed that very hydrophobic chemicals are highly toxic, but do not show any excess toxicity over baseline (Escher and Hermens 2002). This implies that they do not bind to specific receptors and/or that accumulation in membranes is the dominant process.

EDCs were tested to evaluate DNT effects of typical environmental chemicals that do not have any primary neurotoxic MOAs. All three EDCs from the NTP library were classified as baseline toxicants and did not show enhanced cytotoxicity or neuronal-specific toxicity in SH-SY5Y cells (Fig. 2). The experimental effect concentrations for 3,3′,5,5′-tetrabromobisphenol A were higher than the expected baseline toxicity possibly due to uncertainty in predicted $IC_{10,baseline}$ for anionic chemicals (Lee et al. 2021).

Neuronal-specific effects can be caused not only by specific MOA affecting neurite outgrowth directly but also by enhanced cytotoxicity. The latter case is not neurite-specific, since their effects on neurite outgrowth just resulted from adverse effects on overall cell health, which necessitates quantification of neurite-specific effects in the following section.

Neurite-specific effects ($SR_{cytotoxicity}$)

For neurite-specific effects, a threshold of 4 was used to define the specific effects on neurite outgrowth compared to cytotoxicity ($SR_{cytotoxicity} > 4$), which was proposed by Krug et al. (2013) and confirmed independently by our calculation (Text S2; Table S4). All chemicals with $SR_{cytotoxicity} > 4$ had EC_{10} which clearly distinguished from IC_{10} considering the overlap of their average + 3 standard deviation or their confidence interval given in Table 2.

All four endpoint-specific controls had neurite-specific effects (Fig. 2). $SR_{cytotoxicity}$ ranged from 7.7 to 1370 for these chemicals, which are all above the defined threshold. Our assay control, narciclasine, inhibited neurite outgrowth specifically ($SR_{cytotoxicity} = 42$) possibly by activation of Rho signaling pathway which regulates actomyosin contractility. Cycloheximide inhibits protein synthesis by interfering with translocation step, and showed the most specific effects on

neurite outgrowth inhibition among all the tested chemicals with $SR_{cytotoxicity}$ of 1370. Colchicine, a microtubule polymerization inhibitor, and rotenone, a mitochondrial toxicant, showed relatively moderate specificity with $SR_{cytotoxicity}$ of 7.7 and 11.7, respectively.

As expected, the six known baseline toxicants all showed nonspecific effects on neurite outgrowth with $SR_{cytotoxicity}$ from 1.2 to 3.1, except for 4-chloro-3-methylphenol having $SR_{cytotoxicity}$ slightly over the threshold (4.3).

AChE inhibitors, which are used as insecticides, showed different patterns depending on their interaction at the target site (Fig. 2). Carbamates bind reversibly to AChE to disturb the enzymatic function, while organophosphates (OP) bind irreversibly (Colovic et al. 2013), and both undifferentiated and differentiated SH-SY5Y cells are known to express AChE (de Medeiros et al. 2019). The two reversible AChE inhibitors, 3-hydroxycarbofuran and carbaryl, showed $SR_{cytotoxicity} > 10$ and their specificity and effect potency for neurite outgrowth inhibition were the highest among the tested pesticides. For the three irreversible AChE inhibitors, $SR_{cytotoxicity}$ stayed fairly constant at around 4.5, close to the $SR_{cytotoxicity}$ threshold of 4. The role of AChE in neurite outgrowth has been reviewed, and can be explained by both enzymatic and non-enzymatic way (Paraoanu and Layer 2008). It was described that secreted acetylcholine could signal to AChE of adjacent cells to direct neurite outgrowth, while AChE also could directly support neurite outgrowth by structural interaction with extracellular matrix protein such as laminin. However, it should be still elucidated whether reversible and irreversible AChE inhibitors could behave differently in these processes.

Other specific MOAs may exist for carbamates which caused specific effects on neurite outgrowth with minor effects on cell viability. While mechanistic understanding remains limited for DNT, it has been reported that impairment of signaling pathways can disturb neurodevelopmental processes including neurite outgrowth (Bal-Price et al. 2018; Masjosthusmann et al. 2020). The interaction with signaling pathways may also be responsible for effects on differentiation of cells and it has been reported that carbofuran impaired neuronal differentiation through transforming growth factor beta (TGF-β) signaling, which mediates neurogenesis, in rat hippocampus (Seth et al. 2017). This observation can explain our results as we tested cells in early differentiation stage with short-term differentiation compared to the previous studies (Constantinescu et al. 2007; Shipley et al. 2016).

The mitochondrial toxicants are all applied as fungicides in agriculture and showed broad specificity of their effects on neurite outgrowth, although these pesticides commonly target mitochondrial respiration representing a basal function of all cells (Fig. 2). Rotenone, one of the endpoint-specific controls, showed specific effects despite of its high hydrophobicity, which suggests that specific toxicity can still manifest if the MOA is highly specific. Other mitochondrial toxicants, strobilurins and hexachlorophene, showed relatively low specific effects. All strobilurins with exception of trifloxystrobin had moderate $SR_{cytotoxicity}$ above 4, and hexachlorophene was nonspecific. This variety in neurite-specific effects could be explained by difference in their MIEs (Delp et al. 2019). Delp et al. (2019) investigated the specific effects of mitochondrial toxicants on neurite outgrowth inhibition and their link to MIEs in LUHMES cells. They observed that rotenone showed highly neurite-specific effects and targeted complex I in mitochondrial respiratory chain, and the other complex I inhibitors commonly showed relatively high neurite-specific effects. In contrast, they found that the strobilurins acted as complex III inhibitors and hexachlorophene was a phenolic uncoupler of oxidative phosphorylation. Both strobilurins and hexachlorophene showed less neurite-specific effects in the study of Delp et al. (2019), which agrees well with our observation.

The redox cyclers diquat and paraquat showed moderate neurite-specific effects, which were accompanied by highly enhanced cytotoxicity (Fig. 2). This indicates that their specific MOAs can contribute not only to neurite-specific effects but also strongly to neuronal-specific and cytotoxic effects. Diquat and paraquat are photosynthesis inhibitors, and were historically applied as herbicides, but have been phased out as plant protection products (Conning et al. 1969). Both were considered as endpoint-specific controls by Aschner et al. (2017), and we not only confirmed their neurite-specific effects in our assay but also brought more details in that their effect is highly enhanced over baseline toxicity. Redox cycling and the subsequent production of reactive oxygen species can generally impair cell health, but this can also possibly explain the specific effects on neurite outgrowth as it has been reported that cytoskeleton dynamics can be regulated by oxidative species in neuronal cells and the redox imbalance can affect neurite outgrowth (Wilson and Gonzalez-Billault 2015).

Stimulating effects

Two endpoint-specific controls for stimulating neurite outgrowth (Aschner et al. 2017) confirmed the capacity of our assay to also capture stimulating effects (Text S3, Table S5, Fig. S5). Stimulating effects over 150% were observed for both HA-1077 and Y-27632 and their hormetic parameter *f* was significant ($p < 0.05$).

All GABA receptor blockers, all sodium channel agonists, hexachlorophene, and 3,3′,5,5′-tetrabromobisphenol A stimulated neurite outgrowth and gave significant parameter *f* with $p < 0.05$ (Fig. 2, Table S6). Especially, hexachlorophene showed the most distinct stimulating effects considering its highest hormesis effect parameter *f*. However, EC_{10} for

stimulating effects could only be derived for five chemicals (fipronil sulfone, α-endosulfan, bifenthrin, 4,4′-DDT, and hexachlorophene) and the EC_{10} values for stimulating effects are given in Table S6. The best-fit curves in Brain–Cousens model did not reach 110% level in neurite length for the rest of chemicals (Fig. S4), and therefore, the stimulating effects could not be quantified. To confirm that the stimulating effects were not due to increased cell number, total neurite length divided by total cell count was compared, and the parameter *f* stayed significant and gave comparable values to the original analysis (Table S6).

The stimulating effects were observed mostly for the chemicals interacting with ion channels. The GABA receptor and sodium channels can be involved in stimulating neurite outgrowth as reported previously (Davis et al. 2004; Michler 1990), but the relevant literature to explain the stimulating effects is still limited and the effects have been rarely quantified. Furthermore, it should be noted that the observed stimulating effects could reflect general stress responses given that they occurred close to concentrations causing cytotoxicity and the hormesis parameter *f* was not high, except for hexachlorophene. Also, considering that the stimulating effects were followed by the inhibiting effects close to cytotoxic level, the stimulating effects can be masked by the cytotoxic effects and might be captured more sensitively from long-term exposure at low concentration. For example, clothianidin showed stimulating effects in differentiated SH-SY5Y cells after co-exposure to brain-derived neurotrophic factor for 3 days (Hirano et al. 2019), while we did not observe any stimulating effects for this chemical in our experimental set up.

Classification based on $SR_{baseline}$ and $SR_{cytotoxicity}$

The test chemicals were categorized into three groups based on neurite- and neuronal-specific toxicity regarding to neurite outgrowth inhibition in Fig. 3: neurite-specific and neuronal-specific chemicals in group 1 ($SR_{cytotoxicity} > 4$, $SR_{baseline} > 10$), exclusively neurite-specific chemicals without enhanced cytotoxicity in group 2 ($SR_{cytotoxicity} > 4$, $SR_{baseline} < 10$), and baseline toxicants in group 3 ($SR_{cytotoxicity} < 4$, $SR_{baseline} < 10$). Chemicals in group 1 are likely to affect cell viability and neurite outgrowth through specific MOAs other than baseline toxicity, while specific MOAs can mainly contribute to neurite outgrowth inhibition with lower effects on cell viability for group 2 chemicals. No chemicals were found in a fourth group that would be neuronal-specific but not neurite-specific.

The majority of chemicals fell into group 1 or 3 (Fig. 3) and the highly neurite-specific effects of group 1 chemicals are prone to accompany elevated cytotoxicity as described above. Both neurite- and neuronal-specific effects were mainly observed for endpoint-specific controls and AChE inhibitors. Endpoint-specific controls were confirmed to show specific effects on neurite outgrowth and our novel analysis also showed that they have even more pronounced enhanced cytotoxicity with $SR_{baseline} > SR_{cytotoxicity}$ (Fig. 3). The same applied for AChE inhibitors with rather distinct SR values for the carbamates, while the OPs had much lower SR values close to the threshold.

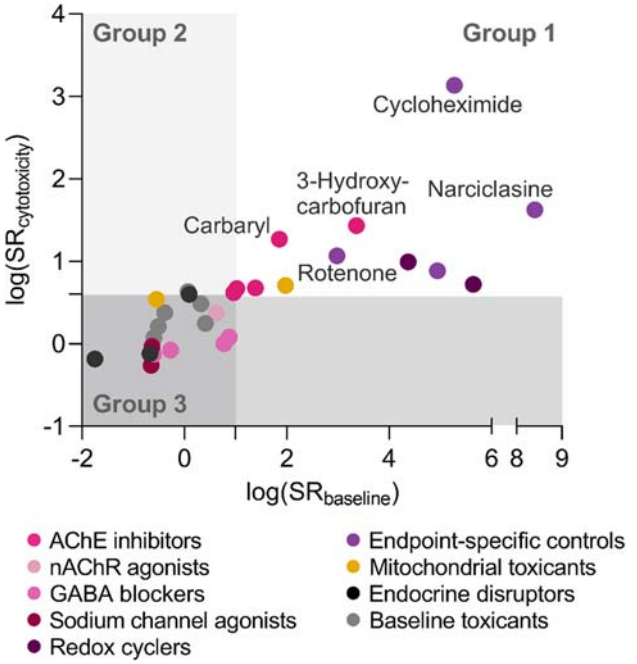

Fig. 3 Classification of test chemicals based on their specificity ratios SR. Neuronal-specific effects were explained by $SR_{baseline}$, and neurite-specific effects were explained by $SR_{cytotoxicity}$. Based on $SR_{baseline}$ and $SR_{cytotoxicity}$, the test chemicals were classified into three groups: neurite-specific and neuronal-specific chemicals (group 1; $SR_{cytotoxicity} > 4$ and $SR_{baseline} > 10$), chemicals with only neurite-specific effects (group 2; $SR_{cytotoxicity} > 4$ and $SR_{baseline} < 10$), and baseline toxicants ($SR_{cytotoxicity} < 4$ and $SR_{baseline} < 10$)

Only a few chemicals were classified into group 2, and the group 2 chemicals can have high uncertainty in their classification as their SRs laid closely to the threshold. One of baseline toxicants, 4-chloro-3-methylphenol, was included in group 2, but its $SR_{cytotoxicity}$ (4.3) is just above the threshold and can be classified differently considering its standard error. Therefore, the chemicals close to the threshold must be regarded with caution as there can be some uncertainty in the definition of the thresholds and their classification can be improved by refining the threshold based on a larger training set of chemicals without specific effects.

Conclusions and outlook

The proposed approach considering both neurite-specific and neuronal-specific effects in the neurite outgrowth assay provides new information that complements the current DNT in vitro testing strategies. On one hand, the specificity ratio $SR_{cytotoxicity}$ can identify chemicals with neurite-specific DNT effects and, therefore, can be used to prioritize test chemicals for further testing. Hereby, we identified two carbamates, 3-hydroxycarbofuran and carbaryl, as highly neurite-specific chemicals in SH-SY5Y cells. On the other hand, $SR_{baseline}$ can be used to identify neurotoxic chemicals whose neurotoxicity is not driven by specific inhibition of neurite outgrowth. Furthermore, $SR_{baseline}$ may serve as a useful measure when comparing effect potency of a given chemical between different cell models as the current DNT in vitro testing strategies utilize multiple cell models with diverse endpoints. It can also support estimation of specificity in case that no cytotoxicity was observed by replacing the use of the highest test concentration or a factor thereof as reference level (Delp et al. 2018). These two specificity ratios can clarify if the effects are triggered by their specific MOAs or merely by baseline toxicity arising from their high hydrophobicity and strong toxic effects can be observed at low concentration for hydrophobic chemicals due to their membrane affinity. Therefore, while cytotoxicity is considered as a reference to identify neurite-specific effects, baseline toxicity provides an anchor to compare the observed toxic effects for individual endpoints.

Mechanistic research underlying specific effects can help build a clear connection between MIEs and adverse outcomes in DNT and expand knowledge of MOAs (Carlson et al. 2020). Other key neurodevelopmental processes such as cell migration could potentially be more sensitive DNT endpoints than neurite outgrowth, and therefore, a battery of endpoints can capture DNT effects more comprehensively (Behl et al. 2019; Harrill et al. 2018; Masjosthusmann et al. 2020). As for our observation on neurite outgrowth, primary MOAs of the pesticides are not necessarily the only specific MOA involved in cytotoxicity and inhibition of neurite outgrowth. The insecticides are usually less potent in mammals due to species specificity and they have secondary targets which can possibly induce toxic effects in non-target organisms (Lushchak et al. 2018). Therefore, multiple MOAs, which can be primary MOA or other secondary MOAs, might contribute to the observed inhibition of neurite outgrowth and cytotoxicity. In case of hydrophobic chemicals, these specific MOAs even can compete with baseline toxicity and baseline toxicity can prevail over the specific MOA for more hydrophobic chemicals due to their high affinity to membranes (Escher and Hermens 2002).

In terms of in vitro models for DNT, although SH-SY5Y cells have been widely used as a model to study neurite outgrowth, their abnormal physiology (Do et al. 2007) originated from tumor origin could limit the interpretation of the observed toxic effects in this model. Therefore, comparison of the effects with those from different models can improve the reliability of this model. LUHMES cells can be applied for this purpose and also can serve as a proper tool to test the effects on neurite outgrowth considering their non-oncogenic human origin. Furthermore, more biologically relevant exposure scenario can be achieved by testing potential DNT chemicals in co-culture with astrocytes.

Supplementary Information The online version contains supplementary material available at https://doi.org/10.1007/s00204-022-03237-x.

Acknowledgements We thank Maria König for technical advice and Sophia Mälzer for experimental support. The experiments were performed using the platform CITEPro (Chemicals in the Environment Profiler) funded by the Helmholtz Association with co-funding by the States of Saxony and Saxony-Anhalt.

Funding Open Access funding enabled and organized by Projekt DEAL.

Declarations

Conflict of interest The authors declare no competing financial interest.

References

Agholme L, Lindstrom T, Kagedal K, Marcusson J, Hallbeck M (2010) An in vitro model for neuroscience: differentiation of SH-SY5Y cells into cells with morphological and biochemical characteristics of mature neurons. J Alzheimers Dis 20(4):1069–1082. https://doi.org/10.3233/JAD-2010-091363

Aschner M, Ceccatelli S, Daneshian M et al (2017) Reference compounds for alternative test methods to indicate developmental neurotoxicity (DNT) potential of chemicals: example lists and criteria for their selection and use. Altex 34(1):49–74. https://doi.org/10.14573/altex.1604201

Bal-Price A, Crofton KM, Leist M et al (2015) International STakeholder NETwork (ISTNET): creating a developmental neurotoxicity (DNT) testing road map for regulatory purposes. Arch Toxicol 89(2):269–287. https://doi.org/10.1007/s00204-015-1464-2

Bal-Price A, Hogberg HT, Crofton KM et al (2018) Recommendation on test readiness criteria for new approach methods in toxicology: exemplified for developmental neurotoxicity. Altex 35(3):306–352. https://doi.org/10.14573/altex.1712081

Behl M, Ryan K, Hsieh JH et al (2019) Screening for developmental neurotoxicity at the national toxicology program: the future is here. Toxicol Sci 167(1):6–14. https://doi.org/10.1093/toxsci/kfy278

Biedler JL, Helson L, Spengler BA (1973) Morphology and growth, tumorigenicity, and cytogenetics of human neuroblastoma cells in continuous culture. Cancer Res 33(11):2643–2652

Bjorling-Poulsen M, Andersen HR, Grandjean P (2008) Potential developmental neurotoxicity of pesticides used in Europe. Environ Health. https://doi.org/10.1186/1476-069x-7-50

Bonneh-Barkay D, Reaney SH, Langston WJ, Di Monte DA (2005) Redox cycling of the herbicide paraquat in microglial cultures. Brain Res Mol Brain Res 134(1):52–56. https://doi.org/10.1016/j.molbrainres.2004.11.005

Brain P, Cousens R (1989) An equation to describe dose responses where there is stimulation of growth at low-doses. Weed Res 29(2):93–96. https://doi.org/10.1111/j.1365-3180.1989.tb00845.x

Carlson LM, Champagne FA, Cory-Slechta DA et al (2020) Potential frameworks to support evaluation of mechanistic data for developmental neurotoxicity outcomes: a symposium report. Neurotoxicol Teratol. https://doi.org/10.1016/j.ntt.2020.106865

Casida JE (2009) Pest toxicology: the primary mechanisms of pesticide action. Chem Res Toxicol 22(4):609–619. https://doi.org/10.1021/tx8004949

Christen V, Rusconi M, Crettaz P, Fent K (2017) Developmental neurotoxicity of different pesticides in PC-12 cells in vitro. Toxicol Appl Pharmacol 325:25–36. https://doi.org/10.1016/j.taap.2017.03.027

Colovic MB, Krstic DZ, Lazarevic-Pasti TD, Bondzic AM, Vasic VM (2013) Acetylcholinesterase inhibitors: pharmacology and toxicology. Curr Neuropharmacol 11(3):315–335. https://doi.org/10.2174/1570159x11311030006

Conning DM, Fletcher K, Swan AAB (1969) Paraquat and related bipyridyls. Br Med Bull 25(3):245. https://doi.org/10.1093/oxfordjournals.bmb.a070712

Constantinescu R, Constantinescu AT, Reichmann H, Janetzky B (2007) Neuronal differentiation and long-term culture of the human neuroblastoma line SH-SY5Y. J Neural Transm Suppl 72:17–28. https://doi.org/10.1007/978-3-211-73574-9_3

Davis TH, Chen CL, Isom LL (2004) Sodium channel beta 1 subunits promote neurite outgrowth in cerebellar granule neurons. J Biol Chem 279(49):51424–51432. https://doi.org/10.1074/jbc.M410830200

de Medeiros LM, De Bastiani MA, Rico EP et al (2019) Cholinergic differentiation of human neuroblastoma SH-SY5Y cell line and its potential use as an in vitro model for Alzheimer's disease studies. Mol Neurobiol 56(11):7355–7367. https://doi.org/10.1007/s12035-019-1605-3

Delp J, Gutbier S, Klima S et al (2018) A high-throughput approach to identify specific neurotoxicants/ developmental toxicants in human neuronal cell function assays. Altex 35(2):235–253. https://doi.org/10.14573/altex.1712182

Delp J, Funke M, Rudolf F et al (2019) Development of a neurotoxicity assay that is tuned to detect mitochondrial toxicants. Arch Toxicol 93(6):1585–1608. https://doi.org/10.1007/s00204-019-02473-y

Delp J, Cediel-Ulloa A, Suciu I et al (2021) Neurotoxicity and underlying cellular changes of 21 mitochondrial respiratory chain inhibitors. Arch Toxicol 95(2):591–615. https://doi.org/10.1007/s00204-020-02970-5

Do JH, Kim IS, Park TK, Choi DK (2007) Genome-wide examination of chromosomal aberrations in neuroblastoma SH-SY5Y cells by array-based comparative genomic hybridization. Mol Cells 24(1):105–112

Escher BI, Hermens JLM (2002) Modes of action in ecotoxicology: their role in body burdens, species sensitivity, QSARs, and mixture effects. Environ Sci Technol 36(20):4201–4217. https://doi.org/10.1021/es015848h

Escher BI, Neale PA, Villeneuve DL (2018) The advantages of linear concentration-response curves for in vitro bioassays with environmental samples. Environ Toxicol Chem 37(9):2273–2280. https://doi.org/10.1002/etc.4178

Escher BI, Glauch L, Konig M, Mayer P, Schlichting R (2019) Baseline toxicity and volatility cutoff in reporter gene assays used for high-throughput screening. Chem Res Toxicol 32(8):1646–1655. https://doi.org/10.1021/acs.chemrestox.9b00182

Escher BI, Henneberger L, Konig M, Schlichting R, Fischer FC (2020) Cytotoxicity burst? Differentiating specific from nonspecific effects in Tox21 in vitro reporter gene assays. Environ Health Perspect. https://doi.org/10.1289/ehp6664

Giordano G, Costa LG (2012) Developmental neurotoxicity: some old and new issues. ISRN Toxicol 2012:814795. https://doi.org/10.5402/2012/814795

Gobas FAPC, Lahittete JM, Garofalo G, Wan YS, Mackay D (1988) A novel method for measuring membrane-water partition coefficients of hydrophobic organic chemicals: comparison with 1-octanol-water partitioning. J Pharm Sci 77(3):265–272. https://doi.org/10.1002/jps.2600770317

Grandjean P, Landrigan PJ (2006) Developmental neurotoxicity of industrial chemicals. Lancet 368(9553):2167–2178. https://doi.org/10.1016/s0140-6736(06)69665-7

Harrill JA, Freudenrich T, Wallace K, Ball K, Shafer TJ, Mundy WR (2018) Testing for developmental neurotoxicity using a battery of in vitro assays for key cellular events in neurodevelopment. Toxicol Appl Pharmacol 354:24–39. https://doi.org/10.1016/j.taap.2018.04.001

Hirano T, Minagawa S, Furusawa Y et al (2019) Growth and neurite stimulating effects of the neonicotinoid pesticide clothianidin on human neuroblastoma SH-SY5Y cells. Toxicol Appl Pharmacol. https://doi.org/10.1016/j.taap.2019.114777

Kovalevich J, Langford D (2013) Considerations for the use of SH-SY5Y neuroblastoma cells in neurobiology. Methods Mol Biol 1078:9–21. https://doi.org/10.1007/978-1-62703-640-5_2

Krug AK, Balmer NV, Matt F, Schonenberger F, Merhof D, Leist M (2013) Evaluation of a human neurite growth assay as specific screen for developmental neurotoxicants. Arch Toxicol 87(12):2215–2231. https://doi.org/10.1007/s00204-013-1072-y

Lee J, Braun G, Henneberger L et al (2021) Critical membrane concentration and mass-balance model to identify baseline cytotoxicity of hydrophobic and ionizable organic chemicals in mammalian cell lines. Chem Res Toxicol 34(9):2100–2109. https://doi.org/10.1021/acs.chemrestox.1c00182

Lein P, Silbergeld E, Locke P, Goldberg AM (2005) In vitro and other alternative approaches to developmental neurotoxicity testing (DNT). Environ Toxicol Phar 19(3):735–744. https://doi.org/10.1016/j.etap.2004.12.035

Lushchak VI, Matviishyn TM, Husak VV, Storey JM, Storey KB (2018) Pesticide toxicity: a mechanistic approach. EXCLI J 17:1101–1136. https://doi.org/10.17179/excli2018-1710

Maeder V, Escher BI, Scheringer M, Hungerbuhler K (2004) Toxic ratio as an indicator of the intrinsic toxicity in the assessment of persistent, bioaccumulative, and toxic chemicals. Environ Sci Technol 38(13):3659–3666. https://doi.org/10.1021/es0351591

Masjosthusmann S, Blum J, Bartmann K et al (2020) Establishment of an a priori protocol for the implementation and interpretation of an in-vitro testing battery for the assessment of developmental neurotoxicity. EFSA Support Publ. https://doi.org/10.2903/sp.efsa.2020.EN-1938

Michler A (1990) Involvement of gaba receptors in the regulation of neurite growth in cultured embryonic chick tectum. Int J Dev Neurosci 8(4):463–472. https://doi.org/10.1016/0736-5748(90)90078-G

Påhlman S, Ruusala AI, Abrahamsson L, Mattsson ME, Esscher T (1984) Retinoic acid-induced differentiation of cultured human neuroblastoma cells: a comparison with phorbolester-induced differentiation. Cell Differ 14:135–144

Paraoanu LE, Layer PG (2008) Acetylcholinesterase in cell adhesion, neurite growth and network formation. FEBS J 275(4):618–624. https://doi.org/10.1111/j.1742-4658.2007.06237.x

Radio NM, Mundy WR (2008) Developmental neurotoxicity testing in vitro: models for assessing chemical effects on neurite outgrowth. Neurotoxicology 29(3):361–376. https://doi.org/10.1016/j.neuro.2008.02.011

Richardson JR, Fitsanakis V, Westerink RHS, Kanthasamy AG (2019) Neurotoxicity of pesticides. Acta Neuropathol 138(3):343–362. https://doi.org/10.1007/s00401-019-02033-9

Ritz C, Baty F, Streibig JC, Gerhard D (2015) Dose-response analysis using R. PLoS ONE. https://doi.org/10.1371/journal.pone.0146021

Ryan KR, Sirenko O, Parham F et al (2016) Neurite outgrowth in human induced pluripotent stem cell-derived neurons as a high-throughput screen for developmental neurotoxicity or neurotoxicity. Neurotoxicology 53:271–281. https://doi.org/10.1016/j.neuro.2016.02.003

Seth B, Yadav A, Agarwal S, Tiwari SK, Chaturvedi RK (2017) Inhibition of the transforming growth factor-/SMAD cascade mitigates the anti-neurogenic effects of the carbamate pesticide carbofuran. J Biol Chem 292(47):19423–19440. https://doi.org/10.1074/jbc.M117.798074

Shipley MM, Mangold CA, Szpara ML (2016) Differentiation of the SH-SY5Y human neuroblastoma cell line. J vis Exp 108:53193. https://doi.org/10.3791/53193

Smirnova L, Hogberg HT, Leist M, Hartung T (2014) Developmental neurotoxicity—challenges in the 21st century and in vitro opportunities. Altex 31(2):129–156. https://doi.org/10.14573/altex.1403271

Vaes WHJ, Ramos EU, Verhaar HJM, Hermens JLM (1998) Acute toxicity of nonpolar versus polar narcosis: Is there a difference? Environ Toxicol Chem 17(7):1380–1384. https://doi.org/10.1002/etc.5620170723

Wilson C, Gonzalez-Billault C (2015) Regulation of cytoskeletal dynamics by redox signaling and oxidative stress: implications for neuronal development and trafficking. Front Cell Neurosci 9:381. https://doi.org/10.3389/fncel.2015.00381

Publication III

Monitoring mixture effects of neurotoxicants in surface water and wastewater treatment plant effluents with neurite outgrowth inhibition in SH-SY5Y cells

Jungeun Lee,[1] Rita Schlichting,[1] Maria König,[1] Stefan Scholz,[2] Martin Krauss,[3] and Beate I. Escher[1,4]*

[1]Department of Cell Toxicology, Helmholtz Centre for Environmental Research – UFZ, Permoserstr. 15, DE-04318 Leipzig, Germany,

[2]Department of Bioanalytical Ecotoxicology, Helmholtz Centre for Environmental Research – UFZ, Permoserstr. 15, DE-04318 Leipzig, Germany,

[3]Department of Effect-Directed Analysis, Helmholtz Centre for Environmental Research – UFZ, Permoserstr. 15, DE-04318 Leipzig, Germany,

[4]Environmental Toxicology, Center for Applied Geoscience, Eberhard Karls University Tübingen, Scharrenbergstr. 94-96, DE-72076 Tübingen, Germany

***Address correspondence to:** beate.escher@ufz.de

Published in ACS Environmental Au, DOI: 10.1021/acsenvironau.2c00026.

ACS ENVIRONMENTAL Au
AN OPEN ACCESS JOURNAL OF THE AMERICAN CHEMICAL SOCIETY

pubs.acs.org/environau

Article

Monitoring Mixture Effects of Neurotoxicants in Surface Water and Wastewater Treatment Plant Effluents with Neurite Outgrowth Inhibition in SH-SY5Y Cells

Jungeun Lee, Rita Schlichting, Maria König, Stefan Scholz, Martin Krauss, and Beate I. Escher*

Cite This: *ACS Environ. Au* 2022, 2, 523–535

Read Online

ACCESS | Metrics & More | Article Recommendations | Supporting Information

ABSTRACT: Cell-based assays covering environmentally relevant modes of action are widely used for water quality monitoring. However, no high-throughput assays are available for testing developmental neurotoxicity of water samples. We implemented an assay that quantifies neurite outgrowth, which is one of the neurodevelopmental key events, and cell viability in human neuroblastoma SH-SY5Y cells using imaging techniques. We used this assay for testing of extracts of surface water collected in agricultural areas during rain events and effluents from wastewater treatment plants (WWTPs), where more than 200 chemicals had been quantified. Forty-one chemicals were tested individually that were suspected to contribute to the mixture effects among the detected chemicals in environmental samples. Sample sensitivity distributions indicated higher neurotoxicity for surface water samples than for effluents, and the endpoint of neurite outgrowth inhibition was six times more sensitive than cytotoxicity in the surface water samples and only three times more sensitive in the effluent samples. Eight environmental pollutants showed high specificity, and those ranged from pharmaceuticals (mebendazole and verapamil) to pesticides (methiocarb and clomazone), biocides (1,2-benzisothiazolin-3-one), and industrial chemicals (*N*-methyl-2-pyrrolidone, 7-diethylamino-4-methylcoumarin, and 2-(4-morpholinyl)benzothiazole). Although neurotoxic effects were newly detected for some of our test chemicals, less than 1% of the measured effects were explained by the detected and toxicologically characterized chemicals. The neurotoxicity assay was benchmarked against other bioassays: activations of the aryl hydrocarbon receptor and the peroxisome proliferator-activated receptor were similar in sensitivity, highly sensitive and did not differ much between the two water types, with surface water having slightly higher effects than the WWTP effluent. Oxidative stress response mirrored neurotoxicity quite well but was caused by different chemicals in the two water types. Overall, the new cell-based neurotoxicity assay is a valuable complement to the existing battery of effect-based monitoring tools.

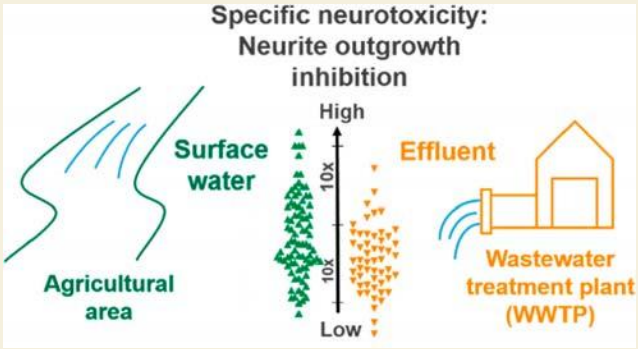

KEYWORDS: *neurotoxicity, neurite outgrowth, water quality monitoring, mixture toxicity, SH-SY5Y cells*

INTRODUCTION

The aquatic environment is contaminated by diverse chemicals of anthropogenic origin. Various sources such as agricultural and road runoff, and release from wastewater treatment plants (WWTPs) contribute to this contamination. While chemicals from road run-off occur almost ubiquitous,[1,2] pesticides are a major group of pollutants in agricultural areas and rain events can increase the chemical load in the water streams.[3,4] In contrast to agricultural or road runoff, WWTPs are point sources of contamination with various chemicals such as pharmaceuticals, personal care products, surfactants, and pesticides.[5−7] Release of the chemicals into aquatic surface waters results in complex mixtures of organic chemicals in low concentrations, that is, micropollutants, which can pose a risk to aquatic life but also drinking water sources. Environmental monitoring using bioassays is able to capture toxicity of micropollutants in an integrative and comprehensive manner, complement chemical analysis, and provide information on environmentally relevant toxicity endpoints.[8] For example, 103 cell-based bioassays were applied to assess water quality for the comprehensive evaluation of toxicity pathways such as activation of the aryl hydrocarbon receptor (AhR), binding to the peroxisome proliferator-activated receptor gamma (PPARγ), activation of the estrogen receptor (ER), and oxidative stress response.[9]

Received: May 2, 2022
Revised: July 20, 2022
Accepted: July 21, 2022
Published: August 17, 2022

https://doi.org/10.1021/acsenvironau.2c00026
ACS Environ. Au 2022, 2, 523–535

Developmental neurotoxicants represent a group of chemicals of particular concern due to their potential impact on human health,[10,11] but high-throughput screening tools for their detection via routine environmental monitoring by testing a large number of samples are still lacking.[12] An *in vitro* test battery for developmental neurotoxicity (DNT) was proposed for testing of single chemicals in the context of human health risk assessment.[13] The DNT testing battery covers multiple key events involved in neurodevelopmental processes, and one of the key events, neurite outgrowth, is crucial for neuronal connectivity and function. Developing neurons produce small processes extending from the cell body. This process is termed neurite outgrowth and has been commonly applied as the endpoint for DNT screening.[14−16] It can serve as endpoint for high-throughput assays considering the sensitive response and relatively short exposure duration compared to the other DNT endpoints in the DNT testing battery.[13] Environmental mixtures have not been tested for their effects on neurite outgrowth, and thus, application of a neurite outgrowth assay to environmental samples is the aim of the present study.

A challenge for DNT assessment is the potential interference of cytotoxicity with the specific endpoint. Therefore, an assessment of specificity is important to discriminate DNT-specific effects from general cytotoxicity.[17,18] The minimal cytotoxicity that would be expected for any chemical is baseline toxicity. Baseline toxicity is caused by membrane intercalation of chemicals and occurs independent of cell types.[19,20] Enhanced level of cytotoxicity relative to this baseline cytotoxicity can arise from specific modes of action (MOA) by chemicals.[21] The specificity of effects on neurite can therefore be quantified by comparing effect concentrations for neurite outgrowth with those for observed cytotoxicity and predicted baseline toxicity.[15,16,22] Neurite-specific effects indicate chemicals that act on neurite outgrowth specifically and thus cause higher toxicity levels for neurite outgrowth compared to the observed cytotoxicity in neuronal cells. The neuronal-specific effect is a composite of the neurite-specific effect and enhanced cytotoxicity over baseline toxicity. Non-neurotoxicants and complex environmental mixtures with diverse MOAs may also result in enhanced cytotoxicity or even specific effects on neurite outgrowth; hence, we always tested cytotoxicity for comparison.

We implemented the combined neurite outgrowth inhibition and cytotoxicity assay as a high-throughput tool for testing environmental samples and for identifying toxicity drivers. The human neuroblastoma SH-SY5Y cell line was used as an *in vitro* model for the high-throughput screening.[22] The assay was applied on samples from small German streams sampled during rain events and WWTP effluents collected across Europe. The water samples were extracted with solid phase extraction and enriched before dosing into bioassays. The responses in SH-SY5Y cells were also compared to responses in bioassays targeting other endpoints, namely, binding to the AhR, PPARγ, ERα, and antioxidant response elements. Therefore, sample sensitivity distributions were used for this comparison to evaluate how sensitive the neurotoxic responses from environmental samples are compared to other endpoints typically used in environmental monitoring. Based on analytical data, single chemicals that were identified in the mixture were subsequently tested to explain the mixture effects and identify potential drivers of the observed effect. Therefore, a so-called iceberg modeling was applied to explain the contribution of detected chemicals to the measured effects of the environmental mixtures.[23,24]

MATERIALS AND METHODS

Water Samples

A total of 140 water samples were investigated in this study: 85 surface water samples were collected during rain events in small streams that were impacted by agriculture and 55 WWTP effluent samples. The surface water samples were collected from stream water in agricultural areas of Germany from April to July in 2019 using event-triggered auto-samplers that started sampling when the water levels rose ≥ 5 cm during rain events. The details of samples and sampling method were already described by Liess et al.[25] The samples were extracted with solid phase extraction (SPE) using Chromabond HR-X cartridges (6 mL, 200 mg sorbent) from Macherey-Nagel (Düren, Germany) with SPE process blanks run in parallel as described for a similar sampling campaign a year earlier.[23] The sample ID consists of an anonymized site number and date of sampling.

The WWTP effluent samples were collected from European WWTPs in 15 different countries over 18 months from August in 2017 to April in 2019. All WWTP samples were enriched with SPE as described previously.[26] The SPE extracts were blown down and re-dissolved in MeOH with enrichment factors (EF; $L_{water}/L_{extract}$) from 250 to 1000. The WWTP sample IDs were anonymized and can be distinguished from surface water sample IDs by the prefix "EU".

There were more samples included in the accompanying analytical studies,[25,26] but only a selection of the samples were used that had sufficient volumes for subsequent testing with at least one experimental run in SH-SY5Y cells as well as four reporter gene assays.

Chemical Analysis

The water samples were analyzed by a target screening method using liquid chromatography high-resolution mass spectrometry (LC−HRMS) via direct injection and a quadrupole-Orbitrap MS (QExactive Plus, Thermo Scientific). A total of 381 chemicals were analyzed for surface water samples according to the analytical method described by Neale et al.[23] For the WWTP effluent, 499 chemicals were analyzed, and the details of the analytical method and results of chemical analysis were published by Finckh et al.[26] As has been previously shown, chemical analysis by direct injection of water samples can be compared with bioassay results from SPE extracts due to the high chemical recovery of the applied SPE method.[24]

Bioanalysis

SH-SY5Y cells were maintained and differentiated prior to the assay as described by Lee et al.[22] The methanol extracts of surface water and WWTP effluent were blown down under a stream of nitrogen gas and reconstituted with the assay medium. The cells were exposed with 11 different concentrations in serial dilution with a relative enrichment factor (REF, $L_{water}/L_{bioassay}$) of 100 as the maximum concentration. Neurite length and cell viability were measured after 24 h exposure using an IncuCyte S3 live cell imaging system (Essen BioScience, Ann Arbor, Michigan, USA). For cell viability, total and dead cells were stained with Nuclear Green LCS1 (Abcam, ab138904) and propidium iodide (Sigma-Aldrich, 81845), respectively. The total neurite length per image was quantified by the IncuCyte NeuroTrack software module, and the effects on neurite outgrowth were expressed based on the neurite length relative to control. An example of image analysis for cell viability and neurite outgrowth is given in Figure S1. The experiment was run once or twice depending on the availability of samples and robustness of the concentration−response curves (CRCs). Subsequent testing of single chemicals was done in the identical procedure with 3 to 4 experimental runs after applying the selection criteria described below.

To compare the sensitivity of responses between bioassays, three mammalian reporter gene assays were conducted according to Neale et al.:[23] AhR-CALUX (H4L7.5c2, based on H4IIe), PPARγ-BLA (HEK293H), and AREc32 (MCF7). Unlike SH-SY5Y cells whose

https://doi.org/10.1021/acsenvironau.2c00026
ACS Environ. Au 2022, 2, 523−535

viability was determined with live/dead cell staining, cell confluency was quantified as a measure of cytotoxicity in reporter gene assays using an IncuCyte S3 live cell imaging system (Essen BioScience, Ann Arbor, Michigan, USA). For the surface water samples only, the ERα-BLA (HEK293T) was performed according to Neale et al.[23] to estimate the contribution of untreated wastewater in the rain-event impacted river samples.

Data Evaluation

Concentration−response relationships are typically linear up to a 30% effect level.[27] For single chemicals, the effect levels up to 30% were included in CRC modeling to determine concentrations causing 10% effect. IC_{10} represents the inhibitory concentration leading to 10% reduction in cell viability, and EC_{10} indicates effect concentrations for 10% reduction in neurite length. In the case of environmental samples, data up to 40% effect were used for CRC modeling due to fewer data points up to 30% effect level. In the case of samples whose CRC did not reach the 10% effect level even at the maximum tested enrichment of REF 100, the CRC was linearly extrapolated to a REF of 150 in order to extrapolate the EC_{10}. This approach was only applied for SH-SY5Y cells to increase the number of samples for specificity analysis. For chemicals or samples where a plateau was observed in their CRC with poor linearity, a log-logistic model was applied for CRC modeling. The details of image and data analysis and the equations for CRC models including the linear regression and log-logistic model were described by Lee et al.[22] For the reporter gene assays, data were analyzed as described by Neale et al.,[23] and a 30% effect cutoff was applied for the linear CRC without extrapolation for both chemicals and samples.

For sensitivity distribution, water samples were ranked based on their IC_{10} and EC_{10} values, and their cumulative probability distributions were derived. Samples without any effect up to an REF of 150 were ranked but no IC_{10}/EC_{10} was assigned to them. The rank of logarithmic IC_{10} and EC_{10} were converted into the probit scale, and the 50th percentile IC_{10} and EC_{10} were derived from a linear regression of log IC_{10} and EC_{10} against probit for probit = 5. It relies on testing if distribution of logarithms of effect concentration of different samples were normally distributed and, if yes, if log−normal distributions differed between sample groups and bioassay endpoints.

Selection of Chemicals

Individual chemicals were tested to explain the effects observed in environmental samples. Tested chemicals were selected among detected chemicals in environmental samples based on the flow chart given in Figure S2. A correlation test was the main criterion for the selection. The correlation test was performed between log $SR_{cytotoxicity}$ of the surface water samples and the logarithm of the detected concentration of a certain chemical i (C_i) in the sample. The detected concentrations C_i were normalized by their $IC_{10,baseline}$ (eq 1) to avoid overestimating the contribution by hydrophilic chemicals prior to drawing the logarithm $[\log(C_i/IC_{10,baseline}(i))]$. The $IC_{10,baseline}$ is the concentration causing 10% cytotoxicity by baseline toxicity, predicted with eq 1 using a quantitative structure−activity relationship (QSAR) based on the liposome-water partition constants ($K_{lip/w}$).[19,20] The baseline toxicity QSAR (eq 1) uses a mass-balance model to convert the critical membrane concentration of baseline toxicity into nominal concentration. To facilitate the prediction of baseline toxicity, an empirical QSAR was fitted to the mass-balance model with $K_{lip/w}$ as the sole descriptor and used to calculate baseline toxicity specific for differentiated SH-SY5Y cells as described by Lee et al.[20]

$$\log(1/IC_{10,baseline}(M)) = 1.26 + 5.63 \times (1 - e^{-0.202 \log K_{lip/w}}) \quad (1)$$

The Pearson correlation coefficient r was used to select 40 chemicals with the highest positive correlation ($r > 0$) between log $SR_{cytotoxicity}$ of samples and log $(C_i/IC_{10,baseline}(i))$. Significance of the correlation was not considered due to different number of data pairs included in the correlation test for individual chemicals. In the case of chemicals that were detected in less than three samples, the correlation test could not be applied. Therefore, these chemicals were only included for testing when they were detected at least once in the samples with highly specific effects on neurite outgrowth ($SR_{cytotoxicity} > 10$).

Specificity Analysis for Individual Chemicals

The specificity of effects on neurite outgrowth was determined compared to observed cytotoxicity and predicted baseline cytotoxicity.[16,22,28] The specificity ratio $SR_{cytotoxicity}$ (eq 2) compares the effects on neurite outgrowth (EC_{10}) and cytotoxicity (IC_{10}), which were experimentally determined in SH-SY5Y. Chemicals with $SR_{cytotoxicity}$ above a previously defined threshold of 4 were considered as neurite-specific effects.[15,16,22]

$$SR_{cytotoxicity} = \frac{IC_{10}}{EC_{10}} \quad (2)$$

The specificity ratio $SR_{baseline}$ (eq 3) compares the effects on neurite outgrowth (EC_{10}) with the predicted baseline cytotoxicity ($IC_{10,baseline}$; eq 1) and quantifies how specific the toxicity on certain endpoints is compared to minimal toxicity. A threshold of $SR_{baseline}$ of 10 was applied to identify neuronal-specific effects of chemicals.[22,28]

$$SR_{baseline} = \frac{IC_{10,baseline}}{EC_{10}} \quad (3)$$

Iceberg Modeling

Iceberg modeling compares the effects measured directly with bioassays in the sample with the predicted effects in the mixture. This is achieved by using effect concentrations of the detected chemicals and application of mixture models.[8] Bioanalytical equivalent concentrations (BEQ_{bio}) derived from bioanalysis can capture the entire mixture effects and express them in concentrations of an appropriate potent reference chemical in each bioassay that would trigger the same effect as the mixture. The BEQ_{bio} can be compared to mixture effects of individual chemicals that are detected from chemical analysis (BEQ_{chem}). The analogous concept of toxic units (TUs) was applied for cytotoxicity, which does not require reference chemicals for calculation.[29,30] The iceberg modeling was performed for SH-SY5Y as well as AREc32, AhR-CALUX, and PPARγ-BLA reporter gene assays using a workflow developed in KNIME (version 4.4.1, Zurich, Switzerland). The details of KNIME workflow can be found on GitHub.[31]

BEQ were expressed in concentrations of reference chemicals. EC_{10} of environmental samples were converted into BEQ_{bio} compared to EC_{10} of the reference chemical (eq 4; Table S1).

$$BEQ_{bio} = \frac{EC_{10}(ref)}{EC_{10}(sample)} \quad (4)$$

For neurite outgrowth inhibition in differentiated SH-SY5Y cells, narciclasine was used as the reference chemical,[16,22] and BEQ were expressed as narciclasine equivalent concentrations (narciclasine-EQ). For the oxidative stress response detected with AREc32, BEQ were expressed as dichlorvos-EQ, for AhR as benzo[a]pyrene-EQ (B[a]P-EQ), for PPARγ-BLA as rosiglitazone-EQ.[32]

For BEQ_{chem}, relative effect potencies for each chemical i (REP_i; eq 5) were calculated based on the EC ratio of the reference chemical and chemical i in molar units. The detected concentration (C_i) of chemical i was then multiplied by REP_i to calculate BEQ_i for individual chemicals. The sum of BEQ_i for all detected chemicals is BEQ_{chem}, as shown in eq 6.

$$REP_i = \frac{EC_{10}(ref)}{EC_{10}(i)} \quad (5)$$

$$BEQ_{chem} = \sum_{i=1}^{n} BEQ_i = \sum_{i=1}^{n} REP_i \cdot C_i \quad (6)$$

The IC_{10} for cytotoxicity of the sample was converted into TU_{bio} using eq 7. For cytotoxicity or baseline cytotoxicity, TU_{chem} was

https://doi.org/10.1021/acsenvironau.2c00026
ACS Environ. Au 2022, 2, 523−535

calculated for cytotoxicity ($TU_{chem(cytotoxicity)}$; eq 8) and baseline cytotoxicity ($TU_{chem(baseline)}$; eq 9) by summing up the ratio of the detected concentration of chemical i and associated IC_{10} or $IC_{10,baseline}$, respectively.

$$TU_{bio} = \frac{1}{IC_{10}(sample)} \quad (7)$$

$$TU_{chem(cytotoxicity)} = \sum_{i=1}^{n} \frac{C_i}{IC_{10}(i)} \quad (8)$$

$$TU_{chem(baseline)} = \sum_{i=1}^{n} \frac{C_i}{IC_{10,baseline}(i)} \quad (9)$$

The effects from entire mixture can be explained by the detected chemicals by comparing BEQ_{bio} with BEQ_{chem}, and TU_{bio} with TU_{chem}. The individual detected chemical i explains BEQ_{chem} or TU_{chem} with different percent contributions, which can be calculated by eqs 10 and 11.

$$\%\ \text{contribution of } i \text{ to } BEQ_{chem} = \frac{BEQ_i}{BEQ_{chem}} \times 100\% \quad (10)$$

$$\%\ \text{contribution of } i \text{ to } TU_{chem} = \left(\frac{C_i}{IC_{10}(i)} \cdot \frac{1}{TU_{chem}}\right) \times 100\% \quad (11)$$

The input for chemical effect concentrations (IC_{10} and EC_{10}) were retrieved from the literature for the four cell lines or newly determined for SH-SY5Y cells in this study, which is given in Table S2. $IC_{10,baseline}$ was predicted for all detected chemicals using $K_{lip/w}$ in Table S2.

RESULTS AND DISCUSSION

Chemical Profiles

Chemical composition was investigated for 85 surface water samples (Table S3) and had been reported previously for 55 WWTP effluent samples (Table S4).[26]

For surface water, 243 chemicals were detected among 381 chemicals analyzed (Table S3). The herbicide sulcotrione was detected at the highest concentration of 490 μg/L among all surface water samples but only in one sample (S17_20190610). The second highest detected chemical was another herbicide, pethoxamid, which was detected in 22 samples with the highest concentration of 187 μg/L. Two industrial chemicals, triphenylphosphine oxide and 5-methyl-1H-benzotriazole, were detected most frequently and found in all 85 samples. For the rest of the chemicals, the detection frequency varied a lot for individual chemicals, indicating the diversity of chemical composition, which is typical for rain-event impacted water as has been shown previously.[23]

366 out of 499 analyzed chemicals were detected in WWTP effluents (Table S4 reprinted from Finckh et al.[26]). Twenty-five chemicals were detected in all 55 WWTP effluent extracts, and 107 chemicals were detected frequently with more than 90% of detection frequency. The highest detected concentration of 461 μg/L (EU009) was observed for hexa-(methoxymethyl)melamine (HMMM), which was detected in all 55 WWTP effluent extracts. HMMM is used for coatings and plastics and has been reported as the emerging contaminant in German rivers.[33] A more thorough discussion of detected chemicals in these WWTP effluent samples is given by Finckh et al.[26]

Sensitivity Distribution of Responses from Surface Water and WWTP Effluent

IC_{10} and EC_{10} for surface water and WWTP effluent were derived from the CRCs depicted in Figures S3 and S4. The IC_{10} for cytotoxicity in SH-SY5Y cells ranged from REF 2.8 to 147 (Table S5), which means that the samples had to be enriched 3 to 147 times to cause 10% cytotoxicity. Fifteen samples (6 surface water and 9 WWTP effluent extracts) were not cytotoxic up to an enrichment of 150 times. The EC_{10} for inhibitory effects on neurite outgrowth ranged from REF 0.2 to 80 (Table S5), and the EC_{10} was up to 49 times more sensitive than the IC_{10}. The bioassay setup can also identify stimulating effects on neurite outgrowth[22] not just inhibition. However, no stimulation was observed for the present set of samples.

To compare toxicity of surface water and WWTP effluent, the IC_{10} and EC_{10} were ranked, and cumulative distributions are visualized in Figure 1 with all details in Table S6. We

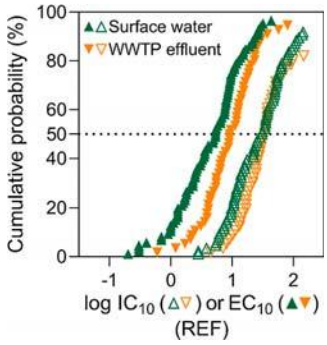

Figure 1. Sensitivity distribution of cytotoxic effects (IC_{10}) and inhibition of neurite outgrowth (EC_{10}) for surface water and WWTP effluent samples in SH-SY5Y cells.

derived the sample sensitivity distributions at the population level to evaluate the sensitivity of cellular response in many different water samples to figure out which type of water samples would respond more sensitively to neurite outgrowth and how sensitive the effects were compared to other bioassays typically applied in water quality monitoring.

For each data set, the IC_{10} and EC_{10} were log-normally distributed but differed in sensitivity. Surface water elicited higher toxicity on both cell viability and neurite outgrowth than the WWTP effluent (Figure 1). The difference in sensitivity between surface water and WWTP effluent was more obvious for neurite outgrowth inhibition than for cytotoxicity. Hence, on average there were higher concentrations of chemicals and/or more potent chemicals acting on neurite outgrowth in surface water samples than in WWTP effluent. The higher sensitivity for neurite outgrowth in the surface water sample could have been caused by pesticides from agriculture or chemicals from road runoff released into water bodies during rain events. Considering that the effluent is further diluted when received by surface water, the contribution of effect from treated wastewater to the surface water appears to be smaller than from other sources during the rain events. Untreated wastewater from combined sewer overflows appears to also be another potential source of micropollutants in surface water samples, given the occasional high occurrence of caffeine, a typical marker of untreated wastewater, and estrogenicity observed in several surface water samples. Additionally, the artificial sweetener sucralose was

https://doi.org/10.1021/acsenvironau.2c00026
ACS Environ. Au 2022, 2, 523−535

also considered as a wastewater tracer[34] and was either non-detected or detected at high concentrations up to micromolar level, which indicates possible influence by wastewater at several sampling sites. Together, these measures indicated impact of untreated or poorly treated wastewater.[23]

The 50th percentiles of the distributions are marked with a dotted line in Figure 1, and the descriptors of the probit regressions are given in Table S6. For surface water, the 50th percentile of the IC_{10} distribution was REF 27.8 and that of EC_{10} was REF 4.5, with a corresponding $SR_{cytotoxicity}$ of 6.1. In the case of WWTP effluent, the 50th percentiles of IC_{10} and EC_{10} distributions were REF 35.1 and REF 9.4, respectively, and a corresponding $SR_{cytotoxicity}$ of 3.7. The lower median IC_{10} and EC_{10} distributions of surface water samples demonstrated their overall higher toxicity. Also, surface water samples were more likely to affect neurite outgrowth specifically considering higher $SR_{cytotoxicity}$ derived from 50th percentile values.

The responses in SH-SY5Y cells were compared with other bioassays typically applied for water quality monitoring including AhR-CALUX, PPARγ-BLA, and AREc32 (IC_{10} and EC_{10} in Table S5; distributions in Table S6 and Figure S5). Since each of these reporter gene assays is based on a different cell line, the cytotoxicity was assessed for each of them. For all cell lines, the IC_{10} distributions of surface water (Figure S5a) showed higher toxicity than the WWTP effluent (Figure S5b) with H4IIe cells (AhR-CALUX) being most sensitive, followed by HEK293H (PPARγ-BLA) of equal sensitivity. SH-SY5Y and MCF7 (AREc32) exhibited the lowest sensitivity. The cytotoxicity distributions were analyzed jointly for all sample types and also followed a log−normal distribution (Figure S5c, Table S6).

In the previous work on the baseline toxicity of single chemicals, the difference in cytotoxicity between different cell lines triggered by baseline toxicity was attributed to differences in bioavailability with similar cell-internal effect concentrations, and any differences were larger for more hydrophobic chemicals than for hydrophilic chemicals.[19,20] The mixture effect of the water samples did not follow this ranking. AhR-CALUX was equipotent with AREc32 for predicted baseline toxicity but 5.4 times more potent at the median with respect to measured cytotoxicity of water samples. PPARγ-BLA was three times more potent than AREc32 for the water samples, which is very similar to the ratio for the predicted baseline toxicity of hydrophobic chemicals. SH-SY5Y was only 1.6 times more sensitive than AREc32 at the 50th percentile of the distribution of the water samples but up to nine times more sensitive toward baseline toxicants. Overall differences were within an order of magnitude, which supports cytotoxicity as an apical effect little influenced by specific MOAs.

The distributions of effects (EC_{10} and $EC_{IR1.5}$) differed much more between surface water (Figure S5d) and WWTP effluent (Figure S5e) than cytotoxicity although the combined distribution still exhibit a good log−normal distribution (Figure S5f, r^2 from 0.87 to 0.99 for the probit regression in Table S6). The effects on neurite outgrowth in SH-SY5Y cells were the least sensitive in WWTP effluent compared to the other endpoints, that is, activation of PPARγ and AhR, as well as oxidative stress response. However, SH-SY5Y responded more sensitively in surface water, and the sensitivity of neurite outgrowth was similar to the two most sensitive endpoints, AhR and PPARγ, in surface water. Neurite outgrowth is a more apical endpoint than the receptor-mediated effects from other bioassays, which might contribute to a relatively low sensitivity of responses in SH-SY5Y cells. However, it is striking that the rank order was different between the event-triggered surface water and effluent samples.

AREc32, which is an indicator of oxidative stress response, showed overlapping distributions between surface water and WWTP, although surface water had fewer activity detects due to masking by cytotoxicity. In comparison with neurite outgrowth in SH-SY5Y, AREc32 was less sensitive for surface water and more sensitive for WWTP effluent.

The responses in the surface water samples were expressed as BEQ_{bio} based on reference chemicals (Table S1) and compared to the results from a similar sampling campaign a year earlier,[23] and the responses in effluent were compared with various data from the literature[32,35] in Figure S6. Higher effects were observed for surface water than for WWTP effluent in AhR-CALUX and AREc32, while the distribution of rosiglitazone-EQ_{bio} was similar in PPARγ-BLA, and this corresponded to the differences and similarities in sample types seen in the literature (Figure S6). This would indicate that the samples used in this study can represent the characteristics of each water types. Thus, the identified toxicity on neurite outgrowth in surface water above is representative of the risk for DNT in various surface water samples.

The estrogen receptor in ERα-BLA was only activated in 60% of the surface water extracts (Table S5). Estrogenicity was not assessed in the WWTP effluent extracts, but we know that BEQ for ERα-BLA expressed as 17β-estradiol-EQ (EEQ; Table S1) ranged from the detection limit of 0.7 to 51.4 ng_{E2}/L from previous studies on WWTPs with diverse treatment types.[35] If estrogenicity was detected in surface water, the effect levels were often rather high, up to an EEQ of 18 ng_{E2}/L (Figure S6d), many of them exceeding the effect-based trigger value for estrogenicity of 0.34 ng_{E2}/L,[32] even if they remained below the levels of WWTPs with primary treatment. Likewise, the 2018 sampling campaign of rain events at the same sites had revealed estrogenic effects ranging from 0.06 to 37 ng_{E2}/L and wastewater markers such as caffeine in several surface water samples, indicating that urban runoff and combined sewer overflow during rain events contributed to the chemical load.[23] Studies on pesticides in these surface water samples had concluded that the rivers contained mainly agricultural runoff,[25] which is not supported by the results on estrogenicity.

Specific Effects on Neurite Outgrowth of Surface Water and WWTP Effluent

The effects on cell viability and neurite outgrowth were compared to quantify specificity of the effects on neurite outgrowth for individual samples (Figure 2a). The IC_{10} and EC_{10} were plotted together on an inverted logarithmic scale to compare the degree of toxicity. Their ratio, that is, the $SR_{cytotoxicity}$, represents an indicator of the specificity of effects (Figure 2a). Previously, this indicator $SR_{cytotoxicity}$ has exclusively been used to interpret effect data of single chemicals but lends itself also to mixture effects if one keeps in mind that the ratio is then a composite of many chemicals and could be driven by a small number of chemicals with very high individual $SR_{cytotoxicity}$ or by many with moderate to low $SR_{cytotoxicity}$.

For the samples with similar cytotoxicity, the toxicity on neurite outgrowth was more likely to be higher in surface water than in WWTP effluent (Figure 2a). The higher toxicity on neurite outgrowth led to higher $SR_{cytotoxicity}$ in surface water samples compared to WWTP effluent considering overall

https://doi.org/10.1021/acsenvironau.2c00026
ACS Environ. Au 2022, 2, 523−535

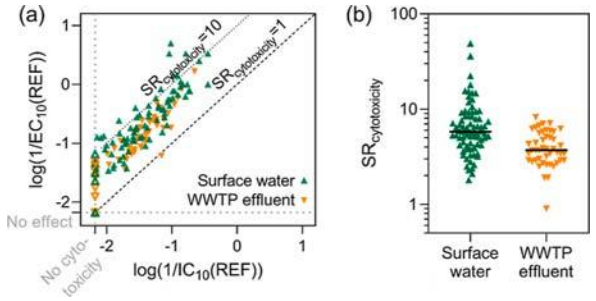

Figure 2. Specificity of effects on neurite outgrowth compared to cytotoxicity for surface water and WWTP effluent samples in SH-SY5Y cells. (a) Comparison of IC_{10} and EC_{10} and (b) their ratio $SR_{cytotoxicity}$ as an indicator of specificity of effect. Empty symbols in (a) stand for no effects on cell viability or neurite outgrowth. The bold line in (b) indicates median values. All data are given in Table S5.

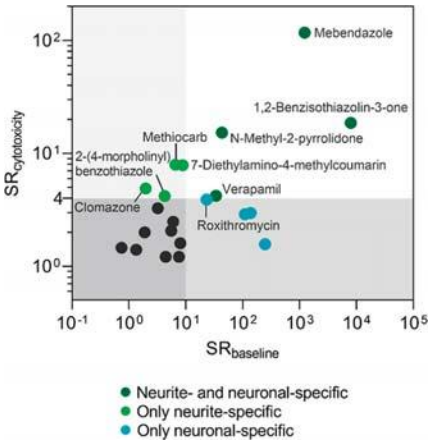

Figure 3. Specific effects on neurite outgrowth compared to cytotoxicity ($SR_{cytotoxicity}$) and baseline cytotoxicity ($SR_{baseline}$) for detected chemicals in surface water. Chemicals with $SR_{cytotoxicity}$ above 4 were considered as neurite-specific, and those with $SR_{baseline}$ above 10 were considered as neuronal-specific.

distribution in Figure 2b. $SR_{cytotoxicity}$ ranged from 1.8 to 49 (median 5.8) for 79 surface water samples and from 0.9 to 8.2 (median 3.7) for 46 WWTP effluent samples (Figure 2b).

Identification of Neurite-Specific Toxicants in Water Samples

To identify chemicals that induced specific effects on neurite outgrowth in surface water, single chemicals were selected among the detected chemicals in surface water samples according to the flow chart given in Figure S2 and tested in the neurite outgrowth assay. The correlation coefficient *r* in the correlation test between $SR_{cytotoxicity}$ of surface water samples and detected level of chemicals in the samples was mainly considered for selection of additional chemicals for neurotoxicity testing (Table S7). The CRCs of the tested chemicals are given in Figure S7 with their IC_{10} and EC_{10} in Table S8. Effect concentrations for clothianidin and fipronil were already available for SH-SY5Y cells together with a number of other chemicals that were tested in a previous study,[22] not all of which were active and/or cytotoxic (Table S2, total number of tested chemicals 97, active 59).

Among the newly prioritized 41 chemicals, the specificity ratios, $SR_{cytotoxicity}$ and $SR_{baseline}$, could be determined only for 21 chemicals. The other 20 chemicals showed either only reduced neurite length (n = 3) or no effects on both neurite outgrowth and cell viability up to maximum solubility (n = 17).

Based on the threshold for $SR_{cytotoxicity}$ at 4,[16,22] 8 chemicals acted on neurite outgrowth specifically compared to cytotoxicity and were identified as neurite-specific chemicals (Figure 3): mebendazole, 1,2-benzisothiazolin-3-one (BIT), *N*-methyl-2-pyrrolidone, methiocarb, 7-diethylamino-4-methylcoumarin, clomazone, verapamil, and 2-(4-morpholinyl)-benzothiazole. $SR_{cytotoxicity}$ above the threshold would indicate that the chemicals have MOA involved in specific effects on neurite outgrowth.

Mebendazole had the highest $SR_{cytotoxicity}$ of 49 and was also the most potent neurotoxicant with the lowest EC_{10} (107 nM) among all tested chemicals (Figure 3; Table S8). Mebendazole is an antihelmintic human and veterinary drug that inhibits polymerization of microtubule by binding to tubulin, which corresponds to the MOA of a known neurite-specific toxicant, colchicine.[13,15,22] Mebendazole was more frequently detected in the WWTP effluent and at higher concentrations than in surface water. The second most neurite-specific toxicant, BIT, is used as antimicrobial and is an electrophile that can react with functional groups in enzymes or other proteins.[36,37] This MOA could be linked to a molecular initiating event of reactivity to seleno proteins established for DNT.[38]

Three of the neurite-specific chemicals were pesticides, which have been considered as major toxicity drivers in surface water.[3] Methiocarb reversibly inhibits acetylcholinesterase (AChE) as an insecticide, and clomazone is a herbicide that inhibits carotenoid biosynthesis but was also reported to act as the AChE inhibitor.[39,40] Highly neurite-specific effects were previously observed for reversible AChE inhibitors (e.g., carbaryl and 3-hydroxycarbofuran), while other neurotoxicants did not specifically act on neurite outgrowth such as GABA blockers and sodium channel agonists.[22] Verapamil is also a neurotoxicant blocking calcium channels and used as a medication for high blood pressure. The primary MOA of verapamil may also be relevant for DNT, since calcium channel blockers have been reported to inhibit neurite outgrowth by regulating calcium influx in neurons from chick embryos and snails.[41,42]

The remaining three neurite-specific chemicals represented industrial chemicals that lack information about their potential MOAs. *N*-Methyl-2-pyrrolidone is widely applied as a solvent in petrochemical and plastic industries and was not analyzed in WWTP effluent but occurred frequently and at high concentrations in surface water. 7-Diethylamino-4-methylcoumarin is a fluorescent dye with various applications[43] and was mainly found in WWTP effluent. 2-(4-Morpholinyl)-benzothiazole is a vulcanization accelerator used in car tires and is a marker of road runoff. It was mainly detected in surface water and only in low concentrations in WWTP effluent.

Neurite-specific effects were not restricted to agricultural chemicals but were also observed for contaminants from the urban environment. It is still possible that small amount of many pesticides below the detection limit could contribute to the mixture effects; however, agricultural chemicals such as pesticides are not necessarily the only major contributors to the neurite-specific effects in surface water. Testing of more chemicals can help to figure out whether agricultural chemicals induced neurite-specific effects or removal of micropollutants reduced neurite-specific effects in WWTP effluent.

https://doi.org/10.1021/acsenvironau.2c00026
ACS Environ. Au 2022, 2, 523−535

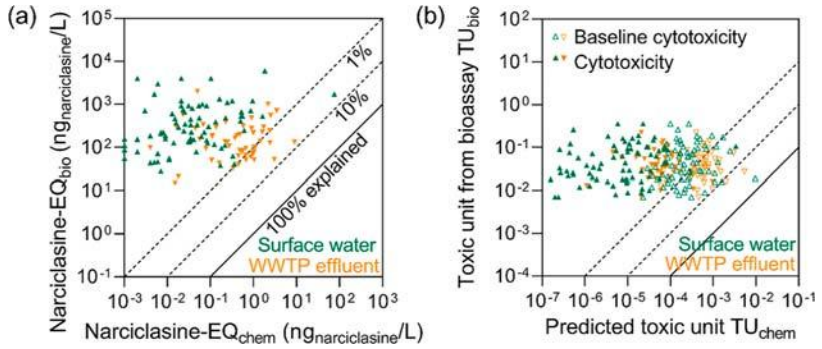

Figure 4. (a) Effects from bioanalysis explained by the mixture effect of the detected chemicals in surface water and WWTP effluent samples for neurite outgrowth inhibition by comparing narciclasine-EQ_{chem} with measured narciclasine-EQ_{bio}. (b) Comparison of measured cytotoxicity with estimated cytotoxicity based on experimental effect concentrations of individual chemicals and with predicted baseline cytotoxicity (TU: toxic unit).

While highly neurite-specific effects were accompanied by neuronal-specific effects, only neuronal-specific effects were observed for four chemicals: clarithromycin, 2-naphthalene sulfonic acid, citalopram, and roxithromycin. Their neurite-specific effects would be minor, but they still inhibited neurite outgrowth with enhanced toxicity compared to the minimal toxicity.[22] This indicates that there can exist specific MOAs that may secondarily impact on neurite outgrowth for these chemicals.

The remaining nine chemicals had both $SR_{cytotoxicity}$ and $SR_{baseline}$ below the thresholds, indicating that they are likely to act on both cell viability and neurite outgrowth via baseline toxicity rather than specific MOAs. Nevertheless, such chemicals will still contribute to the mixture effects.

Iceberg Modeling

Mixture effects were predicted from measured effects of individual chemicals, which were detected in at least one of the samples (IC_{10} for 25 and EC_{10} for 34 chemicals detected in surface water; IC_{10} for 19 and EC_{10} for 28 chemicals detected in WWTP effluent; Table S2). For neurite outgrowth inhibition, the sample's mixture effect corresponds to narciclasine-EQ_{bio}, which was compared to the predicted mixture effect of the detected chemicals, narciclasine-EQ_{chem} (Figure 4a, Table S9).

With few exceptions, less than 1% of the experimental mixture effects for neurite outgrowth inhibition were explained by the predicted mixture effects of the detected chemicals (Figure 4a). Overall, narciclasine-EQ_{bio} were better explained by narciclasine-EQ_{chem} in WWTP effluent than in surface water. For samples whose measured mixture effects were explained by the detected chemicals relatively well (around 5%), not only high chemical potency but also high detected concentration contributed to the higher mixture effects. For example, 4.4% of narciclasine-EQ_{bio} was explained by narciclasine-EQ_{chem} in surface water sample S7_20190616 (Table S9). This was the only sample that contained the highly neurite-specific chemical BIT. BIT was not only potent (REP 0.0212) but also detected at high concentration (1.8 μg/L) and therefore explained nearly 100% of narciclasine-EQ_{chem} in this sample (Table S10). In the case of WWTP effluent, all detected chemicals explained 6.8% of narciclasine-EQ_{bio} in the WWTP effluent EU016 (Table S9), and 7-diethylamino-4-methylcoumarin contributed to 95% of narciclasine-EQ_{chem} due to its high detected concentration of 30.1 μg/L (Table S11). The very potent neurotoxicant mebendazole (REP 0.0367) explained 70% of narciclasine-EQ_{chem} in the WWTP effluent EU122, where 5.9% of narciclasine-EQ_{bio} was explained by narciclasine-EQ_{chem} (Table S11).

It is difficult to relate the differences between surface water and WWTP effluents to specific chemicals, given that only a portion of the chemicals present in the samples might be detected by analytical chemistry. This can be illustrated by comparison of the percentages of narciclasine-EQ_{bio} explained by narciclasine-EQ_{chem}. The higher the number of detected and bioactive chemicals is, the higher will be the percentage of the effect explained by the detected chemicals (Figure S8). If we extrapolate the relationship depicted in Figure S8 linearly on a log−log scale to "100% explained", we would require at least 152 quantified bioactive chemicals. This is only a very rough estimate given the high scatter in the data but illustrates that many more chemicals than detected are present in the samples. Hence, in order to relate the effect levels for neurite outgrowth to the presence of certain chemicals, the analytical target list would need to be expanded and the corresponding effect concentration would be required for all detected chemicals. Despite the large scatter, a trend is evident in Figure S8 that the WWTP effluent has a higher number of bioactive chemicals detected and accordingly also higher percentage of effect explained. This might be by chance due to selection and higher number of target chemicals in WWTP effluents (499 vs 381 in surface water) and effect data biased to those present in WWTP effluents.

The corresponding measures for cytotoxicity are TU_{bio} and TU_{chem} (Figure 4b, Table S9). TU_{bio} was explained by $TU_{chem(cytotoxicity)}$ to a higher extent in WWTP effluent than in surface water despite the similar degree of toxicity (Figure 4b). The predicted baseline cytotoxicity $TU_{chem(baseline)}$ of detected chemicals explained the TU_{bio} better than $TU_{chem(cytotoxicity)}$ from experimental single chemical cytotoxicity (Figure 4b). This can be explained by the different number of chemicals included for iceberg modeling since only experimental cytotoxicity IC_{10} could be used for $TU_{chem(cytotoxicity)}$, but the baseline cytotoxicity $IC_{10,baseline}$ of all detected chemicals could be predicted for $TU_{chem(baseline)}$. Even if all chemicals were captured, baseline cytotoxicity cannot explain 100% of the effects if there are any chemicals with specific MOAs that induce enhanced cytotoxicity, which can only be experimentally determined.

When we have a closer look at the effect drivers in SH-SY5Y over different samples, the chemicals contributing to narciclasine-EQ_{chem} varied a lot in the surface water samples

https://doi.org/10.1021/acsenvironau.2c00026
ACS Environ. Au 2022, 2, 523−535

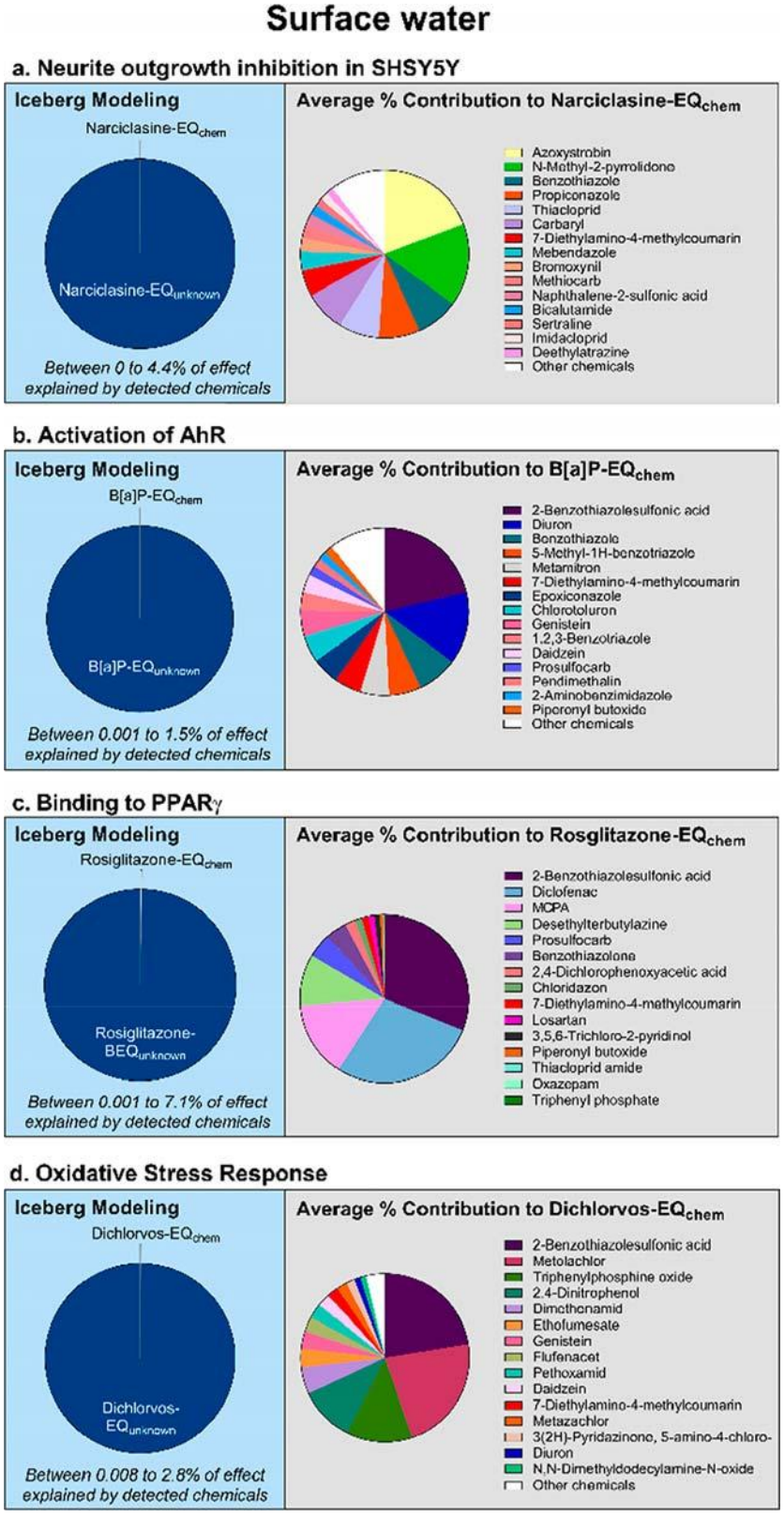

Figure 5. continued

https://doi.org/10.1021/acsenvironau.2c00026
ACS Environ. Au 2022, 2, 523−535

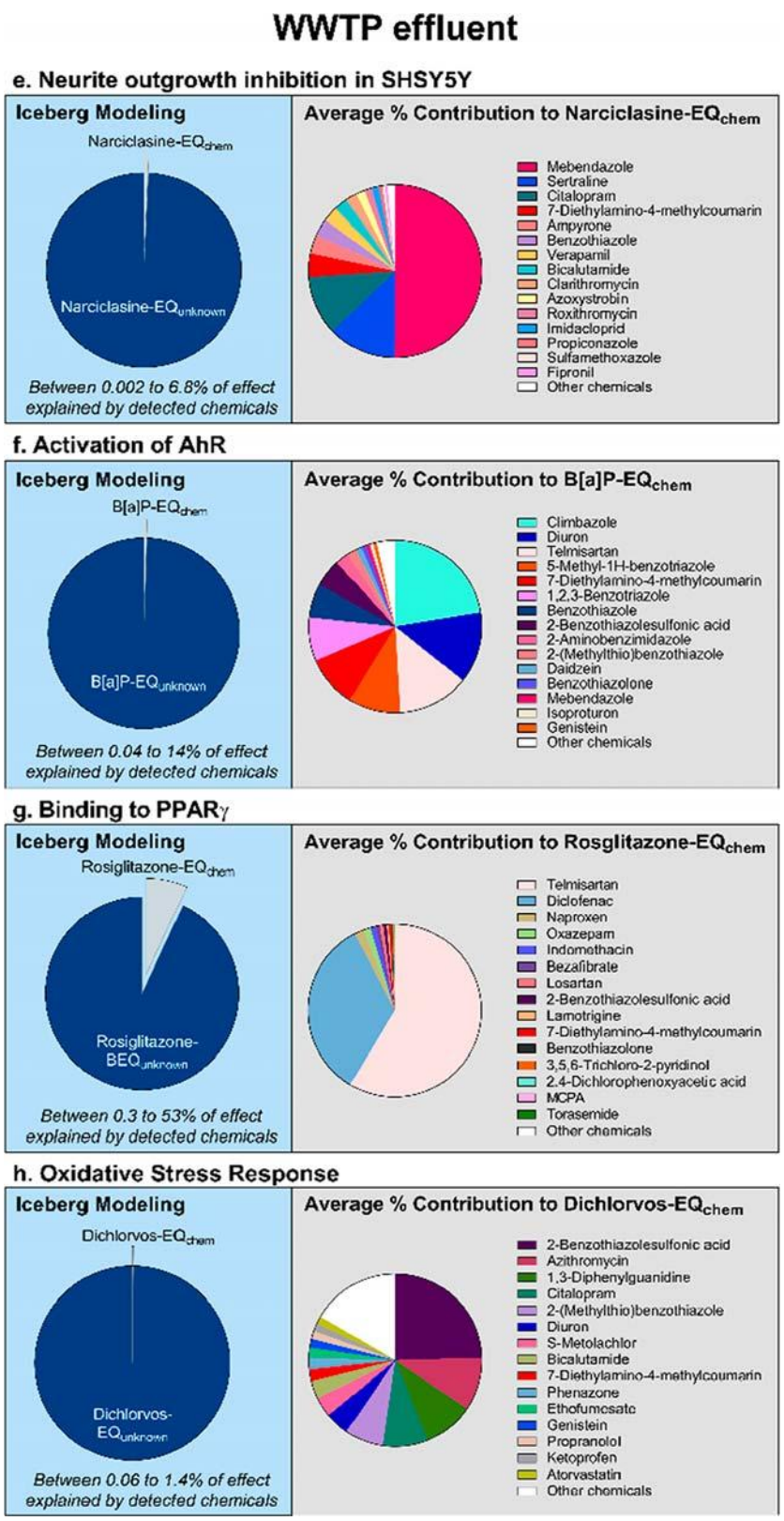

Figure 5. (a) Average fraction of BEQ_{bio} that was explained by BEQ_{chem} (left, BEQ_{chem}/BEQ_{bio}) and contribution to BEQ_{chem} by top 15 chemicals (right, BEQ_i/BEQ_{chem}) for (a) SH-SY5Y, (b) AhR-CALUX, (c) PPARγ-BLA, and (d) AREc32 in the surface water extracts and for (e) SH-SY5Y, (f) AhR-CALUX, (g) PPARγ-BLA, and (h) AREc32 in the WWTP effluent extracts. The detailed data of the SH-SY5Y assay for each sample are given in Table S10 for surface water and S11 for WWTP effluent.

(Figure S9a, Table S10). The average contribution to narciclasine-EQ_{chem} was the highest for azoxystrobin (Figure 5a), which explained on average 19% of narciclasine-EQ_{chem} of surface water (between 0 and 100% explained). This high

https://doi.org/10.1021/acsenvironau.2c00026
ACS Environ. Au 2022, 2, 523−535

contribution by azoxystrobin could be due to its high detected concentration in several surface water samples up to 1.3 μg/L, but the contribution was highly variable between samples. Diverse chemicals also contributed to more than 90% of narciclasine-EQ_{chem} in a few surface water samples, such as *N*-methyl-2-pyrrolidone, benzothiazole, and carbaryl (Figure S9a, Table S10).

Mebendazole was the dominant contributor to the narciclasine-EQ_{chem} in the WWTP effluent extracts (Figures 5e and S9b, Table S11). Although mebendazole was selected from surface water samples for further testing, both detection frequency and detected concentration were higher in the WWTP effluent (Tables S3 and S4), which led to its high contribution to the narciclasine-EQ_{chem} (Table S11). The contribution of mebendazole dominated in half of the WWTP effluent extracts (Figure S9b), which indicates that mebendazole would be one of the major toxicity drivers in WWTP effluent.

Since mebendazole turned out to be the most neurite-specific ($SR_{cytotoxicity}$ = 118; Table S2) among the chemicals included for iceberg modeling, we checked if neurite-specific effects were pronounced in the sample with high concentration of mebendazole. This was not the case because the highest detected concentration of mebendazole (88.4 ng/L; Tables S3 and S4) was observed in sample EU021 among all the tested samples, and this sample showed relatively low specific effects on neurite outgrowth with a $SR_{cytotoxicity}$ of 4.8 (Table S5). Therefore, detection of individual neurite-specific chemicals does not necessarily mean the mixture would show specific effects on neurite outgrowth, which necessitates evaluation of entire mixture effects in bioassays in addition to chemical analysis.

Iceberg modeling was also applied for the other three bioassays AhR-CALUX, PPARγ-BLA, and AREc32 using effect concentrations of detected chemicals from the literature (Tables S1 and S2) for derivation of BEQ_{bio} and BEQ_{chem} (Table S9). As observed for neurotoxicity, only a small part of the BEQ_{bio} could be explained by BEQ_{chem} (Figure S10a–c), which is consistent with previous observations.[23,44,45] Since cytotoxicity data of more chemicals were available for these three bioassays, TU_{chem} was higher for cytotoxicity than baseline cytotoxicity, and therefore, the mixture effects were better explained (Figure S10d–f).

Contribution of individual chemicals to BEQ_{chem} were derived for each surface water extract (Tables S12–S14) and WWTP effluent extract (Tables S15–S17) in the three bioassays, and the toxicity drivers are visualized in Figures S11 and S12. Again there was a high diversity of the chemicals contributing to the mixture effects but, in each sample, there were only a few chemicals that explained most of the mixture effect. Especially in PPARγ-BLA, more than 50% of rosiglitazone-EQ_{chem} was explained by 2-benzothiazolesulfonic acid, diclofenac, or telmisartan for most of the samples (Figures S11b and S12b, Tables S13 and S16).

For comparison between sample types and bioassays, we summarized the average BEQ in all bioassays in Figure 5. This presentation neglects the diversity of mixtures within one sample type but is still a way to visualize differences and commonality. There were very different chemicals dominating and contributing to the mixture effects in each bioassay, but there was also little commonality between the sample types.

In the neurotoxicity assay with SH-SY5Y cells, mebendazole, the dominant mixture effect contributor in the WWTP effluents, was included but played a minor role in surface water and the other way around for azoxystrobin (compare Figure 5a with 5e). Other overlapping mixture effect contributors were propiconazole and 7-diethylamino-4-methylcoumarine. The agricultural pesticides thiacloprid and carbaryl were only important for surface water, but another pesticide imidacloprid appeared in both water types as the mixture contributor. Pharmaceuticals such as antiandrogen medication bicalutamide and the antidepressant sertraline were not only found in both sample types but also were important for the mixture effects.

The industrial chemical 2-benzothiazolesulfonic acid was not characterized in the neurotoxicity assay but contributed to on average a quarter of BEQ_{chem} for surface water in the three bioassays AhR-CALUX, PPARγ-BLA, and AREc32 (Figure 5). This corresponds to what has been observed in the 2018 sampling campaign.[23] The high contribution of 2-benzothiazolesulfonic acid could attribute its overall high detected concentration in surface water (Table S3).

Unlike for surface water, the major toxicity drivers were different between the four bioassays for WWTP effluent (Figure 5). While 2-benzothiazolesulfonic acid was still a dominant contributor in AREc32, diverse chemicals such as mebendazole, climbazole, and telmisartan contributed the most to BEQ_{chem} in the other three bioassays. The concentration of 2-benzothiazolesulfonic acid was also high in WWTP effluent, but climbazole and telmisartan, which were only analyzed in WWTP effluent, were also highly detected (Table S4) and showed higher effect potency than 2-benzothiazolesulfonic acid (REP in Table S2), and therefore, their contribution was pronounced in WWTP effluent.

The toxicity drivers and their rank of contribution were consistent between sample types for AREc32 (Figure 5). However, diuron and diclofenac contributed to the substantial amount of BEQ_{chem} commonly for both sample types in AhR-CALUX and PPARγ-BLA, respectively, which indicates those two chemicals can be the potential toxicity drivers regardless of water types.

A limitation of this analysis is that the list of target chemicals (Tables S3 and S4) differed slightly between the two sample types. We still did the analysis on all chemicals detected and not only on the overlapping chemicals, but such an additional analysis is possible. While a large database of single chemical's effect data has been collected over the last decade for chemicals occurring in European waters, the neurotoxicity assay with SH-SY5Y cells has been applied for the first time for water samples, and therefore, the number of individual chemicals tested was much lower. As the selection of those followed a prioritization, BEQ_{chem} captured still a comparable fraction of BEQ_{bio} as in the other bioassays, but future work could expand the number of individual chemicals tested, especially for chemicals with high occurrence such as 2-benzothiazolesulfonic acid.

CONCLUSIONS

Neurotoxicants pose a risk for both humans and environment. Chemicals could play a role in observed vulnerability of humans to adverse impacts on learning, memory, and cognitive functions. A variety of bioassays are already available for testing certain aspects of the so-called adult neurotoxicity, that is, the toxicity on the function of the already differentiated nervous system, such as acetylcholinesterase inhibition. However, more sensitive and irreversible neurotoxicity may arise from early-life

https://doi.org/10.1021/acsenvironau.2c00026
ACS Environ. Au 2022, 2, 523–535

exposure to toxicants causing DNT. With the novel high-throughput screening assay, we can not only screen single chemicals but also environmental samples for evaluation of water quality in terms of neurite outgrowth, one of the key endpoints in DNT. The neurite outgrowth assay was used here as a bioanalytical tool to identify the presence of chemicals and mixtures with the potential to cause an effect on the nervous system. For inferring a risk of individual chemicals or mixtures to human, a full exposure assessment to estimate the exposure level in the human body and the ability to cross the blood–brain barrier would need to be combined with hazard assessment. Risk assessment is beyond the goals of the present study, but the proposed bioassay might find some application in the future as a bioanalytical tool in human biomonitoring.

The neurite outgrowth assay was successfully implemented and applied for environmental samples ranging from WWTP effluent to diverse surface water samples, indicating the wide applicability and responsiveness of this novel assay. Although a relatively high number of chemicals (243 of 381 targeted in surface water, and 366 of 499 targeted in WWTP effluent) were analytically quantified to identify chemicals contributing to mixture effects, the iceberg modeling indicated that the number remains too limited to explain the observed mixture effects in environmental waters and relate differences in effects to certain type of chemicals. Testing of even more chemicals might not be the solution as one would need to test hundreds of chemicals. Even then, many chemicals below analytical detection limits will contribute to mixture effects, and the multitude of degradation products and unknown chemicals can never be included comprehensively.[46] Therefore, we recommend using the BEQ_{bio} and BEQ_{chem} approach always side by side to understand the full magnitude of the mixture effects but also the relative role of known environmental pollutants.

Effect-directed analysis (EDA) represents an alternative approach to identify causative chemicals,[47] but it is rather suited to bioassays that quantify highly specific, receptor-mediated effects. It has not been explored yet whether the neurite outgrowth effect analysis provides enough specificity, and EDA can be used to identify mixture effect drivers for this bioassay. Furthermore, one may create artificial mixtures to better understand what type of chemicals may drive the observed effects.

Further research should aim at better interpretation of the results in terms of risk of water-borne pollutants to human health and whether it can be used to diagnose major source of chemical contaminations such as agriculture. This also includes the development of effect-based trigger values that can differentiate between acceptable and poor water quality. Considering higher toxic effects on neurite outgrowth observed for surface water and the toxicity drivers identified in this study, environmental monitoring should be focused in the case of surface water or tire-wear and direct road runoff. Given the paucity of DNT evaluation of single chemicals, the mixture-driven approach for identification of DNT-specific chemicals can help to prioritize potential DNT chemicals also considering their environmental relevance. We applied an assay that has been recommended for neurotoxicity assessment because it is anticipated to capture multiple potential molecular initiating event. Inclusion of additional key events (e.g., migration and synaptogenesis)[13] or assessment of specific targets such as inhibition of signal transduction (e.g., inhibition of acetylcholinesterase)[12,48] would allow one to cover an even wider range of effects relevant for DNT in water quality monitoring.

■ ASSOCIATED CONTENT

Supporting Information

The Supporting Information is available free of charge at https://pubs.acs.org/doi/10.1021/acsenvironau.2c00026.

Examples for image analysis, flow chart to select test chemicals, CRCs of chemicals and environmental samples, as well as percentage contribution of individual chemicals to narciclasine-EQ_{chem} (PDF)

Detected concentration of chemicals in environmental samples, effect concentrations of single chemicals and environmental samples, sensitivity distribution, as well as iceberg modeling results (XLSX)

■ AUTHOR INFORMATION

Corresponding Author

Beate I. Escher − *Department of Cell Toxicology, Helmholtz Centre for Environmental Research−UFZ, DE-04318 Leipzig, Germany; Environmental Toxicology, Center for Applied Geoscience, Eberhard Karls University Tübingen, DE-72076 Tübingen, Germany;* orcid.org/0000-0002-5304-706X; Email: beate.escher@ufz.de

Authors

Jungeun Lee − *Department of Cell Toxicology, Helmholtz Centre for Environmental Research−UFZ, DE-04318 Leipzig, Germany;* orcid.org/0000-0001-8336-2952

Rita Schlichting − *Department of Cell Toxicology, Helmholtz Centre for Environmental Research−UFZ, DE-04318 Leipzig, Germany*

Maria König − *Department of Cell Toxicology, Helmholtz Centre for Environmental Research−UFZ, DE-04318 Leipzig, Germany*

Stefan Scholz − *Department of Bioanalytical Ecotoxicology, Helmholtz Centre for Environmental Research−UFZ, DE-04318 Leipzig, Germany;* orcid.org/0000-0002-6990-4716

Martin Krauss − *Department of Effect-Directed Analysis, Helmholtz Centre for Environmental Research−UFZ, DE-04318 Leipzig, Germany;* orcid.org/0000-0002-0362-4244

Complete contact information is available at: https://pubs.acs.org/10.1021/acsenvironau.2c00026

Author Contributions

CRediT: **Jungeun Lee** conceptualization (equal), data curation (lead), formal analysis (lead), investigation (equal), visualization (lead), writing-original draft (lead); **Rita Schlichting** conceptualization (equal), data curation (supporting), formal analysis (supporting), software (lead), supervision (equal), writing-review & editing (equal); **Maria König** investigation (equal); **Stefan Scholz** conceptualization (equal), supervision (equal), writing-review & editing (equal); **Martin Krauss** data curation (supporting), formal analysis (equal), investigation (supporting), methodology (supporting), writing-review & editing (supporting); **Beate I. Escher** conceptualization (equal), formal analysis (equal), funding acquisition (lead), supervision (equal), visualization (equal), writing-original draft (equal), writing-review & editing (lead).

https://doi.org/10.1021/acsenvironau.2c00026
ACS Environ. Au 2022, 2, 523−535

Notes

The authors declare no competing financial interest.

■ ACKNOWLEDGMENTS

Sampling of the WWTP effluent samples was supported by the NORMAN network. We gratefully acknowledge the help from all WWTP operators. The surface water samples were collected in the framework of the project "Implementation of the National Action Plan for the Sustainable Use of Plant Protection Products (NAP)—Pilot study to determine the contamination of small streams in the agricultural landscape by pesticide residues" funded within the framework of the departmental research plan of the Federal Ministry for the Environment, Nature Conservation and Nuclear Safety (BMU) (research code 3717634030) and the Helmholtz long-range strategic research funding (POF III), and the study was conducted with POF IV funding. The authors thank Roman Gunold, Liana Liebmann, Moritz Link, Philipp Vormeier, Oliver Weisner, Matthias Liess, Jörg Ahlheim, and Margit Petre for sampling and extraction, Aleksandra Piotrowska for help with chemical analysis, Peta Neale and Saskia Finckh for helpful discussions. The authors gratefully acknowledge access to the CITEPro platform (Chemicals in the Terrestrial Environment Profiler) funded by the Helmholtz Association.

■ REFERENCES

(1) Crawford, S. E.; Brinkmann, M.; Ouellet, J. D.; Lehmkuhl, F.; Reicherter, K.; Schwarzbauer, J.; Bellanova, P.; Letmathe, P.; Blank, L. M.; Weber, R.; Brack, W.; van Dongen, J. T.; Menzel, L.; Hecker, M.; Schüttrumpf, H.; Hollert, H. Remobilization of pollutants during extreme flood events poses severe risks to human and environmental health. *J. Hazard. Mater.* **2022**, *421*, 126691.

(2) Rauert, C.; Charlton, N.; Okoffo, E. D.; Stanton, R. S.; Agua, A. R.; Pirrung, M. C.; Thomas, K. V. Concentrations of Tire Additive Chemicals and Tire Road Wear Particles in an Australian Urban Tributary. *Environ. Sci. Technol.* **2022**, *56*, 2421−2431.

(3) Halbach, K.; Möder, M.; Schrader, S.; Liebmann, L.; Schäfer, R. B.; Schneeweiss, A.; Schreiner, V. C.; Vormeier, P.; Weisner, O.; Liess, M.; Reemtsma, T. Small streams-large concentrations? Pesticide monitoring in small agricultural streams in Germany during dry weather and rainfall. *Water Res.* **2021**, *203*, 117535.

(4) Leu, C.; Singer, H.; Stamm, C.; Müller, S. R.; Schwarzenbach, R. P. Simultaneous assessment of sources, processes, and factors influencing herbicide losses to surface waters in a small agricultural catchment. *Environ. Sci. Technol.* **2004**, *38*, 3827−3834.

(5) Alygizakis, N. A.; Besselink, H.; Paulus, G. K.; Oswald, P.; Hornstra, L. M.; Oswaldova, M.; Medema, G.; Thomaidis, N. S.; Behnisch, P. A.; Slobodnik, J. Characterization of wastewater effluents in the Danube River Basin with chemical screening, in vitro bioassays and antibiotic resistant genes analysis. *Environ. Int.* **2019**, *127*, 420−429.

(6) Gago-Ferrero, P.; Bletsou, A. A.; Damalas, D. E.; Aalizadeh, R.; Alygizakis, N. A.; Singer, H. P.; Hollender, J.; Thomaidis, N. S. Wide-scope target screening of >2000 emerging contaminants in wastewater samples with UPLC-Q-ToF-HRMS/MS and smart evaluation of its performance through the validation of 195 selected representative analytes. *J. Hazard. Mater.* **2020**, *387*, 121712.

(7) Loos, R.; Carvalho, R.; António, D. C.; Comero, S.; Locoro, G.; Tavazzi, S.; Paracchini, B.; Ghiani, M.; Lettieri, T.; Blaha, L.; Jarosova, B.; Voorspoels, S.; Servaes, K.; Haglund, P.; Fick, J.; Lindberg, R. H.; Schwesig, D.; Gawlik, B. M. EU-wide monitoring survey on emerging polar organic contaminants in wastewater treatment plant effluents. *Water Res.* **2013**, *47*, 6475−6487.

(8) Escher, B. I.; Neale, P. A.; Leusch, F. *Bioanalytical Tools in Water Quality Assessment*, 2nd ed.; IWA Publishing: London, U.K., 2021.

(9) Escher, B. I.; Allinson, M.; Altenburger, R.; Bain, P. A.; Balaguer, P.; Busch, W.; Crago, J.; Denslow, N. D.; Dopp, E.; Hilscherova, K.; Humpage, A. R.; Kumar, A.; Grimaldi, M.; Jayasinghe, B. S.; Jarosova, B.; Jia, A.; Makarov, S.; Maruya, K. A.; Medvedev, A.; Mehinto, A. C.; Mendez, J. E.; Poulsen, A.; Prochazka, E.; Richard, J.; Schifferli, A.; Schlenk, D.; Scholz, S.; Shiraishi, F.; Snyder, S.; Su, G.; Tang, J. Y.; Burg, B.; Linden, S. C.; Werner, I.; Westerheide, S. D.; Wong, C. K.; Yang, M.; Yeung, B. H.; Zhang, X.; Leusch, F. D. Benchmarking organic micropollutants in wastewater, recycled water and drinking water with in vitro bioassays. *Environ. Sci. Technol.* **2014**, *48*, 1940−1956.

(10) Grandjean, P.; Landrigan, P. J. Developmental neurotoxicity of industrial chemicals. *Lancet* **2006**, *368*, 2167−2178.

(11) Bjorling-Poulsen, M.; Andersen, H. R.; Grandjean, P. Potential developmental neurotoxicity of pesticides used in Europe. *Environ. Health* **2008**, *7*, 50.

(12) Legradi, J. B.; Di Paolo, C.; Kraak, M. H. S.; van der Geest, H. G.; Schymanski, E. L.; Williams, A. J.; Dingemans, M. M. L.; Massei, R.; Brack, W.; Cousin, X.; Begout, M. L.; van der Oost, R.; Carion, A.; Suarez-Ulloa, V.; Silvestre, F.; Escher, B. I.; Engwall, M.; Nilén, G.; Keiter, S. H.; Pollet, D.; Waldmann, P.; Kienle, C.; Werner, I.; Haigis, A. C.; Knapen, D.; Vergauwen, L.; Spehr, M.; Schulz, W.; Busch, W.; Leuthold, D.; Scholz, S.; Vom Berg, C. M.; Basu, N.; Murphy, C. A.; Lampert, A.; Kuckelkorn, J.; Grummt, T.; Hollert, H. An ecotoxicological view on neurotoxicity assessment. *Environ. Sci. Eur.* **2018**, *30*, 46.

(13) Masjosthusmann, S.; Blum, J.; Bartmann, K.; Dolde, X.; Holzer, A. K.; Stürzl, L. C.; Keßel, E. H.; Förster, N.; Dönmez, A.; Klose, J.; Pahl, M.; Waldmann, T.; Bendt, F.; Kisitu, J.; Suciu, I.; Hübenthal, U.; Mosig, A.; Leist, M.; Fritsche, E. Establishment of an a priori protocol for the implementation and interpretation of an in-vitro testing battery for the assessment of developmental neurotoxicity. *EFSA Supporting Publ.* **2020**, *17*, 1938E.

(14) Radio, N. M.; Mundy, W. R. Developmental neurotoxicity testing in vitro: models for assessing chemical effects on neurite outgrowth. *Neurotoxicology* **2008**, *29*, 361−376.

(15) Krug, A. K.; Balmer, N. V.; Matt, F.; Schönenberger, F.; Merhof, D.; Leist, M. Evaluation of a human neurite growth assay as specific screen for developmental neurotoxicants. *Arch. Toxicol.* **2013**, *87*, 2215−2231.

(16) Delp, J.; Gutbier, S.; Klima, S.; Hoelting, L.; Pinto-Gil, K.; Hsieh, J. H.; Aichem, M.; Klein, K.; Schreiber, F.; Tice, R. R.; Pastor, M.; Behl, M.; Leist, M. A high-throughput approach to identify specific neurotoxicants/ developmental toxicants in human neuronal cell function assays. *ALTEX* **2018**, *35*, 235−253.

(17) Aschner, M.; Ceccatelli, S.; Daneshian, M.; Fritsche, E.; Hasiwa, N.; Hartung, T.; Hogberg, H. T.; Leist, M.; Li, A.; Mundi, W. R.; Padilla, S.; Piersma, A. H.; Bal-Price, A.; Seiler, A.; Westerink, R. H.; Zimmer, B.; Lein, P. J. Reference Compounds for Alternative Test Methods to Indicate Developmental Neurotoxicity (DNT) Potential of Chemicals: Example Lists and Criteria for their Selection and Use. *ALTEX* **2017**, *34*, 49−74.

(18) Bal-Price, A.; Hogberg, H. T.; Crofton, K. M.; Daneshian, M.; FitzGerald, R. E.; Fritsche, E.; Heinonen, T.; Bennekou, S. H.; Klima, S.; Piersma, A. H.; Sachana, M.; Shafer, T. J.; Terron, A.; Monnet-Tschudi, F.; Viviani, B.; Waldmann, T.; Westerink, R. H. S.; Wilks, M. F.; Witters, H.; Zurich, M. G.; Leist, M. Recommendation on Test Readiness Criteria for New Approach Methods in Toxicology: Exemplified for Developmental Neurotoxicity. *ALTEX* **2018**, *35*, 306−352.

(19) Escher, B. I.; Glauch, L.; König, M.; Mayer, P.; Schlichting, R. Baseline Toxicity and Volatility Cutoff in Reporter Gene Assays Used for High-Throughput Screening. *Chem. Res. Toxicol.* **2019**, *32*, 1646−1655.

(20) Lee, J.; Braun, G.; Henneberger, L.; König, M.; Schlichting, R.; Scholz, S.; Escher, B. I. Critical Membrane Concentration and Mass-Balance Model to Identify Baseline Cytotoxicity of Hydrophobic and Ionizable Organic Chemicals in Mammalian Cell Lines. *Chem. Res. Toxicol.* **2021**, *34*, 2100−2109.

https://doi.org/10.1021/acsenvironau.2c00026
ACS Environ. Au 2022, 2, 523−535

(21) Escher, B. I.; Ashauer, R.; Dyer, S.; Hermens, J. L.; Lee, J. H.; Leslie, H. A.; Mayer, P.; Meador, J. P.; Warne, M. S. Crucial role of mechanisms and modes of toxic action for understanding tissue residue toxicity and internal effect concentrations of organic chemicals. *Integr. Environ. Assess. Manage.* **2011**, *7*, 28−49.
(22) Lee, J.; Escher, B. I.; Scholz, S.; Schlichting, R. Inhibition of neurite outgrowth and enhanced effects compared to baseline toxicity in SH-SY5Y cells. *Arch. Toxicol.* **2022**, *96*, 1039−1053.
(23) Neale, P. A.; Braun, G.; Brack, W.; Carmona, E.; Gunold, R.; König, M.; Krauss, M.; Liebmann, L.; Liess, M.; Link, M.; Schäfer, R. B.; Schlichting, R.; Schreiner, V. C.; Schulze, T.; Vormeier, P.; Weisner, O.; Escher, B. I. Assessing the Mixture Effects in In Vitro Bioassays of Chemicals Occurring in Small Agricultural Streams during Rain Events. *Environ. Sci. Technol.* **2020**, *54*, 8280−8290.
(24) Neale, P. A.; Brack, W.; Aït-Aïssa, S.; Busch, W.; Hollender, J.; Krauss, M.; Maillot-Maréchal, E.; Munz, N. A.; Schlichting, R.; Schulze, T.; Vogler, B.; Escher, B. I. Solid-phase extraction as sample preparation of water samples for cell-based and other in vitro bioassays. *Environ. Sci.: Processes Impacts* **2018**, *20*, 493−504.
(25) Liess, M.; Liebmann, L.; Vormeier, P.; Weisner, O.; Altenburger, R.; Borchardt, D.; Brack, W.; Chatzinotas, A.; Escher, B.; Foit, K.; Gunold, R.; Henz, S.; Hitzfeld, K. L.; Schmitt-Jansen, M.; Kamjunke, N.; Kaske, O.; Knillmann, S.; Krauss, M.; Küster, E.; Link, M.; Lück, M.; Möder, M.; Müller, A.; Paschke, A.; Schäfer, R. B.; Schneeweiss, A.; Schreiner, V. C.; Schulze, T.; Schüürmann, G.; von Tümpling, W.; Weitere, M.; Wogram, J.; Reemtsma, T. Pesticides are the dominant stressors for vulnerable insects in lowland streams. *Water Res.* **2021**, *201*, 117262.
(26) Finckh, S.; Beckers, L.; Busch, W.; Carmona, E.; Dulio, V.; Kramer, L.; Krauss, M.; Posthuma, L.; Schulze, T.; Slootweg, J.; Von der Ohe, P. C.; Brack, W. A risk based assessment approach for chemical mixtures from wastewater treatment plant effluents. *Environ. Int.* **2022**, *164*, 107234.
(27) Escher, B. I.; Neale, P. A.; Villeneuve, D. L. The advantages of linear concentration-response curves for in vitro bioassays with environmental samples. *Environ. Toxicol. Chem.* **2018**, *37*, 2273−2280.
(28) Escher, B. I.; Henneberger, L.; König, M.; Schlichting, R.; Fischer, F. C. Cytotoxicity Burst? Differentiating Specific from Nonspecific Effects in Tox21 in Vitro Reporter Gene Assays. *Environ. Health Perspect.* **2020**, *128*, 77007.
(29) Beckers, L. M.; Busch, W.; Krauss, M.; Schulze, T.; Brack, W. Characterization and risk assessment of seasonal and weather dynamics in organic pollutant mixtures from discharge of a separate sewer system. *Water Res.* **2018**, *135*, 122−133.
(30) Kuzmanovic, M.; Ginebreda, A.; Petrovic, M.; Barcelo, D. Risk assessment based prioritization of 200 organic micropollutants in 4 Iberian rivers. *Sci. Total Environ.* **2015**, *503*−*504*, 289−299.
(31) CITE-KNIME. Iceberg_modelling. GitHub repository. 2022 https://github.com/CITE-KNIME/Iceberg_modelling.git [accessed on July 04, 2022].
(32) Escher, B. I.; Aït-Aïssa, U.-A.; Behnisch, P. A.; Brack, W.; Brion, F.; Brouwer, A.; Buchinger, S.; Crawford, S. E.; Du Pasquier, D.; Hamers, T.; Hettwer, K.; Hilscherová, K.; Hollert, H.; Kase, R.; Kienle, C.; Tindall, A. J.; Tuerk, J.; van der Oost, R.; Vermeirssen, E.; Neale, P. A. Effect-based trigger values for in vitro and in vivo bioassays performed on surface water extracts supporting the environmental quality standards (EQS) of the European Water Framework Directive. *Sci. Total Environ.* **2018**, *628-629*, 748−765.
(33) Dsikowitzky, L.; Schwarzbauer, J. Hexa(methoxymethyl)-melamine: An Emerging Contaminant in German Rivers. *Water Environ. Res.* **2015**, *87*, 461−469.
(34) Oppenheimer, J.; Eaton, A.; Badruzzaman, M.; Haghani, A. W.; Jacangelo, J. G. Occurrence and suitability of sucralose as an indicator compound of wastewater loading to surface waters in urbanized regions. *Water Res.* **2011**, *45*, 4019−4027.
(35) Neale, P. A.; O'Brien, J. W.; Glauch, L.; König, M.; Krauss, M.; Mueller, J. F.; Tscharke, B.; Escher, B. I. Wastewater treatment efficacy evaluated with in vitro bioassays. *Water Res.: X* **2020**, *9*, 100072.
(36) Lindner, W. In Fields of application: surface coatings. *Directory of Microbicides for the Protection of Materials*; Paulus, W., Ed.; Kluwer Academic, 2004; pp 347−375.
(37) Silva, V.; Silva, C.; Soares, P.; Garrido, E. M.; Borges, F.; Garrido, J. Isothiazolinone Biocides: Chemistry, Biological, and Toxicity Profiles. *Molecules* **2020**, *25*, 991.
(38) Spinu, N.; Bal-Price, A.; Cronin, M. T. D.; Enoch, S. J.; Madden, J. C.; Worth, A. P. Development and analysis of an adverse outcome pathway network for human neurotoxicity. *Arch. Toxicol.* **2019**, *93*, 2759−2772.
(39) Santi, A.; Menezes, C.; Duarte, M. M.; Leitemperger, J.; Lópes, T.; Loro, V. L. Oxidative stress biomarkers and acetylcholinesterase activity in human erythrocytes exposed to clomazone (in vitro). *Interdiscip. Toxicol.* **2011**, *4*, 149−153.
(40) dos Santos Miron, D.; Crestani, M.; Rosa Shettinger, M.; Maria Morsch, V.; Baldisserotto, B.; Angel Tierno, M.; Moraes, G.; Vieira, V. L. Effects of the herbicides clomazone, quinclorac, and metsulfuron methyl on acetylcholinesterase activity in the silver catfish (Rhamdia quelen) (Heptapteridae). *Ecotoxicol. Environ. Saf.* **2005**, *61*, 398−403.
(41) Suarez-Isla, B. A.; Pelto, D. J.; Thompson, J. M.; Rapoport, S. I. Blockers of calcium permeability inhibit neurite extension and formation of neuromuscular synapses in cell culture. *Brain Res.* **1984**, *14*, 263−270.
(42) Mattson, M. P.; Kater, S. B. Calcium regulation of neurite elongation and growth cone motility. *J. Neurosci.* **1987**, *7*, 4034−4043.
(43) Muschket, M.; Brack, W.; Inostroza, P. A.; Beckers, L. M.; Schulze, T.; Krauss, M. Sources and Fate of the Antiandrogenic Fluorescent Dye 4-Methyl-7-Diethylaminocoumarin in Small River Systems. *Environ. Toxicol. Chem.* **2021**, *40*, 3078−3091.
(44) Neale, P. A.; Altenburger, R.; Aït-Aïssa, S.; Brion, F.; Busch, W.; de Aragão Umbuzeiro, G.; Denison, M. S.; Du Pasquier, D.; Hilscherová, K.; Hollert, H.; Morales, D. A.; Novák, J.; Schlichting, R.; Seiler, T.-B.; Serra, H.; Shao, Y.; Tindall, A. J.; Tollefsen, K. E.; Williams, T. D.; Escher, B. I. Development of a bioanalytical test battery for water quality monitoring: Fingerprinting identified micropollutants and their contribution to effects in surface water. *Water Res.* **2017**, *123*, 734−750.
(45) Escher, B. I.; van Daele, C.; Dutt, M.; Tang, J. Y. M.; Altenburger, R. Most oxidative stress response in water samples comes from unknown chemicals: the need for effect-based water quality trigger values. *Environ. Sci. Technol.* **2013**, *47*, 7002−7011.
(46) Escher, B. I.; Stapleton, H. M.; Schymanski, E. L. Tracking complex mixtures of chemicals in our changing environment. *Science* **2020**, *367*, 388−392.
(47) Brack, W.; Ait-Aissa, S.; Burgess, R. M.; Busch, W.; Creusot, N.; Di Paolo, C.; Escher, B. I.; Mark Hewitt, L. M.; Hilscherova, K.; Hollender, J.; Hollert, H.; Jonker, W.; Kool, J.; Lamoree, M.; Muschket, M.; Neumann, S.; Rostkowski, P.; Ruttkies, C.; Schollee, J.; Schymanski, E. L.; Schulze, T.; Seiler, T. B.; Tindall, A. J.; De Aragão Umbuzeiro, G. D.; Vrana, B.; Krauss, M. Effect-directed analysis supporting monitoring of aquatic environments - An in-depth overview. *Sci. Total Environ.* **2016**, *544*, 1073−1118.
(48) Lee, J.; Huchthausen, J.; Schlichting, R.; Scholz, S.; Henneberger, L.; Escher, B. I. Validation of an SH-SY5Y cell-based acetylcholinesterase inhibition assay for water quality assessment. *Environ. Toxicol. Chem.* **2022** (in revision).

https://doi.org/10.1021/acsenvironau.2c00026
ACS Environ. Au 2022, 2, 523−535

Publication IV

Validation of a SH-SY5Y cell-based acetylcholinesterase inhibition assay for water quality assessment

Jungeun Lee,[1] Julia Huchthausen,[1] Rita Schlichting,[1] Stefan Scholz,[2] Luise Henneberger,[1] and Beate I. Escher[1,3]

[1]Department of Cell Toxicology, Helmholtz Centre for Environmental Research – UFZ, Permoserstr. 15, DE-04318 Leipzig, Germany,

[2]Department of Bioanalytical Toxicology, Helmholtz Centre for Environmental Research – UFZ, Permoserstr. 15, DE-04318 Leipzig, Germany,

[3]Environmental Toxicology, Center for Applied Geoscience, Eberhard Karls University Tübingen, Scharrenbergstr. 94-96, DE-72076 Tübingen, Germany

***Address correspondence to:** beate.escher@ufz.de

Published in Environmental Toxicology and Chemistry, DOI: 10.1002/etc.5490.

Environmental Toxicology and Chemistry—Volume 41, Number 12—pp. 3046–3057, 2022
Received: 1 May 2022 | Revised: 23 June 2022 | Accepted: 23 September 2022

Environmental Toxicology

Validation of an SH-SY5Y Cell–Based Acetylcholinesterase Inhibition Assay for Water Quality Assessment

Jungeun Lee,[a] Julia Huchthausen,[a] Rita Schlichting,[a] Stefan Scholz,[b] Luise Henneberger,[a] and Beate I. Escher[a,c,*]

[a]Department of Cell Toxicology, Helmholtz Centre for Environmental Research—UFZ, Leipzig, Germany
[b]Department of Bioanalytical Ecotoxicology, Helmholtz Centre for Environmental Research—UFZ, Leipzig, Germany
[c]Department of Environmental Toxicology and Geosciences, Eberhard Karls University of Tübingen, Tübingen, Germany

Abstract: The acetylcholinesterase (AChE) inhibition assay has been frequently applied for environmental monitoring to capture insecticides such as organothiophosphates (OTPs) and carbamates. However, natural organic matter such as dissolved organic carbon (DOC) co-extracted with solid-phase extraction from environmental samples can produce false-negative AChE inhibition in free enzyme-based AChE assays. We evaluated whether disturbance by DOC can be alleviated in a cell-based AChE assay using differentiated human neuroblastoma SH-SY5Y cells. The exposure duration was set at an optimum of 3 h considering the effects of OTPs and carbamates. Because loss to the airspace was expected for the more volatile OTPs (chlorpyrifos, diazinon, and parathion), the chemical loss in this bioassay setup was investigated using solid-phase microextraction followed by chemical analysis. The three OTPs were relatively well retained (loss <34%) during 3 h of exposure in the 384-well plate, but higher losses occurred on prolonged exposure, accompanied by slight cross-contamination of adjacent wells. Inhibition of AChE by paraoxon-ethyl was not altered in the presence of up to 68 mg_c/L Aldrich humic acid used as surrogate for DOC. Binary mixtures of paraoxon-ethyl and water extracts showed concentration-additive effects. These experiments confirmed that the matrix in water extracts does not disturb the assay, unlike purified enzyme-based AChE assays. The cell-based AChE assay proved to be suitable for testing water samples with effect concentrations causing 50% inhibition of AChE at relative enrichments of 0.5–10 in river water samples, which were distinctly lower than corresponding cytotoxicity, confirming the high sensitivity of the cell-based AChE inhibition assay and its relevance for water quality monitoring. *Environ Toxicol Chem* 2022;41:3046–3057. © 2022 The Authors. *Environmental Toxicology and Chemistry* published by Wiley Periodicals LLC on behalf of SETAC.

Keywords: Acetylcholinesterase inhibitors; dissolved organic matter; effects-based monitoring; neurotoxicity; SH-SY5Y cells; volatility

INTRODUCTION

The enzyme acetylcholinesterase (AChE; acetylcholine [ACh] acetylhydrolase, E.C. 3.1.1.7) modulates neurotransmission by breaking down the neurotransmitter ACh. In cholinergic neurons, depolarization of the presynaptic membrane triggers the release of ACh into the synaptic cleft, enabling a time-resolved transmission of excitation. Subsequent binding to the AChE receptor at postsynaptic membranes activates cholinergic or motor neurons. Inhibition of AChE, therefore, can hinder degradation of ACh and lead to overstimulation of the ACh receptor, which could disrupt neurotransmission. Acetylcholinesterase can be inhibited by diverse insecticides that have an affinity to its active site (Čolović et al., 2013; Pohanka, 2011). Depending on the interaction of the AChE inhibitors with the active sites, the insecticides bind either irreversibly or reversibly to AChE. Inhibitors of AChE have been mainly used as insecticides (Fukuto, 1990), but some are also potentially used for therapeutic purposes to treat neurological disorders such as Alzheimer's disease (Sharma, 2019).

Insecticides that act as AChE inhibitors have raised concern because of their presence in the environment and their adverse effects on nontarget organisms. Among the neurotoxic modes of action, AChE inhibition had the highest hazard quotient in environmental monitoring from three European river basins considering the ratio of environmental concentration and effect

This article includes online-only Supporting Information.

* Address correspondence to beate.escher@ufz.de
Published online 9 March 2022 in Wiley Online Library (wileyonlinelibrary.com).
DOI: 10.1002/etc.5490

concentration for the detected chemicals (Legradi et al., 2018). In addition, AChE has already been employed as biomarker of neurotoxicity, and organ homogenates collected from exposed species were used for environmental monitoring (Lionetto et al., 2011; Nunes, 2011). Alternatively, a simple enzyme-based assay (using purified enzyme) can be used to assess inhibition of AChE activity by environmental pollutants in water samples (Escher et al., 2009; Hamers et al., 2000; Macova et al., 2011; Molica et al., 2005).

Diverse AChE inhibition assays have been applied for screening the inhibitory potency of environmental chemicals or samples. High-throughput screening of inhibition of AChE activity was performed using purified enzyme, human neuroblastoma SH-SY5Y cells, and neural stem cells for chemicals in the Tox21 program (Li et al., 2021). Approximately 2.25% of the tested chemicals (187 of 8312) inhibited the AChE activity in that study. Inhibition assays based on purified AChE have been commonly applied because of low cost and simple operation (Cao et al., 2020). Despite its wide application, the enzyme-based AChE inhibition assay may be adversely impacted by natural organic matter that is co-extracted with the micropollutants during the extraction process of environmental samples. For example, matrix effects from diverse water samples were observed, and the co-extracted dissolved organic carbon (DOC) contributed to reduced sensitivity of enzyme-based AChE inhibition assays (Neale & Escher, 2013). Furthermore, cell-based AChE inhibition assays may better reflect in vivo physiology considering cellular environment and localization of AChE (Li et al., 2017, 2021). Given that localization of AChE anchored to the cell membrane or in the cytoplasm can prevent the direct interaction between DOC and AChE (Hicks et al., 2013; Thullbery et al., 2005), a cell-based assay could provide an alternative screening tool for environmental samples; but this has not been explored yet.

Loss of chemicals can occur because of partitioning of volatile chemicals from the bioassay medium to the air. Previously, a "volatility" cutoff was determined empirically. When this cutoff was applied to Tox21 high-throughput screening data, approximately 20% of the chemicals investigated in Tox21 were estimated to be partially lost during testing (Escher et al., 2019). In the typical setup of cellular assays, microplates have an air headspace, which can cause chemical partitioning to the gas phase. In bioassays, the partition constant between medium and air ($K_{medium/air}$) can serve as the best proxy to estimate loss of chemicals because it considers not only their distribution between air and water but also the retaining capacity of medium components such as proteins and lipids (Escher et al., 2019). Volatile chemicals can hinder precise quantification of effect concentrations and even can cause cross-contamination in the bioassay (Birch et al., 2019; Proenca et al., 2021). Some AChE inhibitors are likely to volatilize during incubation in bioassays, and their volatility could represent a limitation in bioassays including the assessment of AChE inhibition.

The aim of the present study was to optimize a cell-based AChE inhibition assay for testing environmental samples. We explored the experimental condition using human neuroblastoma SH-SY5Y cells, which express AChE with cholinergic characteristics (de Medeiros et al., 2019). Irreversible and reversible inhibitors were considered to optimize the assay condition. Four main challenges were evaluated: (1) interference by assay medium with the assay, (2) proper exposure duration, (3) loss processes during the assay due to volatility of certain AChE inhibitors, and (4) disturbance by DOC. The assay was then applied to water extracts to demonstrate its practical applicability.

MATERIALS AND METHOD

Tested chemicals

Irreversible and reversible AChE inhibitors were tested in the present study. The irreversible AChE inhibitors included three organothiophosphates (OTPs; chlorpyrifos, diazinon, parathion) and their active metabolite organophosphates (OPs; chlorpyrifos-oxon, diazoxon, paraoxon-ethyl). Three carbamates (carbaryl, carbofuran, 3-hydroxycarbofuran) were included as reversible AChE inhibitors. Detailed information on test chemicals (Chemical Abstracts Service number, abbreviation of name, source, and purity) is given in Supporting Information, Table S1. Methanol was used to prepare the stock solutions of the chemicals, and its final concentration in assay plates was allowed up to 1%, which did not cause any effects on cell viability and AChE activity in our assay condition. Humic acid sodium salt (Sigma-Aldrich; H16752) was used as a reference of DOC.

Cell culture and medium

Sigma-Aldrich SH-SY5Y cells (94030304) were maintained in growth medium composed of 90% Dulbecco's modified Eagle medium (DMEM)/F12 (Gibco; 11320074) and 10% heat-inactivated fetal bovine serum (hiFBS; Gibco; 10500064) with 100 U/ml penicillin and 100 μg/ml streptomycin (Gibco; 15140122). The cells were cultured in 5% CO_2 in an incubator at 37 °C, and the passage of cells for the assay was limited from 5 to 15 to avoid senescence.

The differentiation medium consisted of Neurobasal medium with phenol red (Gibco; 21103049) and was supplemented with 2% B-27 Supplement (Gibco; 17504044), 2 mM GlutaMAX (Gibco; 35050061), as well as 100 U/ml penicillin and 100 μg/ml streptomycin (Gibco; 15140122). For the assay, the differentiated SH-SY5Y cells were seeded, and the test chemicals were diluted in phenol red-free Neurobasal medium (Gibco; 12348017) containing the same supplement. To compare assay media, not only this Neurobasal assay medium but also other candidate assay media were considered and prepared with 99% DMEM/F12 and 1% diverse types of FBS: nontreated FBS (Gibco; 10099141), charcoal-stripped FBS (csFBS; Gibco; 12676029), dialyzed FBS (dFBS; Gibco; 26400044), and hiFBS (details above).

Cell plating and dosing

The SH-SY5Y cells were differentiated for 72 h in flasks containing differentiation medium with 10 μM all-trans retinoic acid

(Sigma-Aldrich; R2625). The differentiated cells were plated in collagen I–coated 384-well plates (Corning; 354667) using a MultiFlo™ Dispenser (Biotek). Each well contained 15 000 cells in 30 µl of assay medium. The cells were further differentiated in the plates with 10 µM all-trans retinoic acid for 48 h. The last column of the plates was used as a control without cells.

The chemical stocks in methanol were directly added into the assay medium. The methanolic extracts of water samples were blown down with nitrogen and subsequently diluted in assay medium. The highest concentration tested was determined based on the solubility of the respective chemical in the medium and the effect level observed in a preliminary test (data not shown). The chemicals in the assay medium were diluted serially, and 10 µl of the final dilution was transferred into the wells of the plates that contained cells using a Hamilton Microlab STAR platform (Hamilton, Bonaduz, Switzerland) except for the second to last column of the 384-well plate, which was only treated with assay medium. Two independent experimental runs were repeated, and each run had 11 test concentrations with two technical replicates for each chemical. The plates were then kept in the incubator at 37 °C until measurement.

Viability test

For measurement of cell viability, the exposure duration was 24 h to clearly visualize cytotoxicity. The cells were prepared and dosed according to the procedure above. After 24 h of exposure, total and dead cells were stained with Nuclear Green™ LCS1 (Abcam; ab138904) and propidium iodide (Sigma-Aldrich; 81845), respectively. The stained cell objects were counted in fluorescence images using an IncuCyte® S3 live cell imaging system (Essen BioScience). Cell viability was derived as the ratio of live cells to total cells. The inhibitory concentration causing 50% reduced cell viability (IC50) was derived using a log-logistic concentration–response model.

In case of environmental samples, cytotoxicity was already measured for the identical samples by Lee et al. (2022) with the same assessment protocol as in the present study but at lower cell density. The measured cytotoxicity (percentage) was taken from Lee et al. (2022) and reanalyzed to derive the IC50 for the present study.

AChE inhibition assay

For detection, change in AChE activity was measured based on absorbance according to the method of Ellman et al. (1961). Detection mixture was prepared using acetylthiocholine iodide (ATCh iodide; Sigma-Aldrich; A5751) and 5,5'-dithiobis(2-nitrobenzoic acid) (DTNB; Sigma-Aldrich; D8130). The assay medium was removed by inverting the microplates and blotting them on a paper towel to take out as much of the medium as possible. Then, 20 µl of the detection mixture was added into each well using a multichannel pipette. The absorbance at 410 nm was measured every min for 30 min using a Tecan Infinite M1000 plate reader (Tecan). With the method of Ellman et al. (1961), the absorbance of 2-nitro-5-thiobenzoate dianion can be quantified from the reaction of DTNB and hydrolysates of ATCh.

The data were analyzed using two consecutive workflows set up in KNIME (Ver 4.4.1), and the details of the KNIME workflows can be found on GitHub (CITE-KNIME, 2022). The slope of change in absorbance over time is the enzyme velocity (v), and AChE inhibition (percentage) was calculated using Equation 1, where $v_{control}$ and v_i indicate the enzyme velocity of control (nontreated cells) and test chemicals, respectively. Derivation of enzyme velocity and AChE inhibition was visualized for paraoxon-ethyl as an example in Supporting Information, Figure S1. Inhibition of AChE from all experimental runs was plotted together against the concentration using a log-logistic concentration–response model with fixed minimum (0%) and maximum (100%) using the drc package in R Studio, Ver 4.0.4, and the effect concentration for 50% of maximum AChE inhibition (EC50) was calculated using the ED command in the statistical computing language R (2020) (Equation 2).

$$\text{AChE inhibition}(\%) = \left(1 - \frac{v_i}{v_{control}}\right) \times 100\% \quad (1)$$

$$\text{AChE inhibition}(\%) = \frac{100}{1 + \exp[\text{slope} \times \log(\text{concentration}/EC50)]} \quad (2)$$

Prediction of potential loss of chemicals to the air

A mass balance model was applied to predict if chemicals are likely to be lost to the air (Escher et al., 2019). The physicochemical properties of the chemicals that serve as input to this model were retrieved from the linear solvation energy relationships database (Ulrich et al., 2017): protein–water partition constants ($K_{protein/w}$), liposome–water partition constants ($K_{lip/w}$), and air–water partition constants (K_{aw}). Bovine serum albumin (BSA) served as a surrogate for protein to derive the $K_{protein/w}$ (Fischer et al., 2017). The input parameters regarding the composition of Neurobasal assay medium were taken from Lee et al. (2021). The partition constants and volume fractions were substituted into Equation 3 to calculate $K_{medium/air}$. Previously, a so-called volatility cutoff, which is actually a log $K_{medium/air}$ cutoff, was proposed at a log $K_{medium/air}$ of 4 based on cytotoxic effects in AREc32 cells (Escher et al., 2019). The predicted $K_{medium/air}$ of the nine AChE inhibitors were compared with this volatility cutoff to select test chemicals for further experimental volatility test.

$$K_{medium/air} = \frac{Vf_{lip,medium} \times K_{lip/w} + Vf_{protein,medium} \times K_{BSA\,w} + f_{w,medium}}{K_{aw}} \quad (3)$$

Test for loss and cross-contamination

Chemical stocks in methanol were used to prepare dilutions of the three test chemicals chlorpyrifos, diazinon, and parathion.

The final concentration of the chemicals in the plates corresponded to the highest test concentration of the AChE inhibition assay: 2.2×10^{-5} M for chlorpyrifos, 6.6×10^{-5} M for diazinon, and 3.4×10^{-5} M for parathion (concentration with the maximum solubility in the assay medium).

In a collagen I–coated 384-well plate, 40 µl of spiked medium per well was transferred into the plates with quadruplicates as shown in Supporting Information, Figure S2. The remaining wells were filled with 40 µl of nonspiked assay medium. The plate was covered with a lid and incubated at 37 °C and 5% CO_2 for 24 h in total. Two aliquots of 1 ml of spiked medium were incubated in closed vials under the same condition.

To quantify the initial level of chemicals, two aliquots of 30 µl of the spiked medium were transferred into high-performance liquid chromatography (HPLC) vials with insert and extracted immediately after preparation. After 3 and 24 h of incubation, 30 µl of the spiked medium from two out of the four wells of the quadruplicates and the nonspiked medium from four adjacent wells in the plates, as well as two aliquots from closed vials were collected and transferred into HPLC vials with insert for extraction.

The samples were extracted using solid-phase microextraction (SPME) for subsequent quantification of the chemical amount. The SPME method was based on protocols from previous studies of our group (Henneberger et al., 2019; Huchthausen et al., 2020), and the method parameters were adapted accordingly because of the small sample volume of the 384-well plate. Customized SPME fibers were purchased from Sigma-Aldrich and were made of nitinol wire with a coating of C18 particles embedded in polyacrylonitrile. The coating thickness was 45 µm, and the coating length was 2 mm, leading to an approximate coating volume of 69 nL. The SPME fibers were stored in methanol and conditioned in Milli-Q water for 20 min before the experiment. The fibers were transferred to the sample vials, and the vials were shaken at 37 °C and 1800 rpm (BioShake iQ; Quantifoil Instruments) for 2 h. For the chemical desorption from the fibers, aliquots of 60 µl of 90/10 (v/v) acetonitrile/Milli-Q water (chlorpyrifos) or 50/50 (v/v) acetonitrile/Milli-Q water (diazinon and parathion) were pipetted into HPLC vials with inserts. All solvents used had a purity >99%. The fibers were transferred to the vials containing the desorption solvent and incubated at 37 °C and 1800 rpm for 2 h. The fibers were removed from the vials, and the vials were stored at 4 °C until instrumental analysis.

The chemical concentration in the desorption solvent after SPME was quantified using liquid-chromatography mass-spectrometry (LC-MS). An Agilent 1260 Infinity II system was equipped with a Kinetex 1.7 µm C18, 100 Å, LC column (50 × 2.1 mm) and coupled to a triple-quadrupole MS (Agilent 6420 Triple Quad). The LC and MS parameters are given in Supporting Information, Table S2.

Relative peak area (percentage) was calculated based on an initial peak area of samples before incubation (at 0 h). Instead of converting peak area to mass using standard curves, relative peak area was used so that the data below the standard range could be included for some samples with a low concentration level, for example, samples from neighboring wells. At least two experimental runs were conducted with additional repeats in case the data from the first two runs were not comparable.

Environmental samples

Water samples were collected from diverse small streams in Germany during rain events that were impacted by agriculture, road runoff, and combined sewer overflow, leading to a highly diverse pattern of organic pollutants. The detailed information for sampling was already described by Liess et al. (2021), and 381 chemicals were analyzed by a target screening method using LC high-resolution MS. Details of chemical analysis and detected concentrations of chemicals were published by Lee et al. (2022). Among these 85 river water samples, 13 were selected for testing in the AChE inhibition assay based on the sum of the detected concentrations of AChE inhibitors. The availability of samples (enough volume for testing) represented another selection criterion. Samples were only run once, although in a proper monitoring study, duplicate experiments would need to be performed; but the available extract volume was limited.

To calculate the sum of detected concentrations, we only considered chemicals that were classified as AChE inhibitors by the Insecticide Resistance Action Committee (2021). Non-insecticide OPs (e.g., triphenyl phosphate) typically have no or very weak AChE-inhibiting potency and were therefore not considered. The EC50 for AChE inhibition was derived as described above in units of relative enrichment factor (REF; liters of water per liters of bioassay).

Role of DOC in the AChE inhibition assay

Humic acid and paraoxon-ethyl were exposed together for 3 h, followed by the AChE inhibition assay described above to evaluate the effects of DOC on AChE inhibition. Humic acid was serially diluted and tested up to 68 mg_C/L in the presence of paraoxon-ethyl at its EC50 obtained in this assay. The relative AChE inhibition level by the co-exposure of humic acid and paraoxon-ethyl was determined compared with the inhibition level triggered by the constant paraoxon-ethyl concentration.

Mixture experiments

The toxicity of binary mixtures of chemicals or mixtures of a chemical and an extract of environmental sample were evaluated based on an isobologram approach (Altenburger et al., 1990). A fixed concentration ratio design was used, which means that stock solutions containing 10 times the EC50 of each component were mixed in ratios of 80:20, 60:40, 40:60, and 20:80 (Supporting Information, Figure S3); and these stocks with sum of concentrations in the mixture (C_{sum}) were diluted as in a single-chemical experiment to derive concentration–response curves (CRCs).

The concentration fraction of each component in the mixture (p_i) was calculated by Equation 4, and $EC50_{mix}$ was

deduced from the CRCs of the mixture experiments that used C_{sum} as the concentration.

$$p_i = \frac{C_i}{C_{sum}} \quad (4)$$

The toxic units of each mixture component i (TU_i) in Equation 5 were calculated from the experimental $EC50_{mix}$ multiplied by the p_i and divided by the EC50 of the mixture component i ($EC50_i$).

$$TU_i = \frac{p_i \times EC50_{mix}}{EC50_i} \quad (5)$$

The binary mixture of paraoxon-ethyl and diazoxon was tested as reference with four different fixed ratios plus the components alone. While the $EC50_{mix}$ was determined individually for each experimental run because of the diverse combination of mixtures, $EC50_i$ was derived from all experimental runs together to improve the robustness of TU_i. The experiment was repeated two or three times.

Subsequent testing of paraoxon-ethyl and environmental samples was performed to investigate the influence of DOC on the mixture toxicity and to test if a water sample containing a complex mixture behaves in a concentration-additive way with respect to the target mode of action. Two river water samples were tested in the same isobologram design using nine or 10 different fixed concentration ratios of binary mixtures with paraoxon-ethyl. The two river water samples were selected considering following criteria: (1) no cytotoxicity accompanied by AChE inhibition, and (2) different degree of AChE inhibition potency (high and moderate). For C_{sum} in the mixture of paraoxon-ethyl with environmental samples, the highest tested concentration of paraoxon-ethyl (1.99×10^{-8} M) was set at an REF of 1 to unify their units.

RESULTS AND DISCUSSION

Type of FBS and cells used

Many cell-based AChE inhibition assays use assay medium with FBS, which can result in additional AChE in the bioassay with inconsistent composition from different species. Our assay used SH-SY5Y cells, originated from human tissue, as the source of AChE. Because FBS contains active AChE from cow (Ralston et al., 1985), FBS-containing medium can provide another source of AChE in this SH-SY5Y cell–based AChE inhibition assay. The enzymes in FBS could possibly be filtered out or inactivated by heat via additional treatment of FBS, but the type of FBS has often not been indicated clearly. Although the amino acid sequence of AChE and the corresponding enzyme structure are known to be relatively conserved between species, the sensitivity of AChE to several known AChE inhibitors was lower in cow than in horse or rat (Cohen et al., 1985; Karanth & Pope, 2003). Therefore, we compared background AChE levels from assay media containing FBS, csFBS, dFBS, and hiFBS as well as the Neurobasal assay medium to rule out the presence of external AChE and avoid any bias in AChE inhibition determination (Supporting Information, Figure S4).

The AChE activity of the medium itself (without cells) was assessed by measuring the absorbance after incubation with the known AChE inhibitor paraoxon-ethyl or methanol for 1 h. Increased absorbance from methanol-treated wells was observed for assay medium containing 1% FBS and dFBS, which indicates the presence of active AChE in the medium. For the rest of the media (DMEM/F12 with 1% csFBS or hiFBS and Neurobasal assay medium), the absorbance was comparable between paraoxon-ethyl- and methanol-treated wells and was only slightly higher than that of phosphate-buffered saline, which was used as a negative control. To prevent any possible contamination by external AChE from FBS, Neurobasal assay medium was selected as the assay medium in the present study.

Differentiated SH-SY5Y cells were used for the AChE inhibition assay because the AChE activity of the undifferentiated cells was too low and the change in absorbance too subtle to be used for analysis (data not shown). Therefore, we applied differentiated cells in our assay to increase AChE activity and the assay performance. It was reported previously that AChE activity increased 10-fold after differentiation of SH-SY5Y cells (de Medeiros et al., 2019). In addition, it was observed that AChE in undifferentiated SH-SY5Y cells was mainly localized on the neurites and distributed throughout the cytoplasm, while the majority of AChE is closely located to the nucleus for nonneuronal cells (Thullbery et al., 2005). Considering that expression of AChE along the neurites was achieved after differentiation of rat adrenal chromaffin PC-12 cells in the same study, more intense expression of AChE on the neurites and plasma membrane could be expected for differentiated SH-SY5Y cells.

To evaluate the assay quality for the optimized condition, the Z-factor (Zhang et al., 1999) was determined by comparing inhibition rate from paraoxon-ethyl-treated (100% inhibition level, positive control) and methanol-treated (negative control) measurements. The optimized condition using Neurobasal assay medium and differentiated SH-SY5Y cells gave a Z-factor of 0.81, which was above the threshold of 0.5 suggested by Zhang et al. (1999).

Change in EC50 for AChE inhibition over time

Nine AchE inhibitors were tested in differentiated SH-SY5Y cells under the optimized condition with an incubation period of 1–6 h to evaluate the changes in EC50 over time and determine an optimal exposure duration. No cytotoxic effects were observed for the dosed concentration ranges after 24-h exposure (data not shown). The inverse of EC50 was plotted to present the degree of toxicity in Figure 1, and the EC50s were derived from the CRCs in Supporting Information, Figure S5, and are given in Supporting Information, Table S3.

The EC50s of inhibitors with the same moiety (e.g., P=S moiety for OTPs; P=O for OPs) were similar to each other, which indicates comparable inhibitory potency on AchE from

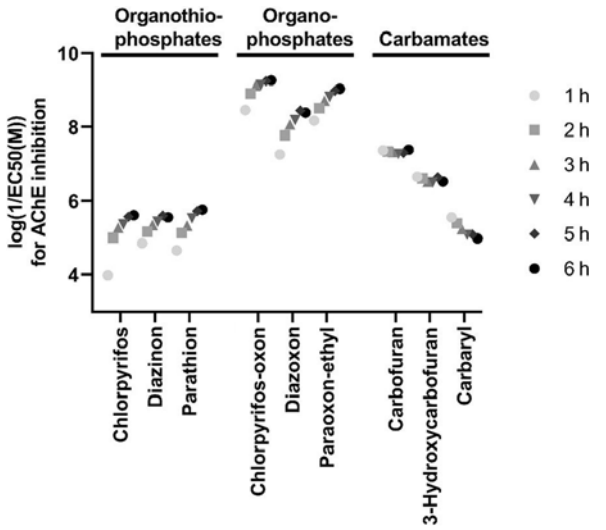

FIGURE 1: Effect concentration for 50% of maximum acetylcholinesterase inhibition for organothiophosphates and carbamates after 1–6-h exposure in differentiated SH-SY5Y cells. EC50 = median effect concentration; AChE = acetylcholinesterase.

their structural similarity. The difference in EC50 between OTPs and between OPs was within a factor of 10 after >3 h of exposure. The ratios of EC50s of the corresponding OPs and OTPs are in the range of 255–30 343, which means that OPs showed much higher effect potency for AchE inhibition than OTPs. It is well known that OTPs need metabolic activation by oxidation for higher inhibitory potency (Čolović et al., 2011; Fukuto, 1990). There appears to be metabolic activation in SH-SY5Y cells, but it appears not to be very efficient compared with the activation by microsomes (Li et al., 2021). Therefore, for future experiments, it might be necessary to metabolically activate chemicals or environmental samples before testing to reflect higher toxicity of the metabolites.

The already oxidized chlorpyrifos-oxon showed the highest effect potency among all tested AchE inhibitors with the lowest EC50, and carbofuran was the most potent among the reversible AchE inhibitors. The potency of AchE inhibition is mainly determined by reactivity to the serine hydroxyl moiety at the active site of AchE and the structural fitness to the AchE (Čolović et al., 2013; Fukuto, 1990). Therefore, chlorpyrifos-oxon and carbofuran are possibly highly reactive to the moiety of AchE or might have strong structural fitness to the active site of AchE.

The Inhibition of AChE Increased over time with decreasing EC50 for the three OTPs and the three OPs (Figure 1). For OPs, a rapid increase in AchE inhibition was observed at 1 to 2 h of exposure, which was followed by a leveling off of EC50 values after longer exposure. In contrast, the maximum effects on AchE inhibition of carbofuran and 3-hydroxycarbofuran were already achieved after 1 h of exposure. This different pattern can be explained by different reaction rates involved in the AchE inhibition (Čolović et al., 2013; Fukuto, 1990). When compared with OPs, carbamates fit relatively well to AchE active sites because of their structural similarity to Ach; thus, the intrinsic reactivity of the carbamyl moiety is generally high, which could accelerate the reaction (Fukuto, 1990).

TABLE 1: Effect concentration for 50% of maximum acetylcholinesterase (AChE) inhibition after 3-h exposure to AChE inhibitors (detailed information in Supporting Information, Table S3) and comparison with literature using a similar cell-based assay and an enzyme-based assay (Li et al., 2021)

	EC50 (μM)		
Chemical	Present study	SH-SY5Y cell–based assay	Enzyme-based assay
3-Hydroxycarbofuran	0.31	Not included	Not included
Paraoxon-ethyl	0.0019	0.1	0.2
Carbaryl	5.8	30.7	24.3
Diazoxon	0.0085	0.2	1.8
Carbofuran	0.047	0.2	0.2
Chlorpyrifos-oxon	0.00076	0.01	0.02
Parathion	4.6	10.9	24.3
Diazinon	4.5	18.6	27.3
Chlorpyrifos	5.4	19.9	60.4

EC50 = median effect concentration.

The time course of carbaryl EC50s differed from the other carbamates, carbofuran and 3-hydroxycarbofuran (Figure 1). Degradation of carbaryl could account for this decrease in toxicity for carbaryl. It was reported that a considerable amount of carbaryl was hydrolyzed already after 3 h of incubation at pH 7.4, and this hydrolysis was facilitated by serum albumin, which is contained in our assay medium (Sogorb et al., 2004, 2007). Therefore, when carbaryl was unbound from AchE by a reverse reaction, the released carbaryl would continuously degrade, leading to a continuous decrease in exposure concentration.

The change In EC50 observed for the tested chemicals was used to Identify an appropriate exposure duration. Considering the lower sensitivity of OPs after a short time but also the fast reverse reaction observed for carbaryl, we decided to apply 3 h as our optimal assay duration.

The EC50 values of the present study ranged over four orders of magnitude and had the same relative order of potency but were overall more sensitive than data reported in the literature for an SH-SY5Y cell–based bioassay (Li et al., 2021; Table 1; Supporting Information, Figure S6A). The new assay was also more sensitive than an enzyme-based assay (Li et al., 2021; Table 1; Supporting Information, Figure S6B). The EC50s from the literature agreed well between cell- and enzyme-based assays (Supporting Information, Figure S6C).

Loss due to partitioning of AchE inhibitors to the airspace in 384-well plates

To evaluate loss of AchE inhibitors, we predicted $K_{medium/air}$ of the nine tested AchE inhibitors based on the distribution between medium and water ($K_{medium/w}$) and the K_{aw} (Table 2). The log $K_{medium/air}$ ranged from 3.59 to 9.80 for our test chemicals. The volatility cutoff in bioassays was initially defined by Escher et al. (2019), and chemicals having a log $K_{medium/air} < 4$ were considered as volatile chemicals in the assays with a 24-h exposure duration. Three OTPs, chlorpyrifos, diazinon, and parathion, had log $K_{medium/air}$ below or just above

TABLE 2: Partition coefficients to predict loss processes from volatility in the bioassay with Neurobasal assay medium for nine acetylcholinesterase inhibitors

Chemical	Log $K_{BSA/w}$ (L_{water}/L_{BSA})[a]	Log $K_{lip/w}$ (L_{water}/L_{lip})[a]	Log $K_{medium/w}$ (L_{water}/L_{medium})[b]	Log K_{aw} (L_{water}/L_{air})[a]	Log $K_{medium/air}$ (L_{air}/L_{medium})[b]
3-Hydroxycarbofuran	0.96	0.56	0.01	−9.79	.80
Paraoxon-ethyl	1.80	1.98	0.06	−6.70	.76
Carbaryl	2.61	2.92	0.31	−6.26	.57
Diazoxon	0.95	0.89	0.01	−6.42	.43
Carbofuran	1.72	1.93	0.05	−5.94	.99
Chlorpyrifos-oxon	2.25	2.53	0.16	−5.64	5.80
Parathion	2.83	3.43	0.44	−4.65	5.09
Diazinon	2.85	3.25	0.45	−3.96	4.41
Chlorpyrifos	3.48	4.30	0.94	−2.65	3.59

[a]UFZ-LSER database (Ulrich et al., 2017); pH 7.4, 37 °C.
[b]Prediction using a mass balance model (Escher et al., 2019).
$K_{BSA/w}$ = partition constants between proteins (bovine serum albumin; BSA) and water; $K_{lip/w}$ = partition constants between lipids and water; $K_{medium/w}$ = partition constants between medium and water; K_{aw} = partition constants between air and water; $K_{medium/air}$ = partition constants between medium and air.

the defined cutoff. Therefore, we selected these three chemicals to verify the predicted loss under our test condition using chemical analysis. We also quantified the chemical losses after 24 h because this is the typical exposure duration of bioassays. For the remaining chemicals including OP metabolites and carbamates, the log $K_{medium/air}$ was clearly above the cutoff, and thus they were considered as not prone to losses to the air for the assay conditions applied.

The Initial levels (0 h) of chlorpyrifos, diazinon, and parathion were compared with the final levels in closed vials as well as with spiked and neighboring wells in 384-well plates after 3 and 24 h of incubation (Figure 2). The chemicals were incubated without cells to exclude loss due to metabolism. The amount of chemicals in closed vials was relatively stable for 24 h for all three OPs (from 85% to 100% of initial level). The constant level of chemicals in the closed system over time would mean there was minor contribution by additional loss from an abiotic process other than volatility, such as photolysis and hydrolysis (Proenca et al., 2021).

When we compared the level in the closed vials with those from spiked wells, most of the test chemicals stayed in the medium for our assay duration of 3 h: 66% of the initial level for chlorpyrifos, 83% for diazinon, and 76% for parathion. The maximum loss of 34% was observed for chlorpyrifos, which was expected from the lowest predicted $K_{medium/air}$ among the test chemicals. The loss due to partitioning to air may be considered acceptable within 3 h of exposure, but one should be cautious with more volatile chemicals whose EC50 values may be affected strongly. It is noteworthy that the observed losses in the spiked wells could also arise from sorption to the plastic

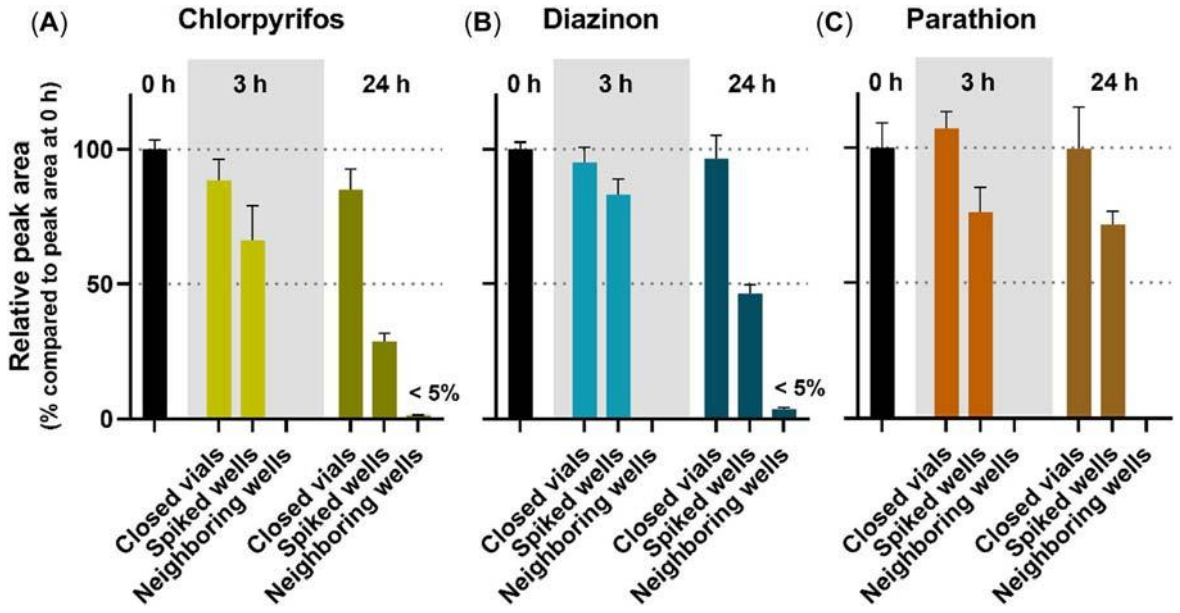

FIGURE 2: Volatility test of three organophosphates in 384-well plates containing Neurobasal assay medium without cells. The chemicals at the highest tested concentration used for testing acetylcholinesterase inhibition were incubated for 3 and 24 h. Relative peak area of (**A**) chlorpyrifos, (**B**) diazinon, and (**C**) parathion in closed vials, spiked wells, and neighboring wells compared to the initial level at 0 h.

of microplates, but this loss process is expected to be negligible because of the high sorptive capacity of medium components (Fischer et al., 2018).

More than 50% of chlorpyrifos and diazinon were lost from the spiked wells after 24 h, which can be rationalized by their predicted $K_{medium/air}$ (Figure 3). The lower the predicted $K_{medium/air}$ was for the chemicals, the higher was the loss in the spiked wells observed after 24 h. Chlorpyrifos had the lowest log $K_{medium/air}$ of 3.59 and the biggest loss from the spiked wells among the three OPs after 3 and 24 h of incubation. Although the spiked wells of chlorpyrifos and diazinon contained chemicals at <50% of the initial level after 24 h of incubation, parathion with a log $K_{medium/air}$ of 5.09 had 71.5% detected in the spiked wells. Loss to the airspace of chemicals in the bioassay depends on K_{aw} and the octanol–water partition coefficient K_{ow}, as shown in Figure 3 (Escher et al., 2019). The K_{aw} of individual chemicals mainly determines the loss in the bioassay, and the higher the K_{aw} is, the more easily chemicals partition into the headspace with some damping by the retaining capacity of the medium. Although the retaining capacity of medium was the highest for these three OPs among the nine AchE inhibitors considering higher $K_{medium/w}$ (Table 2), this had a minor contribution to alleviation of the loss to the airspace, which was confirmed by only slightly elevated $K_{medium/air}$ in simulation with the medium containing 10% FBS (Supporting Information, Figure S7).

Cross-contamination in neighboring wells was observed to a low extent for diazinon after 24 h, whose $K_{medium/air}$ is slightly above the volatility cutoff (Figure 2). The detection level in the neighboring wells was 3.5% of the initial level for diazinon, 1.3% for chlorpyrifos, and 0.5% for parathion. This trend is in line with the previous observation that chemicals with a $K_{medium/air}$ closer to volatility cutoff, that is, diazinon in the present study, caused more severe cross-contamination, whereas highly volatile chemicals were mainly lost without cross-contamination (Escher et al., 2019). Considering that a substantial amount (>60% of initial level) was retained and no cross-contamination was observed during the 3-h exposure duration of the AchE inhibition assay, the previously defined volatility cutoff is still applicable for the AchE inhibition assay; but we recommend analytically verifying the exposure concentrations when testing single chemicals that have a log $K_{medium/air}$ close to 4 and <5.

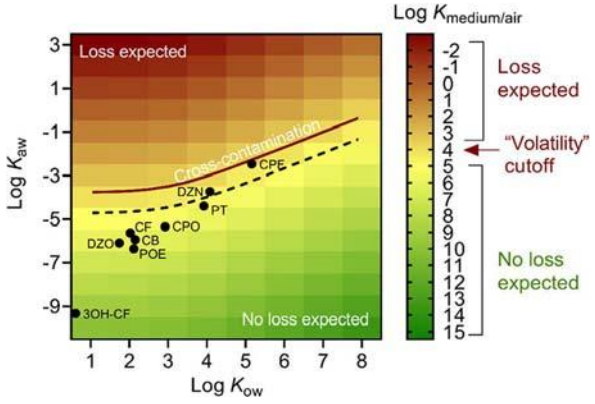

FIGURE 3: Distribution of partition constants between medium and air ($K_{medium/air}$, colored squares) of acetylcholinesterase (AChE) inhibitors overlaying an *x*–*y* plot of partition constants between air and water and between octanol and water (K_{ow}) to determine the cutoff for volatility in bioassay. The previously established volatility cutoff for cytotoxicity (24-h exposure) of $K_{medium/air}$ of 10^4 is shown as a solid red line and is recommended also for the 3-h AChE inhibition assay. The white broken line corresponds to a $K_{medium/air}$ of 10^5, where partial losses occurred at longer exposure times as evidenced in Figure 3 by DZN and CPF after 24-h exposure. K_{aw} = partition constants between air and water; CPF = chlorpyrifos; DZN = diazinon, PT = parathion; CF = carbofuran; CPO = chlorpyrifos-oxon; DZO = diazoxon; CB = carbaryl; POE = paraoxon-ethyl; 3OH-CF = 3-hydroxycarbofuran; K_{ow} = partition constant between octanol and water.

Evaluation of the influence of DOC on the AchE inhibition assay

During sample preparation of surface water and wastewater via solid-phase extraction (SPE), DOC is co-extracted with micropollutants from water samples (Pichon et al., 1996), while metal and inorganic ions can be well removed. Depending on the water type, 40%–70% of the DOC can be recovered in the extract after SPE (Neale & Escher, 2013). It has been shown that DOC interferes with the performance of the enzyme-based AchE assay and suppresses the effect of added AchE inhibitors (Neale & Escher, 2013). However, DOC did not disturb the performance of cell-based bioassays where the receptors of interest are at least partially inside the cells (Neale & Escher, 2014). Given that the AchE is partially located on the neurites of SH-SY5Y cells and therefore potentially in contact with the medium, we explored if this interference by DOC is also observed in the SH-SY5Y cell–based AchE inhibition assay. The inhibition level of AchE from co-exposure to DOC and paraoxon-ethyl as a reference chemical was compared with that from single exposure to paraoxon-ethyl. Aldrich humic acid was applied as representative of DOC according to Neale and Escher (2013).

Inhibition of AchE by paraoxon-ethyl was not influenced by humic acid up to 68 mg_c/L (Figure 4). Any experimental artifacts were prevented by removing the assay medium before detection. The inhibition level by exposure to only paraoxon-ethyl was comparable to that by co-exposure to paraoxon-ethyl and humic acid. This means that no suppressive effects were observed with humic acid. This observation is in striking contrast to what was observed in the enzyme-based AchE inhibition assay, where AchE inhibition by oxidized parathion was suppressed by humic acid at a final assay concentration as low as 2 mg_c/L (Neale & Escher, 2013).

The Interference by DOC has been explained by three different causes: (1) nonspecific binding of DOC to the target site, (2) experimental artifacts due to interference with measurement, and (3) sorption of micropollutants to DOC leading to low bioavailable concentration (Neale & Escher, 2014). Nonspecific binding of DOC to AchE possibly interfered with inhibition by chemicals in the assay using purified AchE (Neale & Escher, 2013). However, in the cell-based assay, AchE is

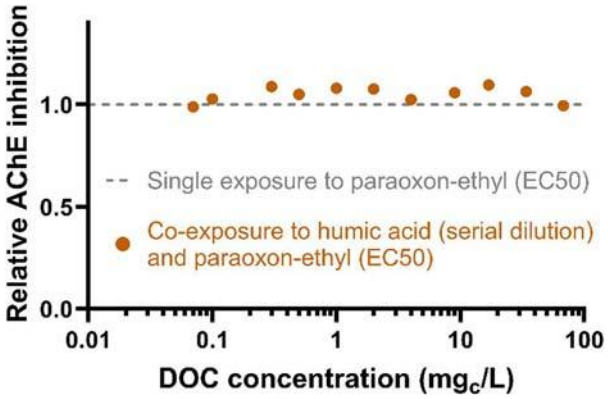

FIGURE 4: Relative inhibition of acetylcholinesterase (AChE) after 3-h exposure to paraoxon-ethyl (POE) at the previously determined median effect concentration of 2×10^{9} M POE in the presence of variable concentrations of Aldrich humic acid (dissolved organic carbon) in the AChE inhibition assay with SH-SY5Y cells. EC50 = median effect concentration; DOC = dissolved organic carbon.

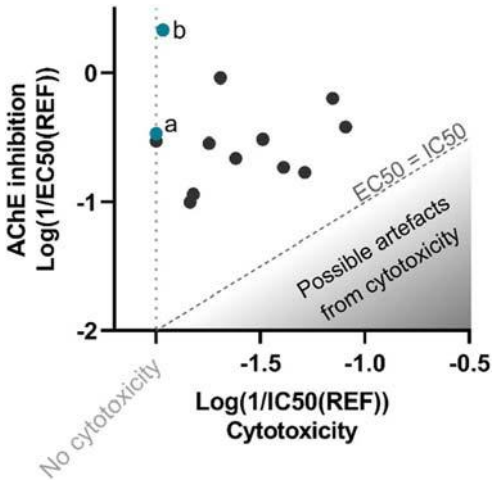

FIGURE 5: Acetylcholinesterase inhibition (median effect concentration for 3-h exposure) and cytotoxic effects (median inhibition concentration for 24 h exposure) of 13 river water samples in differentiated SH-SY5Y cells. Darker gray area indicates higher possibility of artifacts from cytotoxicity. Samples a and b were chosen for the subsequent mixture experiments. AChE = acetylcholinesterase; EC50 = median effect concentration; REF = relative enrichment factor (liters of water per liter of bioassay); IC50 = median inhibition concentration for cytotoxicity.

anchored to the outer cell membrane, and this might deter accessibility of humic acid to AchE. It could be that DOC is too bulky to effectively bind to anchored AchE. Charge repulsion between cell membrane and DOC, because both are negatively charged (Philippe & Schaumann, 2014), also can hinder the access of DOC to the AchE. Another possible explanation for the experimental observations arises from the tetramer structure of anchored AchE. Although two catalytic subunits of the tetramers are oriented outward, the other two subunits are toward the cell membrane (Perrier et al., 2002), and hence possibly less accessible by DOC. Some AchE is located inside the cells, and DOC cannot enter into the cells. In addition, if DOC would disturb the quantification of the enzyme activity by measurement with ATCh, for example, if the bioavailability of ATCh was reduced in the presence of DOC, one would also detect lower activity. In the SH-SY5Y cell assay, the medium is removed prior to running the enzyme inhibition test with ATCh, which could protect against artifacts.

Applicability of the cell-based AchE inhibition assay to environmental water samples

To investigate the applicability to environmental water samples, 13 river water samples were tested in the AchE inhibition assay. Their EC50s ranged from REF 0.5 to 10; that is, the samples had to be diluted by a factor of 2 or enriched 10-fold to achieve 50% AchE inhibition. The EC50s were at least three times lower than the IC50, and cytotoxicity was determined after 24 h of exposure. Therefore, the observed AchE inhibition would be primarily caused by specific inhibition rather than by unspecific reduction due to cytotoxicity. The CRCs of the tested water samples are given for AchE inhibition and cytotoxicity in Supporting Information, Figure S8. The derived EC50s for AchE inhibition are given in Supporting Information, Table S4, together with the 24-h cytotoxicity IC50.

All 13 river water samples inhibited AchE with different effect potency (Figure 5). Higher detected concentrations of AchE inhibitors in the samples did not necessarily lead to higher AchE inhibition. For example, pirimicarb and dimethoate were detected in the sample with the highest AchE inhibition (sample b in Figure 5), but their detected concentrations were lower than the level in other samples with lower AchE inhibition potency (Supporting Information, Table S4). This indicates that there might be a contribution of AchE inhibitors below the detection limit or unknown AchE inhibitors, which demonstrates the sensitivity of our assay to capture those effects.

Two water extracts were selected for subsequent mixture experiments. To evaluate samples with different degrees of effect potency, we chose samples which showed moderate (sample a in Figure 5; EC50 = REF 3.0) and high (sample b in Figure 5; EC50 = REF 0.5) AchE inhibition.

Mixture experiments

We tested binary mixtures of reference chemicals and the two selected water extracts to confirm the applicability of the cell-based assay to environmental samples. Diverse mixtures with different effect concentration fractions of paraoxon-ethyl with diazoxon or water extract were tested, and their experimental toxic unit was compared with the prediction of the concentration addition model (Figure 6). Parallel log-CRCs are a prerequisite for derivation of the toxic unit (Villeneuve et al., 2000), and the slopes of the CRCs were similar within a factor of 1.4 (Supporting Information, Figure S9 and Tables S5 and S6). Detailed information for the calculation of toxic unit is given in Supporting Information, Tables S5 and S6.

The experimentally derived toxic unit agreed well with the concentration addition prediction for binary mixtures of the known AchE inhibitors paraoxon-ethyl and diazoxon (Figure 6A).

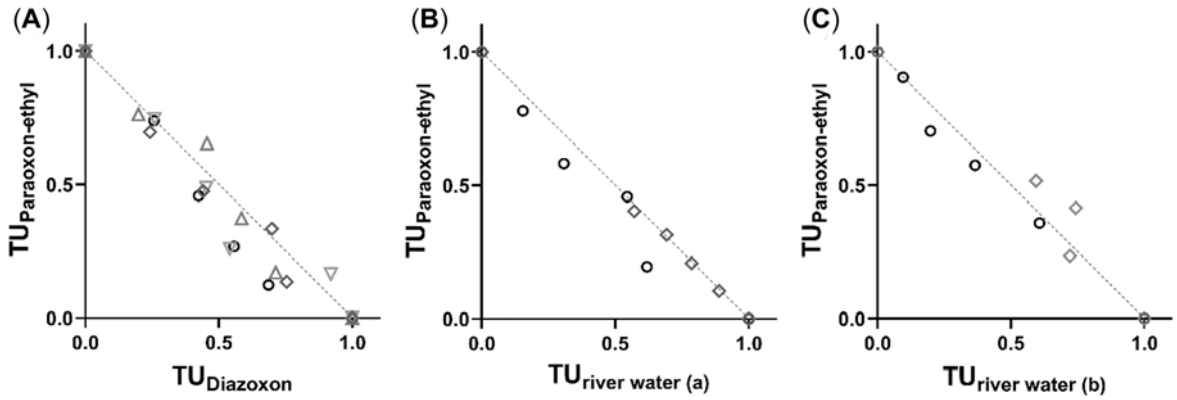

FIGURE 6: Isobolograms for binary mixtures of paraoxon-ethyl with (**A**) diazoxon as well as water extracts with (**B**) moderate and (**C**) high inhibition potency in an acetylcholinesterase inhibition assay using SH-SY5Y cells. The line indicates the concentration addition prediction. Different symbols stand for the results from multiple experimental sets. TU = toxic unit.

Because these two chemicals act through the same mode of action, no deviation is expected from the prediction. This was already demonstrated in the isobologram for oxidized diazinon and parathion in a purified AchE inhibition assay (Neale & Escher, 2013).

The experimental toxic unit of water extracts mixed with single chemicals also agreed well with the prediction for concentration addition (Figure 6B,C). In the isobologram study using purified AchE, on the contrary, the experimental values highly deviated from the predictions for binary mixtures of oxidized parathion with diverse types of water samples (reverse osmosis concentrate, treated effluent, and surface water; Neale & Escher, 2013). This indicates that the AChE inhibition assay using SH-SY5Y cells is not biased by binding to DOC, and hence can be applied to screening of DOC-rich environmental samples.

CONCLUSIONS

Limitations of bioassays for testing chemicals could be loss of chemicals during exposure, for example, by volatilization. To consider volatile loss of chemicals for experimental planning, a volatility cutoff at a log $K_{medium/air}$ of 4 was defined previously considering cytotoxic effects in various cell lines (Escher et al., 2019). While we confirmed that this cutoff is also applicable to the AChE inhibition assay with SH-SY5Y cells after 3 h of exposure, we observed substantial loss and slight cross-contamination after 24 h of incubation for some chemicals whose $K_{medium/air}$ was just around the cutoff. There can be other processes that contribute to the loss of chemicals in bioassays, such as abiotic degradation and sorption to the plastic microplates. In the presence of cells, it must also be kept in mind that SH-SY5Y cells are metabolically active and that a decrease in exposure concentration could occur because of cellular uptake and intracellular metabolism despite the large medium volume to cell volume ratio that would normally assure that depletion due to cell uptake and metabolism is negligible.

The OTPs were substantially less potent than OPs. Oxidation of OTPs into OPs by the metabolic activity of SH-SY5Y cells needs to be investigated further to understand the role of metabolism in this cell-based AChE assay. Potentially, the metabolic activation could be boosted by addition of an external metabolizing enzyme cocktail such as S9 isolated from rat liver, as is common practice in other bioassays. In the free enzyme-based assay, the OTPs are often oxidized with *N*-bromosuccinimide to the corresponding OPs, but even mild oxidation can degrade other mixture components in water samples; therefore, we did not attempt chemical oxidation as part of sample preparation.

Bioanalytical tools are useful to assess the toxicity of micropollutants in environmental samples. Measurement of AChE inhibition has been considered a potential endpoint to detect certain types of neuroactive pesticides such as OPs and carbamates in environmental samples (Legradi et al., 2018). However, environmental matrices such as DOC can hinder precise assessment in bioassays using isolated enzyme because the DOC can bind chemicals and therefore reduce the bioavailability of the chemicals for the receptor—in our case, AChE—or the DOC can disturb the AChE nonspecifically (Neale & Escher, 2013). Considering that DOC can suppress AChE inhibition in assays using purified enzyme, previous testing of water extracts with isolated enzymes might have underestimated AChE inhibition in the environmental samples. Such a negative impact of co-extracted DOC had not been observed for any other cell-based assay (Neale & Escher, 2014). Consistent with these observations, our SH-SY5Y cell–based assay was also unaffected by DOC and is more sensitive toward known AChE inhibitors. Therefore, it appears more suitable for environmental monitoring than any enzyme-based AChE inhibition assay.

Supporting information—The Supporting Information is available on the Wiley Online Library at https://doi.org/10.1002/etc.5490.

Acknowledgment—We thank N. Wojtysiak and S. Mälzer for conducting experiments for the volatility test. The water samples were collected in the framework of the project "Implementation of the National Action Plan for the Sustainable Use of Plant Protection Products (NAP)—Pilot Study to Determine the Contamination of Small Streams in the Agricultural

Landscape by Pesticide Residues," funded within the framework of the departmental research plan of the Federal Ministry for the Environment, Nature Conservation and Nuclear Safety (research code 3717634030) and the Helmholtz long-range strategic research funding (POF III) and led by M. Liess. We gratefully acknowledge access to the CITEPro platform (Chemicals in the Terrestrial Environment Profiler) funded by the Helmholtz Association. Open Access funding enabled and organized by Projekt DEAL.

Author Contributions Statement—**Jungeun Lee**: Conceptualization; Data curation; Formal analysis; Methodology; Investigation; Visualization; Writing—original draft. **Julia Huchthausen**: Investigation; Writing—review & editing. **Rita Schlichting**: Conceptualization; Software; Supervision; Writing—review & editing. **Stefan Scholz**: Supervision; Writing—review & editing. **Luise Henneberger**: Conceptualization; Investigation; Writing—review & editing. **Beate I. Escher**: Conceptualization; Funding acquisition; Supervision; Formal analysis; Visualization; Writing—review & editing.

Data Availability Statement—Data are available in the Supporting Information. Data, associated metadata, and calculation tools are available from the corresponding author (beate.escher@ufz.de).

REFERENCES

Altenburger, R., Bodeker, W., Faust, M., & Grimme, L. H. (1990). Evaluation of the isobologram method for the assessment of mixtures of chemicals. Combination effect studies with pesticides in algal biotests. *Ecotoxicology and Environmental Safety*, *20*, 98–114. https://doi.org/10.1016/0147-6513(90)90049-b

Birch, H., Kramer, N. I., & Mayer, P. (2019). Time-resolved freely dissolved concentrations of semivolatile and hydrophobic test chemicals in in vitro assays—measuring high losses and crossover by headspace solid-phase microextraction. *Chemical Research in Toxicology*, *32*, 1780–1790. https://doi.org/10.1021/acs.chemrestox.9b00133

Cao, J., Wang, M., Yu, H., She, Y., Cao, Z., Ye, J., Abd El-Aty, A. M., Hacimuftuoglu, A., Wang, J., & Lao, S. (2020). An overview on the mechanisms and applications of enzyme inhibition-based methods for determination of organophosphate and carbamate pesticides. *Journal of Agricultural and Food Chemistry*, *68*, 7298–7315. https://doi.org/10.1021/acs.jafc.0c01962

CITE-KNIME. (2022). AChE_evaluation. GitHub repository. https://github.com/CITE-KNIME/AChE_evaluation

Cohen, S. D., Williams, R. A., Killinger, J. M., & Freudenthal, R. I. (1985). Comparative sensitivity of bovine and rodent acetylcholinesterase to in vitro inhibition by organophosphate insecticides. *Toxicology and Applied Pharmacology*, *81*, 452–459. https://doi.org/10.1016/0041-008x(85)90416-8

Čolović, M. B., Krstić, D. Z., Lazarevic-Pasti, T. D., Bondzic, A. M., & Vasic, V. M. (2013). Acetylcholinesterase inhibitors: Pharmacology and toxicology. *Current Neuropharmacology*, *11*, 315–335. https://doi.org/10.2174/1570159X11311030006

Čolović, M. B., Krstić, D. Z., Uščumlić, G. S., & Vasić, V. M. (2011). Single and simultaneous exposure of acetylcholinesterase to diazinon, chlorpyrifos and their photodegradation products. *Pesticide Biochemistry and Physiology*, *100*, 16–22. https://doi.org/10.1016/j.pestbp.2011.01.010

de Medeiros, L. M., De Bastiani, M. A., Rico, E. P., Schonhofen, P., Pfaffenseller, B., Wollenhaupt-Aguiar, B., Grun, L., Barbe-Tuana, F., Zimmer, E. R., Castro, M. A. A., Parsons, R. B., & Klamt, F. (2019). Cholinergic differentiation of human neuroblastoma SH-SY5Y cell line and its potential use as an in vitro model for Alzheimer's disease studies. *Molecular Neurobiology*, *56*, 7355–7367. https://doi.org/10.1007/s12035-019-1605-3

Ellman, G. L., Courtney, K. D., Andres, V., Jr., & Feather-Stone, R. M. (1961). A new and rapid colorimetric determination of acetylcholinesterase activity. *Biochemical Pharmacology*, *7*, 88–95. https://doi.org/10.1016/0006-2952(61)90145-9

Escher, B. I., Bramaz, N., & Ort, C. (2009). JEM spotlight: Monitoring the treatment efficiency of a full scale ozonation on a sewage treatment plant with a mode-of-action based test battery. *Journal of Environmental Monitoring*, *11*, 1836–1846. https://doi.org/10.1039/b907093a

Escher, B. I., Glauch, L., König, M., Mayer, P., & Schlichting, R. (2019). Baseline toxicity and volatility cutoff in reporter gene assays used for high-throughput screening. *Chemical Research in Toxicology*, *32*, 1646–1655. https://doi.org/10.1021/acs.chemrestox.9b00182

Fischer, F. C., Cirpka, O. A., Goss, K. U., Henneberger, L., & Escher, B. I. (2018). Application of experimental polystyrene partition constants and diffusion coefficients to predict the sorption of neutral organic chemicals to multiwell plates in *in vivo* and *in vitro* bioassays. *Environmental Science & Technology*, *52*, 13511–13522. https://doi.org/10.1021/acs.est.8b04246

Fischer, F. C., Henneberger, L., König, M., Bittermann, K., Linden, L., Goss, K. U., & Escher, B. I. (2017). Modeling exposure in the Tox21 in vitro bioassays. *Chemical Research in Toxicology*, *30*, 1197–1208. https://doi.org/10.1021/acs.chemrestox.7b00023

Fukuto, T. R. (1990). Mechanism of action of organophosphorus and carbamate insecticides. *Environmental Health Perspectives*, *87*, 245–254. https://doi.org/10.1289/ehp.9087245

Hamers, T., Molin, K. R., Koeman, J. H., & Murk, A. J. (2000). A small-volume bioassay for quantification of the esterase inhibiting potency of mixtures of organophosphate and carbamate insecticides in rainwater: Development and optimization. *Toxicological Sciences*, *58*, 60–67. https://doi.org/10.1093/toxsci/58.1.60

Henneberger, L., Mühlenbrink, M., Fischer, F. C., & Escher, B. I. (2019). C18-coated solid-phase microextraction fibers for the quantification of partitioning of organic acids to proteins, lipids, and cells. *Chemical Research in Toxicology*, *32*, 168–178. https://doi.org/10.1021/acs.chemrestox.8b00249

Hicks, D. A., Makova, N. Z., Nalivaeva, N. N., & Turner, A. J. (2013). Characterisation of acetylcholinesterase release from neuronal cells. *Chemico-Biological Interactions*, *203*, 302–308. https://doi.org/10.1016/j.cbi.2012.09.019

Huchthausen, J., Mühlenbrink, M., König, M., Escher, B. I., & Henneberger, L. (2020). Experimental exposure assessment of ionizable organic chemicals in *in vitro* cell-based bioassays. *Chemical Research in Toxicology*, *33*, 1845–1854. https://doi.org/10.1021/acs.chemrestox.0c00067

Insecticide Resistance Action Committe. (2021). *The IRAC mode of action classification* (Version 10.1). https://irac-online.org/mode-of-action/

Karanth, S., & Pope, C. (2003). In vitro inhibition of blood cholinesterase activities from horse, cow, and rat by tetrachlorvinphos. *International Journal of Toxicology*, *22*, 429–433. https://doi.org/10.1177/109158180302200604

Lee, J., Braun, G., Henneberger, L., König, M., Schlichting, R., Scholz, S., & Escher, B. I. (2021). Critical membrane concentration and mass-balance model to identify baseline cytotoxicity of hydrophobic and ionizable organic chemicals in mammalian cell lines. *Chemical Research in Toxicology*, *34*, 2100–2109. https://doi.org/10.1021/acs.chemrestox.1c00182

Lee, J., Schlichting, R., König, M., Scholz, S., Krauss, M., & Escher, B. I. (2022). Monitoring mixture effects of neurotoxicants in surface water and wastewater treatment plant effluents with neurite outgrowth inhibition in SH-SY5Y cells. *ACS Environmental Au*. Advance online publication. https://doi.org/10.1021/acsenvironau.2c00026

Legradi, J. B., Di Paolo, C., Kraak, M. H. S., van der Geest, H. G., Schymanski, E. L., Williams, A. J., Dingemans, M. M. L., Massei, R., Brack, W., Cousin, X., Begout, M. L., van der Oost, R., Carion, A., Suarez-Ulloa, V., Silvestre, F., Escher, B. I., Engwall, M., Nilen, G., Keiter, S. H., … Hollert, H. (2018). An ecotoxicological view on neurotoxicity assessment. *Environmental Sciences Europe*, *30*, Article 46. https://doi.org/10.1186/s12302-018-0173-x

Li, S., Huang, R., Solomon, S., Liu, Y., Zhao, B., Santillo, M. F., & Xia, M. (2017). Identification of acetylcholinesterase inhibitors using homogenous cell-based assays in quantitative high-throughput screening platforms. *Biotechnology Journal*, *12*, Article 1600715. https://doi.org/10.1002/biot.201600715

Li, S., Zhao, J., Huang, R., Travers, J., Klumpp-Thomas, C., Yu, W., MacKerell, A. D., Jr., Sakamuru, S., Ooka, M., Xue, F., Sipes, N. S.,

Hsieh, J. H., Ryan, K., Simeonov, A., Santillo, M. F., & Xia, M. (2021). Profiling the Tox21 chemical collection for acetylcholinesterase inhibition. *Environmental Health Perspectives*, *129*, Article 47008. https://doi.org/10.1289/EHP6993

Liess, M., Liebmann, L., Vormeier, P., Weisner, O., Altenburger, R., Borchardt, D., Brack, W., Chatzinotas, A., Escher, B., Foit, K., Gunold, R., Henz, S., Hitzfeld, K. L., Schmitt-Jansen, M., Kamjunke, N., Kaske, O., Knillmann, S., Krauss, M., Kuster, E., … Reemtsma, T. (2021). Pesticides are the dominant stressors for vulnerable insects in lowland streams. *Water Research*, *201*, Article 117262. https://doi.org/10.1016/j.watres.2021.117262

Lionetto, M. G., Caricato, R., Calisi, A., & Schettino, T. (2011). Acetylcholinesterase inhibition as a relevant biomarker in environmental biomonitoring: New insights and perspectives. In J. E. Visser (Ed.), *Ecotoxicology around the globe* (pp. 87–115). Nova Science.

Macova, M., Toze, S., Hodgers, L., Mueller, J. F., Bartkow, M., & Escher, B. I. (2011). Bioanalytical tools for the evaluation of organic micropollutants during sewage treatment, water recycling and drinking water generation. *Water Research*, *45*, 4238–4247. https://doi.org/10.1016/j.watres.2011.05.032

Molica, R. J. R., Oliveira, E. J. A., Carvalho, P. V. V. C., Costa, A. N. S. F., Cunha, M. C. C., Melo, G. L., & Azevedo, S. M. F. O. (2005). Occurrence of saxitoxins and an anatoxin-a(s)-like anticholinesterase in a Brazilian drinking water supply. *Harmful Algae*, *4*, 743–753. https://doi.org/10.1016/j.hal.2004.11.001

Neale, P. A., & Escher, B. I. (2013). Coextracted dissolved organic carbon has a suppressive effect on the acetylcholinesterase inhibition assay. *Environmental Toxicology and Chemistry*, *32*, 1526–1534. https://doi.org/10.1002/etc.2196

Neale, P. A., & Escher, B. I. (2014). Does co-extracted dissolved organic carbon cause artefacts in cell-based bioassays? *Chemosphere*, *108*, 281–288. https://doi.org/10.1016/j.chemosphere.2014.01.053

Nunes, B. (2011). The use of cholinesterases in ecotoxicology. *Reviews of Environmental Contamination and Toxicology*, *212*, 29–59. https://doi.org/10.1007/978-1-4419-8453-1_2

Perrier, A. L., Massoulié, J., & Krejci, E. (2002). PRiMA: The membrane anchor of acetylcholinesterase in the brain. *Neuron*, *33*, 275–285. https://doi.org/10.1016/s0896-6273(01)00584-0

Philippe, A., & Schaumann, G. E. (2014). Interactions of dissolved organic matter with natural and engineered inorganic colloids: A review. *Environmental Science & Technology*, *48*, 8946–8962. https://doi.org/10.1021/es502342r

Pichon, V., Coumes, C. C. D., Chen, L., Guenu, S., & Hennion, M. C. (1996). Simple removal of humic and fulvic acid interferences using polymeric sorbents for the simultaneous solid-phase extraction of polar acidic, neutral and basic pesticides. *Journal of Chromatography A*, *737*, 25–33. https://doi.org/10.1016/0021-9673(95)01339-3

Pohanka, M. (2011). Cholinesterases, a target of pharmacology and toxicology. *Biomedical Papers of the Medical Faculty of Palacky University in Olomouc*, *155*, 219–229. https://doi.org/10.5507/bp.2011.036

Proenca, S., Escher, B. I., Fischer, F. C., Fisher, C., Gregoire, S., Hewitt, N. J., Nicol, B., Paini, A., & Kramer, N. I. (2021). Effective exposure of chemicals in in vitro cell systems: A review of chemical distribution models. *Toxicology In Vitro*, *73*, Article 105133. https://doi.org/10.1016/j.tiv.2021.105133

R: A language and environment for statistical computing. (Ver 4.0.4) [Computer software]. (2020). R Foundation for Statistical Computing.

Ralston, J. S., Rush, R. S., Doctor, B. P., & Wolfe, A. D. (1985). Acetylcholinesterase from fetal bovine serum. Purification and characterization of soluble G4 enzyme. *Journal of Biological Chemistry*, *260*, 4312–4318.

Sharma, K. (2019). Cholinesterase inhibitors as Alzheimer's therapeutics (review). *Molecular Medicine Reports*, *20*, 1479–1487. https://doi.org/10.3892/mmr.2019.10374

Sogorb, M. A., Alvarez-Escalante, C., Carrera, V., & Vilanova, E. (2007). An in vitro approach for demonstrating the critical role of serum albumin in the detoxication of the carbamate carbaryl at in vivo toxicologically relevant concentrations. *Archives of Toxicology*, *81*, 113–119. https://doi.org/10.1007/s00204-006-0142-9

Sogorb, M. A., Carrera, V., & Vilanova, E. (2004). Hydrolysis of carbaryl by human serum albumin. *Archives of Toxicology*, *78*, 629–634. https://doi.org/10.1007/s00204-004-0584-x

Thullbery, M. D., Cox, H. D., Schule, T., Thompson, C. M., & George, K. M. (2005). Differential localization of acetylcholinesterase in neuronal and non-neuronal cells. *Journal of Cellular Biochemistry*, *96*, 599–610. https://doi.org/10.1002/jcb.20530

Ulrich, N., Endo, S., Brown, T. N., Watanabe, N., Bronner, G., Abraham, M. H., & Goss, K.-U. (2017). *UFZ-LSER database (Ver 3.2.1)*. Helmholtz Centre for Environmental Research-UFZ. http://www.ufz.de/lserd

Villeneuve, D. L., Blankenship, A. L., & Giesy, J. P. (2000). Derivation and application of relative potency estimates based on in vitro bioassay results. *Environmental Toxicology and Chemistry*, *19*, 2835–2843.

Zhang, J. H., Chung, T. D., & Oldenburg, K. R. (1999). A simple statistical parameter for use in evaluation and validation of high throughput screening assays. *Journal of Biomolecular Screening*, *4*, 67–73. https://doi.org/10.1177/108705719900400206

